



**RESERVOIR QUALITY OF PERMIAN SANDSTONES
IN THE STRZELECKI - KIDMAN - KERNA AREAS,
COOPER BASIN, SOUTH AUSTRALIA.**

J. Eleftheriou
University of Adelaide, 1990

RESERVOIR QUALITY OF PERMIAN SANDSTONES IN THE STRZELECKI-KIDMAN-KERNA AREAS, COOPER BASIN, SOUTH AUSTRALIA.

by
John Eleftheriou (B.App.Sc., Grad Dip App.Sci.).

August 1990

National Centre for Petroleum Geology and Geophysics, 1990.
P.O. Box 498, Adelaide, South Australia.

This thesis is submitted as partial fulfilment for the degree of Master of Science, in Petroleum Geology and Geophysics, the University of Adelaide.

Declaration

To the best of the writer's knowledge and belief, this thesis contains no material previously published or written by another person, except where due reference is made in the text of the thesis. This thesis also contains no material accepted for the award of any other degree or diploma in any University.

John Eleftheriou.

Acknowledgments

I am indebted to Sally Phillips for her constructive criticism, tolerance and good humour; Bill Stuart for further constructive criticism and lateral thinking; John Willoughby's resourcefulness; SANTOS for access to precious data and resources, and to petroleum geology in general.

To my family Sia, Alex and Joanna for their moral and practical support, I thank you.

Key words

Aroona	Bagundi	Cooper Basin	diagenesis
Dieri	dickite	Dilchee	facies
Kidman	Kerna	Lepena	Marana
Marabooka	overpressures	permeability	Permian
porosity	reservoir	Strzelecki	Wanara

TABLE OF CONTENTS

Section	contents	page
	Frontispiece	i
	Title page	ii
	Contents	iii
	List of figures	v
	List of tables	vi
	List of appendices	vi
	List of plates	vi
	Abstract	viii
1	Introduction	1
1.1	Preface	1
1.2	Aim and results	2
2	Available information	2
3	Methods	3
4	Geological setting	6
4.1	Introduction	6
4.2	Regional setting	6
4.3	Stratigraphy	7
4.4	Structural setting	8
4.5	Hydrocarbon setting	10
5	Field descriptions	12
5.1	Strzelecki area	12
5.2	Kidman Complex	13
5.3	Kerna area	13
6	Sedimentology	14
6.1	Nomenclature	14
6.1.1	Patchawarra Formation subdivision	14
6.1.2	Toolachee Formation subdivision	15
6.2	Geological history	15
6.3	Facies mapping	17
6.3.1	Previous work	18
6.3.2	Correlations	19
	Plates 1 to 5	
7	Petrology and diagenesis	21
7.1	General description	21
7.2	Rock composition	21
7.3	Petrography	21
7.3.1	Quartz	21
7.3.1.1	Quartz observations	22
7.3.1.2	Timing of quartz authigenesis	23
7.3.1.3	Quartz dissolution	24
7.3.1.4	Origin of quartz	25
7.3.1.5	Discussion of quartz authigenesis	29
7.3.1.6	Conclusions - quartz	31
7.3.2	Illite	31
7.3.2.1	Illite / smectite	32
7.3.2.2	Origins of illite	32
7.3.2.2.1	Detrital illite	32
7.3.2.2.2	Authigenic illite	33
7.3.2.3	Conclusions - illite	35

Table of Contents (continued)

Section	contents	page
7.3.3	Kaolin (kaolinite & dickite) clay	35
7.3.3.1	Origin of kaolin	36
7.3.3.2	Conclusions - kaolin	38
7.3.4	Micas	38
7.3.5	Feldspar	39
7.3.5.1	Feldspar dissolution	39
7.3.6	Rock fragments	40
7.3.7	Carbonates	40
7.3.7.1	Micritic siderite	41
7.3.7.2	Sparry siderite	42
7.3.7.3	Conclusions - carbonates	42
7.3.8	Chlorite	43
7.3.9	Other minerals	43
7.4	Hydrocarbons	44
7.4.1	Discussion of hydrocarbon occurrence	44
7.4.2	Conclusions - hydrocarbon occurrence	46
7.5	Porosity observations	47
7.6	Permeability observations	47
7.7	Compaction effects	48
7.8	Diagenetic sequence	48
7.9	Previous diagenetic studies	49
8	Petrophysics	52
8.1	Core plug data analysis	52
8.2	Flow data analysis	54
8.3	Groundwater	55
8.3.1	Water sample data analysis	56
9	Reservoir quality	57
9.1	First order porosity variation	57
9.2	Second order porosity variation	58
9.3	Other porosity variations	58
9.4	Permeability variations	59
9.5	Influence of unconformity on reservoir quality	60
9.5.1	Unconformity effects - observations	60
9.5.2	Nature of the unconformity	61
9.5.3	Mechanism of unconformity related diagenesis	61
9.5.4	Discussion of unconformity influence on reservoir quality	63
9.5.5	Conclusions - unconformity effects	64
9.6	Geological influences on porosity and permeability	64
9.6.1	Lithology	65
9.6.2	Lithofacies	65
9.6.3	Depositional facies	65
9.6.4	Facies associations	66
9.6.5	Discussion of geology and permeability/porosity	66
9.7	Overpressures	68
9.7.1	Conclusions - overpressures	70
9.8	Summary of reservoir quality	71
10	Summary and conclusions	72
11	Figures 1 to 64a	
12	References	
13	Appendices 1 to 8	

LIST OF FIGURES

<i>Figure</i>	<i>Contents</i>
1	Study area location.
2	Structural cross section A-A'.
3	Structural cross section B-B'.
4	Structural features of the study area.
5	Localities referred to in this report and major structural features of the Cooper Basin.
6	Study area well location plan.
7	Structural cross section showing Patchawarra Formation facies association correlations.
8	Structural cross section showing Toolachee Formation facies association correlations.
9	Palaeogeographic reconstruction of the Patchawarra Formation.
10	Palaeogeographic reconstruction of the Toolachee Formation.
11	Illite/kaolin vs average grain size.
12	Dickite & kaolinite vs average grain size.
13	Illite/kaolin vs kaolinite.
14	EDS spectra for K.
15	Siderite vs average grain size.
16	Siderite vs illite/kaolin.
17	Kaolin vs illite.
18	Porosity vs permeability.
19	Illite vs primary porosity.
20	Kaolin vs primary porosity.
21	Dickite vs porosity.
22	Plug porosity vs average grain size.
23	Primary porosity vs average grain size.
24	Plug porosity vs maximum grain size.
25	Plug porosity vs illite/kaolin.
26	Plug porosity vs sorting.
27	Plug permeability vs average grain size.
28	Secondary porosity vs plug permeability.
29	Primary porosity vs plug permeability.
30	Sorting vs plug permeability.
31	Illite vs plug permeability.
32	Siderite vs plug permeability.
33	Proposed sequence of diagenetic events.
34	Porosity vs formation interval.
35	Porosity vs depth from Jurassic.
35a	Porosity vs depth from Jurassic.
36	Plug permeability vs depth from Jurassic.
37	Log plug permeability vs depth from Jurassic.
38	Section porosity vs depth from Jurassic.
39	Plug residual oil vs depth from Jurassic.
40	39 DST results from 4 Toolachee Formation facies associations.
41	23 DST results from the upper two Patchawarra Formation facies associations.
42	DST results of testing channel sands, overbank sands and all sands.
43	Histogram of DST results, all sands.
44	DST rating vs distance from Strzelecki 2.
45	Groundwater TDS vs depth from Jurassic.
46	Strzelecki 10 porosity / depth plot.
47	Vitrinite reflectance vs depth.
48	Plug porosity vs depth.
49	Dickite vs plug permeability.
50	Plug permeability vs grain size.

List of Figures (continued)

<i>Figure</i>	<i>Contents</i>
51	Log(permeability)/porosity vs grain size.
52	Log(permeability)/porosity vs depth.
53	Porosity vs plug residual oil.
54	Kaolin & illite vs depth from Jurassic.
55	Kaolin vs depth from Jurassic.
56	Siderite vs depth from Jurassic.
57	Illite/kaolin vs depth from Jurassic.
58	Porosity vs formation position.
59	Permeability vs formation position.
60	Illite/kaolin vs plug porosity.
61	Illite/kaolin vs plug permeability.
62	Illite/kaolin vs siderite.
63	Illite/kaolin vs average grain size.
64	Permeability vs porosity.
64a	Permeability vs porosity.

LIST OF TABLES

<i>Table</i>	<i>Contents</i>	<i>Page</i>
1	Plug analysis of samples 305 & 308.	3
2	Sample analyses carried out for this report.	5
3	Environments of hydrocarbon formation in the Strzelecki area.	10
4	Details of hydrocarbon fields in the study area.	12
5	Details of core plugs.	53
6	Drill stem test rating scheme.	54
7	Facies reference data	Adj Plate 1

LIST OF APPENDICES

<i>Appendice</i>	<i>Contents</i>
1	Core logging methods and results.
2	Petrological descriptions.
3	XRD results and analysis.
4	Miscellaneous data.
5	Facies associations limits for wells.
6	Electrical log to core logging correlations.
7	Drill Stem Test results and analysis.
8	Water sample chemistry data.

LIST OF PLATES

(SEM = electron microscope, CL = cathodoluminescence, TL = transmitted light)

Plate 1: SEM micrographs of quartz

- 1a quartz & kaolin
- 1b etching of quartz
- 1c intergrown quartz & kaolin
- 1d quartz & kaolin
- 1e intergrown quartz & kaolin
- 1f clay rich rock fragment
- 1g druse quartz
- 1h druse quartz

Plate 2: SEM micrographs of clays, feldspar & siderite

- 2a platy grain coating illite
- 2b bent mica
- 2c mica altering to kaolin
- 2d corroded detrital feldspar
- 2e fibrous illite
- 2f vermiform euhedral dickite
- 2g partly dissolved micritic siderite
- 2h primary porosity

Plate 3: TS and CL micrographs of quartz

- 3a multiple stage quartz overgrowths (CL)
- 3b multiple stage quartz overgrowths (TL)
- 3c fine grained sample with few quartz overgrowths (CL)
- 3d quartz dust rings (TL)
- 3e quartz dust rings (TL)
- 3f quartz dust rings (TL)

Plate 4: TS and CL micrographs of quartz

- 4a patchy silicification (CL)
- 4b patchy silicification (TL)
- 4c quartz overgrowths and porosity (CL)
- 4d quartz overgrowths and porosity (TL)
- 4e quartz overgrowths and meniscus cement (CL)
- 4f quartz overgrowths and meniscus cement (TS)

Plate 5: TS, CL micrographs of quartz, feldspar & siderite

- 5a spar siderite (TL)
- 5b spar siderite (TL)
- 5c dissolution seams and microstylolites (CL)
- 5d dissolution seams and microstylolites (TL)
- 5e partial dissolution of a quartz grain (CL)
- 5f quartz overgrowths and remnant feldspar (CL)

Abstract

"Reservoir quality of Permian arenites in the Strzelecki-Kidman-Kerna areas, Cooper Basin, South Australia."

Permian Cooper Basin gas and oil bearing reservoir arenites are examined from the Strzelecki, Marabooka, Kidman, Kerna and adjacent hydrocarbon fields, South Australia. The aim of the study is to identify genetic, diagenetic and physical influences on reservoir quality. Techniques used include lithofacies-based core logging, thin section petrology, scanning electron microscopy, X-ray diffraction and cathodoluminescence. Existing wireline logs, core plug tests, drill stem tests, groundwater analyses and hydrocarbon maturity data are also used.

Reservoir rock types are mostly fluvialite sublithic quartzarenites in which porosity is reduced by authigenic minerals and diagenetic fabrics. Identified diagenetic processes include mechanical compaction, multiple phase quartz cementation and kaolin and illite authigenesis. Less common results of framework grain dissolution and siderite and chlorite authigenesis are also observed.

Major factors influencing reservoir quality of arenites from the study area are sedimentary (e.g. original pore size, grain packing, sand thickness), physical (e.g. sediment loading and compaction, pore water pressure) and chemical (e.g. quartz overgrowths, kaolin authigenesis). Most reservoir porosity is attributed to remnant primary porosity which is best preserved in coarse grained, poorly sorted arenites with little detrital clay matrix. Reduced porosity and permeability values of arenites generally occur towards the base of the Cooper Basin sequence, towards the base of the Toolachee and Patchawarra Formations and towards the top 100 metres (350 feet) of the Cooper Basin sequence.

A model of the post-depositional history of the study area involving several, mostly overlapping diagenetic events is proposed. This model differs from previous interpretations of Cooper Basin diagenesis in three ways:

- (a) some quartz cementation may have occurred at elevated temperatures and depth during Cretaceous hydrocarbon generation;
- (b) unconformities associated with (?) Late Triassic erosion may have produced localised diagenetic effects that reduce porosity and permeability within 100 metres below the top of the Cooper Basin;
- (c) some quartz cement is possibly formed in overpressured zones within initially porous sands.

Permeability appears loosely dependent on porosity but is field dependent and varies with grain size and depth. Channel deposits displaying sedimentary structures associated with high flow regimes are potentially the most productive sands in the study area. Future exploration plays for hydrocarbons may be formulated with respect to changes of reservoir quality below local unconformities.

1 Introduction

1.1 Preface

The Cooper Basin is an oil and gas bearing sequence of subsurface Carboniferous, Permian and Triassic fluvial sediments up to 1.5 kilometers thick that extend over an area of 127,000 square kilometers of northeast South Australia and southwest Queensland. The basin has been exploited for major reserves of gas and minor amounts of oil since the 1960's.

Together with the overlying Jurassic to Cretaceous Eromanga Basin sequence, the Cooper Basin forms the most prolific hydrocarbon producing onshore basin in Australia.

Exploration for hydrocarbons within the Cooper Basin has reached a mature stage with most larger prospective structural traps having been drilled. During the 1980's the application of facies mapping, "genetic interval mapping", higher quality seismic data and detailed geochemical analysis has aided exploitation of existing fields and exploration for stratigraphic traps. However, reservoir porosity has been identified as the major influence on the "success rate of the primary objectives of wells" drilled into the Cooper Basin (Hunt & Piper 1986).

This thesis examines the main influences on porosity and permeability of major Permian reservoir sandstones within part of the southern Cooper Basin, referred to as the Strzelecki-Kidman-Kerna area, or the study area.

The Strzelecki-Kidman-Kerna area contains the Permian gas producing fields of Strzelecki, Marabooka, Lepena, Bagundi/Aroona, Kidman and Kidman North along with several cased and suspended potential gas producing wells. The western boundary of the area is approximately fifty kilometres southeast of Moomba, South Australia (Figure 1) and it extends as a corridor 15 kilometers wide to the Queensland state border 50 kilometers to the east.

The results of this study also form part of NERDDC funded project 1175 being undertaken by the National Centre for Petroleum Geology & Geophysics based at the University of Adelaide. Objectives of this project include the determination of factors controlling the regional quality of Permian reservoir sandstones in the Southern Cooper Basin.

1.2 Aim and results

The aim of this study is to define and predict the best types of hydrocarbon bearing sands in Permian reservoir units of the study area, based on identified genetic, diagenetic and physical controls.

As outlined in the last chapter of this report, it is believed this aim has been substantially achieved. It is concluded that physical diagenetic processes (e.g. sediment loading and compaction, pore water pressure) and chemical diagenetic processes (e.g. quartz overgrowths, kaolin authigenesis) have produced major porosity and permeability reductions in Permian sands after deposition. It is also considered that initially coarse grained and high porosity sediments such as channel sands displaying high flow regime sedimentary structures are the best hydrocarbon reservoir targets.

2 Available information

The Cooper Basin has been extensively studied over the past few decades, particularly in regard to the occurrence of hydrocarbons and the regional geological setting of reservoir intervals (Kapel 1966, Gatehouse 1972, Kapel 1972, Stuart 1976, Kanstler et al 1978 and others). However, apart from geological synopses included in some well completion reports and field reserve summaries, few geological reports are specific to any part of the study area. Available literature is reviewed where relevant in the report.

Core and cuttings samples from all the study area wells are kept in good condition at the South Australian Department of Mines and Energy core storage library. Details of core plug testing, pore water analyses, drill stem testing etc are maintained as computer online data at Santos Ltd.

3 Methods

The Cooper Basin is entirely subsurface so all primary data are from cores, well cuttings and wireline logs acquired from wells. Cored intervals of wells in the study area, generally within the known hydrocarbon reservoir intervals of the Toolachee, Epsilon and Patchawarra Formations, were logged and sampled to determine their geological setting. Vertical and lateral sedimentary "facies" variations within uncored intervals of the study area were predicted using electrical log signatures of the logged sections.

A total of 317 metres (1040 feet) of core was logged in 14 wells and the graphic logs are included in Appendix 1.

A series of cross-sections were established using selected wells. Correlation of electrical logs of these wells by time stratigraphic principles used viable associations or groupings of interpreted sedimentary facies. Isopach maps and seismic information were also used for correlation. Because of common interfingering of sands and shales, the generally transitional nature of formation boundaries and restricted coverage of well data, correlations can only be considered approximate.

Core samples were generally taken next to core plugs to utilize the existing porosity and permeability data. 89 core samples and 23 cuttings samples were taken for further analysis and two core plug analyses were taken for porosity and permeability measurements by the consulting laboratory, Amdel (Table 1). It was found that most core has been intensively sampled for core plug data and all of this data were made available for this project by SANTOS Ltd. and the South Australian Department of Mines and Energy.

sample	306	304
well	Kidman 1	Marana 1
driller's depth	6601'3"	6328'5"
permeability (md)	0.016	13.5
porosity (%)	2.0	13.0
bulk dry density (g/cc)	2.5	2.33
grain density (g/cc)	2.55	2.67

Table 1 Core plug test results from Amdel.

Samples were examined by means of conventional transmitted light microscopy, Scanning Electron Microscopy (SEM), bulk sample X-Ray diffraction (XRD) analysis and cathodoluminescence (CL) techniques.

Petrological examinations of thin sections were used to determine genetic and paragenetic mineral

relationships and to characterise porosity types. Thin sections were prepared from all samples. Araldite with blue dye was used as the mounting medium to assist in porosity recognition. Mineral abundances and grain sizes were estimated visually. Petrological description summaries are included in Appendix 2.

Bulk mineral identification of all samples was carried out by XRD analysis. Samples of total rock were wet ground for 30 seconds using alcohol in a tungsten-carbide mill, then oven dried at temperatures less than 100° C. Samples were run as front mounted powder pressings from 3 to 75° 2 theta at 4° per minute in a "Siemens" X-Ray diffractometer at 50kV and 35mA using Co K alpha radiation.

All core samples were examined by a SEM enabling the identification and morphology of mineral types and pore spaces to be obtained. Samples were prepared by fracturing core samples and mounting fresh 1 cm³ size fragments on an aluminium pin type stub. The sub-samples were then evaporatively coated with carbon and gold/palladium. A "Philips 505" SEM was used to view and image the sub-samples. Mineral identification was based on elements identified in an "Tracor Northern TN5500" energy dispersive spectrometer (EDS) system connected to the SEM.

Cathodoluminescence (CL) studies of 13 samples helped determine the paragenetic sequence of diagenetic minerals, in particular that of quartz. Polished thin sections 0.3 mm thick were irradiated using electron gun voltages of 15 to 25 kV at 200 to 500 mA in vacuum levels of 0.05 to 0.02 Torr. A "Technosyn 8200" generator and stage were used.

Details of samples selected and examined for this report are shown in Table 2.

METHOD	COMMENT	NUMBER OF SAMPLES	RESULTS
Core logging		1040 feet	Appendix 1
Thin Section	Used blue dyed araldite for mounting	110	Appendix 2
XRD	Wet ground, powder pressing	110	Appendix 3
SEM	EDS spectra obtained from all samples.	87	
CL	Polished sections	13	
Plug Analysis	Tested by AMDEL	Samples 305,308	Table 1

Table 2 Sample analyses carried out for this report.

Other data used in this report include 706 Permian and 436 Jurassic to Cretaceous core plug analyses, the results of 79 drill stem tests, 40 analyses of groundwater and 43 determinations of vitrinite reflectance. This data was made available by Santos Ltd. ("SAS" data files, unpublished reports and well completion reports) and the South Australian Department of Mines and Energy.

4 Geological setting

4.1 Introduction

The Cooper Basin is a northeast to southwest elongate Permian to Triassic intracratonic basin located in northeast South Australia and southwest Queensland, central Australia (Figure 1). The basin covers an area of 127,000 square kilometres and contains sediments with total thickness of up to 1,500 metres in the central Nappamerri Trough (Battersby 1976). Sediments consist of sandstones, siltstones, shales and coals deposited in fluvial, deltaic and lacustrine systems. They unconformably overlie Silurian to Carboniferous metasediments & volcanics of the Warburton Basin and underlie thick Jurassic to Recent sediments of the Eromanga Basin (Battersby 1976).

4.2 Regional setting

The stratigraphic nomenclature used for this report is that formalised by Kapel (1966), Gatehouse (1972), Williams (1982) and Powis (1989) that subdivides the Cooper Basin sediments into the Gidgealpa and Nappamerri Groups.

The Cooper Basin sediments were deposited during the Late Carboniferous to Late Triassic and unconformably overlie eroded clastics and volcanics of the Early Cambrian to Devonian Warburton Basin (Battersby 1976). Sedimentation was initiated by intracratonic subsidence (Coles, Nikiforuk, Pennell 1987) with the earlier Cooper Basin sediments being relatively thin or absent in the study area because of onlap onto structural highs.

Initial Cooper Basin sedimentation occurred with the deposition of the glacial Merrimelia Formation (Williams 1982), while the rest of the sequence mainly contained strata typical of cyclic fluvial and deltaic conditions (Tirrawarra Sandstone, Patchawarra, Epsilon, Daralingie, Toolachee and Nappamerri Formations) and mostly lacustrine conditions (Murteree and Roseneath Shales).

Sedimentation in the Cooper Basin was active over most of the Late Carboniferous to the mid-Triassic (Gausden 1979). All formations have conformable, diachronous boundaries (Thornton 1978) with the exception of an angular unconformity at the base of the Toolachee Formation, which has been delineated by drilling, palynology and seismic investigations (Wopfner 1972, Pycroft 1973, Thornton 1978).

Structural cross sections of the Cooper Basin interval across the study area are presented as Figures 2 and 3 and show the pronounced angular unconformity at the base of the Toolachee Formation.

The Cooper Basin sequence is disconformably overlain by the Jurassic to Cretaceous Eromanga

Basin which is, in turn, disconformably overlain by the Cainozoic Birdsville Basin (Battersby 1976).

4.3 Stratigraphy

The earliest Cooper Basin sediments are sandstones, diamictites, conglomerates, shales and siltstones of the Late Carboniferous to Early Permian **Merrimelia Formation**. They are interpreted to be of glacial origin (Battersby 1976) and deposited in glacio-fluvial, lacustrine and aeolian environments (Williams & Wild 1984). They are present in the west to central part of the study area.

The **Tirrawarra Sandstone** consists mainly of relatively clean sandstones and minor shales that were deposited principally in braided stream regimes (Kapel 1972), possibly with glacial conditions persisting from Merrimelia Formation deposition (Thornton 1978).

Although the Tirrawarra Sandstone occurs at the Big Lake Field 30 km west of the Strzelecki Field (Coles, Nikiforuk, Pennell 1987), it is not intersected in wells in the study area except in Strzelecki 10 where 50 metres (157 feet) of mostly clean sands were reported as Tirrawarra Sandstone on the well logs and well completion report.

The **Patchawarra Formation** marks a gradual change to a predominantly meandering stream depositional environment. Sedimentation over a lengthy period of time overlapped pre-Permian highs and filled in palaeo-topographic lows, with sediment thickness of over 770 metres (2,500 feet) in the deeper portions of the Cooper Basin (Taylor & Thomas 1989). The thickest Patchawarra Formation interval in the study area is 230 metres (750 feet) in Coochilara 1.

The Patchawarra Formation consists of sandstones, siltstones, shales and coals which were deposited in channels, point bars, crevasse splays, overbank and backswamp environments (Grasso 1986). The upper part of the formation represents a general decrease in fluvial energy that ends with the lacustrine deposits of conformably overlying Murteree Shale. Stuart et al (1988) point out that compaction, local structural growth and faulting were contemporaneous with fluvial deposition of the Patchawarra Formation.

The overlying **Murteree Shale** represents quiescent deposition of fine grain sediments into a lake or restricted sea, under essentially fresh water conditions (Stuart 1976, Thornton 1979). The Murteree Shale consists of buff to dark grey siltstone and shale.

The regressive **Epsilon Formation** conformably overlays the Murteree Shale and consists mostly of siltstone with minor sandstone and coal deposited in a fluvio-lacustrine to fluvio-deltaic environment (Smith 1987). The Epsilon Formation sediments may have been sourced from an uplifted area south

of the basin (Battersby 1976) and/or represent a reduction in the rate of subsidence of the Murteree lake allowing it to infill (Stuart 1976).

The **Roseneath Shale** overlays the Epsilon Formation as a lacustrine sequence similar to the Murteree Shale. It is a thick sequence of dark grey carbonaceous siltstone with minor sandstone.

Conformably overlying the Roseneath Shale are the deltaic prograding **Daralingie Formation** siltstones and shales with minor backswamp coals and thin sands.

The **Toolachee Formation** consists of a thick, laterally extensive sequence of interbedded siltstones, sandstones and coals which unconformably overlie the older formations. The Toolachee Formation was deposited in an alluvial floodplain environment dominated by meandering fluvial processes producing laterally extensive point bar, overbank, and back swamp sequences (Battersby 1976, Stuart 1976, Thornton 1978). Differential compaction and growth faulting (Stuart 1976) has influenced overall thicknesses. The Toolachee Formation attains a maximum thickness in the study area of 110 metres in Kidman 3.

Erosion associated with the basal Toolachee Formation unconformity is variable and has cut down to the pre-Permian basement in Strzelecki 3 and Strzelecki 17. Only towards the east of the study area is the full Cooper Basin sequence present below the Toolachee unconformity (Figures 2, 3). The unconformity at the base of the Toolachee Formation represents a 10 million year break in deposition (Price et al 1985). The Toolachee Formation may be conformable with the Daralingie Formation in the deeper depositional troughs of the Cooper Basin, away from the study area.

The **Arrabury Formation** is part of the **Nappamerri Group** and consists of Late Permian to Early Triassic sandstone, siltstone, and shale deposited in fluvial lacustrine conditions (Powis 1989). It conformably overlies the Toolachee Formation.

4.4 Structural setting

The Cooper Basin is a northeast to southwest trending intracratonic basin beneath the Eromanga Basin. The origin of the Cooper/Eromanga Basins has been variously attributed to tectonic subsidence associated with compressional plate movement (Battersby 1976), wrench tectonics (Kuang 1985), complex compression (Petroleum Management Associates 1986), crustal metamorphism producing producing thermal compression or crustal extension and other associated mechanisms such as isostatic adjustment and phase transition at depth (Zhou 1989).

Following initial Cooper Basin sedimentation the earliest regional deformation of the Cooper Basin which caused structural closure to develop occurred in the Early Permian (Kapel 1966) and is

represented by the unconformity at the base of the Toolachee Formation. The unconformity surface extends into the underlying basement in the Strzelecki area. Permian structural traps were later enhanced by structural reactivation commencing in the Late Cretaceous and probably peaking in the Mid Tertiary (Mancktelow 1979).

The end of Cooper Basin sedimentation was caused by Upper Triassic to Jurassic uplift and erosion which resulted in a loss of section of up to 500 metres across most of the Cooper Basin, as indicated by vitrinite reflectance trends reported by Kanstler et al (1983). Fluid inclusion thermometry by Russell & Bone (1989) indicates a loss of section between one to two kilometers in various parts of the southern Cooper Basin away from the study area.

Post Cooper Basin sedimentation commenced with the unconformable Eromanga Basin sediments in the Early Jurassic.

A major increase in subsidence occurred at 100 Ma during Cretaceous Eromanga Basin sedimentation (Zhou 1989). This subsidence is variously attributed to crustal shortening that reactivated existing faults (Kuang 1985), extensional tectonics (Mancktelow 1979), isostatic compensation (Petroleum Management Associates 1986) or crustal sag following compression (Zhou 1989).

Most of the Eromanga Basin has been quiescent since the Late Cretaceous except in the remote basin edges of the Eromanga Basin that were uplifted and eroded, exposing the Mesozoic sequence to outcrop and groundwater flushing (Gausden 1979).

The main structural elements of the southern Cooper Basin are three slightly arcuate southwest to northeast trending troughs (Tennapera, Nappamerri and Patchawarra) separated by three similarly trending structural highs (Toolachee, Nappacoongee-Murteree and Gidgealpa-Merrimelia-Innamincka). Sedimentary thicknesses of all the Cooper Basin formations generally increase within the major troughs to a maximum of 1800 metres in the Nappamerri Trough. These troughs were major depo-centres during the deposition of the Cooper Basin sediments.

Most Cooper Basin hydrocarbon fields have been found in en-echelon, steep sided, often fault controlled anticlines formed along major trends attributed to previously existing Warburton Basin basement features (Kantsler et al 1983). These trends were often vertically reactivated during Permo-Triassic deposition and in the Tertiary (Windsor 1983). Kuang (1985) suggested these anticlinal features were caused by the accommodation of reactivated major southwest to northeast basement thrust faults.

Main structural features of the study area are shown in Figure 4. The study area is situated to the north of the Tennapera Trough, with the Murteree-Nappacoongee anticlinal trend occurring to the

west (Figure 5). Cooper Basin sediments generally thicken towards the southeast of the study area.

While faults and folds within the Cooper Basin generally display a northeast to southwest trend with cross cutting northwest to southeast and north to south structural trends (Mancktelow 1979), these trends are not generally apparent within the study area.

Within the Permian sequence of the study area, faults appear to have greater displacement at depth and fault surfaces are generally steep sided and normal. Mancktelow (1979) reports onlap thinning, drape and differential compaction of sediments associated with most fault related structural features.

4.5 Hydrocarbon setting

Tybor (1986) examined Permian organic matter from 15 core samples of Strzelecki 1, Strzelecki 5 and crude oil from Strzelecki 10. He identified three groupings of hydrocarbon types with similar origins, as shown in Table 3 below.

WELL	FORMATION	ENVIRONMENT OF FORMATION
1	Patchawarra	Microbial activity & organic matter deposited in mixed reducing-oxidising conditions of high acidity
10	Toolachee	Microbial activity & organic matter in reducing, low to moderate acidity conditions
1	Murteree	" " "
5	Toolachee	Microbial activity in low acidity, mixed reducing - oxidising environment

Table 3 Environments of hydrocarbon formation in Strzelecki wells reported by Tybor (1986).

Hydrocarbons in the Cooper Basin are principally sourced from the abundant organic matter (3% to 6% TOC) of the carbonaceous shales of the Toolachee and Patchawarra Formations. Most authors (for example Smyth 1983, Taylor et al 1988, Hunt et al 1989) generally accept the abundant coal measures in these formations as a major source rock type.

The Cooper Basin is mainly gas prone. Attempts to find and produce from economic oil

accumulations in the Cooper Basin sequence have been disappointing because of the overmature nature of the hydrocarbons, thin oil columns, common waxy nature of the oil and marginal reservoir qualities (Yew & Mills 1989). However, Permian oil has been found in commercial quantities within the Tirrawarra Sandstone and numerous subeconomic discoveries of Permian oil reservoirs have been made towards the edge of the Cooper Basin (Yew & Mills 1989) and in the Strzelecki area (Richards 1984).

Tybor (1986) attributed the bulk of the hydrocarbons present within the overlying Eromanga Basin rocks in the Strzelecki area to be sourced from Permian source rocks. Other workers (Jenkins 1989, Gilby & Mortimore 1989, Heath et al 1989) also believe that a considerable proportion of oil found in the Eromanga Basin at various stratigraphic levels was generated in and migrated from underlying Cooper Basin source beds. Numerous mechanisms invoked for upwards migration of oil include erosional truncation of regional seals (e.g. basal Nappamerri Group, Murteree Shale), fault zone paths and partially competent seals.

The abundance of local organic matter, existing structural traps formed before hydrocarbons were expelled, reduced charge of hydrocarbons to structural traps at the edge of the Cooper Basin and geochemical indicators (gas wetness, water washing and alkane fractionation reported by Heath et al 1989) do not indicate long hydrocarbon migration pathways into the Eromanga Basin.

Most Cooper and Eromanga Basin source rocks are thought to have generated oil during major basin subsidence in the late Early Cretaceous (Kantler et al 1983, Gilby & Mortimore 1989). Oil generation is indicated by vitrinite reflectances (V_r) of 0.7 to 1.0 percent R_o max. Most authors (e.g. Kantler et al 1983, Hunt et al 1989) accept that only one hydrocarbon generation event occurred within the Permian sequence of the southern Cooper Basin, following rapid Cretaceous subsidence. Hunt et al (1989) report a sharp onset of significant hydrocarbon accumulation at V_r of 0.95%.

Padmasiri & Cook (1983) interpret Cooper Basin vitrinite reflectance - depth relationships as indicating an early pre-Permian and later post Mesozoic heating events which may have influenced hydrocarbon generation. Staughton (1985) calculated a mean geothermal gradient of 45°C/km for the Strzelecki area based on bottom hole temperatures of wells, making reservoir temperatures in the shallow Strzelecki region comparable to those encountered in generally deeper Cooper Basin fields which have lower geothermal gradients.

Russell & Bone (1989) report appreciable cooling of the deeper Cooper-Eromanga Basin sediments based on fluid inclusion thermometry.

5 Field descriptions

The study area is broadly and informally divided into a western Strzelecki area, a central Kidman Complex and an eastern Kerna area. Well locations in the study area are shown in Figure 6. The producing intervals of wells within the individual fields of the study area are described in Table 4.

FIELD	WELLS	STATUS: (T=Toolachee,E=Epsilon,P=Patchawarra)
Aroona	1	T,E,P gas
Bagundi	2	T E gas
Dilchee	1	P gas suspended
Kerna	4	P,T,E gas suspended (3 wells)
Kidman	5	P,T producer, some E gas
Kidman Nth	2	P,T gas suspended (1 well)
Lepena	1	P,T gas suspended
Marabooka	4	T gas producer
Marana	1	T gas suspended
Pira	2	T gas suspended (1 well)
Strzelecki	25	T gas producer, some T oil

Table 4 Details of Permian hydrocarbon fields in the study area. Information is derived from DeGolyer & McNaughton (1986) and from well completion reports.

5.1 Strzelecki area

The Strzelecki area contains the Strzelecki and Marabooka oil and gas producing fields, suspended gas wells Marana 1 and Wanara 1 and the dry Strzelecki 2 well to the southwest.

The Strzelecki area is situated on a pre-Permian high that trends northeast from the Murteree high into Strzelecki then north through Marabooka and into the Della gas Field (Palanyk 1987). The structural high results in the absence of the Tirrawarra Formation and thinning of the Patchawarra Formation in the Strzelecki area. The Toolachee Formation similarly thins at Strzelecki Field whereas the Triassic sediments generally thicken towards the north, indicating complex structural reactivation events.

The Strzelecki and Marabooka structures are both broad, simple domes with thickening of the Permian sedimentary pile away from the crest. Major faults occasionally truncate both structures.

The Strzelecki Field produces gas from the Toolachee Formation and oil from the Eromanga Basin sequence (Hutton and Murta Formations). A small amount of Permian oil has been intersected in the Toolachee Formation interval in Strzelecki 10.

5.2 Kidman Complex

The Kidman complex contains the Permian gas producing fields of Aroona, Bagundi, Kidman and Kidman North and the suspended gas fields of Dieri, Coochilara, Pira and Dilchee.

Within the complex, gas and condensate occurs in potentially commercial quantities mostly in the Toolachee Formation "Unit C". The higher Toolachee Formation "Unit B", Epsilon Formation and Patchawarra Formation are often water wet or tight (Gordon 1978). The Epsilon Formation is productive in Kidman 1 and Bagundi 1 and the Patchawarra Formation is gas and minor condensate productive or prospective in Aroona, Bagundi, Dilchee and Lepena Fields and Kidman 3 and Kidman North 1 wells.

The Kidman complex consists of several structures. The Kidman 1 structure is a discrete culmination with an elongate nose dipping northwest while the elongate Kidman 2 structure consists of three culminations, separated by saddles and trending northwest (Arndt 1986). Lepena 1, Aroona 1, Bagundi 1 and 2 and Kidman 5 and 2 were drilled into structural highs along this feature and have yielded Toolachee and Patchawarra Formation gas.

Arndt (1986) considers the en echelon culminations of the Kidman 2 structure consistent with regional thrusting and wrenching from the southeast, as postulated by Kuang (1985). Arndt considers the steep gradient over the eastern edge of the Kidman Complex to be a drape fold over faulting below the Toolachee Formation.

5.3 Kerna area

The Kerna Field is a simple north to south anticline to the far east of the study area. The Patchawarra Formation has been the only stratigraphic level intersected with good gas flows. The Toolachee and Epsilon Formations have only marginal pay sands (Richards 1982). The field is suspended pending future production (DeGolyer & McNaughton 1986).

6 Sedimentology

6.1 Nomenclature

The subdivision of the Permian sequence of the Cooper Basin sediments was initially outlined by Kapel (1966) who named it the Gidgealpa Formation and later the Gidgealpa Group (Kapel 1972). The subdivision of the Permian sequence was revised by Gatehouse (1972). Thornton (1979) studied and described the Gidgealpa Group in detail. Williams and Wild (1984) recommended inclusion of the Merrimelia Formation into the basal Gidgealpa Group. Powis (1989) redefined the Triassic interval as the Nappamerri Group consisting of the Arrabury, Tinchoo and Cuddapan Formations.

Subdivision of the Gidgealpa Group into formations by most authors is based on lithological and palynological criteria. There is no outcrop of the Cooper Basin sediments.

6.1.1 Patchawarra Formation subdivision

The Patchawarra Formation was divided into three general units by Kapel (1972). The basal unit comprises lower deltaic carbonaceous shale, siltstone and minor sandstone and coal. The middle unit is sandstone dominated with thick coal intervals of meandering fluvial to upper delta plain origin. The upper unit consists of deltaic to lacustrine shales and siltstone.

Other workers (Battersby 1976, Thornton 1979, Williams 1982, Faridi & Hunt 1987) have divided the Patchawarra Formation into facies based associations, some or all of which may be absent within a well depending on non-deposition or erosion. For example, Faridi & Hunt (1987) divided the Patchawarra Formation into ten genetic and lithologic associations in the southern Cooper Basin based on palaeogeographic reconstructions using well correlations by depositional facies associations. They also identified six syn-depositional tectonic episodes involving subsidence, tilting and fault controlled uplift that influenced these associations.

Problems often encountered when determining depositional settings of the Patchawarra Formation have been outlined by Williams (1982). They include:

- (1) the multiple depositional facies and transitions related to the diachronous nature of the basal sediments.
- (2) the long period of Patchawarra Formation deposition.
- (3) a great variability of formation thickness (to (?)590 metres in parts of the Cooper Basin) due to non - deposition, uplift, onlap and penecontemporaneous faulting.

6.1.2 Toolachee Formation subdivision

The Toolachee Formation in the Moomba Field was divided into two main units by Thornton (1973) and by Stuart (1976). The lower unit, Unit C of Stuart (1976), consists of fluvial sands, silts and coals and the higher unit, Unit B, consists of siltstone and shale and minor coal and sandstone of lower delta / lacustrine origin. Williams (1982) divided the Toolachee Formation into facies associations which are generally equivalent to Units B and C within individual study area fields.

The main problem associated with dividing the Toolachee Formation is the poor log response that precludes reliable correlations between fields.

6.2 Geological history

Deposition in the Cooper Basin began with glacial and paraglacial sequences of tillites, fluvio-glacial, glaciolacustrine and glacial-aeolian sediments of the **Merrimelia Formation** (Williams 1982) deposited over an irregular surface.

The **Tirrawarra Sandstone** occurs as moderately sorted arenites with very minor shales representative of anastomosing braided stream channel deposits (Coles, Nikiforuk, Pennell 1987). It marks a progression from the fluvio-glacial deposition of the Merrimelia Formation through to the lower energy meandering stream deposition represented by the Patchawarra Formation (Thornton 1979). Both upper and lower Tirrawarra Sandstone rock boundaries are considered diachronous by Thornton (1979).

The **Patchawarra Formation** is a result of high sediment input associated with a period of regional peneplanation (Gravestock & Morton 1984). It consists of sands, shales and abundant coals mostly deposited in a floodplain environment.

Early deposition of the Patchawarra Formation sediments occurred towards the centre of the major depositional troughs and consisted of abundant carbonaceous shales with thin interbeds of coal and sandstone (Petroleum Management Associates 1986). Later deposition within the middle part of the formation consisted of interbedded thick sandstones, coals and shales marking fairly rapid sedimentation. The upper part of the formation is predominantly shaley.

Faridi & Hunt (1987) identified six syn-depositional tectonic episodes within the southern Cooper Basin including the study area, involving subsidence, tilting and fault controlled uplift. These structures had local effects on depositional patterns.

Towards the end of Patchawarra Formation deposition, the regional slope gradually diminished through erosion and a large inland lake advanced from the central basinal region onto marginal areas, depositing the **Murteree Shale** (Thornton 1979). The Murteree Shale conformably overlies the Patchawarra Formation and exhibits only a small amount of thinning onto structural highs compared with the Patchawarra Formation, indicating a relatively smooth depositional surface and low relief.

It is possible that the Murteree Shale may have been a restricted sea with access to the open sea off the eastern coast of Australia (Stuart 1976).

With the slow retreat of the lake the regressive **Epsilon Formation** shales, siltstones and thinly interbedded fine sands were deposited in deltaic and shoreline environments, similar in distribution to the Murteree Shale sediments (Petroleum Management Associates 1986).

A second lacustrine or marine encroachment onto marginal areas deposited the **Roseneath Shale** sequence of fine silts and shales. The Roseneath Shale marks the end of the second gross cycle of fluvial sedimentation, similar to but not as extensive as that of the Murteree Shale.

A regressive series of sands, shales and coals of the **Daralingie Formation** were then conformably deposited in a floodplain and deltaic environment.

Palynological data indicate a substantial 10 million year time break between the top of the Early Permian Daralingie Formation and the base of the overlying Late Permian Toolachee Formation (Price et al 1985). Structural movements and erosion during this period removed substantial thicknesses of the underlying Cooper Basin sequence from the major northeast trending anticlines, leaving only low relief topography (Coles, Nikiforuk, Pennell 1987).

Following these episodes of uplift and erosion a substantial thickness of **Toolachee Formation** sediments were regionally deposited. They consist of stacked fining upwards sequences of sands, shales and coals deposited by large meandering rivers in extensive floodplains covered by coal forming forests and lakes (Fairburn 1989). The lower Toolachee Formation sands are generally thick and exhibit good lateral continuity while the upper Toolachee Formation sands are generally thin and poorly developed.

The transition of the Toolachee Formation to the overlying **Arrabury Formation** of the Triassic **Nappamerri Group** is marked by an abrupt lithological change from coal measures to relative uniform, organically lean Triassic arenites (Powis 1989). Thornton (1979) notes the transition is diachronous. Palynological evidence indicates an hiatus between the Toolachee and Arrabury Formations with the latter being accorded a Late Permian to Middle Triassic age (Powis 1989).

The Arrabury Formation consists of fine grained lacustrine to fluvial shales and minor sands. Minor red beds and lack of carbonaceous material suggest hot, humid and oxidising climatic conditions.

Younger mid to late Triassic Nappamerri Group sediments overlying the Arrabury Formation are not found in the study area but occur in the northern Cooper Basin (Barr & Youngs 1981). Powis (1989) groups these sediments into the Tinchoo and Cuddapan Formations and reports basal unconformities in each.

Major widespread tectonism, possibly in the Late Triassic (Padmasiri & Cook 1983) eroded some of the Cooper Basin sequence. Continental downwarping in Early Jurassic initiated Eromanga Basin deposition over the Cooper Basin.

6.3 Facies mapping

As a guide to understanding the origin of the main reservoir units in the study area and to quantify the depositional nature of samples, the Toolachee and Patchawarra Formations are subdivided into facies associations (Appendix 5).

A facies (or more precisely, lithofacies) is described by Reading (1978) as "a body of rock with specified characteristics defined on the basis of colour, bedding, composition, texture, fossils and sedimentary structures". It is generally inferred that the term facies also applies to a distinctive body of rock formed under certain conditions of sedimentation, reflecting a particular process or environment.

A problem particularly pronounced with fluvial environments is that several sedimentary environments and processes operate when sediment is being deposited. This can produce laterally and vertically discontinuous lithologies or lithofacies that are not unique, both of which have and will result in ambiguous correlations.

A useful method for correlating such lithologically discontinuous strata are depositional facies or "Genetic Increment of Strata". Busch (1974) defined a Genetic Increment of Strata (G.I.S.) as:

"an interval of strata representing one cycle of sedimentation in which each lithological component is genetically related to all others. The upper boundary must be a lithologic time marker and the lower boundary may be either a lithologic time marker or an unconformity."

Busch also defined a Genetic Sequence of Strata (G.S.S.) as:

"two or more contiguous genetic increments of strata that represent more or less continuous sedimentation."

The intervals of strata chosen for correlation are genetic sequences of strata or facies associations. One facies association may contain one or several GIS bounded by lithologic time markers. The use of facies associations, with direct analogy to depositional environment allows a facies model of the study area to be made.

As with other studies of this nature, coal seams were chosen as good lithologic time markers to delineate GIS, as coal seams can be correlated with a fair degree of certainty by wireline log signatures. These coals represent slow overbank and flood basin sedimentation that were relatively widespread across the Cooper Basin. Taylor & Thomas (1989) point out that the lack of coal seam splitting in the basin indicates slow subsidence.

The logging of core as presented in Appendix 1 forms the basis of facies and GIS recognition and is matched with wireline log signatures in Appendix 6. The recognition of wireline log traces representative of identified facies and GIS units forms the basis for subdivision of the Toolachee and Patchawarra Formations into facies associations. Facies descriptions are summarised in Table 7.

A series of cross sections were constructed using subdivided Toolachee and Patchawarra intervals of selected wells. Correlation between wells was achieved using electrical log traces of associations of depositional facies showing evidence of time stratigraphic equivalence. Isopach maps of associations and seismic information were also used to supplement correlations between wells. Because of common interfingering of sands and shales and the generally transitional nature of formation boundaries, correlations are only approximate in some areas.

Geological variables derived from facies mapping are lithofacies types, depositional facies (G.I.S.) and facies associations (G.S.S.). Together with lithologies, these parameters form a framework from which the geology of the study area can be quantified. It must be remembered that facies mapping is based on poor well control, particularly in the central part of the study area.

6.3.1 Previous work

Devine & Gatehouse (1977) used Busch's Genetic Increment of Strata (G.I.S.) to predict the continuity of six Patchawarra sand bodies in the Toolachee Field.

Gravestock & Morton (1984) mapped major Toolachee and Patchawarra Formation lithofacies associations across the Della Field. Incomplete preservation of the Patchawarra Formation sequence was attributed to erosion during active channel migration whereas the Toolachee Formation is mostly preserved. They divided the Toolachee Formation into a "lateral accretion association" and a "vertical accretion association" corresponding to Units B and C of Stuart (1976) respectively; both units seem to apply to the Toolachee Formation of the Marabooka and Strzelecki Fields. The choice of subunits for the Patchawarra Formation was more difficult because of the poor correlation of coals caused by seam splitting and the absence of coals by either non deposition or erosion.

Faridi and Hunt (1987) divided the Patchawarra Formation of the southeast Cooper Basin, including the study area, into ten facies associations of which the lower, predominantly swampy coal measures are only completely developed in the deeper pre-Permian troughs. They outlined three main depositional environments:

- (1) fluvial channel sandstones, overlain by overbank or swamp deposits (fining upward sequences).
- (2) prograding crevasse splay sandstones adjacent to channel systems (coarsening upwards sequences).
- (3) flood basin/lacustrine sediments (combined coarsening-upward and minor fining upward units).

Facies associations limits determined for the Patchawarra Formation in the study area wells (Appendix 5) are similar to Faridi & Hunt's limits except for correlations across some structural highs (e.g. Marana 1, Bagundi 1) where reduced facies association thicknesses are interpreted as condensed sequences or the result of erosion and deposition associated with local tectonic movements. Faridi and Hunt delineate locally thin or absent facies associations for these structural highs that indicate non continuous deposition instead.

6.3.2 Correlations

Facies associations limits for the Toolachee and Patchawarra Formation in the study area wells are listed in Appendix 5. Figures 7 and 8 are two cross sections that illustrate typical facies association correlations for the Toolachee and Patchawarra Formations

Three facies associations of the uppermost Patchawarra Formation in the study area wells are identified and represent a variable depositional setting ranging from the fluvial and upper deltaic plain to the lower deltaic plain and associated back swamps. Patchawarra Formation facies associations vary substantially in thickness across the study area and reflect the variable topography

of the original depositional surface.

Four facies associations are delineated for the whole of the Toolachee Formation in study area wells and are numbered from 1 (youngest) to 4 (oldest). Two major divisions of the Toolachee Formation corresponding to Unit B and Unit C of Stuart (1976) are recognised. Unit C is a high energy, vertically accreting type sand and is overlain by the lower energy, laterally accreting Unit B.

The uppermost two facies associations correspond to Unit B and the lower two facies associations correspond to Unit C.

The stratigraphically lower facies associations 3 & 4 (Unit C) have a blocky, multi-storey nature in vertical profile. They consist of coarse to medium grained sands with common channel lag conglomeratic gravels and sharp conglomeratic sand bases associated with scour structures. This indicates pulsed channel formation and deposition. Common sharp tops to the fluvial channel packets of sediment indicate channel abandonment. The thick, stacked nature of this unit indicates dominant vertical accretion.

The higher facies associations 1 and 2 (Unit B) of the Toolachee Formation represent a low energy laterally accreting depositional environment. They generally consist of medium to fine grained arenites fining to siltstone and sometimes coals, typical of a meandering suspended load river in an alluvial floodbasin setting. Fine overbank deposits are dominant. Sandstone deposition occurs as sinuous thin channels, levees and crevasse splays. Occasional coarse intraclasts of clay within matrix supported gravel deposits indicate reworking and deposition of channel banks.

The vertical lithological characters of facies associations 1 & 2 are highly variable.

Block diagrams showing palaeogeographic reconstructions of sedimentary environments during deposition of the various facies associations are presented in Figures 9 and 10 and are based on isopach maps and sandstone % maps of facies associations in Appendix 5. Features to notice from these reconstructions are the prominence of Strzelecki and Kidman 5 structural highs during deposition of the Patchawarra Formation and some of the Toolachee Formation sediments, and the localised nature of fault controlled block emergence and subsidence that result in localised erosion and sediment deposition.

Deposit Types	Grain size			Gamma ray				Facies Associations	Lithofacies	Samples	Examples
	mud	sand	gravel	40	80	120	160				
stacked channel								(T1),T3,T4 (P1),P2,(P3)	Ge Gms Sm Sh Sr Sp St	310 339 340 462 475	Toolachee Fm in Kidman 1 6610-6640'; Fig 4, App 6
								T2,T3,T4 (P1),P2,P3	Sm Sh Sr Sp St Sg Fl	296 298	Toolachee Fm in Strzelecki 1 6350-6390'; Fig 11 App 6
								P3	Sm Sr Sp St Sb Sd Sg Sw/Fw Fl Fm Fb	498-505 274	Patchawarra Fm in Dilchee 1 8260-8290'; Fig 2 App 6
overbank + floodplain								T1,T2,T4 P1,P3	Sm Sr Sp St Sb Sd Sg Sw/Fw Fl Fm Fb	489 490 476 477 478 288	Patchawarra Fm in Kerna 1 8110-8155'; Fig 3 App 6
								T1,T2 P1,(P3)	Sm Sr Sp St Sb Sd Sw/Fw Fl Fm Fb	311 294 293	Toolachee Fm in Pira 2 7140-7195'; Fig 9 App 6

see Appendix 6

see Appendix 6

see Appendix 5
page 19

see Appendix 1 page 18

see Appendix 6

Table 7: Facies reference data.

SEM MICROGRAPHS, PLATE 1 (facing page)
QUARTZ

- 1(a) General view of fine grained arenite with coarse quartz and fine kaolin. Minor (?)primary porosity.
Field of view 0.62 x 0.46mm, scale bar = 0.1mm; 194x. Sample 310 from the gas bearing Toolachee Formation of Kidman 2, 2036.6 metres (6677.5 ft) deep.
- 1(b) Close-up of the central left area of 1(a) shows irregular and oriented V shaped depressions and pitting caused by chemical etching of quartz, possibly due to localised pore water reactions between the quartz and (?)previously adjacent siderite, organic matter or feldspar grain.
Field of view 0.16 x 0.12mm, scale bar = 0.1mm, 745x. Sample 310 as above.
- 1(c) Detail of 1(b) showing intergrown subhedral plates of kaolin (K) and authigenic quartz cement (Q). Corrosion of kaolin has not occurred.
Field of view = 0.037 x 0.027mm, scale bar = 10 microns, 2980x. Sample 310 as above.
- 1(d) General view to the right of 1(b) showing intergrown quartz and well formed pseudo-hexagonal plates of kaolin.
Field of view = 0.16 x 0.12mm, scale bar = 0.1mm, 745x. Sample 310 as above.
- 1(e) Detail of 1(d) showing intergrown quartz and plates of kaolin.
Field of view = 0.037 x 0.027mm, scale bar = 10 microns, 2980x. Sample 310 as above.
- 1(f) Clay rich fine grained arenite fragment, in a medium grained arenite. Clays tend to inhibit quartz overgrowths.
Field of view = 0.09 x 0.05mm, scale bar = 10 microns, 1550x. Sample 482 from a gas bearing interval of the upper Patchawarra Formation of Kerna 1, 2480.3 metres (8132.1 ft) deep.
- 1(g) Well formed prismatic quartz druse on a substrate of quartz (Q) in a medium grained sandstone. Clays partly cover the quartz substrate.
Field of view = 0.28 x 0.21mm, scale bar = 0.1mm, 442x. Sample 302 from a tight interval of the lower Toolachee Formation of Marana 1, 1928.8 metres (6324 ft) deep.
- 1(h) Detail of () showing mostly irregularly shaped kaolinite and illite at the base of the druse quartz prisms.
Field of view = 0.064 x 0.045mm, scale bar = 10 micron, 177x. Sample 302 as above.

1(a)



1(b)



1(c)



1(d)



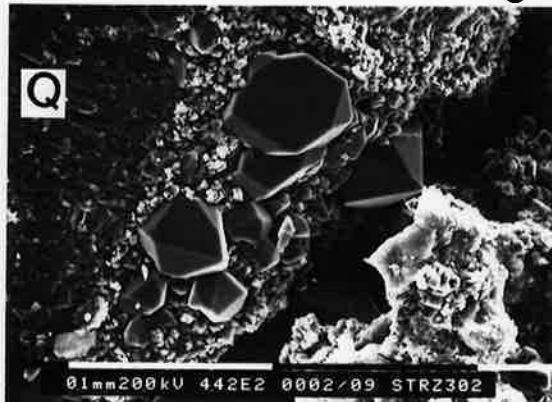
1(e)



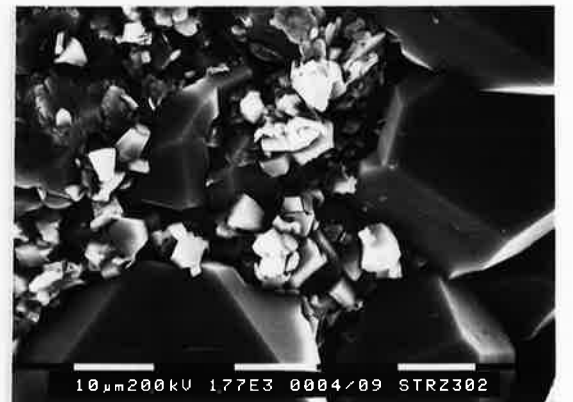
1(f)



1(g)



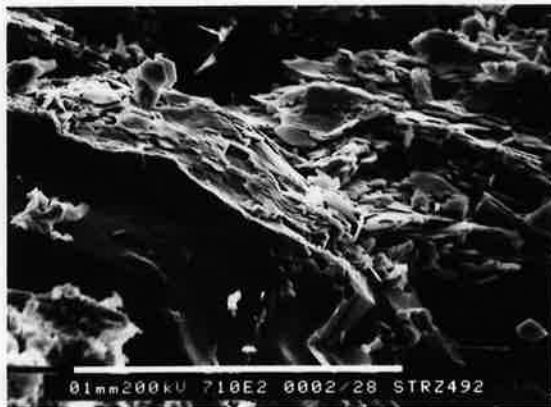
1(h)



SEM MICROGRAPHS, PLATE 2 (facing page)
ILLITE, KAOLIN, FELDSPAR, SIDERITE

- 2(a) Small, closely packed plates of detrital illite. Similar forms of illite are common in fine grained and silty sediments.
Field of view = 0.16 x 0.12mm, scale bar = 0.1mm, 710x. Sample 492 from the water bearing upper Patchawarra Formation of Strzelecki 1, 1993 metres (6535 ft) deep.
- 2(b) Bent biotite with blocky kaolin (arrowed) growing between flakes.
Field of view = 0.13 x 0.1mm, scale bar = 0.1mm, 885x. Sample 302 from the tight lower Toolachee Formation of Marana 1, 1928.8 metres (6324 ft) deep.
- 2(c) Mica flakes mostly converted to blocky kaolin.
Field of view = 0.047 x 0.033mm, scale bar = 10 microns, 2500x. Sample 468 from the gas bearing lower Toolachee Formation of Strzelecki 1, 1940.6 metres (6362.5 ft) deep.
- 2(d) Corroded detrital K feldspar, in centre of field of view.
Field of view = 0.14 x 0.11mm, scale bar = 0.1mm, 775x. Sample 308 from the gas bearing lower Toolachee Formation of Kidman 1, 2014 metres (6603 ft) deep.
- 2(e) Pore filling vermiform books of dickite with ragged edges and minor pore lining fibrous wisps of authigenic illite, from a poorly sorted medium grained arenite. Compare this form of illite with detrital illite in Plate 2(a).
Field of view = 0.13 x 0.11mm, scale bar = 0.1mm, 845x. Sample 340 from a tight, (?) water bearing lower Toolachee Formation of Pira 2, 2526.6 metres (8283.9 ft) deep.
- 2(f) Vermiform, euhedral dickite on euhedral quartz.
Field of view = 0.44 x 0.38mm, scale bar = 0.1mm, 274x. Sample 329 from the tight gas bearing upper Patchawarra Formation of Kidman 1, 2236.2 metres (7331.8 ft) deep.
- 2(g) Partly dissolved micritic siderite.
Field of view = 0.17 x 0.13mm, scale bar = 1mm, 680x. Sample 460 from the water bearing lower Toolachee Formation of Strzelecki 1, 2022 metres (6630 ft) deep.
- 2(h) Occasional but typical porous and permeable medium grained arenite. Most porosity is attributed to remnant primary porosity and is mostly occluded by either pore filling clays or quartz cement. Most other arenite samples have less visual porosity. Core plug testing of core immediately adjacent to the sample gave a porosity value of 12.8% and permeability value of 80md.
Field of view = 3.8 x 2.9mm, scale bar = 1mm, 30x. Sample 309 from the gas bearing lower Toolachee Formation of Kidman 1, 2015.6 metres (6608.5 ft) deep.

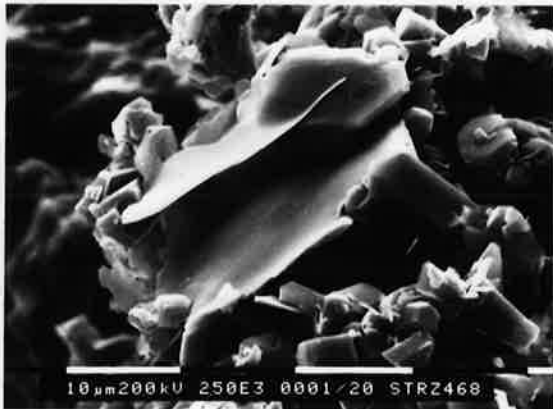
2(a)



2(b)



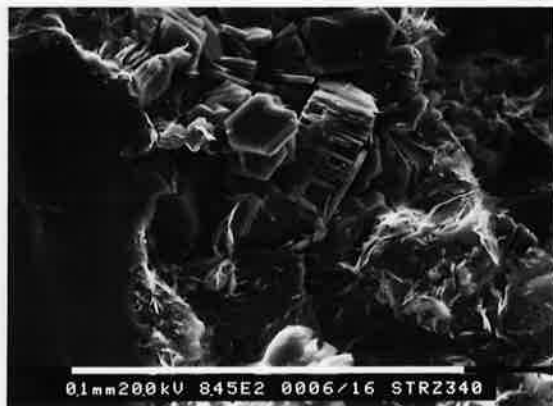
2(c)



2(d)



2(e)



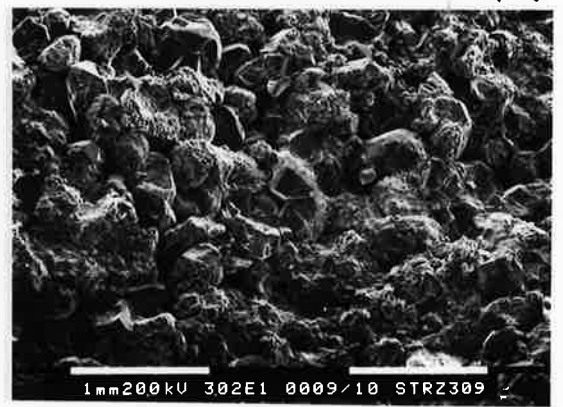
2(f)



2(g)



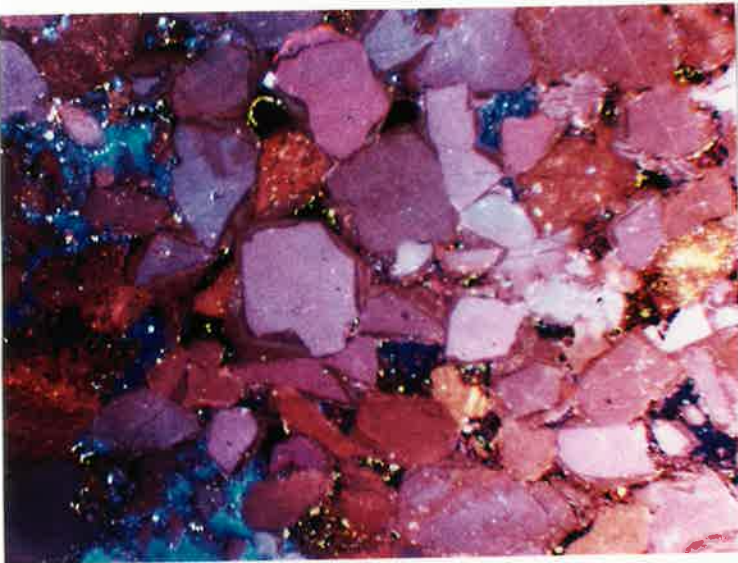
2(h)



THIN SECTION and CL MICROGRAPHS, PLATE 3 (facing page)

- 3(a) CL of a medium grained sandstone showing zoned overgrowths around detrital quartz grains and blue luminescing pore filling kaolin. Remnant primary porosity appears black. The large central grain shows 5 overgrowth zones. Such multiple zoning of quartz overgrowths are patchy and occasional.
Field of view = 1.5 x 1.0mm, 10.2x. Sample 505 from the water bearing upper Patchawarra Formation of Strzelecki 1, 2009.3 metres (6588 ft) deep.
- 3(b) Same field of view as 3(a) in plane polarised light. There is an appreciable fracturing of grains.
- 3(c) CL of a siltstone with brown detrital quartz grains and blue illite/kaolin. White to yellow patches are diamond dust from sample preparation. There are few quartz overgrowths evident in fine grained samples where clays are common.
Field of view = 30 x 20mm, 20.2x. Sample 295 from the tight upper Toolachee Formation of Strzelecki 2, 1873.2 metres (6141.8 ft) deep.
- 3(d) Thin section micrograph of a rare dust lining separating a detrital quartz grain from its quartz overgrowth.
Field of view = 3.1 x 2.1mm, scale bar = 1mm. 50x. Sample 465 from the gas bearing lower Toolachee Formation of Strzelecki 1, 1940 metres (6360.9 ft) deep. Crossed nicols.
- 3(e) Detail of 3(d) showing clays along dust rim and minor pore lining siderite (S). Crossed nicols. Scale bar is 0.25 mm.
- 3(f) Detail of 3(d) in plane polarised light showing (?)bitumen staining of the dust lining and pore. The central pore is stained light blue during sample preparation. Scale bar is 0.25mm.

3(a)



3(b)



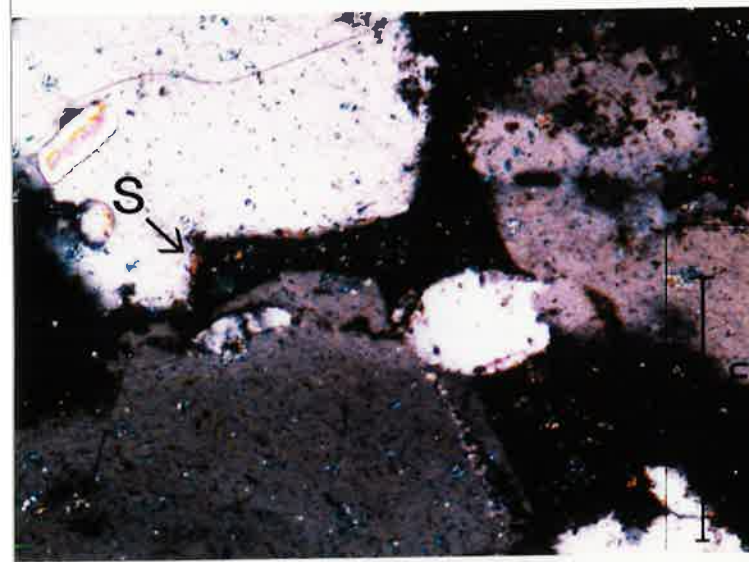
3(c)



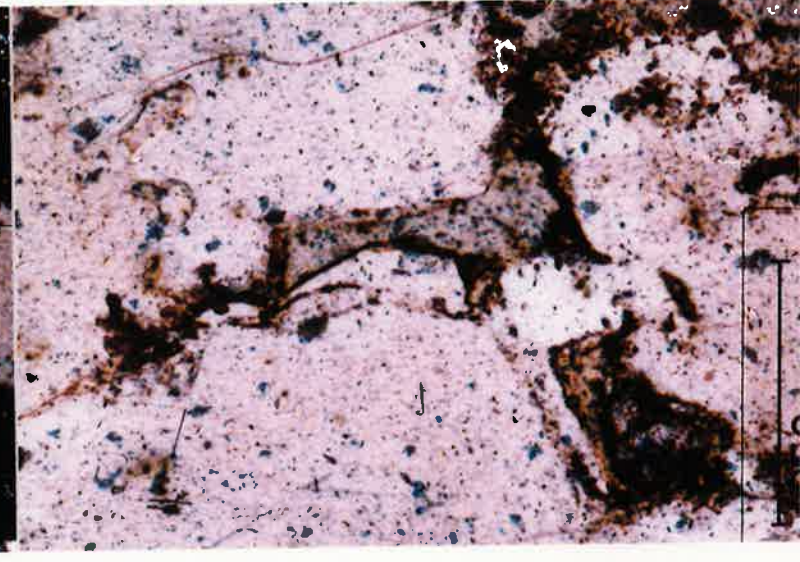
3(d)



3(e)



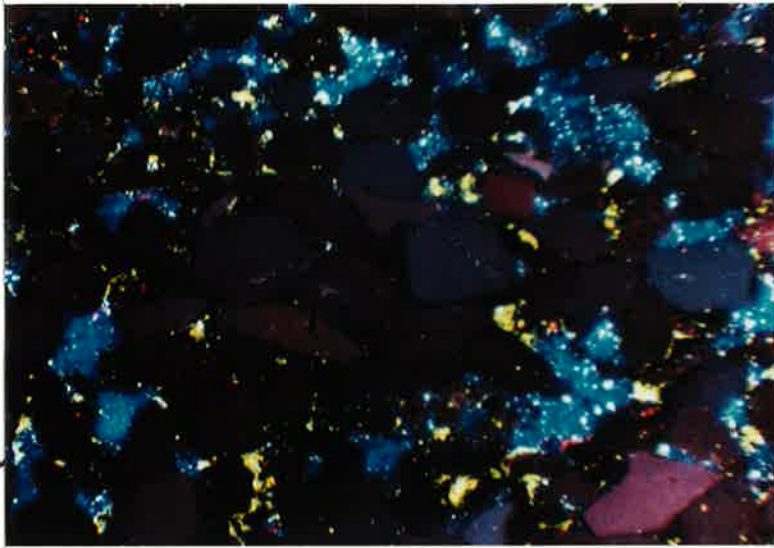
3(f)



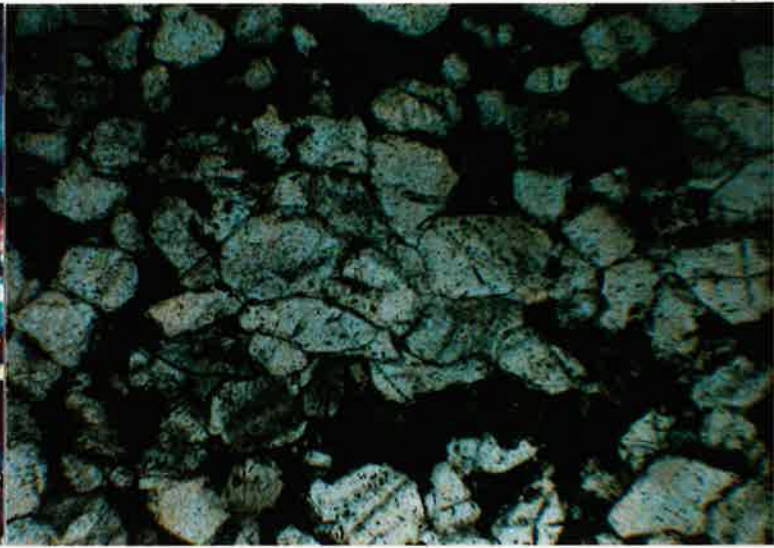
THIN SECTION and CL MICROGRAPHS, PLATE 4 (facing page)

- 4(a) CL of a medium grained sandstone showing the variable distribution of quartz overgrowths and pore filling kaolin. The central area shows predominant multi-zoned quartz cement while surrounding areas of blue, kaolin filled pore spaces are bordered by quartz grains with a single dark quartz overgrowth. This overgrowth appears as a first formed, meniscus type cement to all the quartz grains. Note also the loose packing of the original detrital grains.
Field of view = 20 x 13mm, 12.8x. Sample 501 from the water bearing upper Patchawarra Formation of Strzelecki 1, 2004.9 metres (6573.3 ft) deep.
- 4(b) Same field of view as 4(a) in plane polarised light.
- 4(c) CL micrograph of a medium grained arenite showing fair porosity (seen as light brown areas in Plate 4(d)). Primary porosity was initially quite large and has been reduced by multiple phases of silica cement or by pore filling kaolin, which luminesces blue. A rock fragment (R) does not show silica overgrowths.
Field of view = 6 x 4mm, 25x. Sample 308 from the gas bearing lower Toolachee Formation of Kidman 1, 2014 metres (6603 ft) deep.
- 4(d) Same field of view as 4(a) in plane polarised light. Note that the central large grain is shown as three separate silica cemented quartz grains by CL in Plate 4(c).
- 4(e) CL micrograph of the same sample in Plate 4(c) showing an unusual light blue quartz grain. A single, dark brown luminescing quartz overgrowth forms a (?)meniscus cement that is sometimes intergrown with the blue luminescing pore filling kaolin.
Field of view = 15 x 10mm, 10.2x. Sample 308 as above.
- 4(f) Same field of view as 4(e) in plane polarised light. There is some bitumen staining at (B) that has outlined embayed kaolin to quartz contacts.

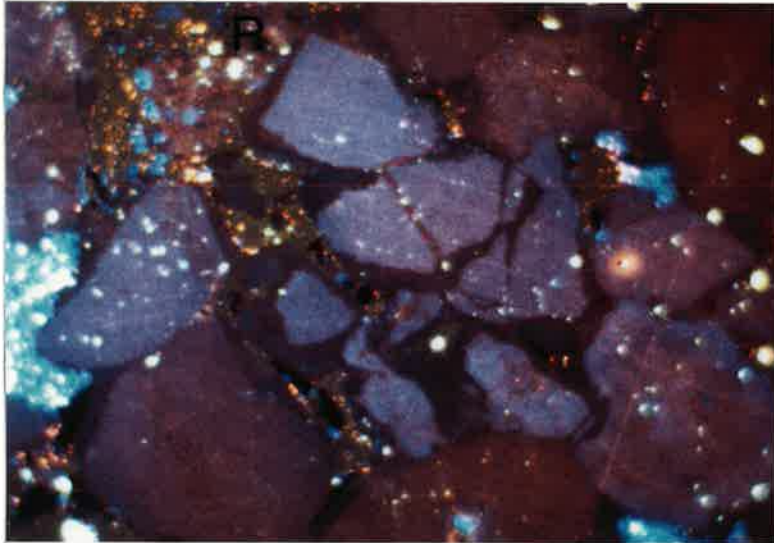
4(a)



4(b)



4(c)



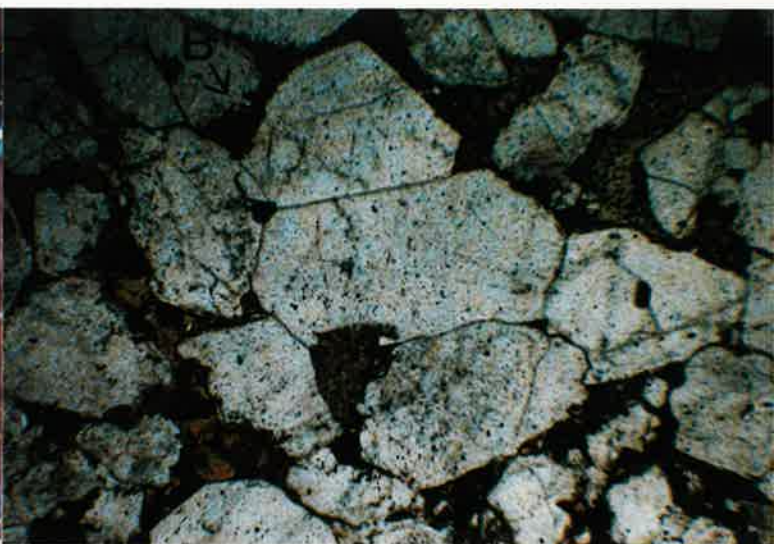
4(d)



4(e)



4(f)



THIN SECTION and CL MICROGRAPHS, PLATE 5 (facing page)

- 5(a) Rhombic spar siderite engulfing quartz grains and rock fragments. Most of the quartz grains and rock fragments are smaller than surrounding framework grains, indicating dissolution by siderite has occurred.
Field of view = 3 x 2mm, scale bar = 1mm, 50x. Sample 463 from the gas bearing lower Toolachee Formation of Strzelecki 1, 1940 metres (6360.4 ft) deep.
- 5(b) Same field of view as 5(a) with crossed polars.
- 5(c) CL micrograph of dissolution seam (D) and microstylolite (M) between adjacent quartz grains.
Field of view = 15 x 10mm, 10.2x. Sample 287 from the gas bearing lower Toolachee Formation of Strzelecki 16, 1901.7 metres (6235.2 ft) deep.
- 5(d) Same field of view as 5(c) in plane polarised light.
- 5(e) CL of the same sample in 5(c) showing partial dissolution of a light blue quartz grain along a stringer of poorly luminescing organic matter.
Field of view = 15 x 10mm, 10.2x. Sample 287 as above.
- 5(f) CL of a medium grained arenite showing a red framework grain of feldspar and other feldspar remnants. Generally, corrosion of feldspar appears to be the major cause of secondary porosity within the study area. White to yellow patches are diamond dust from slide preparation and pore filling kaolin is dark blue. The variation in colour of the framework quartz grains indicate variable provenance.
Field of view = 15 x 10mm, 10.2x. Sample 287 as above.

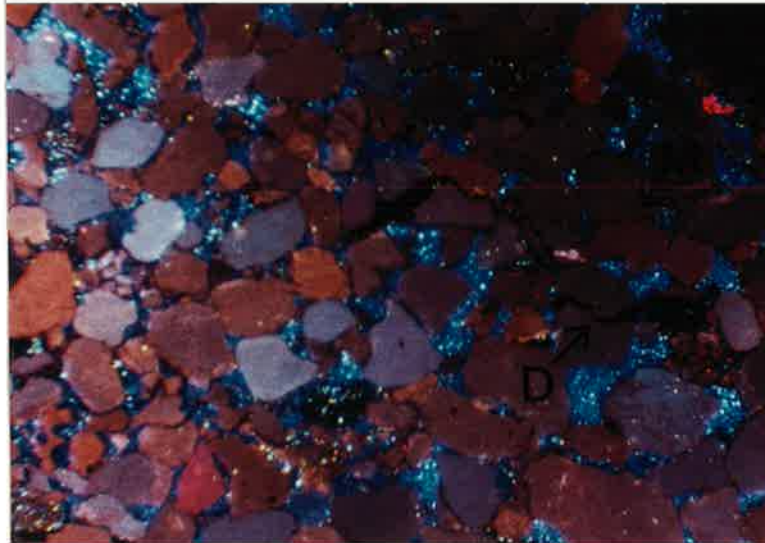
5(a)



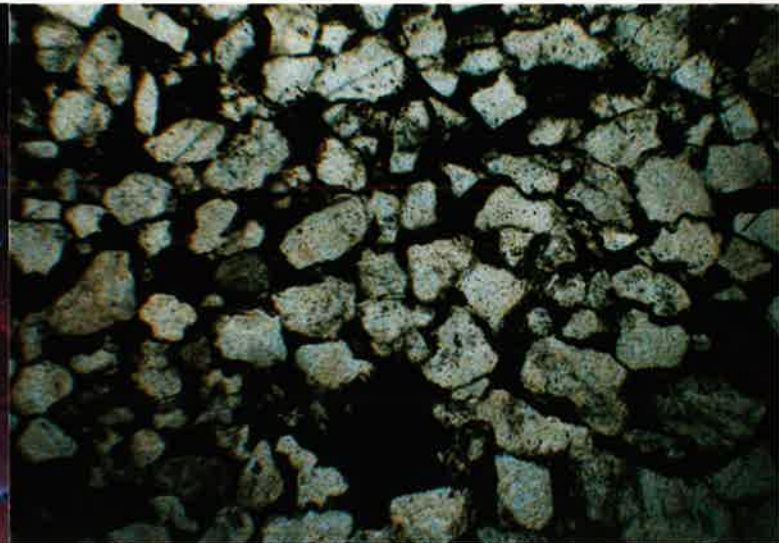
5(b)



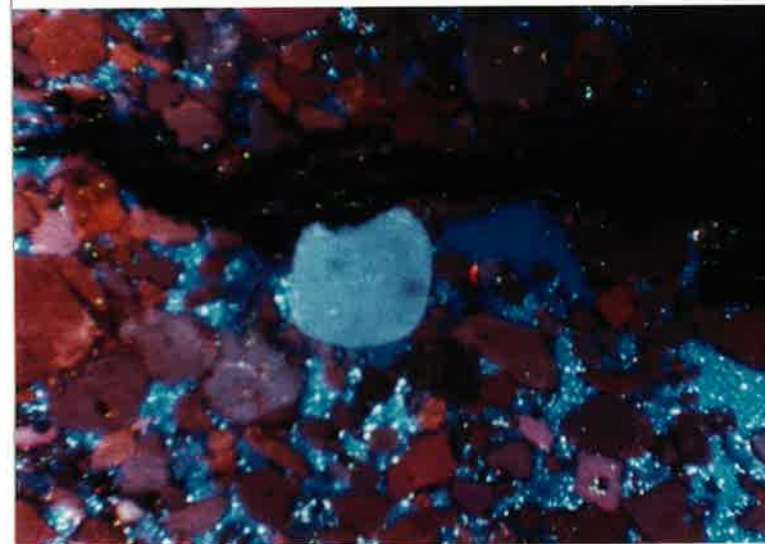
5(c)



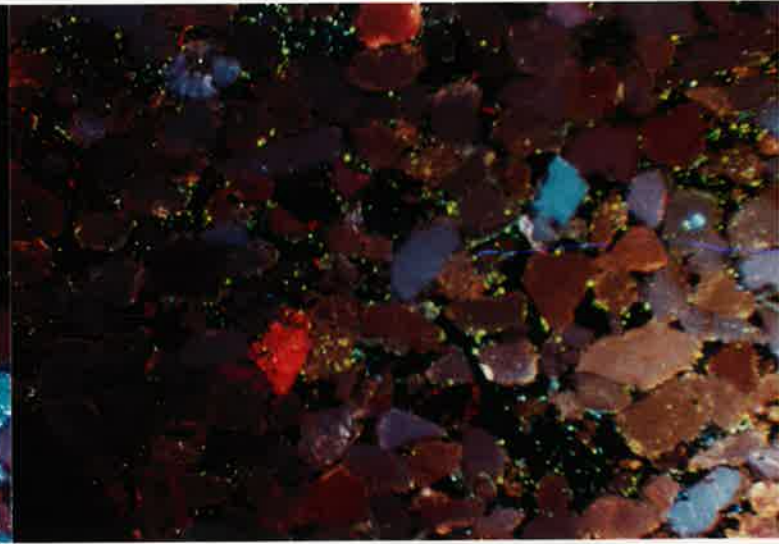
5(d)



5(e)



5(f)



7 Petrology and diagenesis

7.1 General description

Reservoir rock types found in the Cooper Basin sequence are mostly sublithic quartzarenites, siltstones and minor lithic quartzarenites and conglomerates. Other rock types are carbonaceous siltstones, shales and coals. The mineralogy recognised within each rock type is broadly similar.

Samples of reservoir rock types were identified by petrology, X-ray diffraction (XRD) and electron microscopy (SEM). Rock substance constituents are, in mostly decreasing order of abundance, quartz, illite, dickite, kaolin, rock fragments, plant or carbonaceous material, siderite, muscovite, biotite, chlorite, feldspar and traces of rutile and tourmaline.

All samples studied showed diagenetic fabrics and authigenic minerals. Minerals with diagenetic origins include pore filling kaolin, quartz overgrowths and spar siderite, all of which are volumetrically important. Diagenetic fabrics observed include dissolution seams, dissolved framework grain sites, bent muscovite and grain fracturing.

7.2 Rock composition

All the arenites are quartz rich. Quartz generally occurs as sedimentary, monomineralic, well rounded and fair sphericity grains that are generally overgrown by syntaxial euhedral to subhedral quartz overgrowths. Rock fragments are dominant over feldspar grains.

Finer grained argillites are clay and quartz rich. Detrital illite is the most common clay type.

7.3 Petrography

7.3.1 Quartz

This section is divided into observations of quartz, quartz authigenesis and quartz dissolution, and a discussion of possible sources and mechanisms of silica authigenesis. A conclusion summarises the section.

7.3.1.1 Quartz observations

Quartz is the dominant detrital and authigenic mineral in all the arenites studied. Arenites consist mostly of detrital quartz commonly overgrown by epitaxial euhedral to subhedral quartz overgrowths. Argillaceous rocks have common to dominant quartz with poorly developed or no quartz overgrowths.

Criteria for distinguishing detrital grains from associated quartz overgrowths are thin dust linings of illite, organic matter and small void spaces that outline a detrital grain shape, the absence of vacuoles in overgrowths and colour zoning in cathodoluminescence (CL) petrography. A typical, infrequent dust rim is shown in Plates 3d, 3e and 3f.

Where neighbouring detrital grains have tangential contacts only occasional interpenetration of adjacent grain boundaries (microstylolites), commonly associated with pressure solution of quartz is observed. Cathodoluminescence of the arenites show loose grain packing of detrital grain kernels with occasional minor pressure solution effects of the detrital quartz grains and overgrowths. Microstylolitic contacts between adjacent quartz grains are shown in Plates 5c and 5d.

The amount of authigenic quartz within arenites is estimated by CL studies as ranging from 0% to 20% of the total detrital grain volume. Within argillaceous samples authigenic quartz forms approximately 5% and lower. The lower authigenic quartz content of argillites can be seen by comparing the CL micrograph of a fine grained sample in Plate 3c with other CL micrographs of coarser grained samples such as Plates 3a, 4a, 4c and 4e.

Quartz overgrowths are predominantly anhedral in fine grained samples to euhedral and drusey in coarse grained samples. Quartz overgrowths seen in the SEM are best developed in the coarser grained samples where some remnant primary porosity is preserved. Some of the euhedral quartz overgrowths have been chemically etched and some are intergrown with kaolin.

At least two stages of quartz overgrowths in coarse grained samples are shown by SEM (e.g. Plates 1g, 1h); a volumetrically larger stage of overgrowths with common euhedral faces immediately surrounding the detrital material and a less prominent quartz overgrowth stage associated with druse formation. Druse quartz overgrowths as seen by the SEM are patchy but common.

CL studies show a single shade of luminescence within most quartz overgrowths but occasionally up to five concentric zones can be identified within a single overgrowth, as in Plate 3a. The more common single zoned quartz overgrowths form a "meniscus" type of cement around detrital quartz grains and are pervasive within most arenites studied. Kaolin filled pores rimmed by these single zoned overgrowths often display embayed quartz to kaolin contacts.

The more common single zone quartz overgrowths form the innermost zone of the multiple zoned overgrowths. Multiple zoned quartz overgrowths generally border remnant primary pores or occur where silica has substantially cemented primary porosity, whereas the single zoned overgrowths are associated with pore filling kaolin.

Some of the euhedral quartz faces observed with the SEM show chemical etching in the form of irregular and oriented V shaped depressions. An example of this etching is shown in Plate 1b.

Bone (1988) and Bone & Russel (1988) report that many of the fluid inclusions observed within authigenic quartz overgrowths of both the Eromanga and Cooper Basin sediments contained fluorescent hydrocarbons.

7.3.1.2 Timing of quartz authigenesis

Major quartz cementation of original sediments is attributed to precipitation from silica saturated pore water to form common euhedral overgrowths. Zoning of these overgrowths may be attributed to many causes such as evolving pore water chemistry, changes in the source of authigenic silica for cement, groundwater flushing, discrete pulses of cement precipitation etc..

The presence of clay minerals appears to have inhibited nucleation of quartz overgrowths (Heald 1955, Imam & Shaw 1987). Large, euhedral quartz overgrowths do not occur where illite is identified as grain coating.

The presence of well formed plates of kaolin partly incorporated within the outer euhedral rim of the main stage of quartz overgrowths (e.g. Plate 1e) indicates that authigenesis of quartz cement and kaolin is at least partly contemporaneous (refer to the discussion of this feature in the kaolin description, this section). Coexisting euhedral quartz and well formed kaolin intergrowths indicate stable conditions of formation

Post main overgrowth stage quartz cementation is typified by patchy distribution of druse quartz (e.g. Plates 1g, 1h) and multiple CL zoning (e.g. Plate 3a), although some druse quartz may be attributed to limited grain coating by illite during the main overgrowth stage, allowing thin pinnacles of drusey prismatic quartz or small mounds of anhedral quartz to grow where illite cover is absent.

Chemical etching of euhedral quartz faces is attributed to localised alkaline pore water reaction between quartz and adjacent siderite, organic matter or feldspar that has since been dissolved, or the preferential leaching of quartz along crystal defects (S. Phillips, pers comm.).

7.3.1.3 Quartz dissolution

Staughton (1985) reported that total silica levels in deeper Permian formations in the Strzelecki area are less than those of the overlying Jurassic Eromanga Basin sequence, consistent with an increase of silica solubility with pressure, temperature and pH. Martin (1980) reported increasing quartz solution in Toolachee Formation sandstones with depth, manifested as pressure solution effects; some zones within sandstones display quartz overgrowths while other zones show pressure solution effects with few overgrowths.

Two types of solution effects were observed by thin section and CL in several of the samples studied:

(a) Microstylolites occasionally observed between adjacent quartz overgrowths as erratic, sinuous, grain size contacts (e.g. Plate 5c).

(b) Often common dissolution seams (e.g. Plates 5c, 5d, 5e) that occur as sublinear, mostly horizontal, often bitumen stained, organic matter rich zones up to 5mm wide. Most lithics are disaggregated within the seams and muscovite flakes are generally oriented parallel to the zones. Dissolution seams contain a greater concentration of non-quartz grains than the rest of the sample rock substance. The concentration of non-quartz components do not generally exceed twice that of the rock substance; therefore a 5mm thick seam represents up to 5mm of dissolution. Where dissolution seams are present they often occur as a swarm of partly discontinuous "meandering" seams up to 15 millimetres wide.

The low observed incidence of stylolites and microstylolites preclude pressure solution as a major source of silica for overgrowths. No significant variation of dissolution seam or pressure solution effects were noticed between formations nor were any significant increases of these features observed with depth.

Several workers (Wehl 1959, Bjorlykke 1988) have reported that pressure solution of quartz grains is enhanced by the presence of clay or mica. Martin (1980) also reported that Toolachee Formation arenites in various parts of the Cooper Basin display common pressure solution effects. He considered the lack of quartz overgrowths near microstylolites and the abundance of decomposed biotite associated with stylolites indicate that decomposing biotite caused localised higher pH conditions in porewater and marked silica solubility.

Dissolution seams are more prevalent than pressure solution effects and may be an important source of silica, particularly from the dissolution of silt size detrital quartz particles. The common occurrence of fine organic matter within dissolution seams tends to indicate increased solubility of

silica near organic matter, although McBride (1989) summarises work that indicates pressure solution is a more important source of silica than passive dissolution, with only minute increases of silica solubility associated with very small quartz grains.

McBride (1989) comments that qualitative data at which pressure solution begins in siliciclastics are sparse and inconsistent with most workers reporting a depth of between 1 to 2 kilometers, below which quartz solution occurs. Subsidence curves for the overlying Eromanga Basin sediments published by Zhou (1989) indicate this scale of sediment loading occurred during major basin subsidence in the Cretaceous at 100 Ma. It is likely that pressure solution of quartz and hydrocarbon generation occurred under similar conditions during this period.

7.3.1.4 Origin of quartz

Considerable attention has been given by many authors (Davis 1964, Dapples 1979, Smosna 1988, Bjorlykke 1988, McBride 1989) to identifying the source and amount of authigenic quartz endemic to most of the world's hydrocarbon bearing sandstones. In his summary paper McBride (1989) lists 23 possible sources of silica for quartz cement in sandstones. The most relevant possible sources of authigenic silica to the study area are listed below:

(1) Precipitation from flushing, silica saturated groundwater. Most authors (e.g. Blatt 1979, Bjorlykke 1979) believe this to be a minor source of silica because of the huge flux of groundwater needed to precipitate relatively small amounts of quartz as overgrowths. Bjorlykke (1988) also discounts compacting shales and mudstones as an important silica source within thicker sandstone bodies because of similar problems of inadequate groundwater flux.

However, the open grained nature of the arenaceous sediments prior to major quartz cementation make the circulation of meteoric water a feasible method of transporting silica. The location of the study area on the side of the Tennapera Trough may also promote flushing and precipitation of silica rich groundwater towards lower Permian sediments towards the southeast. Quartz overgrowths are reported to be more voluminous and euhedral in Permian arenites of the Toolachee Field, south of the study area (Figure 5; David Alsop, pers. comm.).

The possible "meniscus" appearance of the main quartz overgrowth as seen by CL also indicates initial silica cement precipitated during non-equilibrium chemical conditions such as meteoric groundwater flushing. Where present, subsequent overgrowths appear to evenly coat previous overgrowths or grains without displaying the meniscus appearance of the first formed overgrowth.

Assuming precipitation from flushing, silica rich groundwater occurred, plausible sources of authigenic silica within meteoric groundwater may have been:

(a) Recently deposited sediments consistently providing silica for subsequent quartz cementation. The detrital quartz sediments may act both as a source of dissolved silica and as a nucleation site for precipitated silica, both processes needing high flow rates in the meteoric water zone. Blatt (1979) points out that voluminous quartz cementation is mostly associated with mineralogically mature sediments, inferring that sedimentary process contributes to quartz mobilisation by dissolution of labile grains.

However, no endemic dissolution of the original arenaceous or argillaceous quartz grains is observed, although post depositional quartz dissolution may be invoked to explain the paucity of grains showing dust rims.

(b) Weathered structural highs or remnant topography above the groundwater table, with downwards percolating rain water transporting silica. Local high areas were common during Cooper Basin sedimentation (see, for example, palaeogeographic reconstructions in Figures 9 & 10). Silica rich groundwater may have also been introduced from topographically higher areas from outside the Cooper Basin during the Permian.

(c) Unconformities or periods of non-deposition with increased chemical weathering.

(d) Climatic changes from arid conditions with low silica solubility to humid, warm conditions with high silica solubility (Davis 1964) and increased transport potential by recharge to groundwater.

The apparent lack of variation of main quartz overgrowth development in arenites from different geological formations indicates a systemic input of silica rich fluids occurred after deposition, either from quartz mobilisation associated with sedimentation as outlined in (a) or from percolating groundwater introduced from outside the Cooper Basin as outlined in (b).

(2) Pressure solution of detrital quartz grains. Evidence of compaction in samples are minor stylolites, minor microstylolitic contacts between adjacent quartz grains, occasional disintegrated and deformed lithic fragments, minor bent circular muscovite grains, minor patchy dissolution seams and deformed illite and muscovite. Of these, only stylolites, microstylolites and dissolution liberate silica.

Few pressure related dissolution effects were noticed in samples from the study area, indicating sufficient competency of the rock mass was attained before significant loading by overlying

sediments occurred. Generally, competence of a rock mass is gained by cementation. The formation of cement reduces pressure solution by increasing the contact area and load bearing capacity of individual grain contacts in the sediment (McBride, 1989).

The lack of abundant pressure solution effects in siltstones, shales and silt bounded arenites compared to thicker arenite beds preclude any major increase of silica solubility associated with the presence of clays or mica (Martin 1980, Bjorlykke 1988).

Bearing in mind the low observed incidence of pressure solution of quartz and the substantial depths at which it occurs, it is likely that pressure solution has provided a minor amount of silica late in the diagenetic history of the Cooper Basin arenites.

(3) The transformation of clay minerals. Both the transformation of smectite to illite in shales (Hower et al 1976, Boles & Franks 1979, Goodchild & Whitaker 1986, Stewart 1986, O'Shea & Frappe 1988) or the illitisation of kaolinite (Hurst 1980, Hurst & Kunkle 1985, AlDahan & Morad 1986) have been identified as clay mineral transformations that can release silica.

The transformation of smectite to illite via mixed layer smectite/illite occur as consistent changes of clay chemistry with depth in several basins with thick mudstone/sandstone sequences (Perry & Hower 1970, Hower et al 1976, Boles & Franks 1979, Boles 1981, Goodchild & Whitaker 1986). The transformation requires an external source of potassium and releases silica and calcium during the transformation with increasing temperature and supply of potassium, such as that derived from dissolution of feldspars or micas (Curtis 1978) at temperatures below 60°C (Smosna 1988).

No smectite was identified in bulk and oriented XRD analyses of less than 10 micron particle size of samples 298, 302 and 309 (Raven & Milnes 1989; Appendix 4), nor from SEM petrography.

However, several minor occurrences of smectite in Cooper Basin arenites have been reported. Martin (1980) recorded smectite as a fine brown coating around the edges of some pore spaces in the most permeable samples from Della 5A in the Della Field (Figure 5) but suggested it may have been introduced by drilling mud infiltration. Stanley & Halliday (1984) reported trace illite-smectite in the Tirrawarra and Patchawarra Formations of the Big Lake Field (Figure 5). Almon & Davies (1981) reported the presence of mixed layer illite/smectite in 31 samples of various wells in Permian Cooper Basin sandstones. Smectite is also found in minor proportions in clay fractions in the overlying Eromanga Basin sequence of some Strzelecki wells (AMDEL 1986).

Trace amounts of chlorite found in some samples by SEM may be ambiguously attributed as a product of the smectite to illite transformation (Reinson & Foscolos 1986, Bjorlykke 1988). Chlorite can also be formed from the alteration of K-feldspar, biotite or some lithics (Curtis et al 1985, AlDahan & Morad 1986).

Illitisation of kaolinite in arenites is interpreted by Hancock & Taylor (1978) and Hurst (1980) as an advanced diagenetic process that postdates kaolinite and illite/chlorite assemblage authigenesis. Bjorlykke (1988) reports that, on heating, kaolinite becomes unstable between 120 to 150 °C. Assuming a average geothermal gradient for the Strzelecki area of 5 °C per 100 metres vertical depth (Kantsler et al 1983) this process would commence at 2400 metres. Minor amounts of authigenic illite within some samples may indicate these conditions may have just been achieved.

Compaction of clay beds is generally proposed for the transport of silica derived from the transformation of clay minerals into adjacent sand bodies. Muller (1967) indicated high initial water content and porosities of argillaceous muds result in greater pore fluid expulsion for muds than for sands. The degree of compaction depends on the ratio of fine to coarse material, the character of the sediment framework and the clay type (Wolf & Chilingarian 1976).

The association of silica cement adjacent to clay beds has frequently been attributed to silica transport from mud into sand during compaction or by diffusion. For example, Fuchtbauer (1967) showed that quartz cementation in Dogger Sandstone arenite beds less than 3 metres wide increases towards the shaley margin of the bed. The interbedded shale/sand sequences and complex cement stratigraphy of the Cooper Basin sequence would make this effect difficult to quantify, but silicification in arenites did not seem to increase adjacent to argillaceous sediments.

Given the absence of identified smectite or corroded kaolinite within any sample studied and the apparent lack of variation of authigenic quartz content with distance from clay beds, it is unlikely that any large amount of silica has been generated from the transformation of clay minerals within the study area.

(4) Dissolution and alteration of feldspars to kaolinite. (Hawkins 1978, Morad & AlDahan 1987). Bjorlykke (1988) states that kaolinisation of feldspar produces silica "corresponding to 40% of the altered feldspar". The intergrowth of kaolin with abundant quartz overgrowths, minor corroded feldspars (e.g. Plates 2d,5f), the occurrence of kaolin as framework grain replacement and the authigenic texture of kaolin supports the importance of kaolinisation of feldspars as a mechanism to provide silica for grain overgrowths.

It is difficult, however, to determine the proportion of feldspar in the original sediment. Provenance of the Cooper Basin sequence does not include substantial granitic terrains (Petroleum Management Associates 1986) although Pitt (1986) infers a shallow granite in the Strzelecki area to account for high geothermal gradients within the Permian sequence. Only minor, corroded K feldspars and one Ca feldspar have been identified by SEM and CL, and secondary porosity possibly attributed to late feldspar dissolution is not prevalent within the study area.

Detrital and authigenic kaolin abundances visually determined by thin section studies average less than 10% and rarely exceeds 20% (Appendix 4). An ideal sample with 10% authigenic kaolin formed from the total alteration of detrital feldspar to kaolin and quartz would yield between 6% to 7% authigenic quartz (Bjorlykke 1988). This indicates kaolinisation of feldspar can be a major source of authigenic silica.

7.3.1.5 Discussion of quartz authigenesis

It must be emphasised that the proposal of sources and mechanisms for the authigenesis of quartz is generally speculative.

Three of the postulated sources of silica may have provided the bulk of the silica needed for extensive overgrowths observed within the arenites of the study area. Firstly the presence of corroded feldspar, secondary porosity and appreciable amount of authigenic kaolin indicate substantial alteration of detrital feldspar to kaolin and quartz. Secondly an early and pervasive quartz cement with overgrowths restricted to arenites and the dissolution of rock fragments indicate silica precipitation from meteoric groundwater. Thirdly, dissolution seams with common fine organic matter indicates silica dissolution that may be enhanced by the presence of organic matter.

It is likely that feldspar dissolution was enhanced by some groundwater flushing. Early feldspar dissolution in meteoric groundwater conditions may have resulted in a early silica cement, with kaolin later chemically precipitated in some primary pores as silica concentration waned. Remaining pores not filled with kaolin may have been cemented by later phases of silica cement.

Multiple zoning of overgrowths indicated by CL should not be considered as representing separate cement periods with great differences in pressure, temperature or chemical conditions. Zoning may also be caused by a single related cementing event with slight changes in physical or chemical conditions during precipitation, the same event repeated, several mechanisms of cement formation acting concurrently or a series of interdependent events.

One example of an interdependent set of events is described by Bjorlykke (1988). Decomposing feldspars within compactional, low circulation porewater precipitate stable kaolinite and silica and leave elevated potassium levels in the porewater. The conversion of smectite to illite provides a sink for the potassium and also produces silica. A precursor to this set of diagenetic events may be groundwater flushing that also precipitates silica and promotes more rapid kaolinisation of feldspars.

As indicated by cathodoluminescence, the preservation of an open fabric of coarse detrital quartz grains by quartz cement, possibly in a "meniscus" form, and the predominance of authigenic silica within initially permeable coarse sediments infers that precipitation of silica cement is associated

with near surface meteoric groundwater conditions soon after deposition.

However, temperature data from fluid inclusions in quartz overgrowths reported by Russel & Bone (1989) indicates at least some quartz cement formed at substantial depth. The presence of liquid hydrocarbons in these fluid inclusions also indicate some quartz cement formed at depth, generally greater than one kilometer (from the depth of the liquid window at $R_o \text{ max}=0.5$, Figure 5 in Kantsler & Cook 1979). It is not clear which quartz overgrowths contain the types of fluid inclusions reported by Russel & Bone, but it may be the first formed quartz overgrowth phase, as hydrocarbons are also observed in dust rims associated with this phase.

Rising thermal waters enriched in silica may also precipitate large volumes of silica as they cool. An Upper Triassic / Jurassic heating event associated with regional uplift and erosion has been reported (Kantsler et al 1983) on the basis of vitrinite/depth trends, and may have provided a heat source for silica cementation of the Permian sediments.

The occurrence of major initial quartz cementation at depth appears incongruous with the preservation of an open framework of original detrital grains of coarse arenaceous sediments. The preservation of open fabric at substantial depth can only occur in arenites given the following scenarios:

- (1) Cementation at shallow depths occurred by an early cement that has since been dissolved.
- (2) An early, partial cementing by quartz at grain contact sites in the meteoric groundwater zone.
- (3) The vertical migration of hydrocarbons to sites of quartz cementation at shallow depths and lower temperature.
- (4) Development of high pore water pressures immediately after deposition or as a response to sediment loading.

The only direct evidence for any of these alternatives is an initial quartz cement interpreted as having a "meniscus" form that indicates quartz cementation occurred in the meteoric groundwater zone. However, because of similarity of features of the Cooper Basin with other abnormally pressured hydrocarbon bearing basins (Gretener 1978, Hunt 1989), the existence of overpressured zones during diagenesis should be considered. Evidence for, and the implications of, high pore water pressure zones are discussed in Section 9.7.

7.3.1.6 Conclusions - quartz

Quartz is the dominant detrital and authigenic mineral component in all samples studied. Authigenic quartz occurring as overgrowths and drusy crystals are common in coarser arenites. Zoning of quartz overgrowths is sometimes observed and several stages of quartz cement is inferred.

The preservation of an open detrital framework in arenites, (?)meniscus quartz cement, common kaolin and corroded feldspar indicates the formation of an early quartz cement within the meteoric groundwater zone, partly associated with feldspar dissolution. Other subsequent quartz overgrowths do not display the meniscus nature of the early, first formed overgrowth.

Several mechanisms and sources of silica for cement may be postulated for subsequent stages of quartz cement and include clay mineral transformations and continued alteration of rock fragments. Some of these may be interdependent mechanisms.

Hydrocarbons found in fluid inclusions within quartz overgrowths and fluid inclusion work indicates at least one quartz cement stage is associated with hydrocarbon generation at elevated temperatures and depths. It is not clear which quartz overgrowth stage this is, but the possibility that it may have been the first formed quartz overgrowth should not be ruled out. More work is needed to confirm this possibility.

7.3.2 Illite:

The clay mineral illite is typically seen as small, flat lying, closely spaced plates. Its partly oriented nature and the predominance of illite in fine grained samples suggest a detrital origin (e.g. SEM micrograph in Plate 2a). Partial orientation of illite occurs as common tangential alignment of plates to the framework grains.

Illite also forms as less common framework grain replacement of (?)micaceous rock fragments It is often found with kaolinite.

More rarely, illite forms delicate forms such as wisps, fibres and free standing groups of plates seen by SEM that suggest an authigenic origin (Plate 2e).

Illite is less abundant where well formed euhedral quartz overgrowths are common. Where flakey and platey illite barely coat a quartz grain surface, subhedral quartz (Plates 1f, 1g), druse quartz and patchy euhedral kaolin is found.

7.3.2.1 Illite / smectite

The original form of the bulk of the detrital clays during deposition may have been a combination of illite, smectite or mixed layer illite/smectite. Although trace amounts of smectite have been reported in Cooper Basin sediments by several authors (Almon & Davies 1981, Martin 1980) no smectite has been identified by SEM or oriented clay sample XRD within the study and adjacent areas (Raven & Milnes 1989; Appendix 4).

Smectites can also be diagenetic, initially forming instead of illite and given the right conditions, later altering to illite. Authigenic illite may form in alkaline conditions with a source of K, whereas smectite authigenesis requires a source of alkaline ions (Paul 1988).

Conditions for conversion of any possible smectite have existed in the Cooper Basin. The conversion of detrital smectite to illite is reported to occur at temperatures between 60 °C and 100 °C in the Gulf Coast (Perry & Hower 1970, Hower et al 1976). The conversion is also related to the formation of chlorite (Weaver & Beck 1971, O'Shea & Frape 1988, Bjorlykke 1988) with smectite needing a source of K (from K feldspar or mica decomposition) to produce illite, chlorite and quartz.

7.3.2.2 Origins of illite

7.3.2.2.1 Detrital illite

The partly oriented nature of platey illite is attributed to a detrital origin such as the infiltration of illite into the sediment soon after deposition (Molenaar 1986, Smosna 1988), original depositional fabric of the detrital clays and the squeezing of illite, either during compaction or between adjacent quartz overgrowths during silica nucleation and growth.

The higher illite to kaolin ratios of the finer grained samples (Figure 11) reflect the detrital origin of most of the illite within the finer grain size fraction, compared to the authigenic kaolin common to coarser sediments. Reinson & Foscolos (1986) attribute low authigenic illite content in coarse sands to increased levels of Ca and Mg in pore fluids that inhibit K absorption and the formation of illite.

XRD traces of fine grained samples (Appendix 3) generally show a broad peak at 10 Å⁰ indicating the illite being identified is poorly crystalline or possibly interstratified with another mineral. Martin (1980) commented that the crystallinity of detrital illite may have been inherited from the metamorphic parent rock, particularly the 2M poly types. It has frequently been noted (AlDahan & Morad 1986, Hall et al 1986 and others) that illite crystallinity increases with depth and temperature

and with the K content of illite, but no depth related increase in XRD indicated crystallinity of samples was observed.

7.3.2.2 Authigenic illite

Deer et al (1962) report that alkaline conditions are needed for illite growth. Illite formation occurs as direct precipitation from pore fluids (O'Shea & Frape 1988), the "regeneration" of detrital clays (Sarkisyan 1972, Wilson & Pitman 1977) or the replacement of detrital grains such as feldspar or biotite (Boles & Franks 1979, AlDahan & Morad 1986). These three mechanisms are outlined below.

(1) Direct precipitation of illite: Illites formed by direct precipitation from pore fluids (Blatt 1979, Hurst & Irwin 1982) require pore fluids of total dissolved salt content (TDS) greater than seawater (Harder 1974) and moderate pH (Hurst & Irwin 1982). The formation of authigenic smectite is similarly favoured in terms of pH and Mg/Ca ratio by porewater similar to that of a marine origin (Almon et al 1976, Blatt 1979, Smosna 1988). In view of the dominantly fresh water origin of the Cooper Basin sediments, highly saline pore water conditions could occur only when:

- (a) restricted circulation to the sea occurred during sedimentation.
- (b) marine conditions of deposition of the Cretaceous interval of the overlying Eromanga Basin sediments allowed downward circulation of sea water as pore water.
- (c) the upward circulation of concentrated sedimentary basin brines occurred.

Overton & Hamilton (1982) report total dissolved solids measurements of typical Permian sandstone porewater in the Cooper Basin as 12,000 mg/l which is too low to be considered a brine. The underlying Warburton Basin sediments also lack evaporites but does contain marine units.

Stuart (1976) pointed out that the shales within the Cooper Basin sequence did not necessarily have to be deposited in terrestrial conditions but may have been connected to the sea off the eastern coast of Australia, similar to the present Great Lakes of North America.

In either case, groundwater would have been diluted by fresh water input within a fluvial environment, minimising the conditions favorable for direct precipitation of authigenic illite from saline porewaters.

O'Shea & Frape (1988) report that fibrous and hairy illites found in the Cataract Sandstones of Ontario, Canada are found only in areas of sandstone that have measurable quantities of gas present. They interpret the precipitation of these illites as a by-product of hydrocarbon generation or migration in the Cataract Sandstones due to the expulsion of organic acids associated with the diagenesis of hydrocarbons (Surdam et al 1984).

Rare authigenic fibrous illite, as shown in Plate 2e, has been observed in some gas bearing arenites in the study area.

(2) Illite formed from detrital clays: Illite can also form by authigenesis of kaolinite (Bjorlykke 1979, 1984, Hurst & Irwin 1982), theoretically in a closed system at temperatures as low as 50 °C (Bjorkum & Gvelsvik 1988) but no corrosion of kaolinite is observed in the samples studied. Similarly, no corrosion of illite is observed, implying alkaline porewater conditions were prevalent after their formation (Deer et al 1962). The lack of dissolution features of detrital illites common in finer grained sediments may also be attributed to the low permeability of these sediments.

(3) Illite replacing detrital framework grains: Grain replacement illite tends to occur in small patches usually in close proximity to partly decomposed micas, micaceous rock fragments or calcic feldspar. Kaolin tend to be generally associated with the grain replacement of K feldspar.

For localised precipitation of illite to occur, feldspar and mica dissolution and illite authigenesis require restricted pore water circulation. Both processes are likely to be at least partly contemporaneous, so that as feldspar and mica were being corroded, the constituent ions were transported to the sites of illite growth (O'Shea & Frape 1988). However, aluminium is relatively immobile in near neutral pH porewater (Hurst & Irwin 1982, Huang et al 1986), although the complexing of aluminium with locally produced organic acids making aluminium more mobile is proposed by Surdam et al (1984).

The increase in mobility of aluminium ions implies that dissolution of feldspar and mica may have occurred by interaction with organic rich waters derived from the immature to barely mature diagenesis of hydrocarbons, rather than the thermal breakdown of feldspar to produce potassium and aluminium for illite growth, at temperatures between 100 to 120 °C (Boles & Franks 1979, Lonoy et al 1986). Assuming a high current geothermal gradient of 5°C per 100 metres (Kanstler et al 1983, for the Strzelecki area) thermal breakdown of feldspar may occur at 2 kilometers depth.

The presence of undissolved feldspars and micas suggests either changing pore water conditions, or the growth of diagenetic illite limited the circulation of illite forming pore water solutions after a period of time.

7.3.2.3 Conclusions - illite

A substantial component of most fine grained rock types studied is detrital illite. Detrital and less abundant authigenic illite are found in coarser rock types where authigenic illite mostly forms from the dissolution of framework feldspar, mica and rock fragments in locally alkaline porewater conditions. Rare authigenic fibrous illite may have been directly precipitated from porewater solutions associated with hydrocarbon diagenesis.

7.3.3 Kaolin (kaolinite and dickite) clay

Both kaolinite and dickite species of the kaolin clay group have been identified from XRD analyses (Appendix 3). SEM shows kaolin as pseudo-hexagonal platy crystals that are mostly pore filling and lining. At least three sizes of kaolin minerals can be identified by SEM, sometimes all within the same sample; coarse crystals over 30 microns, intermediate at 11 microns and finer with 4 microns average grain width.

The coarsest kaolin is euhedral, often vermiform and displays delicate morphology (Plate 2f). It is usually found in the coarse grained samples pore filling between euhedral quartz overgrowths. Coarse grained arenaceous samples containing appreciable amounts of this type of kaolin are identified by XRD as containing substantial dickite.

The finer sizes of kaolin most commonly found in fine grained sandstones, shales and siltstones are attributed to kaolinite with possibly lesser amounts of dickite, forming more irregular, blocky and subhedral crystals than coarse dickite. Kaolinite forms as detrital masses and as grain replacement often intergrown with illite. Kaolin (probably dickite) is sometimes intergrown with, but not generally engulfed in, euhedral quartz overgrowths (Plates 1c, 1e).

The euhedral form of the dickite and some of the kaolinite, the vermiform nature of some dickite and its delicacy of form (Wilson & Pitman 1977) indicate an authigenic origin for some of the kaolin clays.

SEM studies indicate that kaolin clays may have formed in 4 ways.

- 1) The alteration of feldspar to produce subhedral to anhedral kaolin. Mixtures of kaolinite and illite are often found at altered framework grain sites that were probably rock fragments and feldspars.
- 2) The alteration of mica (?biotite) to produce coarse kaolin (e.g. SEM micrograph in Plates 2b, 2c).
- 3) The growth from pore water solution. At least 3 different sizes of coexisting kaolin (approximate

diameters of 4µm, 11µm and over 30µm) are recognised that probably indicate sequential growth from solution as conditions became more favourable for kaolin precipitation, with coarser dickite usually occurring as the only, last formed clay mineral in the pores it is filling.

Intergrown kaolin and quartz overgrowths are occasionally observed and both are thought to have grown contemporaneously.

4) Detrital kaolin. The predominance of kaolinite in the finer grained sediments indicates kaolinite is the dominant detrital form of kaolin. Kaolinite content is generally constant in sediments with average grain sizes less than 0.5 mm (Figure 12) and illite to kaolin ratio below 2 (Figure 13). Detrital kaolinite appears as masses of single plates with irregular crystal edges commonly mixed with illite displaying a detrital fabric. Both illite and kaolinite clays are often deformed by compaction.

7.3.3.1 Origin of kaolin

The conditions of formation of kaolin are poorly understood (Bjorlykke 1988).

Kaolinite formation is generally attributed to fresh, meteoric groundwater conditions (Blatt 1979, Dutton 1987). Such conditions also result in the partial corrosion of unstable silicate minerals such as feldspar (Shelton 1964, Imam & Shaw 1987) or mica (Bjorlykke & Brendsdal 1986) under slightly acidic conditions. Authigenic titanium minerals may indicate biotite as a precursor for kaolinite (Bjorlykke & Brendsdal 1986) and although patchy, corroded detrital rutile that may have sourced titanium was observed in some samples by SEM, no authigenic titanium minerals were found.

Hurst & Kunkle (1985) state kaolin is characteristic of low to medium temperature, low pH, high Eh conditions of formation that are found in fluvial environments at shallow depths. Compactional water from dissolving feldspars would require a sink for potassium that is provided by the smectite to illite transformation (Bjorlykke 1988) allowing kaolinite and illite to coprecipitate. Kaolinite and illite/chlorite are considered a stable assemblage by Hurst (1980).

Curtis (1983) has suggested that acidic solutions from organic rich mudrocks will contain significant aluminium derived from the dissolution of feldspar and mica for the direct precipitation of kaolinite.

Kaolin is stable between pH 5 to pH 8 (Hurst 1980). Quartz is stable to pH 9 but is dependent on temperature (Pettijohn et al 1987). The presence of corrosion marks on quartz overgrowths and not on immediately adjacent kaolin (SEM micrograph in Plate 1d) indicate some local combination of alkaline porewater conditions were attained after the authigenic precipitation of quartz and kaolin.

Little information exists on the mode of formation of dickite. Shelton (1964) and Bayliss et al (1965) considered dickite to be a more thermodynamically stable replacement product of kaolinite but no corroded kaolin has been observed in the samples studied. Loughnan & Roberts (1986) studied sediments of the Sydney Basin and stated that kaolinite is generally restricted to low permeability silts and muds while dickite is found in coarser, higher permeability intervals of the fluvial Hawkesbury Sandstone. They proposed that migrating groundwater with unusually low concentrations of silica resulted in the slow precipitation of dickite.

This implies that kaolin in the study area precipitated from fresh to slightly acidic migrating groundwater associated with the partial corrosion of feldspar and mica; initially kaolinite was precipitated during and after waning quartz cementation, and later dickite formed as pore filling in more ideal conditions with lower silica levels in porewaters. Decreasing silica levels may be attributed to several causes such as increasing alkalinity, changes in porewater temperature and pressure and decreasing compaction of clay beds.

The association of dickite with waning quartz precipitation, typified by common intergrowths of (?)dickite within the outer shell of euhedral silica overgrowths, represents a single progressive evolution of pore water chemistry. Such an evolution would most likely have occurred within a closed physical and chemical system of primary pores partially sealed by an initial meniscus cement or by clays blocking pore throats. Blebs of bitumen are occasionally found staining pore filling dickite (e.g. Plate 4f) indicating hydrocarbon generation occurred after dickite formation.

The presence of coarse, well formed pore filling vermiform books of dickite within framework grainsize pores indicates dickite precipitated into pores after the dissolution of some labile grains.

Schultz-Rojahn & Phillips (1989) observed dickite as the typically dominant clay in coarser grained Permian arenites in the southern Cooper Basin, except in the Strzelecki area where dickite is associated with some of the finer silty deposits. This suggests that porosity and permeability were initially good in some of the silty deposits in this area, allowing the formation of dickite from solution.

7.3.3.2 Conclusions - kaolin

Kaolinite occurs as detrital grains in fine grained sediments, grain replacement product of labile grains such as feldspar and mica, and as dickite precipitated from pore water.

After deposition, conditions for the direct precipitation of kaolin from porewater gradually became more favorable, possibly due to increases in aluminium mobility accompanying organic maturation

or decreasing silica concentration after the main quartz overgrowth stage. The last stages of kaolin growth occurred within a closed system with euhedral dickite filling pores and dissolved framework grain sites.

7.3.4 Micas

Micas occur as small 0.1mm to large 0.7mm long, tabular to bladed well formed muscovite and biotite crystals that are commonly bent around adjacent framework grains. Extinction characteristics indicate ductile deformation. Bent micas are attributed to mechanical compaction of the rock mass and to the growth of adjacent authigenic minerals. Micas are commonly oriented parallel to sedimentary laminations in finer grained sediments, indicating a detrital origin.

All micas appear detrital in origin. AlDahan & Morad (1986) attribute authigenic muscovite formation to the alteration of illite under conditions of high grade diagenesis to low grade metamorphism (Figure 14 in AlDahan & Morad 1986) which has not been attained in the study area. Biotite has a higher metamorphic grade of formation than muscovite.

Weaver & Pollard (1973) show that illites have less K_2O , more SiO_2 , MgO and H_2O than muscovite. A semiquantative plot of potassium levels based on the EDS spectra of illites, biotites and muscovites observed during SEM studies (Figure 14) indicates that muscovite has higher K levels than illites. The gradation of K levels between illite and muscovite indicates the alteration of muscovite to illite produces excess K which could be taken up during kaolin authigenesis.

Minor amounts of biotite are present as corroded detrital grains in some samples studied in thin section and SEM. Biotite tends to have slightly more Fe than muscovite, as determined by the EDS spectra during SEM studies. Bjorlykke & Brendsdal (1986) report that biotite can alter to K depleted biotite and contain authigenic carbonate (mostly siderite) and kaolin between constituent sheets. Occasional examples of kaolin forming between mica sheets were observed, as in the SEM micrograph in Plate 1c.

7.3.5 Feldspar

Feldspar is observed in thin section, CL and SEM as rare to occasional large, well rounded corroded detrital grains in some of the samples studied. Some EDS spectra of feldspar show a calcium component which indicates a calcic feldspar such as plagioclase, but the lack of twinning and equidimensional character indicates more common K feldspar. Replacement products of feldspar are kaolin and less common illite.

7.3.5.1 Feldspar dissolution

All feldspar observed was well corroded, as seen in CL and SEM micrographs in Plates 2d and 5f.

A number of mechanisms proposed for the dissolution of feldspar and similar minerals generally require the presence of acidic porewater (Lonoy et al 1986). Two of the most relevant mechanisms of feldspar dissolution in the study area include:

(1) Dissolution by carbonic acid during meteoric water flow. Carbonic acid is formed when CO_2 is produced from the maturation and thermal decarboxylation of kerogen in an organic rich mudrock to form acidic porewater solutions (Schmidt & McDonald 1979) or from the absorption of CO_2 from the atmosphere by rainwater.

(2) Organic complexing to form carboxylic acids. Organic (carboxylic) acids are produced from maturation of organic mudstones (Surdam et al 1984). The maximum generation of these acids coincides with the maximum release of water from the smectite-illite clay transformation which assists with the expulsion of the acidic solutions into adjacent sandstone (Goodchild & Whitaker 1986).

Both mechanisms of feldspar dissolution have conceivably operated in the study area. Organic complexing in carboxylic acid solution circulated by meteoric groundwaters has most likely caused the dissolution of most feldspars at shallow depth, as carboxylic acids are destroyed by bacteria at elevated temperatures (Caruthers & Kharaka 1978, Surdam et al 1984). Less common occurrences of oversized pores with little surrounding quartz overgrowths may indicate corrosion of larger, remnant lithics and feldspars at depths associated with hydrocarbon diagenesis. In this case, carbonic acid production does not occur before CO_2 is generated at temperatures greater than 70 to 80 degrees Celsius (Hunt 1979), or at 1.5 to 2 kilometers depth.

Kaolinite, chlorite and illite are common replacement products of feldspar (AlDahad & Morad 1986) with chloritisation or illitisation of feldspar more common with K feldspar alteration or where pore water solution is enriched with potassium (Harder 1974). Garrels & Howard (1959) interpret illite as an intermediate stage of kaolinite formation during feldspar replacement, but no illite corrosion was observed in any sample.

7.3.6 Rock fragments

Lithic fragments form a substantial part of the rock substance. Fragments include phyllites, shales,

sandstones, chert and igneous and metamorphic fragments displaying undulose extinction of quartz.

Lithic fragments observed in thin section and CL do not show more diagenetic influences than the rock substance they are found in. They are sometimes deformed, sometimes partly to completely disaggregated and often illitised or kaolinised. Generally, polycrystalline quartz rock fragments do not display quartz overgrowths except internally in a few coarse grained fragments where minor quartz overgrowths and kaolin pore line what were presumably pre-existing large pores.

Intraformational fragments derived from syndepositional reworking and stream bank collapse are identified from core logging. They show similar diagenetic character to the host rock substance and were presumably unlithified during deposition.

7.3.7 Carbonates

Siderite is identified by XRD and SEM as the only carbonate mineral present in some samples studied. Siderite in hand specimen is yellowish when fresh and dark red where oxidised on exposed core surfaces. Siderite often occurs as microscopic to mesoscopic bands, generally parallel to sedimentary layering; as blotches up to several millimetres wide and more rarely as patchy cement.

Petrographic studies show both micritic and sparry siderite forms. EDS spectra taken during SEM studies show trace amounts of Mn and Mg occasionally occur in the sparry siderite.

Micritic siderite frequently occurs with coals, shales and fine sandstones, in particular adjacent to and along carbonaceous stringers in shales. Increases in siderite content sometimes outline sedimentary structures such as bedding laminae. Bioturbation effects commonly disrupt siderite rich laminae.

Siderite also occurs as sparry pore filling coarsely crystalline cement in fine to medium grained arenites. Common inclusions of sedimentary grains within spar siderite are smaller in size than surrounding framework grains indicating dissolution of quartz has occurred during carbonate growth (Plates 5a, 5b). The sparry siderite occur in clusters of single to several well formed syntaxial rhombic crystals and sometimes as clusters of radiating crystals associated with micritic siderite. The mostly crystalline pore filling nature and lack of corrosion indicate the sparry siderite is late stage and authigenic.

Solution features of the micritic siderite are rarely evident (SEM micrograph in Plate 2g) while no solution or corrosion has been observed of the sparry siderite.

Both micritic and sparry siderite can form substantial proportions of the rock mass (to 30%) but

generally carbonate levels are low in the study area with siderite absent in most samples. Both sparry and micritic siderite are more common in finer grain sized sediments (Figure 15), with micritic siderite restricted to slightly finer sediments.

7.3.7.1 Micritic siderite

The precipitation of micritic siderite during or soon after sediment deposition is indicated by its close association with sedimentary features. Micritic siderite rich layers frequently parallel grain size variation in shale laminae and micrite siderite is often associated with horizontally laminated organic material.

Conditions necessary for direct precipitation of siderite are reducing, low S, non marine environments such as shallow water, rapidly accreting marshes and swamps that are high in organic matter, sulphate reducing bacteria levels and Fe levels (Postma 1977, Berner 1981, Smosna 1988).

The close association of organic matter with micritic siderite indicates precipitation of micritic siderite was mostly caused by the biogenic release of CO₂ from organic matter (Postma 1977, 1982; Curtis 1978). Other possible sources of CO₂ include postulated deep thermal activity such as the emplacement or metamorphism of basement granites (Rigby & Smith 1981) or the metamorphism of Cambrian limestones underlying the Cooper Basin sediments.

Siderite precipitation also requires a source of iron. In his summary work Stanton (1972) outlined many plausible origins for the supply of iron in modern fluvial environments. These include ferrous iron carried in solution in aerated river waters of pH 7 or lower, transport in suspension of fine clays or mineral platelets with a surface coating of iron oxide, iron removed from iron bearing minerals that form the detritus on lake or swamp floors and biological iron precipitation by bacteria or bacterial catalysis. James (1985) also pointed out the increased mobility of iron by the action of chelating agents within soil making iron more soluble.

7.3.7.2 Sparry siderite

Siderite also occurs as sparry disseminated blotches in fine to coarse grained arenites. Sparry siderite is mostly found in clusters of single to several well formed rhombic crystals to 2mm diameter that typically engulf partly dissolved quartz grains. Spar siderite is also found as less common rims and radial intergrowths intimately associated with micritic siderite layers and blotches.

In thin section, quartz and rarer lithic fragments inclusions are observed within spar siderite crystals as seen in Plates 5a and 5b. Quartz inclusions are often smaller in size than surrounding quartz grains, indicating dissolution of quartz has occurred.

The sparry siderite is considered a late stage authigenic cement because of its well crystallised nature, primary porosity pore filling and occasional association with similarly pore filling euhedral kaolin.

There are several explanations for the formation of sparry siderite. They include:

(a) The formation of a neogene siderite cement. The alteration of biotite and iron rich smectite (nontrite) (Bjorlykke & Brendsdal 1986) produces Fe ions that may combine with CO₂ from sources such as thermal decarboxylation of organic matter (Schmidt & McDonald 1979), meteoric infiltration of groundwater enriched in biogenic CO₂ or from the metamorphism of pre-Permian basement granites and limestones. Increased levels of Mg in some siderites indicate the biotite was a possible precursor to siderite (Bjorlykke & Brendsdal 1986)

(b) The dissolution and subsequent precipitation of carbonates from either the underlying Cambrian Limestones, early micritic siderite cement or from the overlying Eromanga Basin sediments, such as the carbonate cemented Namur Sandstone (Richards 1984).

As shown in Figure 15, spar siderite is restricted to slightly coarser grain sizes than the fine grained silts associated with micritic siderite. The similarity of distribution of the spar and micrite siderite with grain size suggests that spar siderite is mostly generated by the dissolution and local reprecipitation of existing micritic cement.

7.3.7.3 Conclusions - carbonates

Micrite and sparry siderite are the only carbonates found in the samples studied. Micritic siderite was precipitated in reducing conditions during or soon after sediment deposition in shallow, rapidly accreting marshes and swamps.

Spar siderite is found either as a patchy late stage cement that typically engulfs partly dissolved

surrounding quartz grains, or as rims and intergrowths associated with earlier formed micritic siderite blotches. The similarity of distribution of both types of siderite with grain size indicates that spar siderite growth may be largely attributed to the dissolution and local reprecipitation of pre-existing micritic siderite.

7.3.8 Chlorite

Iron rich chlorite is occasionally identified by SEM studies as rare pore lining authigenic plates generally smaller than, but associated with illite.

Curtis et al (1985) attribute chlorite formation to precipitation from alkaline porewater and lesser replacement of biotite, feldspar and some lithics. Imam & Shaw (1987) state that chlorite can form from the chemical alteration of rock fragments by reducing, alkaline porewater that liberates Fe, Al and Si for chlorite. The main source of iron and magnesium necessary for chloritisation of K-feldspar is the alteration of associated detrital biotites (AlDahad & Morad 1986), resulting in formation of both chlorite and illite as a stable mineral suite. That chlorite is less abundant than authigenic illite is attributed to the relative abundance of K-feldspar compared to biotite.

The rare occurrence of chlorite and the more commonly observed alteration of micas to kaolin (e.g. Plate 2c), indicates reducing conditions necessary for chlorite authigenesis were not ideal and may have only been achieved locally.

Some chlorite can also form directly from the alteration of illite, typically around illite boundaries (Curtis et al 1985) but this was not observed by SEM.

7.3.9 Other minerals

Rutile and tourmaline occur in trace amounts in some samples and have a detrital character.

Carbonaceous material is quite common in finer grained sediments and has a detrital and biogenic origin.

To examine the premise that coals and carbonaceous shales may be involved in localised diagenetic reactions (e.g. by making porewater more acid), mineral abundances were compared with distance from coal seams or carbonaceous shales. Using petrological observations of 86 core samples and core logging, no correlation of the incidence of kaolinite, dickite, spar siderite, micritic siderite or illite minerals with distance from coal seams or carbonaceous shales could be made. Similarly, no significant variation between diagenetic mineral abundances either above or below coal seams or

carbonaceous shales was noticed, using the same data.

7.4 Hydrocarbons

At least two occurrences of hydrocarbons were recognised in thin sections. Rare fine blebs of bitumen and oil stained clays form dust linings on detrital quartz grains prior to the development of adjacent overgrowths. Bitumen is also identified within pores lined with quartz overgrowths and pore filling kaolin. Typical observations of grain lining and clay staining bitumen are shown as Plates 3f and 4f.

There appears to be no obvious petrographic evidence of increased abundances of siderite, illite and kaolin between samples taken from water wet zones and samples taken from gas bearing zones (Figures 16,17 & 18). This is consistent with major hydrocarbon emplacement occurring after most diagenetic changes had taken place.

Oil staining of clays is often quite common but is not restricted to hydrocarbon rich zones, as common oil staining of clays can be found in intervals yielding tight and water wet results in Drill Stem Tests (DST's).

7.4.1 Discussion of hydrocarbon occurrence

Observations of oil staining of clays within dust rims, bitumen within quartz overgrowths and the presence of hydrocarbons in small fluid inclusions within quartz overgrowths (Russel & Bone 1989) indicate that hydrocarbon generation is associated with quartz cement formation. Within arenites of the study area, the diagenetic events of hydrocarbon generation and quartz cement may be related in situations where:

- (1) hydrocarbons were generated at depth before and during an initial quartz cement period, or
- (2) hydrocarbons migrated into recently deposited sediments, or
- (3) there was early phase of hydrocarbon generation, or
- (4) an initial quartz cement formed at shallow depths and a subsequent quartz cement was formed during hydrocarbon generation at greater depth.

The latter option appears more tenable and is suggested by the preservation of the open grain fabric of arenites, an initial pervasive, possibly meniscus quartz cement and hydrocarbons found within subsequent quartz cements.

Without an initial cement or high pore water pressure formed soon after deposition, the open grained texture of the arenites would not be preserved during sediment burial down to depths associated with hydrocarbon generation. It is also unlikely that migrating hydrocarbons infiltrated and stained uncemented, clay coated grains soon after sediment deposition, as the pre-Permian basement rocks and basal Cooper Basin sediments show minimal source potential or were immature during deposition of the Cooper Basin sequence (Hunt et al 1989). However, limited hydrocarbon generation from the pre-Permian basement during and after the deposition of the Cooper Basin sequence cannot be ruled out.

Most workers (Kantsler et al 1983, Kanstler et al 1986, Pitt 1986) attribute hydrocarbon generation in the Cooper and Eromanga Basins to be initiated by a single, rapid loading during the Cretaceous. This implies that the related processes of hydrocarbon generation (or migration) and quartz cementation occurred during the Cretaceous at depths generally greater than one to two kilometers and that oil generation in the Cooper Basin is consistent with one event.

However, petrology and CL indicate hydrocarbons in coarse arenites of the study area are found either trapped in quartz overgrowths as bitumen, oil stained clays and possibly fluid inclusions, or as more common pore fill. The pore filling hydrocarbons apparently postdate the hydrocarbons found within the earlier formed, pore lining quartz overgrowths, indicating that more than one phase of hydrocarbon generation has occurred.

Several possibilities for early hydrocarbon generation indicated by hydrocarbons found within early formed quartz overgrowths are:

- (1) Localised maturation. Higher and more localised heat flows have been reported for the Cooper Basin interval than the Eromanga Basin sediments (Kanstler & Cook 1979). This, together with variation in depth of burial of sediments in different parts of the Cooper Basin, may have resulted in early hydrocarbon generation and lateral migration. Pitt (1986) explained localised high geothermal gradients in the Strzelecki area by invoking a shallow, but not drilled or seismically defined granite intrusion, or a possible crustal "hot spot".
- (2) Different source types. Taylor et al (1988) report significant submicroscopic alginite within inertinite rich Patchawarra coals in the Patchawarra Trough. Within the study area, disseminated and patchy algae rich organic material within sediment pores may have matured at a different rate to surrounding inertinite rich coal and shales, or were trapped in situ and matured within subsequent quartz overgrowths.
- (3) Transient heating events. Occasional high hydrocarbon palaeo-temperatures have been recorded from fluid inclusions within the southern Cooper and Eromanga Basin sediments by Russell & Bone (1989) in two wells not in the study area. They consider these to possibly be caused by

transient heating events of short duration.

- (4) Initial regional maturation. Estimates of (?) Late Triassic to Early Jurassic Cooper Basin section lost by erosion during the Jurassic unconformity vary from less than 500 metres (Kantsler et al 1983, Pitt 1986), 400-600 metres (Padmasiri & Cook 1983) and 1473 metres for Strzelecki 1 well data (Russel & Bone 1989). If the latter estimate is correct it is conceivable that parts of the Cooper Basin such as the Strzelecki area were generating hydrocarbons before the generally accepted Cretaceous hydrocarbon generation event.
- (5) Early maturation of in-situ organic matter. In-situ or detrital organic matter may have matured earlier than other, more voluminous hydrocarbons that were expelled into coarse sediments during hydrocarbon generation from adjacent source rocks.
- (6) The migration of hydrocarbons from the pre-Permian basement.

Using petrological studies it is not possible to resolve which of these alternatives is applicable, if any.

There are numerous unresolved problems if one accepts that multiple phases of hydrocarbon generation have occurred. It is not clear how or where the first formed hydrocarbons were generated, or whether the two indicated phases of hydrocarbon generation were two mutually exclusive events or a more complex but contemporary single phase. It is also not clear how oil migration has influenced the microscopic occurrence of hydrocarbons or why the presence of hydrocarbons has not apparently inhibited diagenetic events that were presumably concomitant, as there is little petrographic difference of samples taken from water and gas bearing zones in wells.

In brief, one must conclude that the bulk of hydrocarbons generated from source rocks within the Cooper Basin migrated into and along adjacent arenites whose petrographic character was mostly similar to modern day Cooper Basin arenites. Observations of hydrocarbon occurrences in arenites of the study area indicate an early phase of hydrocarbon generation or early migration of hydrocarbons into the Cooper Basin before the Cretaceous.

7.4.2 Conclusions - hydrocarbon occurrence

Hydrocarbons found in arenaceous samples of the study area were generated from source rocks at depths greater than one kilometer. At least some authigenic quartz cement was formed in conditions of pressure and temperature associated with hydrocarbon generation.

There is a possibility that there were two phases of hydrocarbon generation / migration or that the commonly accepted single phase of oil generation was a long and complex event. There appears to be little inhibition of diagenetic events by hydrocarbon emplacement.

7.5 Porosity observations

Volumetrically important types of porosity in the samples studied are primary porosity and the dissolution of unstable components to form secondary oversized pores. There is some micro-porosity associated with the kaolin minerals. Fracture porosity is rare.

Primary porosity (e.g. Plate 2h) appears to be the major effective porosity type. Most larger primary pores within coarse grained samples are lined with subhedral to euhedral quartz overgrowths and porosity appears to be dependent on the extent of quartz overgrowths. Primary porosity estimated from thin section does not appear to be dependent on illite (Figure 19), kaolinite or dickite (Figures 20 & 21), grain size (Figures 22, 23 & 24), or illite/kaolin (Figure 25) of samples.

Porosity appears better developed in poor to moderately sorted arenaceous samples and less developed in well sorted arenaceous samples (Figure 26), regardless of grain size. All sorting estimates apply to the grain size distribution of the framework grains within a sample, not including clays.

7.6 Permeability observations

Permeability could not be empirically estimated from thin section or SEM studies. All permeability data are derived from the testing of core plugs immediately adjacent to core samples.

Permeability is not generally related to grain size (Figure 27), primary or secondary porosity (Figures 28 & 29) but is dependent on sorting (Figure 30), illite (Figure 31) and siderite abundance (Figure 32). The association of illite and siderite with low plug permeabilities may be due to siderite and illite rich sediments commonly being fine grained. As with porosity, plug permeability values are generally less in well sorted than moderate to poorly sorted arenaceous samples with average grain size less than 1mm diameter.

7.7 Compaction effects

Compaction is evident in thin sections from bent mica flakes, deformed lithic fragments, alignment of clay plates, sutured grain contacts (microstylolites), dissolution seams and stylolites. Stylolites and sutured grain contacts are not common.

The finer grained sediments appear to have been most affected by compaction. Deformation effects are more obvious in sediments that contain muscovite, rock fragments, coaly stringers and a high proportion of clay matrix.

Muscovite grains appear as tabular grains that are commonly bent or broken. They appear to be in contact with detrital grain surfaces indicating deformation associated with compaction rather than in response to localised quartz growth of adjacent detrital quartz grains.

Rock fragments, coaly stringers and mud rip up clasts sometimes show ductile deformation. Some fine grained rock fragments are observed to be disaggregated to varying degrees.

7.8 Diagenetic sequence

Very little regional or intraformational variation of diagenetic effects has been recognised in the study area.

The first diagenetic influence on study area sediments was the precipitation of primary micritic siderite soon after deposition of lake and swamp sediments.

Initial compaction by lithostatic pressure in the vadose zone led to partial slumping of fine grained sediments indicative of dewatering of clay laminae. In some shales and silts, considerable bioturbation has disrupted fine laminae, some of which were enriched in micritic siderite.

The dissolution or alteration (kaolinisation) of some feldspar and rock fragments probably occurred during fresh meteoric groundwater flushing of coarser sediments. Both flushing meteoric waters and the kaolinisation of feldspars may have supplied silica for a major early phase of silica cement in arenites, preventing subsequent compaction and preserving the open grained nature of the sediment.

Towards the end of the formation of silica cement the pore water chemistry stabilised allowing initial coprecipitation of (?) dickite and quartz, and later precipitation of dickite to further fill pore spaces. The continued precipitation of authigenic kaolin indicates prevalent non-alkaline conditions.

There may have been limited hydrocarbon migration from the pre-Permian basement into the

Cooper Basin before the Cretaceous.

Some silica later precipitated as overgrowths following sediment burial at depths greater than one kilometer, probably during initial hydrocarbon generation associated with Cretaceous basin subsidence. Most of the cementing silica may have been derived from compacting clays, dissolution seams, rising thermal waters, pressure solution or continued feldspar alteration.

Spar siderite precipitation occurred after most quartz cement formation and is locally associated with the first formed micritic siderite.

Migrating hydrocarbons during the Cretaceous postdate dickite formation and the petrological character of the reservoir sandstones during oil migration appears to have been similar to their present condition.

The final diagenetic events involve the precipitation of minor authigenic fibrous illite and chlorite.

Dissolution or alteration of feldspar, mica and rock fragments may have persisted during and after quartz cementation.

The proposed sequence of diagenetic events is graphically presented in Figure 33.

7.9 Previous diagenetic studies

Staughton (1985) examined 7 Patchawarra Formation samples and 88 Toolachee Formation samples as part of a study to determine diagenetic effects of both Cooper and Eromanga Basin sequences of the Strzelecki Field.

Petrological features reported by Staughton are generally similar to the petrology of samples studied for this report.

Diagenetic features reported from samples of both the Toolachee Formation and Patchawarra Formation were similar. Patchawarra Formation arenites (in Strzelecki 1) were reported to have low authigenic quartz content of usually 2%, with greatest authigenic quartz content in arenites of high porosity and the lowest in rock types with high authigenic clay content.

Porosity was reported to be influenced by compaction, quartz overgrowths, calcite and siderite cementation and growth of kaolinite and minor illite. Considerable secondary porosity is reported for both formations. Permeability was related to the mineralogical composition of the reservoir sandstones (Staughton, in Wall 1987). Staughton proposed a six fold sequence of diagenetic events:

- (1) (earliest); dissolution and partial alteration of feldspars, rock fragments and detrital matrix to form minor secondary porosity.
- (2) significant quartz overgrowths, limited kaolinite and minor illite authigenesis after partial compaction. Initial hydrocarbon formation.
- (3) extensive and intense replacive calcite and siderite cementation after further compaction.
- (4) widespread dissolution of unstable grains and carbonate cement.
- (5) extensive kaolinite and quartz authigenesis.
- (6) (latest); hydrocarbon migration.

Martin (1988) examined 6 samples of core plugs taken from the Patchawarra Formation arenites of Pira 2 to determine petrological effect on reservoir quality. He reported that all diagenetic processes have reduced porosity and permeability with no secondary porosity being developed. The diagenetic features of these samples are listed in decreasing order of importance as:

- (1) Authigenic clay formation from decomposition of lithic, mica and feldspar components of framework grains. Precursors to dickite formation were feldspars and some lithics and micas. Dickite is more densely packed as a framework grain replacement product than loose pore filling kaolinite clays generally found in "many" sands. Illite precursors appear to have been micas and micaceous rock fragments such as shales and phyllites. Illite tends to be more evenly distributed than the patchy grain replacement dickite.
- (2) Quartz overgrowth cementation which is common but restricted by widespread authigenic clays inhibiting overgrowth development. In some places quartz overgrowths have partly enclosed authigenic kaolinite clays and some fragments of dolomite.
- (3) Pressure solution causing suturing and interlocking of grains, apparently related to the decomposition of mica which also line many of the microstylolite dissolution seams.
- (4) Authigenic carbonates mostly confined to mica and carbonaceous material rich laminae and dispersed as replacement of biotite and other micaceous and lithic fragment framework grains. Rare dolomite with corroded edges was recorded.

The diagenetic sequence proposed by Martin (1988) begins with early carbonate formation which may have accompanied the early stages of a long period of decomposition of framework grains to authigenic clays, with most dickite formation probably occurring before that of illite. Subsequent grain suturing, pressure solution and illite formation preceded a phase of carbonate removal followed by the formation of quartz overgrowths into any pore spaces not already filled with clays.

Martin has reported mostly similar diagenetic effects in previous publications on the reservoir quality of other hydrocarbon fields in the Cooper Basin (Martin 1980, Martin & Hamilton 1981, Martin 1981, Martin 1982, Martin 1984). Other workers have also examined diagenetic effects in Cooper Basin hydrocarbon fields outside of the study area, including Almon & Davies (1981) and Stevenson (1985).

One can see that dissension exists between all authors as to the order, timing and complexity of events which mostly reflects the complexity and basin wide variation of diagenetic processes. Even so, two fundamental concepts promoted in this report contrast with previous interpretations of diagenetic history. Firstly, it is considered hydrocarbon generation occurred before and during some phases of quartz cementation and secondly, recrystallisation of spar cement is directly related to the occurrence of micrite siderite.

CL work has both confirmed and emphasised the occasionally substantial amount of authigenic silica derived from several possible sources at substantial depths. These include compacting clays, dissolution seams, rising thermal waters, pressure solution and alteration of lithics. Even so, pressure solution is not considered to have supplied much silica for overgrowths.

Generally, the role of sedimentary processes and environment on the diagenetic character of sediments is not accorded much detail in previous studies, apart from acknowledging the role of provenance and grain size as factors in diagenetic assemblages.

8 Petrophysics

8.1 Core plug data analysis

A substantial amount of the core taken from wells in the study area has been analysed for petrophysical properties by taking small plug samples of core for testing. Core plugs are generally taken from intervals of core that show potential reservoir characteristics and are mostly fine to very coarse arenites. Generally few very fine grained rock types such as shales and siltstones are sampled.

Most plugs are tested for residual water and oil, density, porosity and permeability. Some plugs have been tested for horizontal and vertical permeability, at ambient and overburden pressures and in helium, air and water mediums.

Details of 706 core plug data sourced from the Cooper Basin interval of the study area are listed in Table 5. In addition to this group, data from the testing of 436 core plugs from the Eromanga Basin interval of the study area were combined to study porosity and maturity variations with depth.

Well	Formation	Plugs
Coochilara 1	Epsilon	5
Coochilara 1	Patchawarra	6
Dilchee 1	Patchawarra	6
Kerna 1	Roseneath	11
	Epsilon	9
	Patchawarra	16
Kerna 2A	Patchawarra	17
Kidman 1	Toolachee	25
	Patchawarra	48
Kidman 2	Toolachee	44
	Epsilon	8
Marana 1	Toolachee	29
Pira 2	Toolachee	7
	Patchawarra	28
Strzelecki 1	Toolachee	68
	Patchawarra	26
	Toolachee	38
Strzelecki 2	Toolachee	41
Strzelecki 3	Toolachee	32
Strzelecki 5	Toolachee	86
Strzelecki 10	Toolachee	56
Strzelecki 15	Toolachee	42
Strzelecki 16	Toolachee	58
Wanara 1	Toolachee	
	TOTAL	706

Table 5 Core plug data origin of Cooper Basin interval of wells in the study area. 55% of data comes from the Strzelecki area; 75% of data are the results of testing Toolachee Formation core. Core plug data is sourced from Santos Ltd., South Australian Department of Mines & Energy and this report (Table 1).

Bearing in mind that only competent sands are tested by core plugs, it is expected that porosity decreases with depth within the same reservoir formation in response to increased effective stress with sediment loading. Such a porosity trend is observed for the Toolachee and Patchawarra Formations in Figure 34 with the trend for Patchawarra data showing generally lower, but similarly decreasing porosity values.

When core plug porosity is plotted with depth from the major unconformity at the top of the Cooper Basin sequence (Figure 35) a reduction in porosity is observed within 100 metres (350 feet) below the unconformity. This is confirmed by a similar trend for core plug permeability (Figure 36 & 37) and possibly for primary and secondary porosities measured from thin sections (Figure 38).

It is important to note that most higher levels (2% to 32%) of residual oil are recorded from core plugs taken from the transition area of 60 to 200 metres (200 to 650 feet) below the basal Jurassic unconformity (Figure 39), where porosity and permeability are highest.

Insufficient data for the study area is available to determine the effects of different types of permeability measurements such as water to air, ambient to overburden, vertical to horizontal etc.. Coles, Nikiforuk, Pennell (1987) report a few abnormally high porosity measurement reductions under confining pressure, possibly due to laboratory procedures such as drying, coring and triaxial pressure confinement. Porosity and permeability enhancement is expected for unloading of samples from conditions of high stress at depth.

8.2 Flow data analysis

To examine the influences on *in situ* permeability, the results of the pressure testing, or Drill Stem Testing (DST) of intervals of wells within the study area were used. DST results over intervals containing Patchawarra and Toolachee Formation sands are presented in Appendix 7.

To examine the relationship of DST testing to geology, DST ratings are compared with facies associations and inferred depositional facies in Figures 40,41 and 42. In all, 79 DST results are compared, using a rating scheme presented in Table 6. It was considered necessary to adopt a rating scheme to differentiate between water produced, No Gas To Surface (NGTS) and Rate Too Small to Measure (RTSM) results of DSTs. No drill stem test that extended over sand intervals of more than one facies association is plotted.

DST rating:	DST results:
0	water
1	tight, no gas to surface (NGTS)
2	trace gas, rate too small to measure (RTSM)
3	0.1 to 1 million cubic feet per day (MMCFD)
4	1 to 2 MMCFD
5	2 to 3 MMCFD
6	3 to 5 MMCFD
7	5 to 7 MMCFD
8	7 to 10 MMCFD
9	> 10 MMCFD

Table 6. Terminology used in the listing of DST results.

Histograms of DST results and DST ratings in Figures 42 and 43 respectively show a bimodal distribution of flow rates. It appears that all tested sands will either flow gas copiously or be very tight; there seems to be no gradation between the two flow conditions.

DST results plotted for the four Toolachee Formation facies associations (Figure 40) and the two upper most Patchawarra Formation facies associations (Figure 41) also show a bimodal spread of

DST results with no single association showing consistently higher or lower gas flow rates.

DST results plotted for the more common channel and overbank deposits in Figure 42 show a similar distribution with no genetic sequence showing consistently higher or lower gas flow rates.

DST results for the four Toolachee Formation facies associations are plotted against radial distance from Strzelecki 2, located in the southwest corner of the study area (Figure 44). Again, only test results of single facies associations are used and where only part of a single association was tested, DST results are shown as being greater than the highest DST result for that association.

No pattern of DST results with position is indicated in Figure 44, indicating gas flow permeability as indicated by DST testing is not a regionalised variable on the scale of the study area.

In conclusion, DST results presented here preclude a simple causal relationship between flow rates and single macroscopic geological features such as facies associations and genetic sequences. The bimodal distribution of DST ratings may be caused by a fundamental factor(?s), possibly on a microscopic scale such as types or proportions of clay, interconnection of pore spaces etc.

It is difficult, however, to identify such a cause by petrological analysis of point samples taken from within a DST interval. Other problems with interpreting DST results are listed in Appendix 7 and include formation damage, short test times and less than ideal flow conditions.

8.3 Groundwater

The Cooper Basin and pre Cretaceous Eromanga Basins sediments were all deposited in a freshwater fluvial and lacustrine environment, with possibly some restricted marine influence during the deposition of the Permian shales.

Thick sequences of deltaic to marine shales deposited in the Early Cretaceous effectively sealed low salinity Permian to Jurassic pore waters from overlying marine waters

Regional uplift during the Late Cretaceous to Early Tertiary exposed the Jurassic and Cretaceous sequence to fresh water recharge in artesian conditions that is currently occurring today from the Great Dividing Range area in Queensland, 1000 kilometers east of the study area.

Prior to this uplift, Coles, Nikiforuk, Pennell (1987) surmise that groundwater in the southern Cooper Basin area was essentially static.

Post Jurassic fresh water recharge has removed and replaced a significant proportion of the original

Permian connate water (Faehrmann 1986) by water movement at fault zones and unconformities. Replacement of the original Permian waters is not complete in low permeability areas, in stratigraphic traps and in structural closures. These areas of stagnant waters are marked by higher salinities ranging from 10,000 to 20,000 ppm, compared to salinities of 1000 to 4000 ppm for flushing waters (Faehrmann 1986).

Permian waters also have more NaCl and less HCO_3 than the flushing waters (Faehrmann 1986). Both water types are low in sulfate, nitrate, calcium and magnesium.

Bowering & Burnett (1980) report an overall increase of salinity with depth within both the Toolachee and Patchawarra Formations, caused either by considerable ionic exchange and diffusion between Jurassic and Permian waters or by groundwater flushing. They also report that higher salinity waters are associated with hydrocarbon occurrences in various fields throughout the Cooper Basin.

Abnormally high porosities (to 30%) are reported for Permian reservoir units along the Southern Cooper / Eromanga Basin margin compared to the low porosities (e.g. 9%) in the northern Cooper Basin by Hunt (1985). He attributes this to large scale mass transfer associated with meteoric water movement and diagenesis, possibly made more acidic by concurrent early organic matter maturation.

8.3.1 Water sample data analysis

A total of forty chemical analyses of groundwater taken from Drill Stem Tests (DST's) of Permian intervals of wells within the study area has been analysed. Raw data is listed in Appendix 8.

The abundance of Na, Ca, Mg, Cl and total dissolved salts (Figure 45) generally increase with depth below the Jurassic unconformity. pH and HCO_3 concentration did not show any pattern with depth.

A plot of depth versus groundwater salinity expressed as Total Dissolved Salts (TDS) in Figure 45 show high peaks at 180 to 260 metres (600 to 850 feet) and at 700 metres (2300 feet) below the Jurassic unconformity. These salinity peaks occur at depths immediately below the increased porosity zones indicated by Figure 35 and described in Section 10.2, below.

The lack of high salinities within the reduced porosity and permeability zone up to 100 metres (350 feet) below the Jurassic unconformity may indicate gravity drainage of porewater into the uppermost high porosity zone or a different groundwater regime associated with the unconformity.

However, these high salinity peaks may also be associated with the occurrence of hydrocarbons (Bowering & Burnett 1980). There is insufficient data to assess these or other salinity trends within

the study area.

9 Reservoir quality

This chapter summarises major influences on reservoir characteristics in the study area. Porosity variations are divided into basin wide trends (first order porosity variations) and formation trends (second order porosity variations). Other porosity variations and major influences on porosity and permeability are listed and discussed.

9.1 First order porosity variations

The major control on porosity within the study area is depth.

A plot of porosity with depth in the Eromanga and Cooper Basin intervals of Strzelecki 10 (Fig 46) is typical of a first order variation of porosity with depth, if low porosities of the carbonate cemented Adori Sandstone are excluded. Porosity values of the Eromanga Basin arenites are generally higher than the Cooper Basin arenites because of less depth of burial.

The rate of decrease of porosity is higher for the Cooper Basin sequence than for the Eromanga Basin sequence, with an inflexion point between the two porosity to depth trends occurring at Toolachee Formation or Nappamerri Group depths.

A similar trend is shown in a plot of vitrinite reflectance (V_r) with depth in wells located in the study area (Figure 47). The rate of increase of V_r with depth, is greater in the Cooper Basin than the Eromanga Basin sequence.

The inflexion point between the two V_r /depth gradients is placed by Keiraville Konsultants (1984) at depths corresponding to the Toolachee Formation in Dilchee 1. Kantsler (1979(a) and (b)) places the inflexion point at depths corresponding to the basal Jurassic unconformity for Strzelecki 3 and Kidman 2 wells, while for Coochilara 1, Kantsler (1978) proposed a unique curved relectance/depth relationship rather than a single inflexion point, but commented that more sampling was needed.

Based on the above data, it is possible that both porosity and hydrocarbon thermal maturity are related. Both factors are depth dependent and have inflexion points at similar depths, generally within the Cooper Basin sequence. Insufficient core plug data and corresponding maturity data exists for the study area (43 points in total) to otherwise establish such a relation with any level of statistical certainty.

The relationship between maturity and porosity is probably related to the fact that time and temperature dependent changes associated with maturation are also major physical causes of diagenetic events in the study area.

9.2 Second order porosity variations

As a general trend, porosity decreases with depth within reservoir intervals of the Toolachee and the upper Patchawarra Formation arenites as shown in Figure 48. This relationship is most likely due to increasing effective stress of a mostly competent sandstone body with depth.

In contrast, tested Epsilon Formation reservoir units have generally lower porosities because of thinner and finer sands influencing both flow characteristics and competency. Such low competency arenites would be expected to be affected by burial more than the more competent arenites of the Patchawarra and Toolachee Formations

Lower Patchawarra Formation arenites also show a first order porosity baseline offset with increased porosities at 2500 metres (8200 feet) in Figure 48. Below this depth porosity values again decrease and show a second order trend. Arenites at this depth may be considered a separate, mostly competent arenaceous body within less competent sediments, similar to arenites at the top of the Patchawarra Formation.

In contrast to other reservoir units, porosity and permeability appear to decrease towards the top of the Toolachee Formation, possible due to the influence of unconformities above the Toolachee Formation. Unconformity effects are discussed in Section 9.5, below.

9.3 Other porosity variations

Most porosity identified by thin section is primary porosity, characterised by small, intergranular voids. Other forms of observed porosity include secondary porosity and microporosity.

Secondary porosity formed by the dissolution of feldspars and lithic fragments is sometimes locally abundant. It is not considered to significantly influence effective porosity and permeability of arenites in the study area because of its low incidence and low apparent pore connection.

Microporosity is present as fine pore spaces incorporated within clays. Within study area arenites, higher microporosities visually estimated in thin section as up to 9% are mostly associated with authigenic kaolin, especially coarse grained dickite.

A plot of dickite with permeability in Figure 49 shows permeability shows little increase with increasing dickite content. This implies that microporosity associated with dickite appears to be non-effective porosity that does not greatly influence permeability. This may be due to poor connection of pores, varying crystallinity, crystal size, shape or packing of dickite or as a result of water or oil saturation restricting fluid flow in small pore throat openings.

Core plug porosities represent the sum of all three types of porosities within tested core samples. Relationships between core plug porosity and average grain size, sorting, roundness and sphericity derived from core logging are ill defined. Similarly, little to no correlation between visual primary porosity, secondary porosity and microporosity estimates from core sample thin sections and petrographically derived average and maximum grain size, sorting, roundness and sphericity estimates was apparent.

The lack of correlation between porosity types and primary sedimentological features such as grain size may be attributed to several causes. Most importantly, pervasive quartz overgrowths mask coarse sedimentary grains and make roundness and sphericity estimates of arenites meaningless and also affect grain size and sorting estimates. Other likely causes for poor correlation include complex interactions of influences on porosity and the relatively large uncertainties inherent in visual estimation of grain attributes and porosity.

9.4 Permeability variations

Permeability of plugs taken from near samples studied appears to be more variable in coarse grained sediments than fine grained sediments (Figure 50). Permeability is generally low in fine grained sediments but varies from low to high in coarse grained lithologies.

Many workers (Overton & Hamilton 1986, Coles, Nikiforuk, Pennell 1987, Overton & Evanochko 1987) have demonstrated a generally positive linear relationship between \log_{10} permeability and porosity from core plug data in most areas of the Cooper Basin, including the study area. All relationships appear field specific and show a considerable spread of data points.

The relationship between core plug porosity and permeability within the study area depends on grain size and depth. Figure 51 shows an otherwise constant \log_{10} permeability to porosity ratio that decreases with average grain size below approximately 0.2mm diameter, possibly due to increased clay microporosity in finer sediments. The \log_{10} permeability to porosity ratio also seems to decrease at depths greater than 2400 metres (8,000 feet) in Figure 52 but more data is needed to confirm this trend.

Permeability is generally more sensitive to overburden conditions than porosity. Coles, Nikiforuk,

Pennell (1987) reported that an average core sample with an ambient permeability of 0.5 md has a permeability of 0.1 md when tested at "reservoir" conditions.

However, no systematic variations of different types of permeability measurements (air to water, overburden to ambient, vertical to horizontal etc.) were observed at different depths or geological settings, using core plug data.

There was no clear relationship between high permeability and petrology, even with samples of visually high primary porosity.

9.5 Influence of unconformity on reservoir quality

In this section the apparent reduction of core plug porosity and permeability towards the top of the Toolachee Formation in the study area is discussed. This topic was previously introduced with the analysis of core plug data in Section 8.1 and warrants further discussion.

The following sub-sections consist of observations, a summary of the geological significance of unconformities in the upper part of the Cooper Basin sequence, possible mechanisms of unconformity related diagenesis and a discussion of points raised. A summary concludes the section.

9.5.1 Unconformity effects - observations

Core plug testing indicates a reduction of porosity and permeability in Toolachee Formation reservoir sands within the upper 100 metres (350 feet) of the Cooper Basin sequence (Figure 35 & 38). Porosity and permeability reduction increases towards the top of the sequence.

Most higher levels (2% to 32%) of residual oil (recorded as a percentage of available porosity) in core plugs come from below this zone of reduced porosity and permeability (Figure 39). Residual oil as recorded by core plug measurements is restricted to core plugs with porosities of 3% to 21% (Figure 53). It is not clear whether some oil stained core plugs were cleaned before testing.

There appears to be no obvious variations of petrographic features of arenaceous samples across this zone. There appears to be no relationship between reservoir quality and the Daralingie Unconformity at the base of the Toolachee Formation.

9.5.2 Nature of the unconformity

The Cooper Basin to Eromanga Basin transition involved at least several phases of non-deposition,

exposure and erosion. The unconformity associated with basal Jurassic Eromanga Basin sedimentation is only one of a number of unconformities that may have associated local diagenetic alteration of the underlying Cooper Basin reservoirs. Later periods of erosion has removed some of the unconformity surfaces.

Palynological evidence indicates an hiatus between the Toolachee Formation and the overlying Late Permian to Middle Triassic Arrabury Formation of the Nappamerri Group (Powis 1989). The Arrabury Formation consists of lacustrine to fluvial shales and minor sands. The presence of minor red beds and the lack of carbonaceous material suggests hot, humid and oxidising climatic conditions at deposition.

Although Mid to Late Triassic Nappamerri Group sediments younger than the Arrabury Formation are missing in the study area, they occur in the northern Cooper Basin (Barr & Youngs 1981) as the Tinchoo and Cuddapan Formations. Powis (1989) reports unconformities at the base of each formation.

A widespread Mid to Late Triassic tectonic event terminated Triassic sedimentation and led to a 45 m.y. time break with erosion of 400 - 600 metres of sediment (Padmasiri & Cook 1983). Within wells of the study area, Triassic sediments of the Nappamerri Group vary in thickness from 55 metres (178 feet) in Strzelecki 3 to 214 metres (702 feet) in Dilchee 1.

To summarise, there are several established and inferred unconformities and depositional hiatuses between the end of deposition of the Permian Toolachee Formation and start of deposition of the Jurassic Hutton Formation. Some Triassic unconformity surfaces have been eroded.

9.5.3 Mechanism of unconformity related diagenesis

Shanmugam (1989) reports that porosities in clastic reservoirs increase towards overlying unconformities in many parts of the world. He attributes this to dissolution of unstable grains and cements due to chemical weathering intensified by subaerial exposure under heavy rainfall conditions.

Within the study area a decrease of porosity towards the overlying Jurassic unconformity is noted. Both primary and secondary porosities are observed to decrease in this zone.

The proportions of illite (Figure 54), kaolinite and dickite (Figure 55), siderite (Figure 56) and the illite to kaolin ratio (Figure 57) do not greatly vary across the unconformity zone, indicating the observed reduction of porosity and permeability in the unconformity zone is not attributed to a single lithofacies, genetic unit or facies association. Similarly, the varying depths below the Jurassic

unconformity of the various facies associations and the select testing of reservoir type sands as core plugs preclude rock type changes causing the observed porosity and permeability reduction.

As indicated by petrology, there is no discernible increase in weathering products near the unconformity surface. It is possible that increased silica cementation of primary pores or compaction has caused most of the reduction of porosity within the unconformity zone, but insufficient cathodoluminescence measurements of coarse grain arenites have been taken to confirm this possibility.

Several mechanisms may be invoked to explain reduced porosity within the unconformity zone that do not involve changes in clay or siderite content. These are:

- (1) Reduced rate of sediment loading. The lack of sediment loading caused by non deposition may have led to a lack of high pore water pressures that was possibly endemic to the rest of the Cooper Basin sequence. This would allow more compaction during subsequent loading and therefore reduce porosity.
- (2) Stress redistribution following erosion. Stress redistribution of the upper part of the basin may have accompanied the unloading of the sedimentary pile by Triassic to Lower Jurassic erosion, allowing diagenetic changes in response to decreased effective stress together with more compaction due to reduced pore water pressures.
- (3) The formation of duricrusts. Siliceous and calcareous duricrusts have been reported within the South Australian section of the Jurassic Hutton Formation by Gravestock et al (1983). Similar cemented zones were observed in the Surat Basin and in Middle to Late Jurassic duricrusts from southwest Queensland, where the Eromanga Basin sediments outcrop. Gravestock et al (1983) attribute the origin of these duricrusts to surficial weathering in a warm, arid to humid climate during periods of non deposition.

A similar weathering process is indicated for the Cooper Basin by Wopfner (1972) who states that climate during deposition of the Cooper Basin sediments was initially cool but became rapidly warmer and humid towards the latter part of the Permian and Triassic. However, if duricrusts do exist in the study area they have not been recognised with core logging and as such would not be significant features at that scale.

- (4) The squeezing of oxidizing connate waters from the Nappamerri Group shales downwards and along the Toolachee Formation arenites (N. Lemmon, pers comm). The change in chemistry of porewater within the upper part of the Toolachee Formation may have minimised dissolution or maximised silica cementation during compactional water extraction.

Because of the lack of evidence of duricrusts or zones of increased cementation towards the top of the Cooper Basin sequence it is more likely that erosion or reduced deposition of the Toolachee Formation or the migration of pore water from the Nappamerri Group sediments has caused the observed porosity and permeability reduction in the study area. All involve changes in pore water pressures and the relevance of abnormal pore water pressures or overpressures to the study area is discussed in Section 10.8 below.

9.5.4 Discussion of unconformity influence on reservoir quality

It is important to bear in mind that the reported decrease of porosity and permeability associated with the unconformity zone may just be an aberration of the collected data and in fact, no such effect exists. This may be an artificial result of sampling intensity, a result of sampling different rock types or an incidental combination of factors giving a casual relationship. However, there are several observations that should be considered in confirming the existence of the effect.

Firstly, both permeability and porosity vary in a similar manner in the unconformity zone (Figures 35, 36 and 37).

Secondly, no similar decrease in porosity is observed in core plugs taken towards the top of the Patchawarra Formation.

Thirdly, there is no systematic variation of plug tested porosity and permeability with relative position in the Toolachee Formation (Figures 58 & 59). As there is also little observed systematic variation of illite, kaolin and siderite with depth from the unconformity, it is unlikely a single geological feature within the Toolachee Formation, such as facies or change in provenance has caused the observed depth related decrease of porosity and permeability. For these reasons it is unlikely that the reduced porosity zone can be attributed to the Toolachee Formation Unit B of Stuart (1976) being more silty than the underlying Toolachee Formation Unit C during deposition.

Finally, data has been widely sourced from over 600 data points from core in 17 wells and from various geological settings within the study area.

It is possible that the sands within the Toolachee Formation Unit B (Stuart 1976) are thinner, less competent and are more affected by sediment loading than the thicker sands of the lower Toolachee Formation Unit C.

To confirm the validity of the unconformity effect hypothesis, it is necessary to identify the

relationship between porosity, permeability and depth from the top of the Cooper Basin sequence in other areas of the Cooper Basin, particularly where Triassic sediments are thin or absent.

Bearing in mind the concentration of core plugs with high residual oil measurements below the reduced porosity zone (Figure 39) it is possible that hydrocarbons may be, or have been restricted to a higher porosity and permeability zone 100 to 140 metres (350 to 450 feet) below the Jurassic unconformity. Alternatively, the concentration of hydrocarbons in this zone may have prevented or restricted the effects of diagenesis and preserved some primary porosity.

Future exploration plays for hydrocarbons may be formulated based on the above higher permeability and porosity zone, particularly where it forms as an anticline, terminates against a fault, fold or stratigraphic change or where it provides a fairway for movement into or out of established reservoir beds or other types of traps (Moore 1985).

9.5.5 Conclusions - unconformity effects

It is considered that the apparent reduction of arenite porosity and permeability towards the top of the Toolachee Formation in the study area is real. However, its cause is not clear. One major problem in determining its cause is insufficient measurements of the amount of authigenic quartz within coarse samples, although similar illite, kaolin and siderite abundance towards the top of the Toolachee Formation preclude any single rock type or increase in weathering products to have reduced reservoir quality.

It is possible that changed conditions of sediment loading that accompanied reduced rates of sediment deposition or erosion at the end of Cooper Basin deposition resulted in greater physical compaction than during previous Toolachee sedimentation, thereby reducing porosity.

9.6 Geological influences on porosity & permeability

Geological variables used to examine porosity and permeability trends in the study area are lithology (mineral constituent, grain size, sorting etc), lithofacies (e.g. St, Sm, Gm as used in core logging), depositional facies or G.I.S. and facies associations or G.S.S. The latter three categories were previously defined in Section 6.3.

Comparative porosity and permeability data are sourced from core plug analyses and thin section estimates. Lithological comparisons were made using 54 core samples taken immediately adjacent to core plug samples. Other comparisons were made using data from 338 core plugs taken from core intervals that were logged for this report.

9.6.1 Lithology

No consistent correlation of all types of measured porosity (primary, secondary, total) with physical sample and core logging measurements (average grain size, illite/kaolin, siderite, lithics, sorting etc.) could be made using core samples.

Permeability values of core plug samples tend to be higher in rock types with low illite, kaolin, carbonaceous material, spar siderite and micritic siderite content. Although rocks with low levels of these minerals are typically coarse grained, permeability is not directly related to grain size in the study area. This indicates that more complex, small scale influences on permeability such as grain packing, sorting and pore throat geometries are present.

Permeability is also the most variable, and occasionally high, in samples with lithic components between 5% and 20%. Oil staining of rock fabrics could not be correlated to permeability. Microporosity associated with dickite may be a small factor in permeability.

9.6.2 Lithofacies

No correlation between core logging derived lithofacies of arenites (St, Sh, Sl, Sg, etc. as used for core logging) could be made with grain size, illite, kaolin, siderite or bulk density.

A zonation of plug permeability and porosity values with lithofacies is shown in Figures 60(a) and 60(b). Lithofacies of sands with ripple marks, trough cross laminations, planar cross beds or trough cross beds tend to have the highest porosity and permeability values, horizontally laminated sands slightly lower and gravels have the lowest values. Massive sands have variable porosity and permeability.

9.6.3 Depositional facies

Channel deposits seem to have higher porosity and permeability values (Figure 61) than floodplain, low energy fluvial, overbank and prograding deposits. Channel deposits could not be typified by siderite or illite to kaolin ratio and only a few samples had grain size coarser than samples from other type of deposits.

No generalisation can be made about the characteristics of channel deposits except that they appear more variable than other depositional facies and are potentially the most productive type of sands.

Their porous and permeable nature appears to be intrinsically derived and not due to the thickness or proportions of sand intervals associated with channel deposits.

A characteristic textural feature of possible shoreline facies arenites in the study area (samples 294, 311, 488, 489, 490 of fine grained arenites taken from predominantly prograding sequences) is the common equigranular interlocking of quartz grains, and common dickite. All samples identified as possible shoreline facies arenites had medium to low core plug porosities, low core plug permeabilities (<0.5md) and came from intervals tested by D.S.T. as tight or no gas to surface. The low reservoir potential and prospectivity of shoreline facies arenites within the study area is directly attributed to diagenetic changes of quartz overgrowths and dickite growth.

9.6.4 Facies associations

The poor correlation between DST results with facies associations for the Toolachee and Patchawarra Formations and the high regional variability of DST results (Section 8.2) indicates that local geological influences such as the thickness of sand units, the proportion of channel sands and the distribution of facies types are more important to reservoir quality than formation wide geological influences such as sediment provenance.

9.6.5 Discussion of geology and permeability/porosity

The geological influence on porosity and permeability occurs at several levels. At the lowest level permeability appears to be most influenced by lithological features such as the proportion of illite, kaolin, carbonaceous material, sparry siderite and micritic siderite while the influence of lithology on porosity is not apparent and is most likely masked by compaction, quartz overgrowths or microporosity.

On a larger scale, channel facies deposits and some lithofacies tend to influence porosities and permeabilities in a different manner than that expected of their constituent lithologies. This defies a simple causal relationship between reservoir quality and the sediments or sedimentary processes.

The major complexity in relating the environments of deposition of arenites to present conditions of porosity and permeability is diagenesis. Knowing that most diagenetic processes such as quartz cementation and kaolin pore filling within arenites of the study area have consistently reduced primary porosity after deposition, an important question to ask is:

"what rock types and conditions of initial porosity and permeability would lead to incomplete

diagenetic processes and partial preservation of porosity ?"

Bearing in mind that most porosity observed in all samples is remnant primary porosity, it is found in this study that only the cleaner, coarsest sands have best preserved their initial effective porosity and permeability during diagenesis.

Coarse sediments in a fluvial environment tend to be deposited by rapidly flowing streams or rivers. Apart from coarse grain size, such sediments are typified by ripple marks, trough cross laminations, planar cross beds and trough cross beds associated with deposition in a channel environment. Within the study area, lithofacies containing these sedimentary structures tend to have higher combinations of porosity and permeability (Figure 60b) than gravels, shales and most horizontally laminated and massive sands.

Some horizontally laminated and massive sands with high permeability and porosity may have also been deposited in the upper flow regime of streams, although most would have been deposited in slower flowing streams and consequently display lower porosity and permeability. Gravels from the study area typically have common clay matrix which accounts for their low porosity and permeability.

A distinction must be made between high initial (depositional) porosity and the size of depositional pore spaces present in pre- diagenesis arenites. More diagenetic preservation of porosity occurs in arenites with poor sorting and larger pore sizes than finer, well sorted sediments with equivalent initial porosity. This may explain why fine grained, well sorted monomineralic shoreline sands with high initial porosity now have low porosity and permeability.

To summarise, channel deposits displaying sedimentary structures associated with higher flow regimes are potentially the most productive of sands in the study area. Channel deposits are more likely to have had higher pre-diagenetic porosities and larger pore sizes than other sands.

9.7 Overpressures

In previous sections on quartz cement and hydrocarbon observations in samples, overpressures have been proposed as one of a number of possible mechanisms that may have caused the preservation of an open grained fabric of coarse detrital grains by quartz cement containing hydrocarbons as inclusions. Evidence for whether overpressures, geopressures or abnormally pressured zones exist or have existed in the Cooper Basin is largely circumstantial and warrants further discussion.

Hunt (1989) states:

"Many sedimentary basins have a layered arrangement of two or more superimposed hydrogeological systems. The shallow systems are basin wide in extent and exhibit normal hydrostatic pressure. The deeper systems where the oil is generated are not basin wide and are abnormally pressured. They generally consist of a series of individual fluid compartments which are not in pressure communication with each other nor with the overlying hydrodynamic regime."

A similar setting may be inferred for the Cooper Basin. It exists as a hydrologically isolated infrabasin of the larger Eromanga Basin and contains common but often discontinuous fluvial sand bodies within mostly impermeable shales and coal measures, both rich in organic matter. Hunt (1989) uses the concept of periodic expulsion from abnormally pressured fluid compartments to explain vertical movement of hydrocarbons from source rocks to reservoirs just above seals, similar to Permian oil found within the Eromanga Basin sequence (Hutton and Namur reservoirs) above the Strzelecki dome (Richards 1984).

Overpressures are mostly generated by maturing hydrocarbons but can also be induced by rapid sedimentary loading, diagenetic changes such as smectite to illite conversion, tectonic loading by compression and by heating of pore water (Gretener 1978).

The preservation of an open grained fabric within study area arenites at substantial depths has been attributed to an early "meniscus" quartz cement formed within the meteoric groundwater zone. However, overpressures formed soon after deposition may also preserve the open grained fabric of these arenites.

Initial overpressuring of coarse sands may have been caused by sedimentary loading, tectonic compression or pore water heating. Subsequent hydrocarbon generation may have added to existing pore water pressures that, with increasing maturity, led to expulsion and migration of hydrocarbons.

Arguments and evidence for the existence of overpressures within the Cooper Basin are listed below:

- (1) Isolated permeable fluvial sand cells within impervious silts are conducive to overpressures formed soon after deposition.
- (2) Preservation of open grained fabric without major quartz overgrowths indicates overpressures.
- (3) Dewatering features such as slumping and flame structures within mudstones of the study area indicates high porewater pressures soon after sediment deposition.
- (4) High local geothermal gradient may result in aquathermal pressuring by porewater, possibly producing overpressures.
- (5) Few pressure solution effects seen within overpressured zones.
- (6) Patchy and fairly common dissolution seams within arenites may be caused by leaky overpressure cells.
- (7) Common core and drillhole diameter changes possibly correlated to overpressure zones (see Appendix 1).
- (8) Pre-Cretaceous tectonic activity may have increased pore water pressure, changed overburden pressures or redistributed pore water pressures.
- (9) An indicated reduction of porosity and permeability in arenites found towards the top of the Cooper Basin sequence can be explained by considering overpressures (Section 9.5).

Arguments and evidence against the existence of overpressures within the Cooper Basin are listed below

- (1) Lack of severe excess mud pressure (due to overpressures) and lost circulation drilling conditions (due to fracturing associated with overpressures) experienced with drilling into the Cooper Basin interval.
- (2) Low sedimentation rates as reported by Stuart et al (1988) for Toolachee Unit 'C' sands in Big Lake & Moomba Fields are not conducive to the formation of overpressures by sediment loading.
- (3) If overpressures existed before hydrocarbon generation, hydrocarbons could not have entered some overpressure zones.
- (4) Major quartz cement identified as "meniscus" may have preserved open grained fabric of coarser arenites at depth, instead of overpressures.
- (5) Patchy occurrence of authigenic minerals (quartz, kaolin, illite etc) not indicative of uniform overpressure conditions.

Log responses indicative of overpressures such as decreased sonic velocity, density and shale resistivity (Gretener 1978) are applicable to unconsolidated or weak sediments. Consolidated Cooper

Basin sediments that have been cemented would not show these log signatures. Cementation of an overpressured zone would also reduce fluid movement and minimise the incidence of excess mud pressures in drilling.

The need to invoke overpressures within the Cooper Basin sands stems mostly from the need to reconcile the preservation of an open fabric of coarse detrital quartz grains by quartz cement containing hydrocarbons as fluid inclusions. This indicates that at least some major quartz authigenesis occurred at substantial depth of greater than one kilometer.

If overpressured zones existed during diagenesis, potential silica sources of cement could include fluids associated with the metamorphic alteration of the underlying basement rocks.

It is also possible that overpressures may have dissipated with time or hydrocarbon generation and this may explain the lack of difficult downhole conditions associated with drilling in overpressured zones in the Cooper Basin.

An alternative mechanism of an early meteoric quartz cement period which depends on the recognition of a "meniscus" cement is promoted in this report as preserving the open framework of arenites at depth, instead of overpressures.

There is also a possibility that overpressures were not generated by rapid sedimentation but by a combination of sediment compaction, aquathermal pressuring, mineral phase changes and tectonism after initial quartz and kaolin authigenesis within the meteoric groundwater zone. This would have the effect of restricting diagenetic changes before hydrocarbon generation and restricting initial hydrocarbon migration within the arenites.

In order to resolve the interaction between overpressures, hydrocarbon generation and diagenesis of Cooper Basin arenites it is necessary to do detailed fluid inclusion based palaeogeothermometry on identified quartz overgrowth zones, similar to work carried out by Russell & Bone (1989).

9.7.1 Conclusions - overpressures

Overpressures offer a viable framework for perceived diagenetic events of Cooper Basin arenites within the study area. However, evidence for overpressures is circumstantial and alternate explanations can be invoked for most of the observations supporting overpressures.

9.8 Summary of reservoir quality

Porosity within the study area generally decreases with depth and is termed a first order porosity variation.

A second order porosity variation occurs as a diversion from this trend within the Toolachee and Patchawarra intervals, with porosity decreasing from the top to the bottom of each formation. Both porosity variations occur in response to sediment loading.

Other formation reservoirs such as the Epsilon Formation gas sands in the Kerna Field are not as well developed in the study area and do not show second order porosity variations.

There appears to be a reduction in porosity and permeability within 100 metres (350 feet) of the top of the Cooper Basin sequence.

Generally, porosity observed in all samples is quite low and large pores and pore throats are rare. The most effective porosity is likely to be remnant primary porosity rather than secondary dissolution porosity, fracture porosity and microporosity associated with clays.

Permeability appears loosely dependent on porosity but the interrelationship is field dependent and varies with grain size and depth.

Permeability and porosity appears to be better developed in arenites with low clay content and large initial (depositional) pore spaces. Channel deposit arenites have variable and often higher porosity and permeability values than other types of deposits such as prograding delta, floodplain and overbank deposits. Shoreline sands have generally low permeabilities.

Drill Stem Test (DST) data did not indicate better reservoir conditions to be restricted to any one of the four facies associations of the Toolachee Formation or the three uppermost facies associations of the Patchawarra Formation delineated in this report.

Little variation in diagenetic assemblages that could influence reservoir quality was observed between fields and formations.

10 Summary and conclusions

Arenites within the study area had higher porosity when deposited than at present. Compaction and clastic diagenesis (quartz cementation, kaolin clay growth etc.) have reduced porosity by variable amounts.

Diagenesis and lithofacies (sand thickness, grain size, sorting etc) are major influences on reservoir quality in the study area, with diagenesis the most important control on reservoir production quality.

Diagenetic processes identified from samples in the study area are compaction, multiple phase quartz cementation, siderite, illite, chlorite and kaolin authigenesis, framework grain dissolution and limited dissolution and corrosion of quartz grains, quartz cement and siderite. Most of these observed diagenetic effects have served to reduce porosity and permeability.

A model of the post depositional history of the study area involving several, mostly overlapping diagenetic events is diagrammatically presented in Figure 33. This model differs from previous interpretations of Cooper Basin diagenesis in two respects:

- (1) Some of the major diagenetic events of quartz cementation possibly occurred concurrently with oil formation at elevated temperatures and depth.
- (2) Unconformities associated with the top of the Cooper Basin sequence may have produced localised diagenetic effects that have reduced porosity and permeability within a 100 metre zone below the top of the Cooper Basin.

Overpressured zones may have influenced diagenetic processes within the study area.

Channel deposits appear to offer the most potential for productive sands in the study area. Most porosity and permeability is observed to be remnant primary porosity which is best preserved in coarse grained, poorly sorted arenites with little detrital clay matrix. A reduction of porosity and permeability values in arenites generally occur towards the base of the Cooper Basin sequence, towards the base of the Toolachee and Patchawarra Formations and towards the top 100 metres (350 feet) of the Cooper Basin sequence.

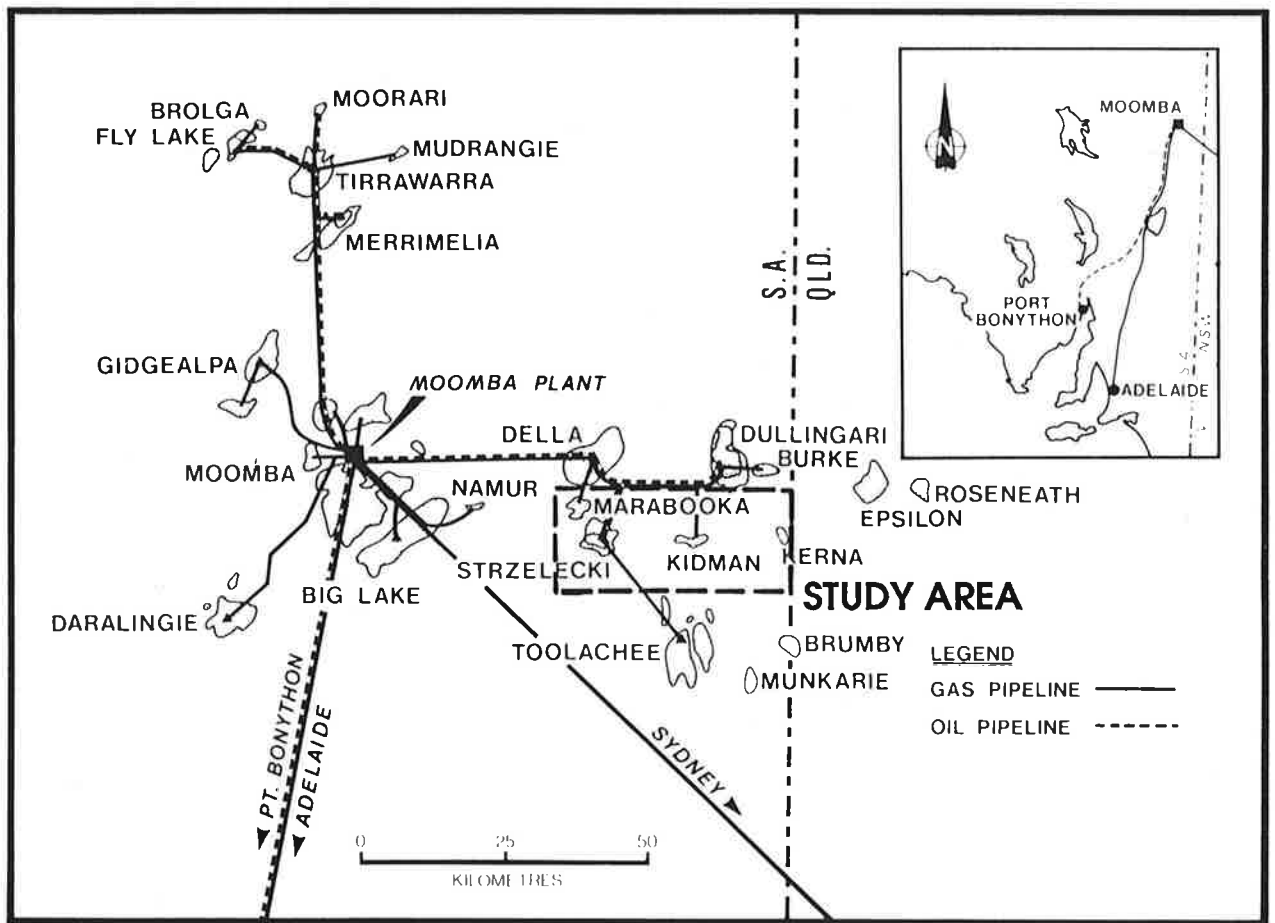
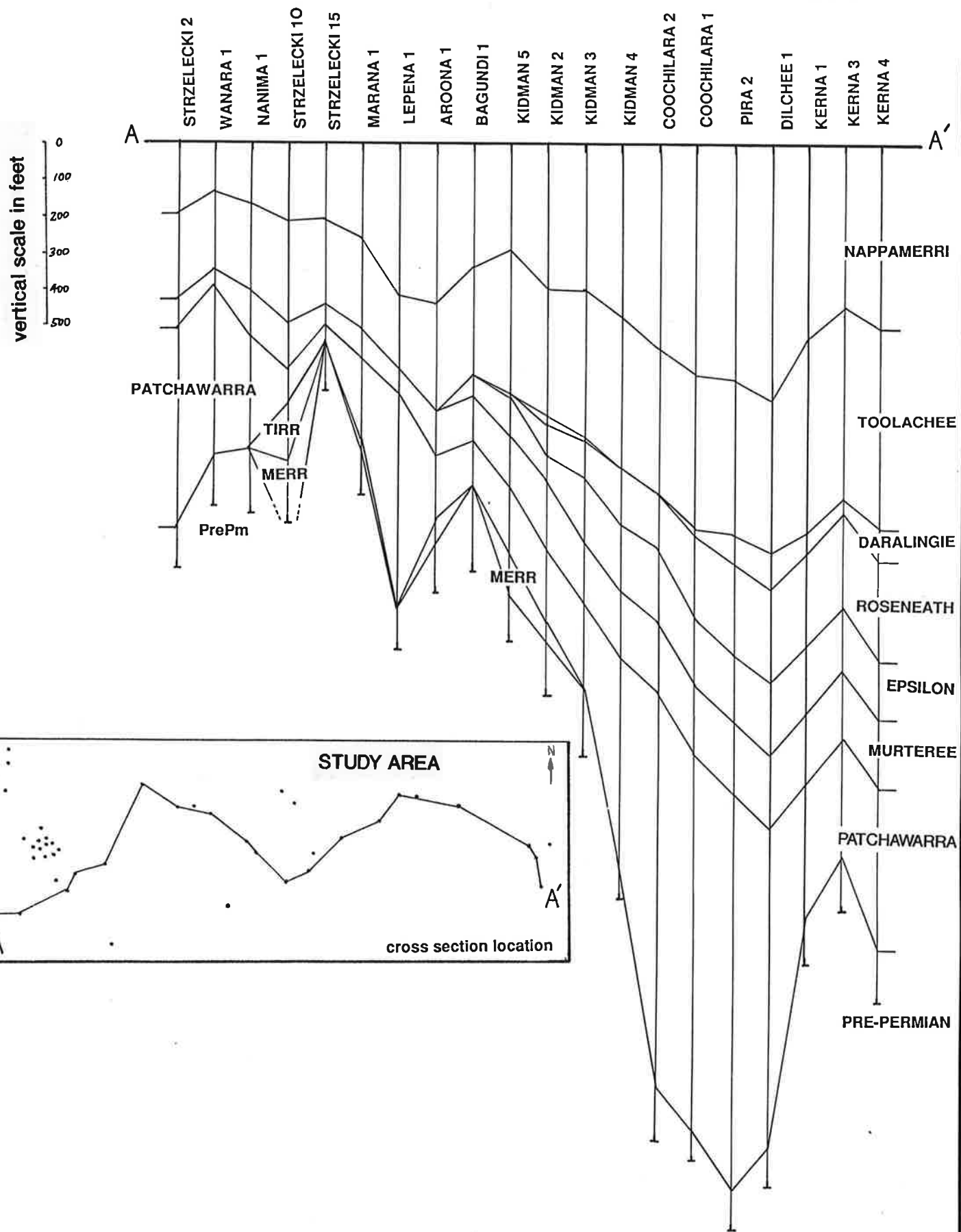


Figure 1

Study area location and southern Cooper Basin gas and oil fields



**Fig 2 STRUCTURAL CROSS SECTION A-A'
 TOP NAPPAMERRI TO END OF HOLE**

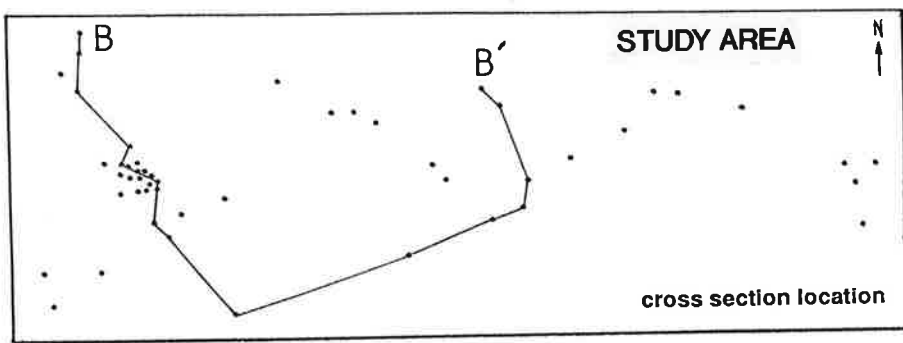
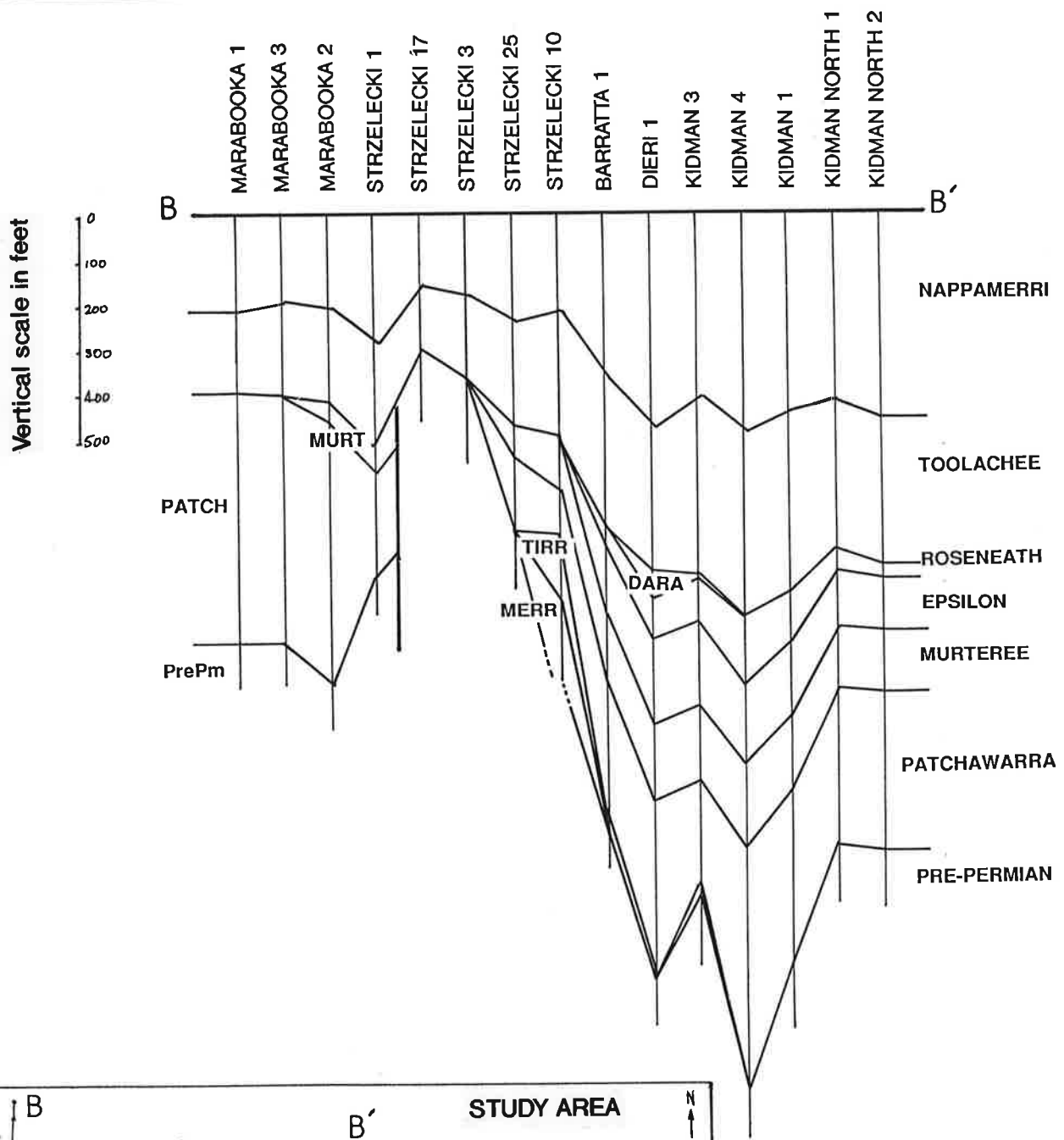


Fig 3 STRUCTURAL CROSS SECTION B-B'
TOP NAPPAMERRI TO END OF HOLE

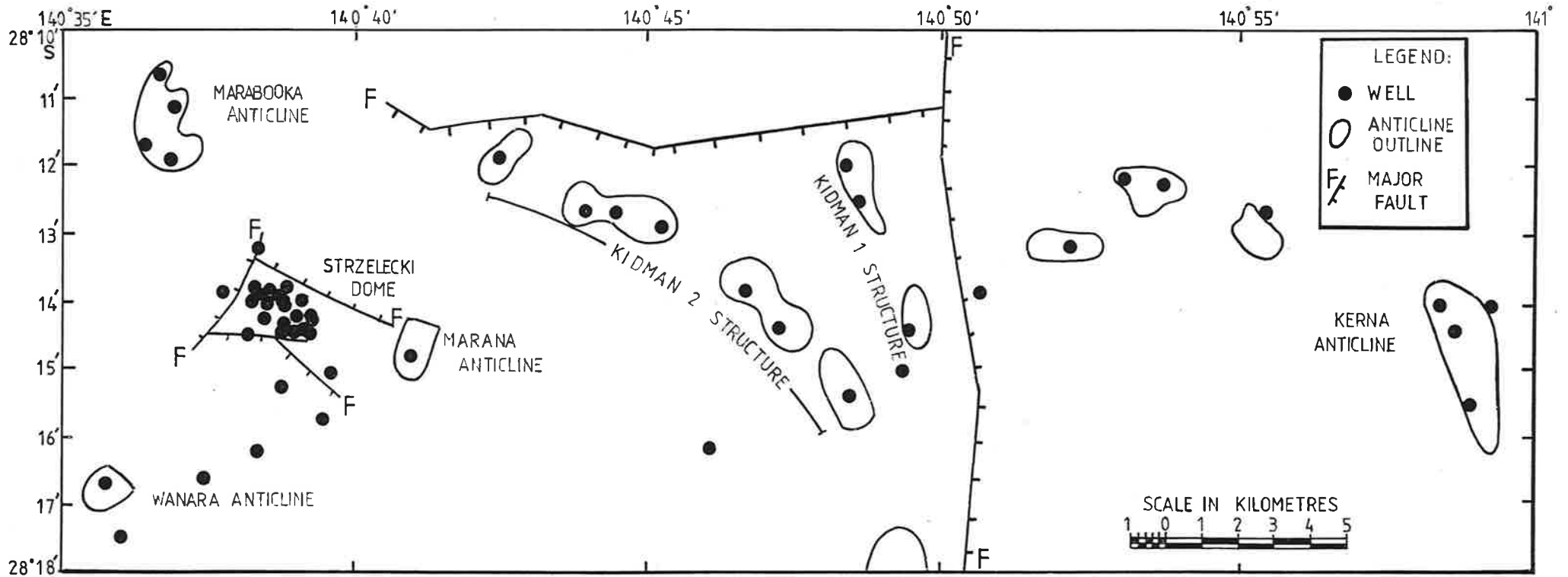


Fig 4 Structural features of the Strzelecki-Kidman-Kerna study area.

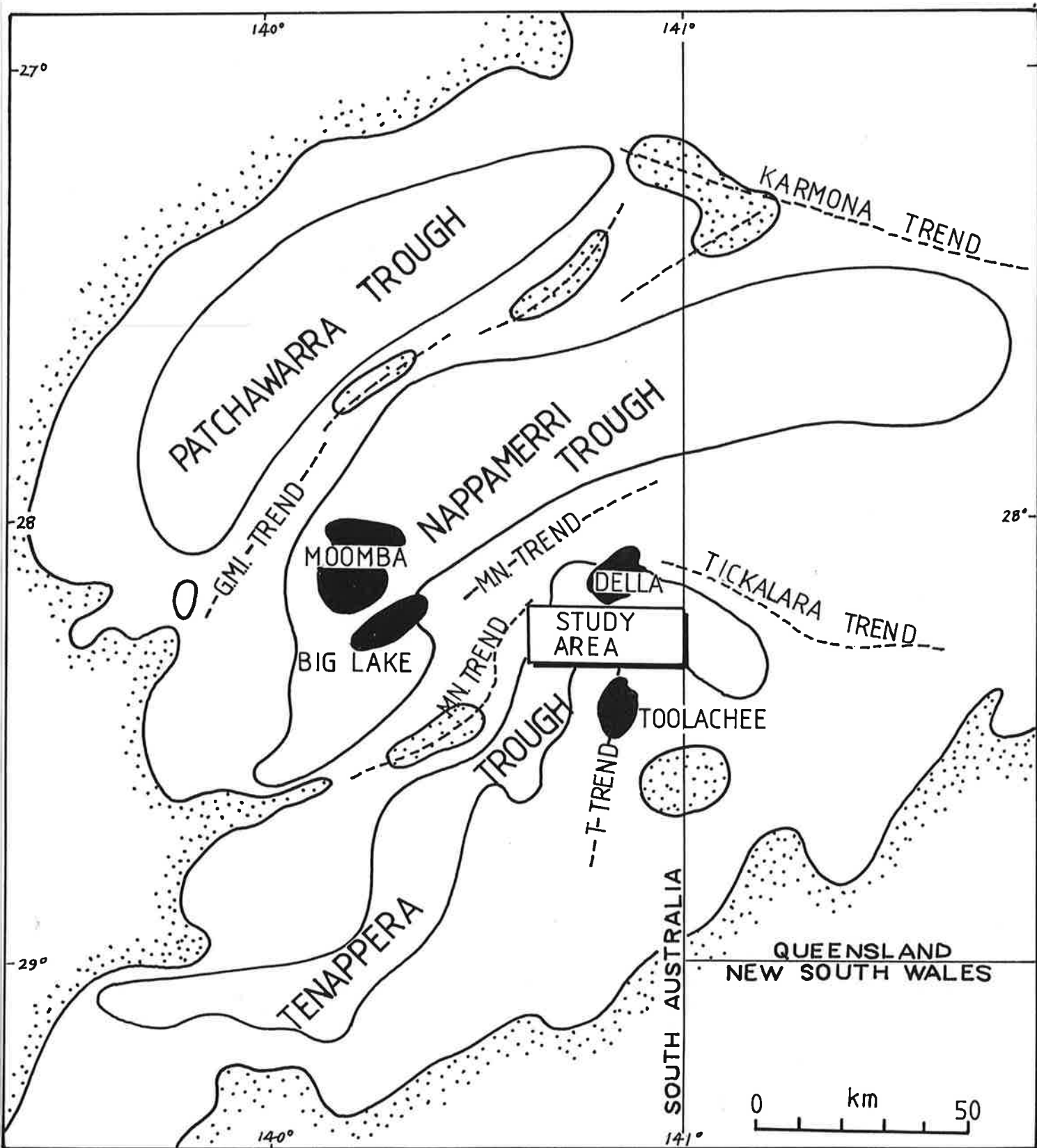


Figure 5 Localities referred to in this report and major structural features of the Cooper Basin.

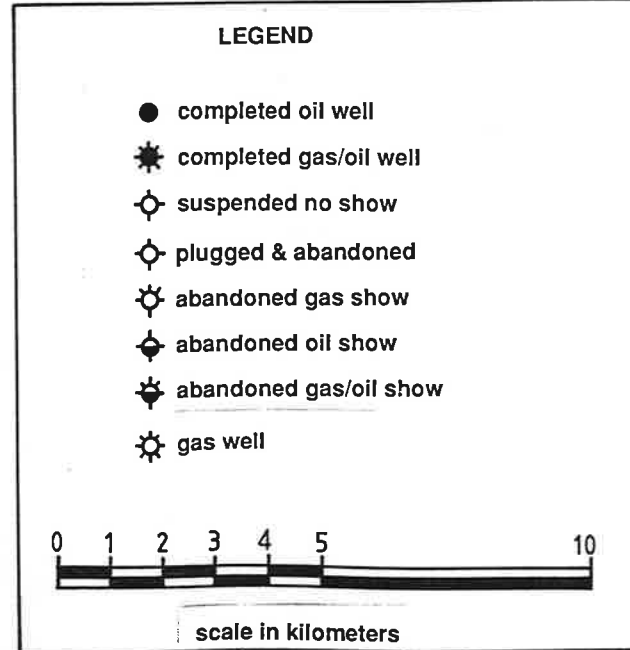
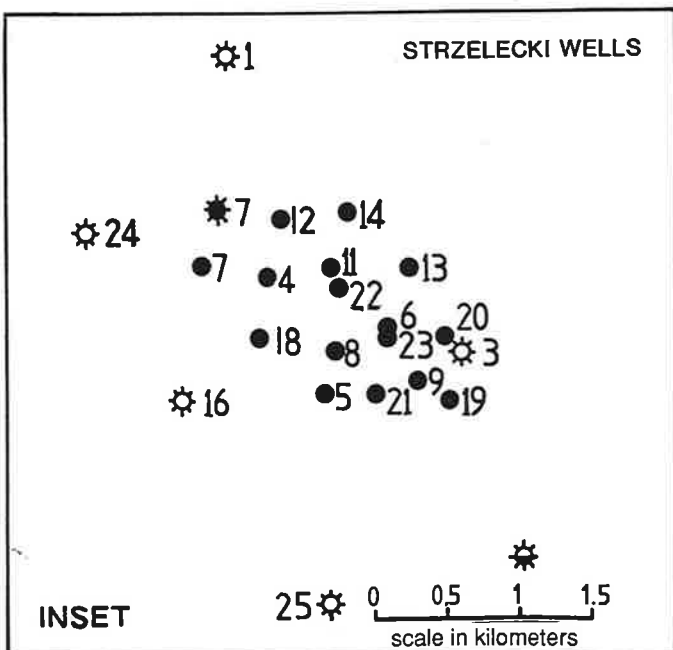
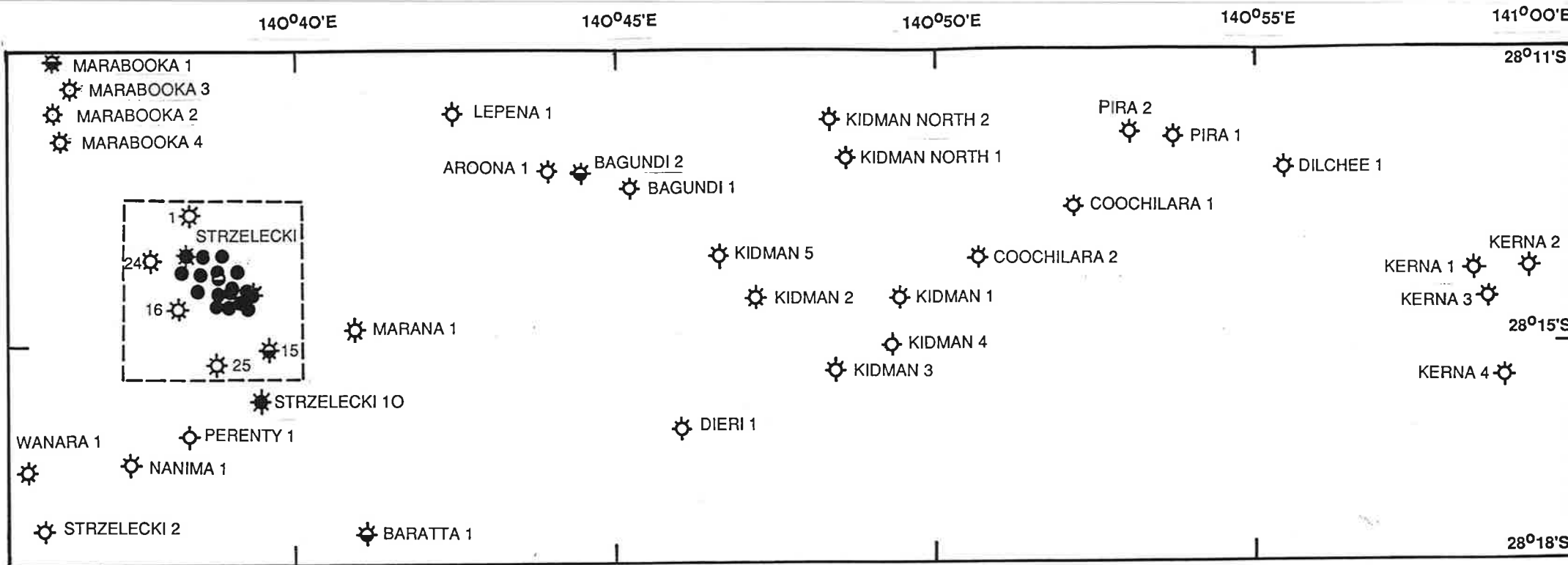


Figure 6
Study area well location plan

STRZELECKI 10

MARANA 1

BAGUNDI 2

KIDMAN 2

KERNA 1

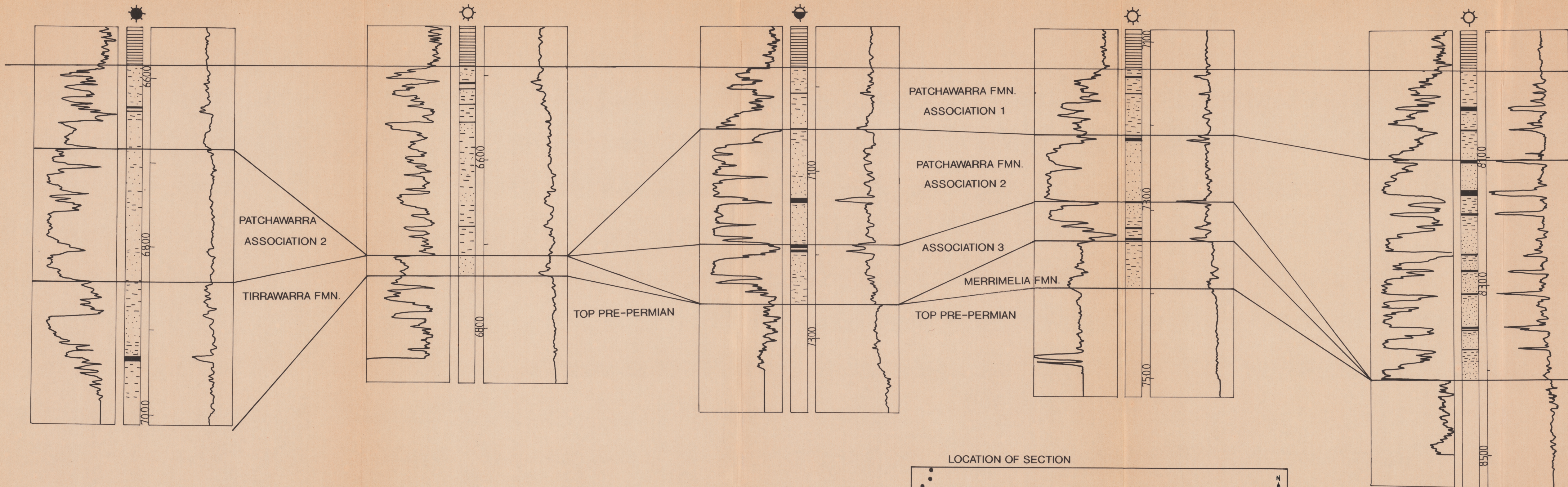
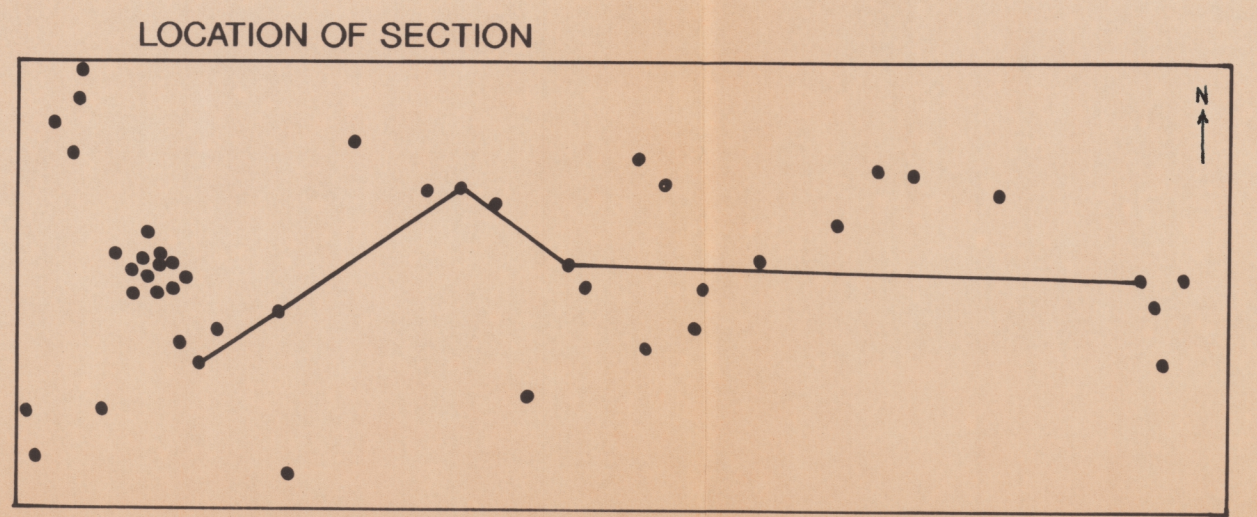
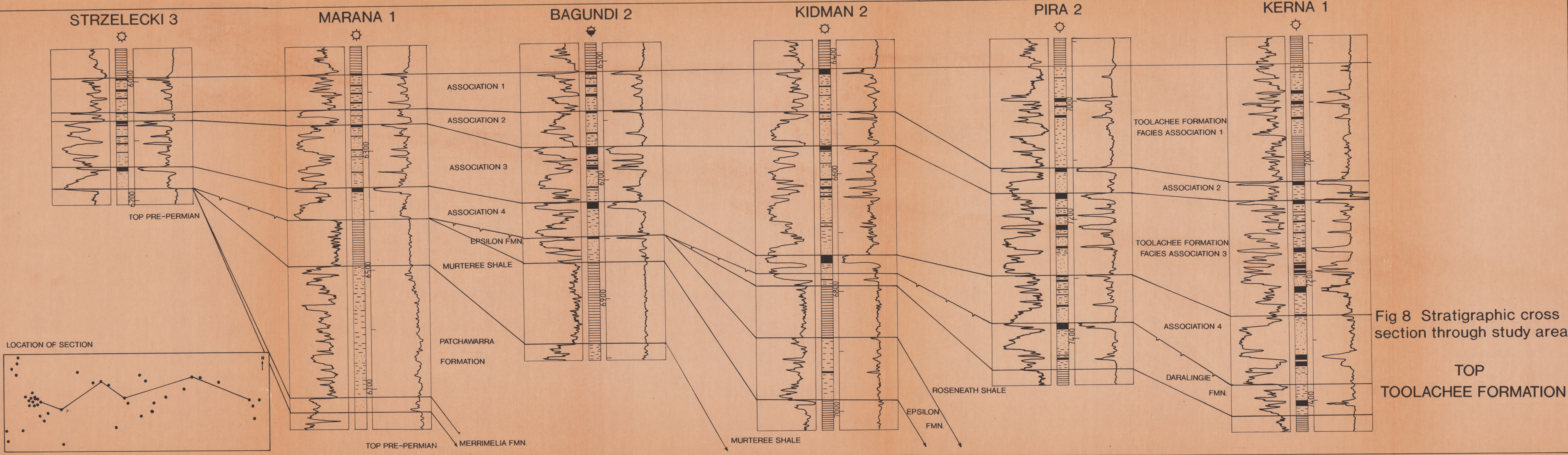


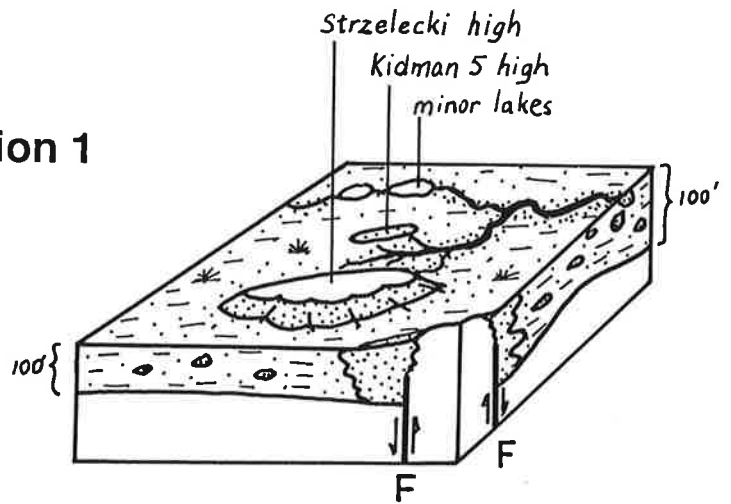
Fig 7 Stratigraphic cross section through study area



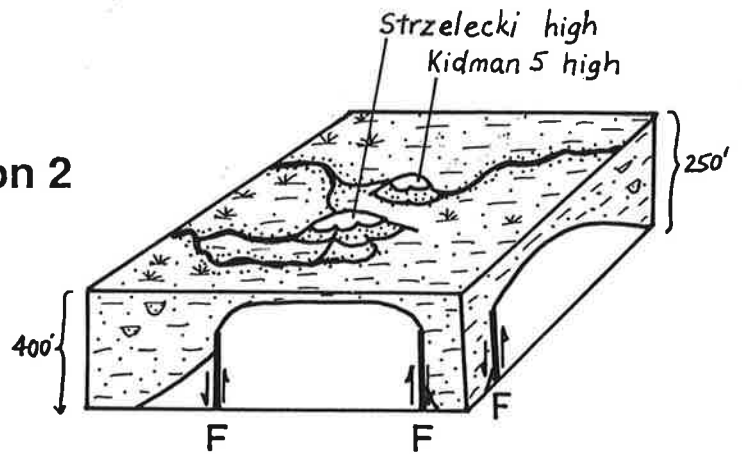
TOP
PATCHAWARRA
FORMATION



Facies association 1



Facies association 2



Facies association 3

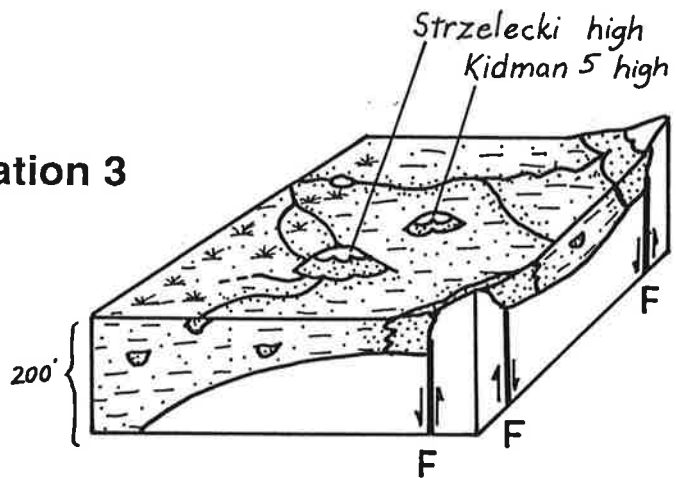
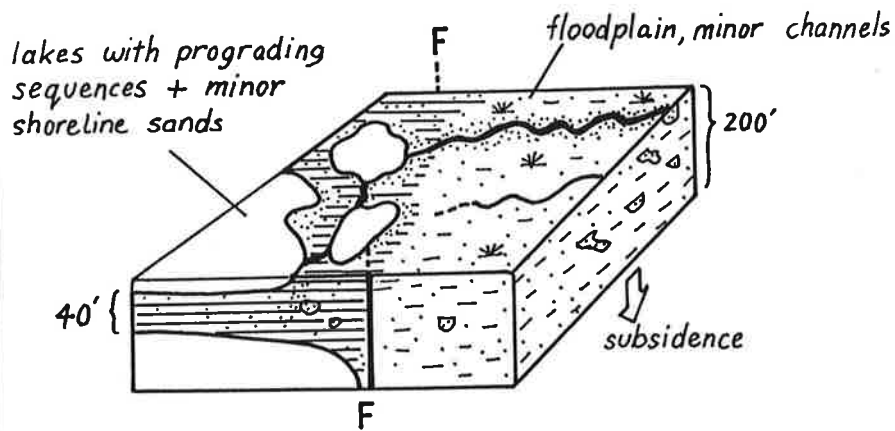
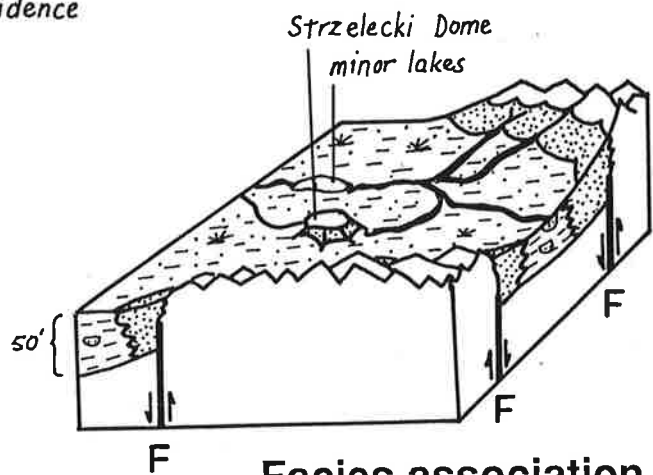


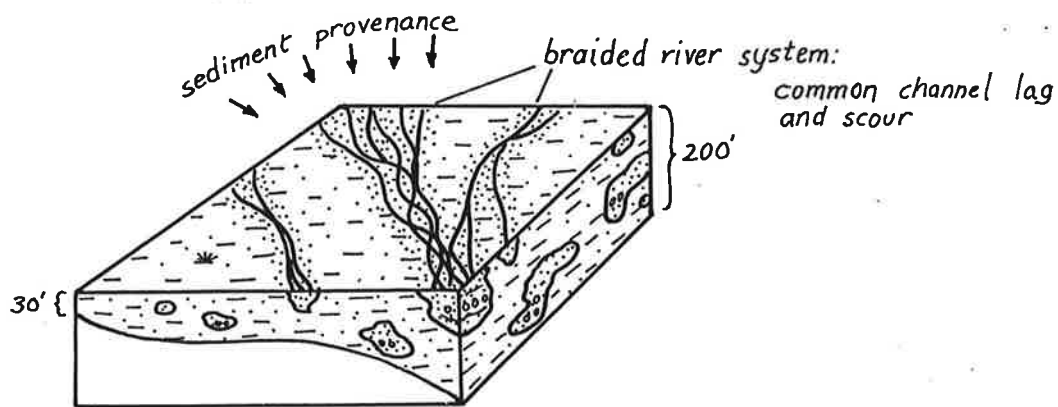
Fig. 9 Palaeogeographic reconstruction of three facies associations of the Patchawarra Formation, North is to the left.



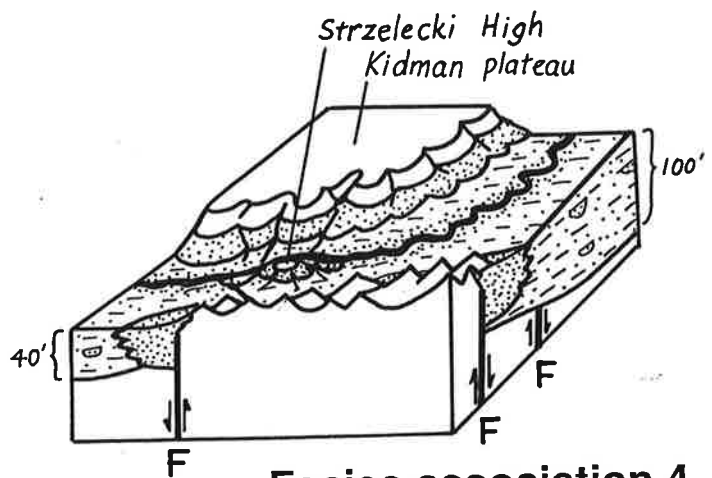
Facies association 1



Facies association 2



Facies association 3



Facies association 4

Fig.10 Palaeogeographic reconstruction of four facies associations of the Toolachee Formation. North is to the left.

Illite/Kaolin vs Average Grain Size

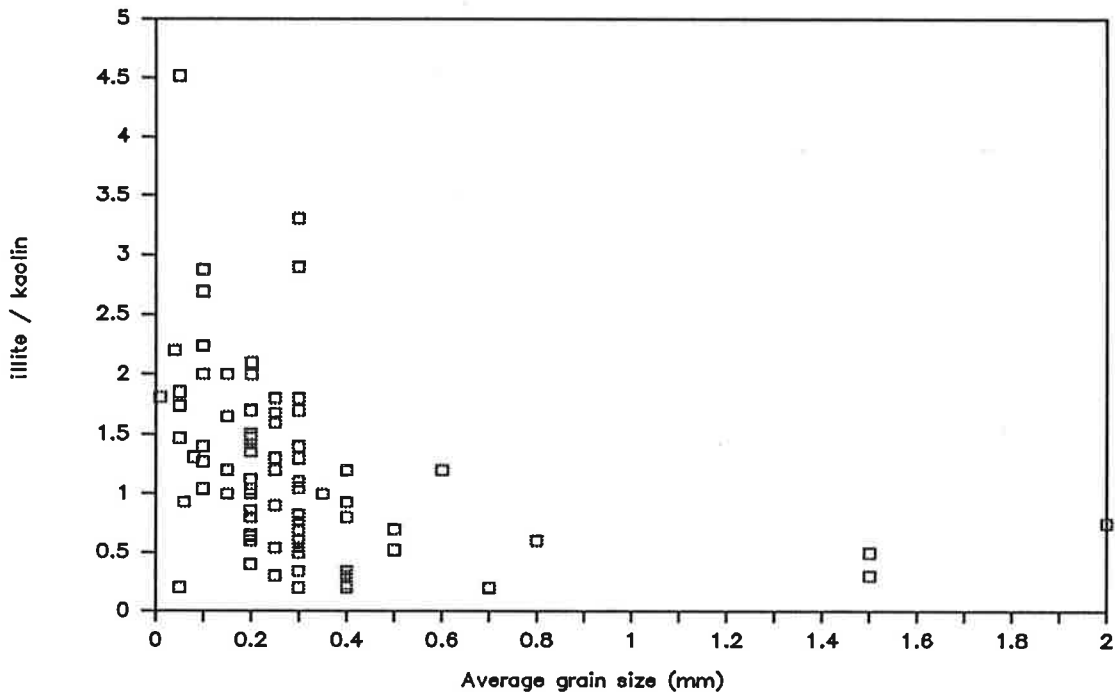


Figure 11. Illite/kaolin vs average grain size. High illite content is restricted to finer grained samples.

Dickite & Kaolinite vs Ave Grain Size

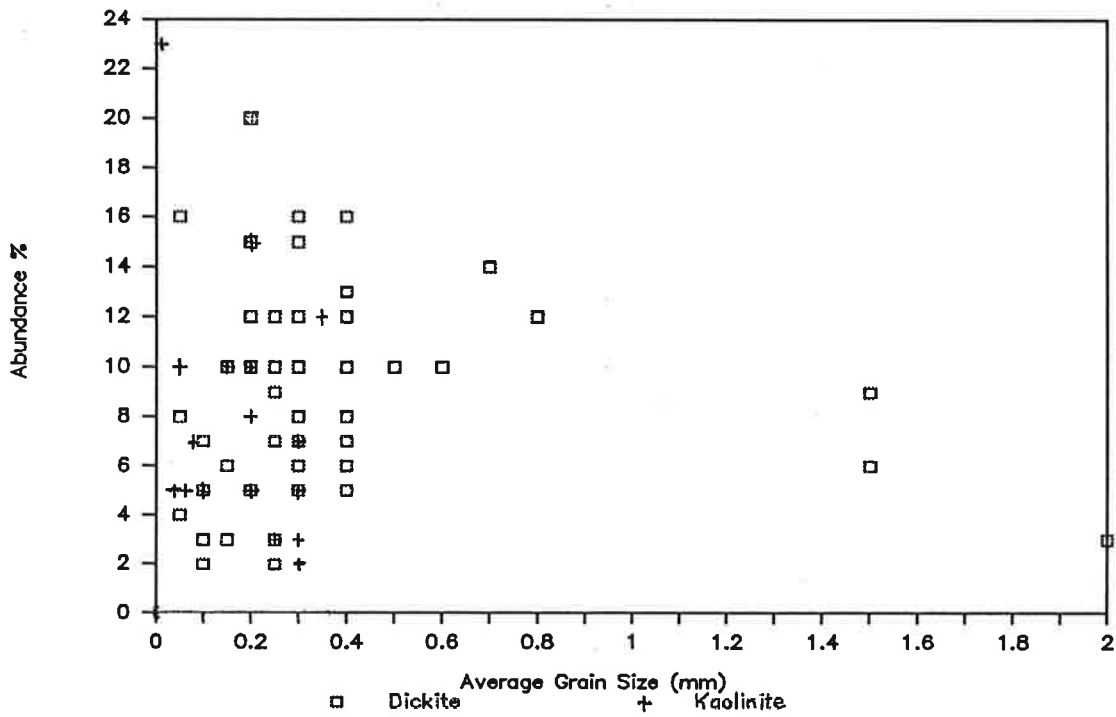


Figure 12: Dickite & kaolinite vs average grain size. Kaolinite is generally constant in sediments with average grain sizes less than 0.5 mm.

Kaolinite vs Illite/Kaolin

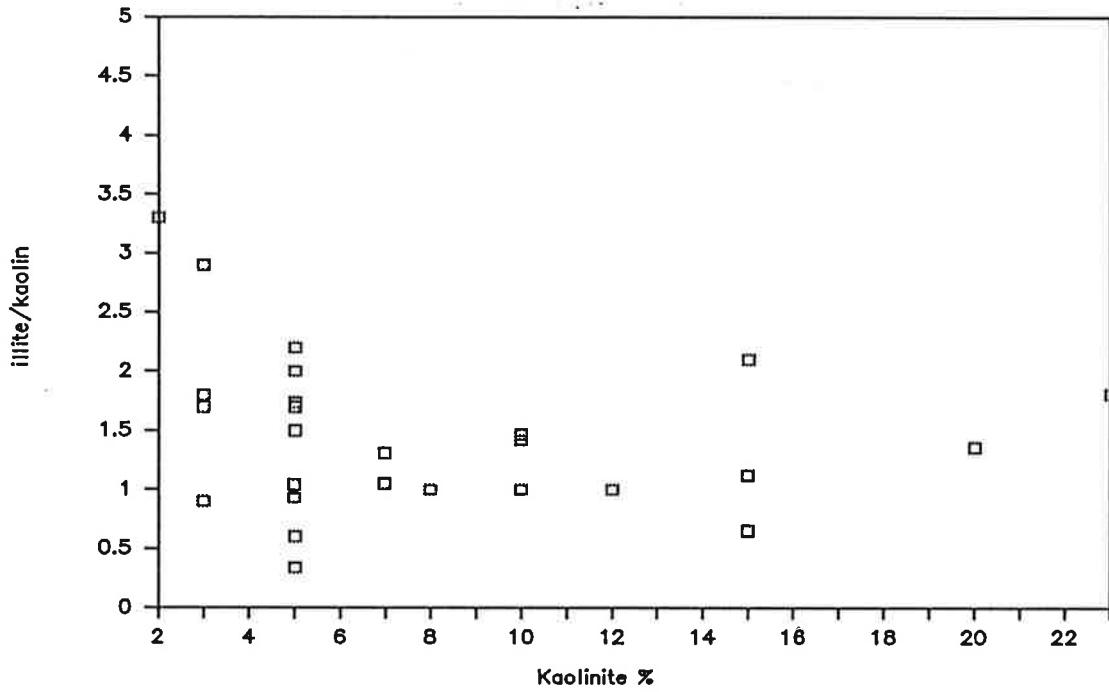


Figure 13: Illite/kaolin vs kaolinite. Kaolinite is generally restricted to $i/k < 2$.

Illite Muscovite Biotite EDX Si/K

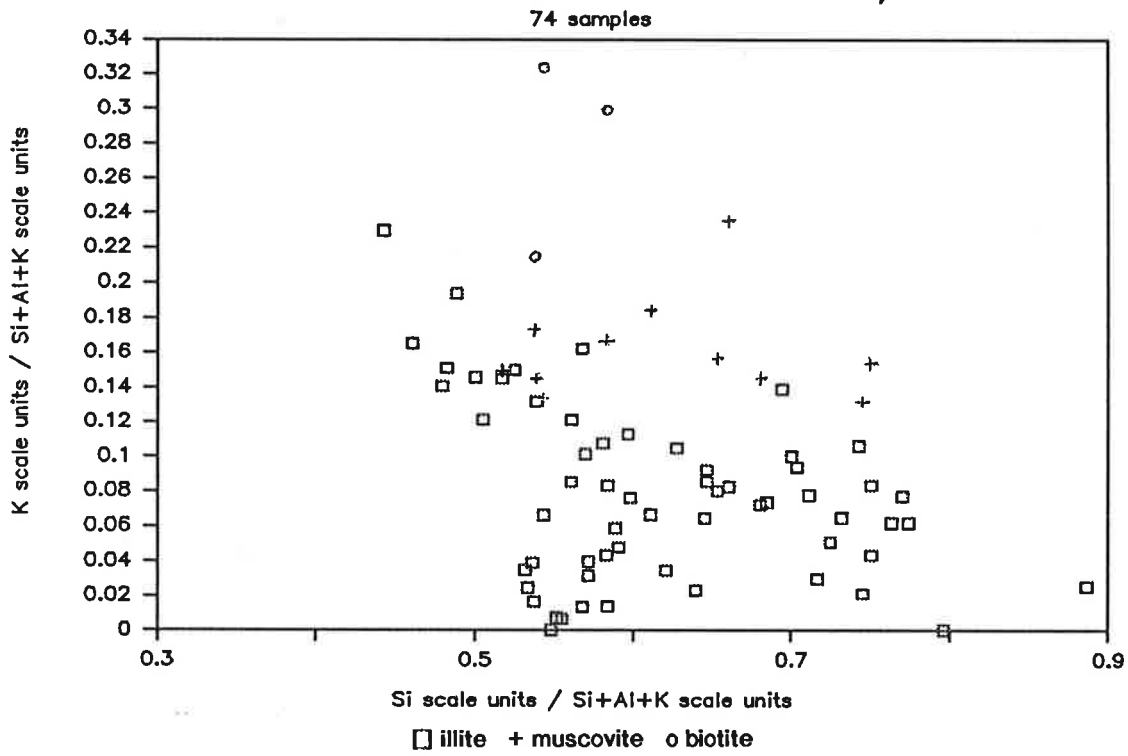


Figure 14: EDS spectra taken during SEM studies showing K variation with illite, biotite and muscovite. Muscovite generally has more K than illite; muscovite altering to illite produces excess K, which could be taken up during kaolin authigenesis. Most of the scatter of data points is attributed to the penetration of the EDS beam through the small illite crystals to register some of the X-ray characteristics of the substrate mineral underneath.

Siderite vs Average Grain Size

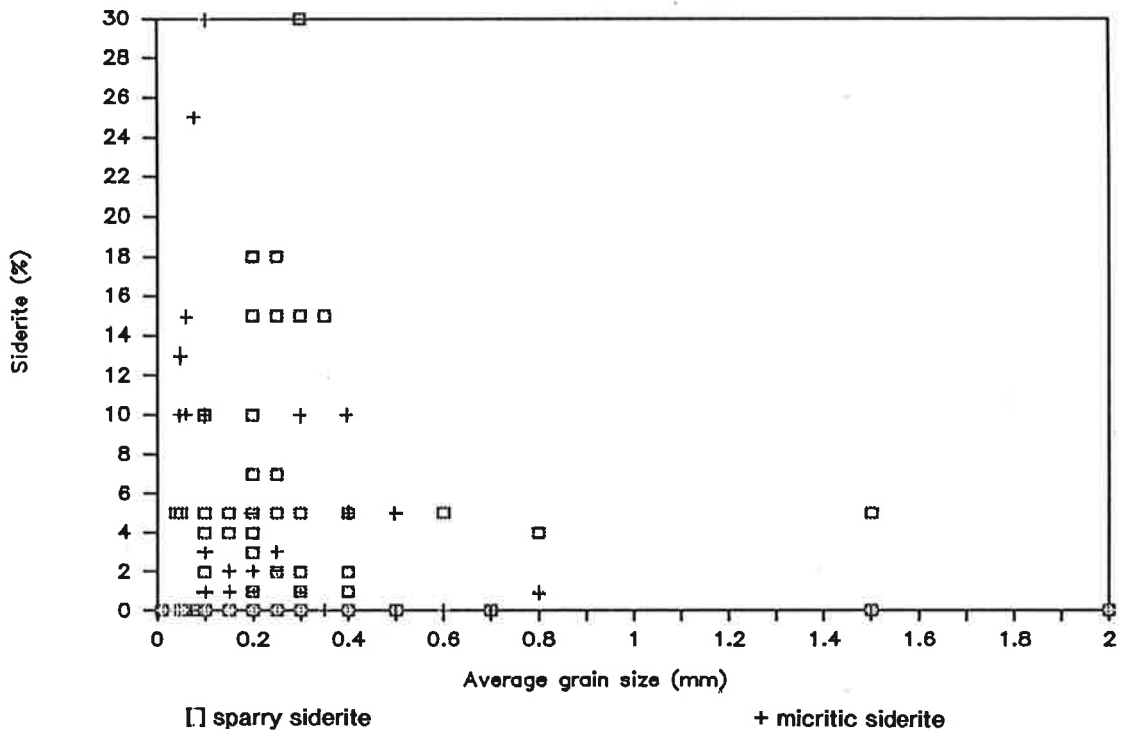


Figure 15: Siderite vs average grain size. Both sparry and micritic siderite are common in fine grain sized sediments with micritic siderite restricted to slightly finer sediments.

Illite/Kaolin vs Siderite

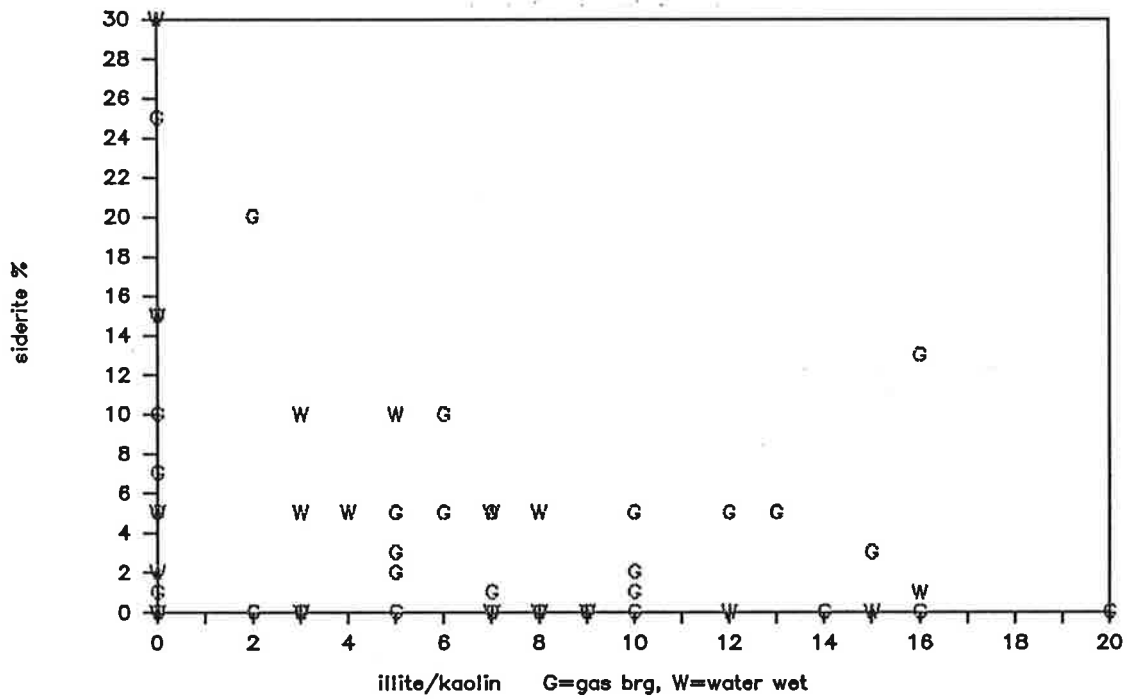


Figure 16: Siderite vs illite/kaolin. There appears to be no differentiation in siderite content or illite/kaolin between samples taken from water wet zones and gas bearing zones. See also Figures 17 & 18.

Illite vs Kaolin

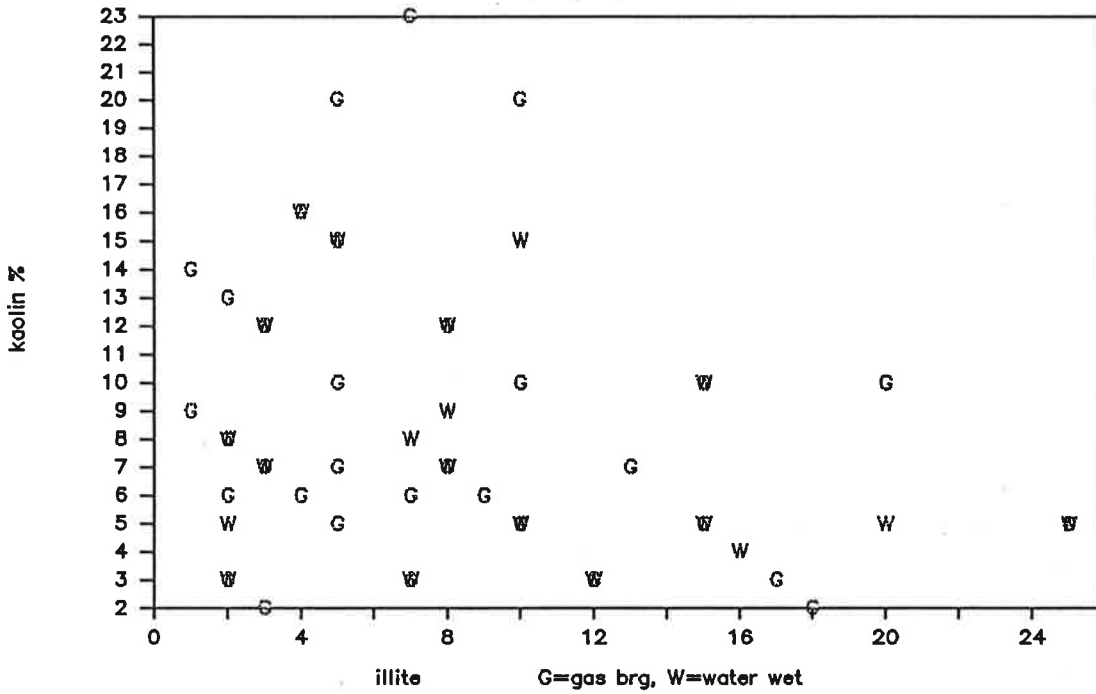


Figure 17: Kaolin vs illite. There appears to be no differentiation in kaolin or illite content between samples taken from water wet and gas bearing zones.

Primary Porosity vs Illite

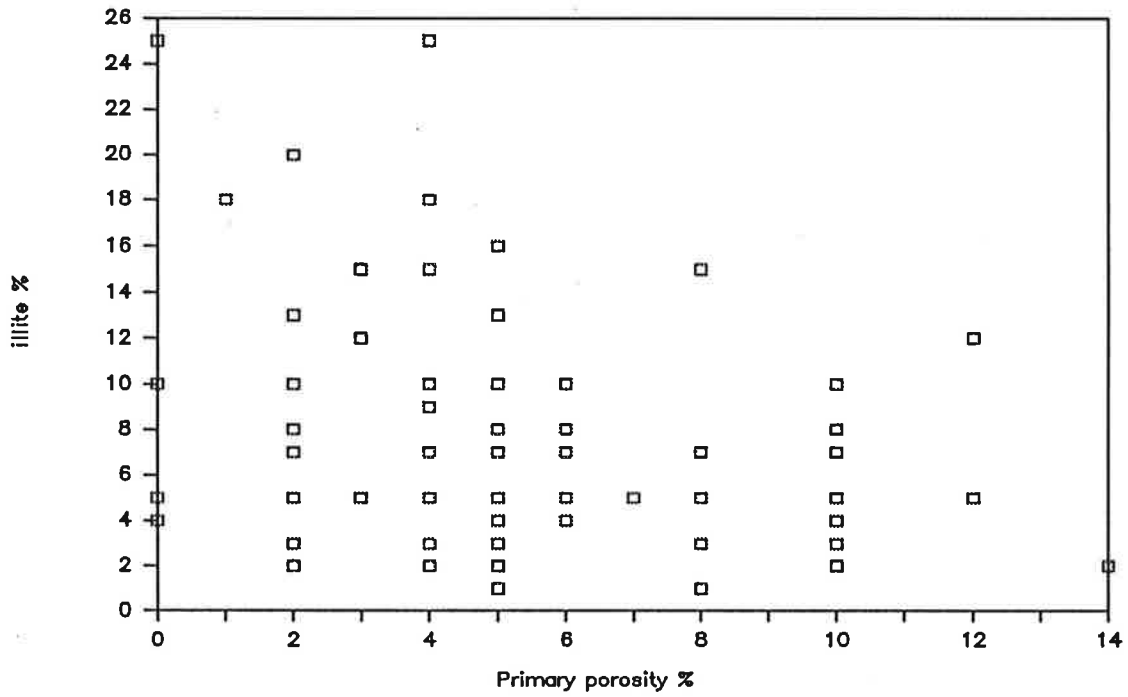


Figure 19: Illite vs primary porosity estimated from thin sections. There appears to be no major influence of illite on primary porosity.

Primary Porosity vs kaolin

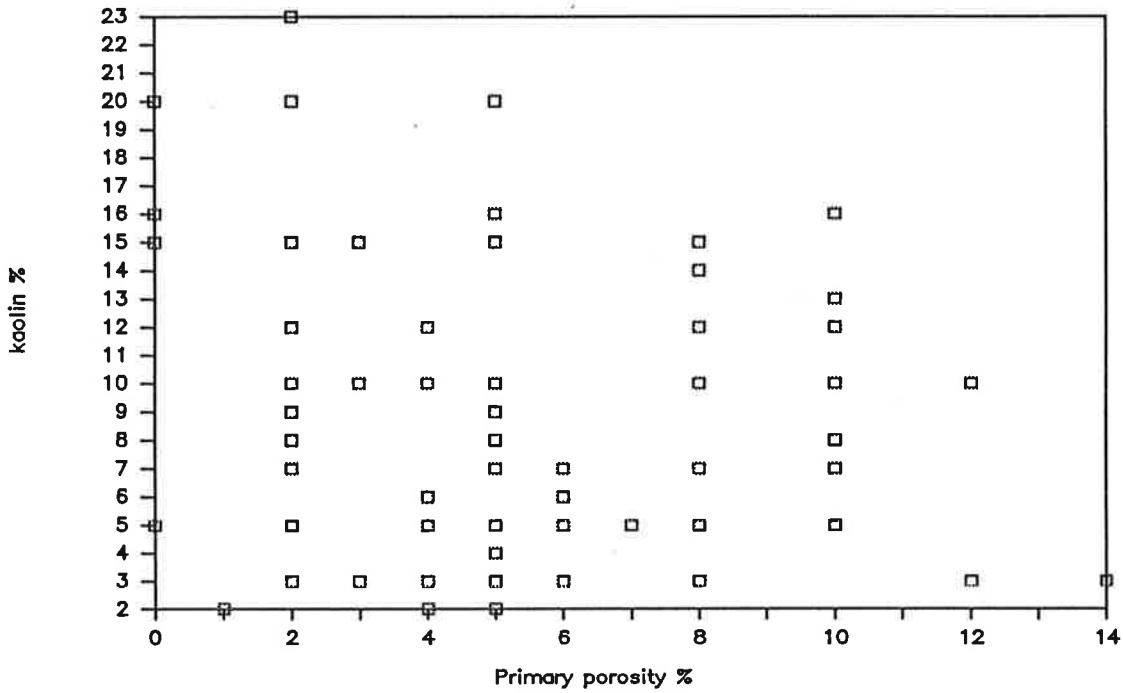


Figure 20: Kaolin vs primary porosity. There appears to be no major influence of kaolinite on primary porosity.

Dickite vs Porosity

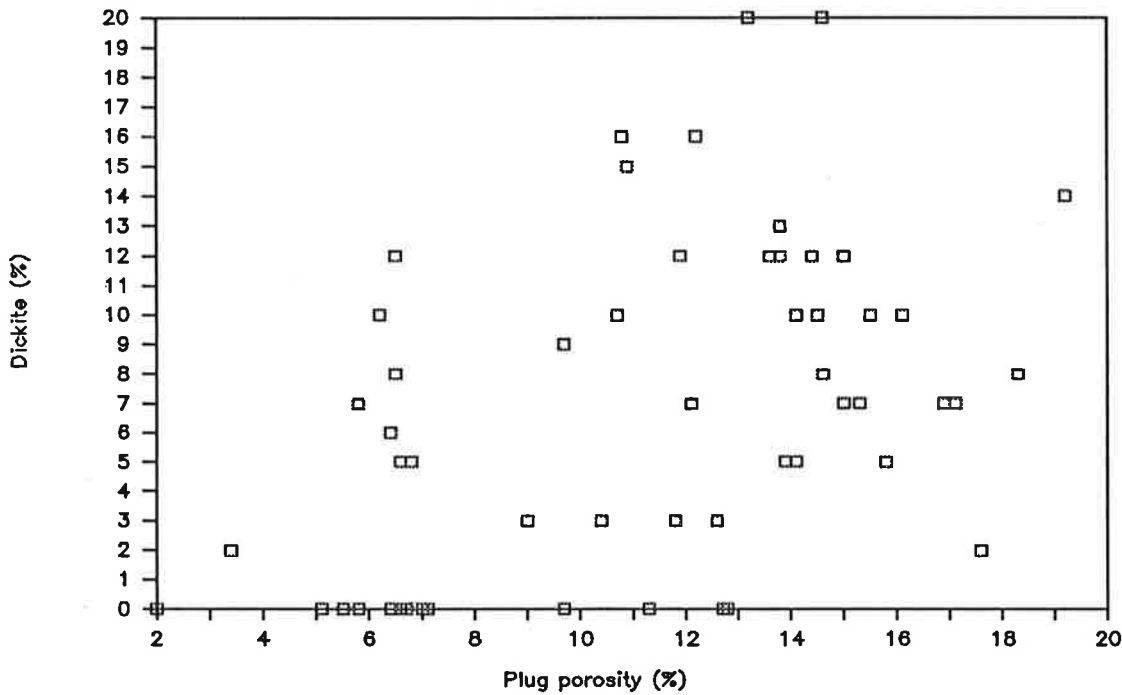


Figure 21: Dickite vs porosity. There appears to be little influence of dickite on primary porosity.

Average Grain Size vs Plug Porosity

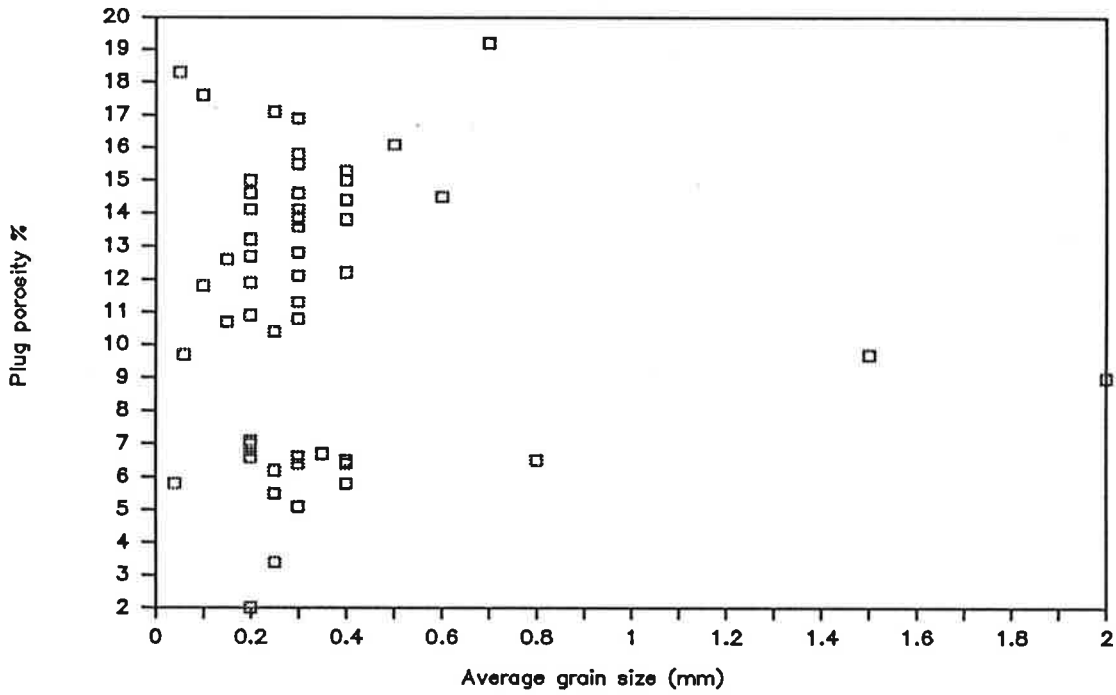


Figure 22: Plug porosity vs average grain size. There appears to be no direct influence of measured grain size on porosity. See also Figures 23 & 24.

Average Grain Size vs Primary Porosity

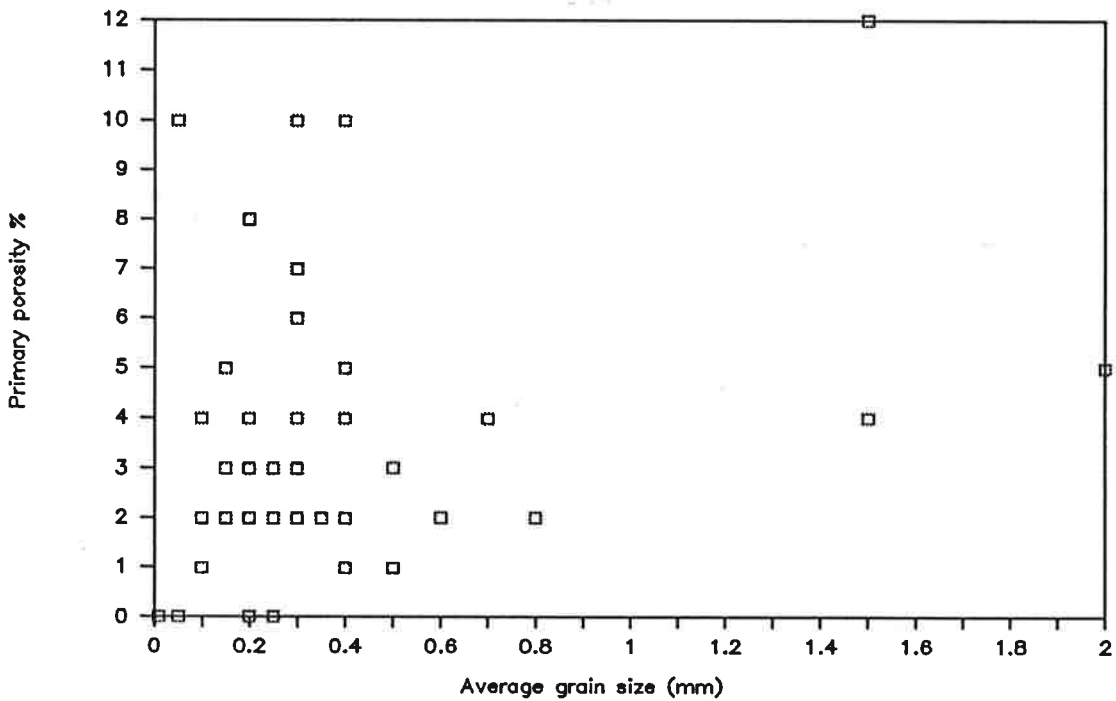


Figure 23: Primary porosity vs average grain size.

Maximum Grain Size vs Plug Porosity

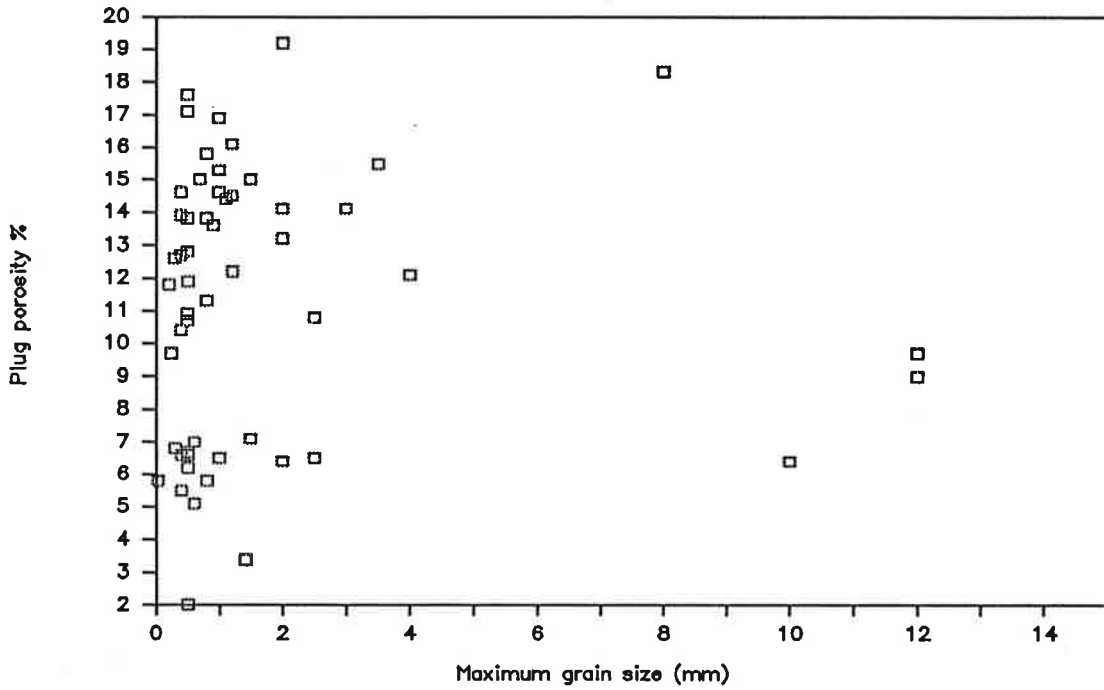


Figure 24: Plug porosity vs maximum grain size.

Primary Porosity vs Illite/Kaolin

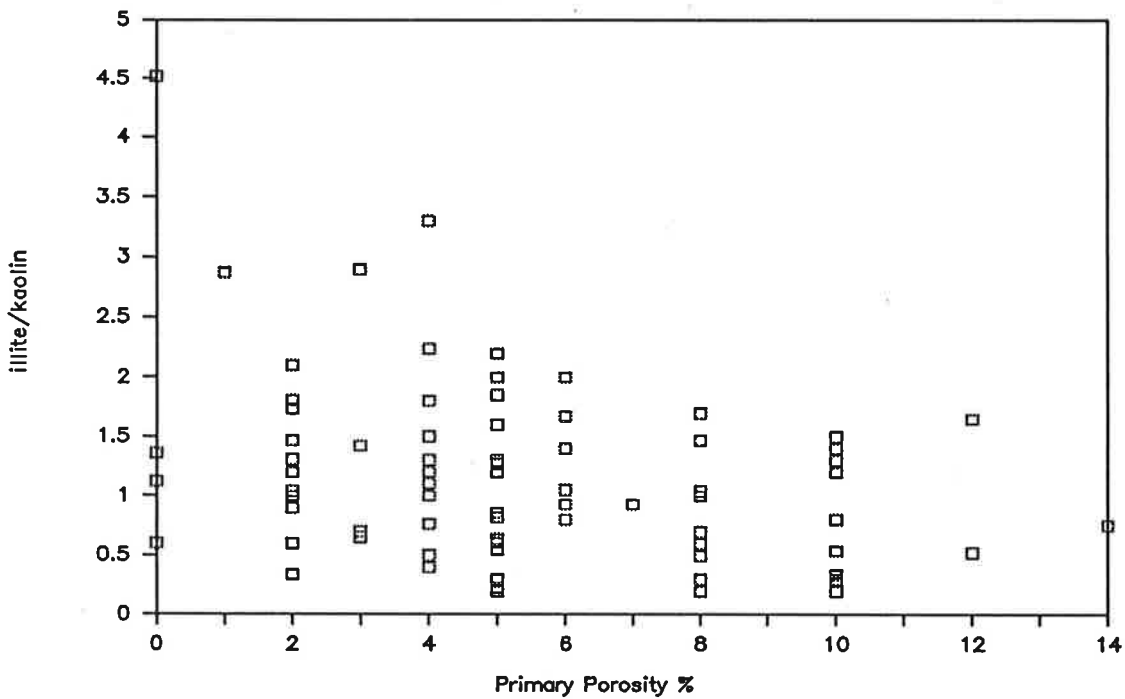


Figure 25. Illite/kaolin vs primary porosity. There appears to be no influence porosity on illite/kaolin.

Sorting vs Plug Porosity

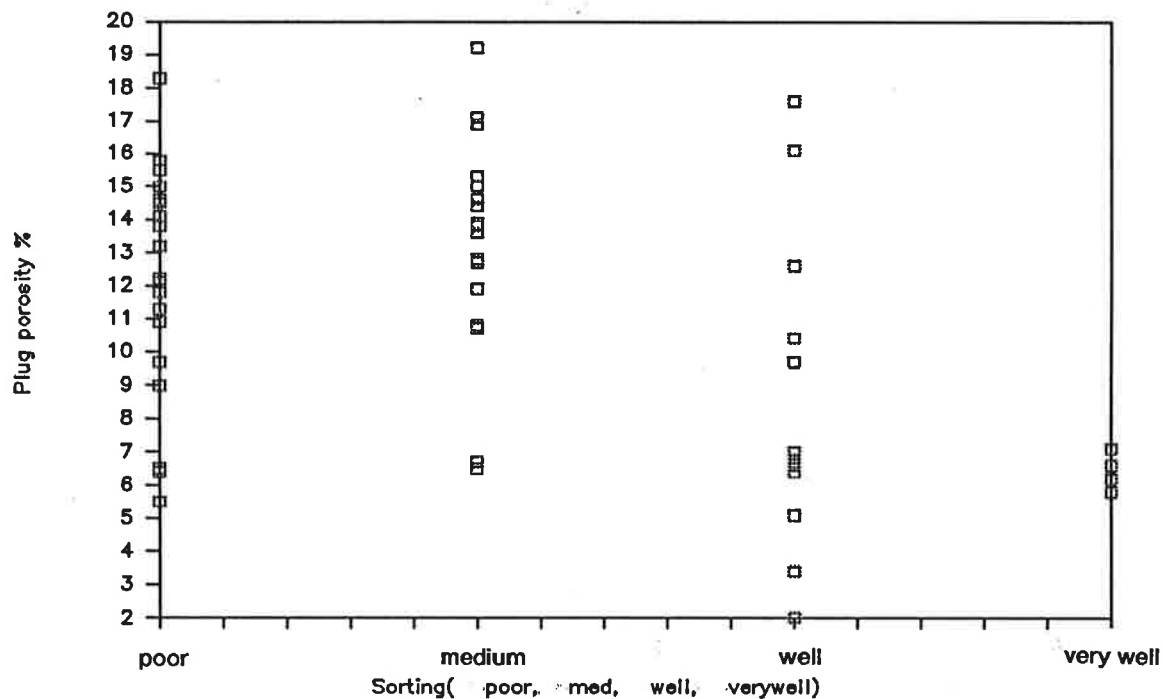


Figure 26: Plug porosity vs sorting. Porosity appears better developed in medium sorted sediments and less developed in poor and well sorted sediments.

Average Grain Size vs Plug Permeability

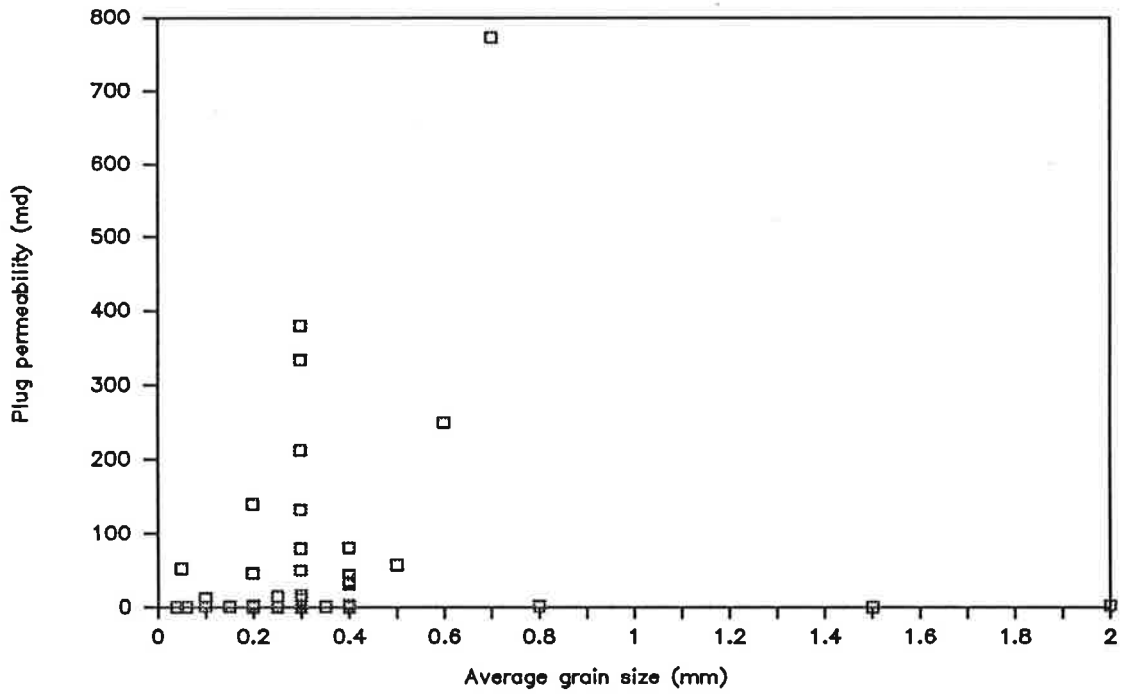


Figure 27: Plug permeability vs average grain size. Permeability is not generally related to grain size.

Plug Permeability vs Secondary Porosity

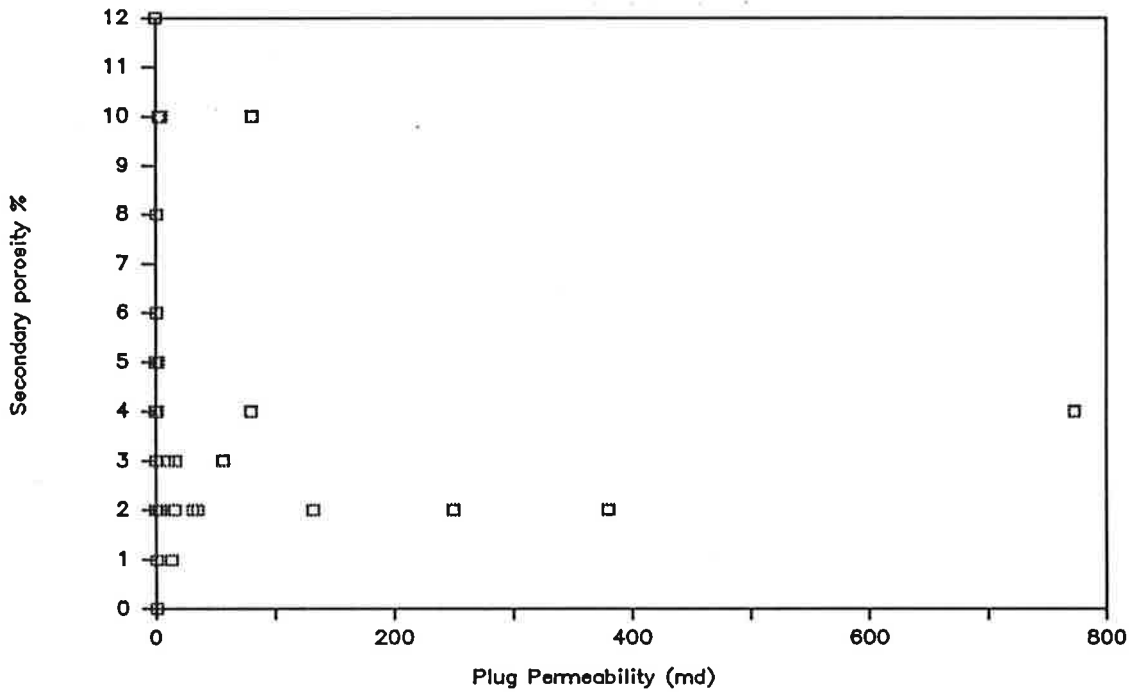


Figure 28: Secondary thin section porosity vs plug permeability. Overall, porosity is not generally related to permeability. See also Figure 29.

Plug Permeability vs Primary Porosity

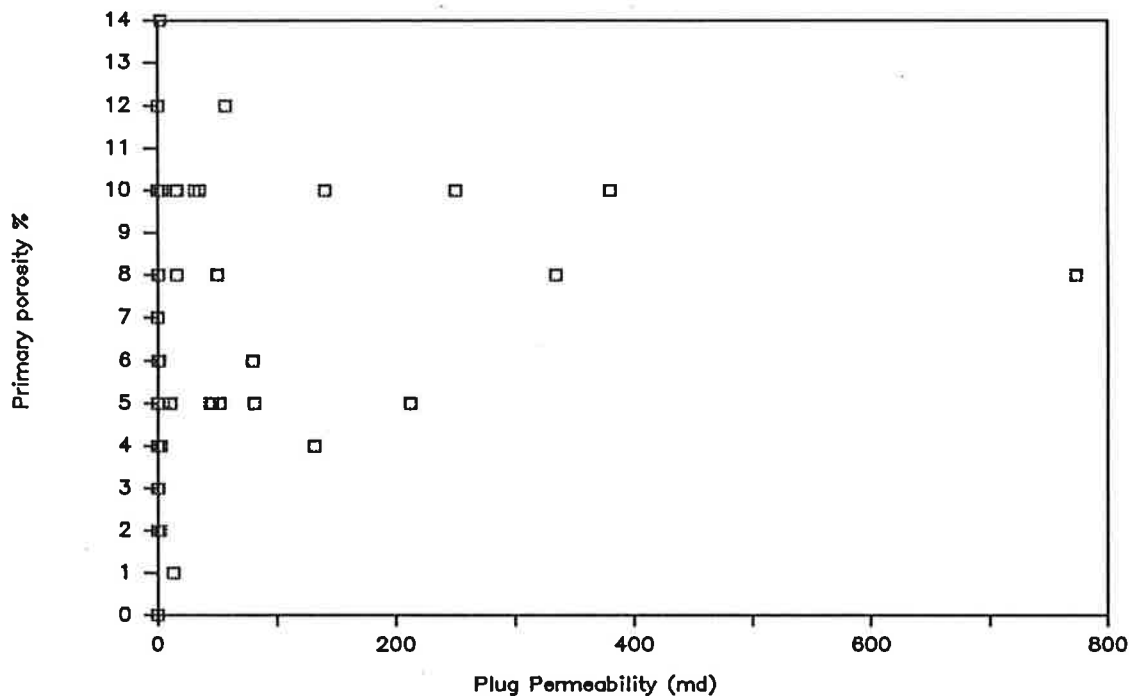


Figure 29: Primary thin section porosity vs plug permeability.

Sorting vs Plug Permeability

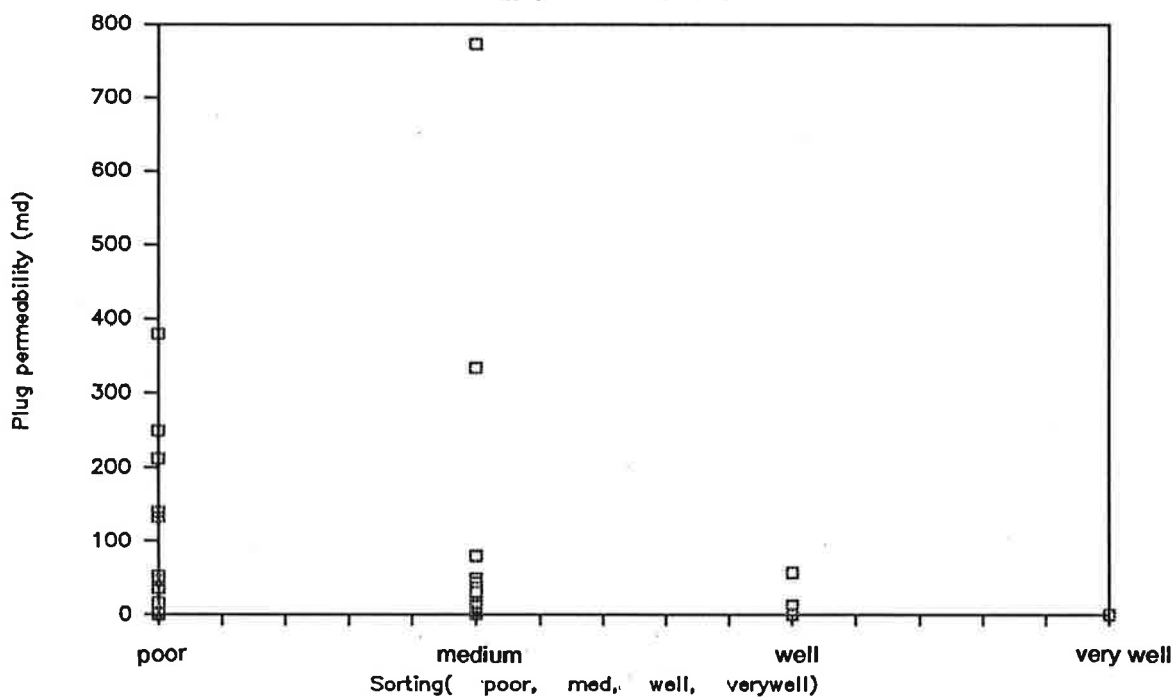


Figure 30: Thin section sorting vs plug permeability. Permeability appears poorer in well sorted samples.

Plug Permeability vs Illite

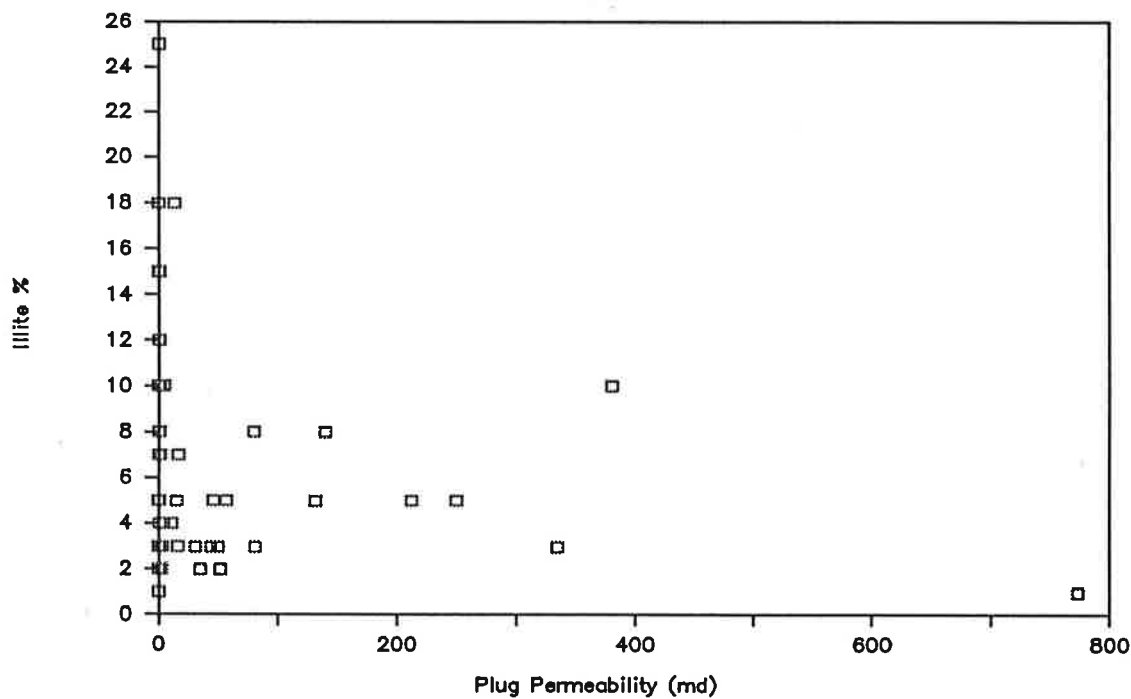


Figure 31: Illite vs plug permeability. Permeability is apparently low in samples with high illite content.

Plug Permeability vs Siderite

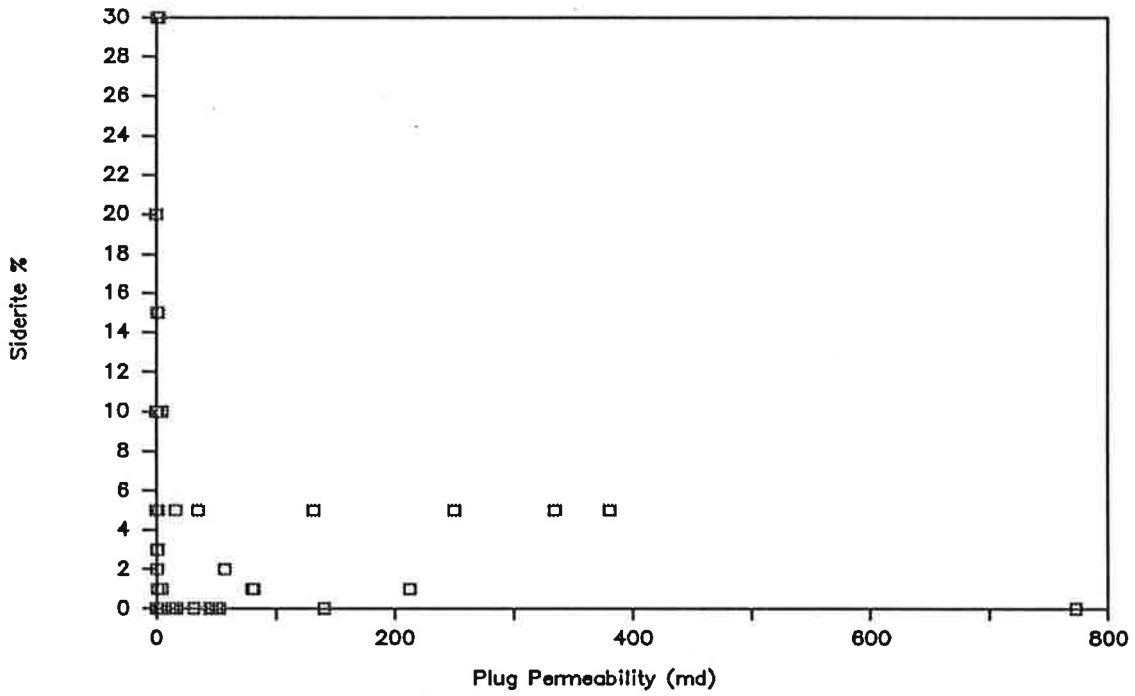


Figure 32: Siderite vs plug permeability. Permeability is apparently low in samples with high siderite content.

Porosity vs Formation Interval %

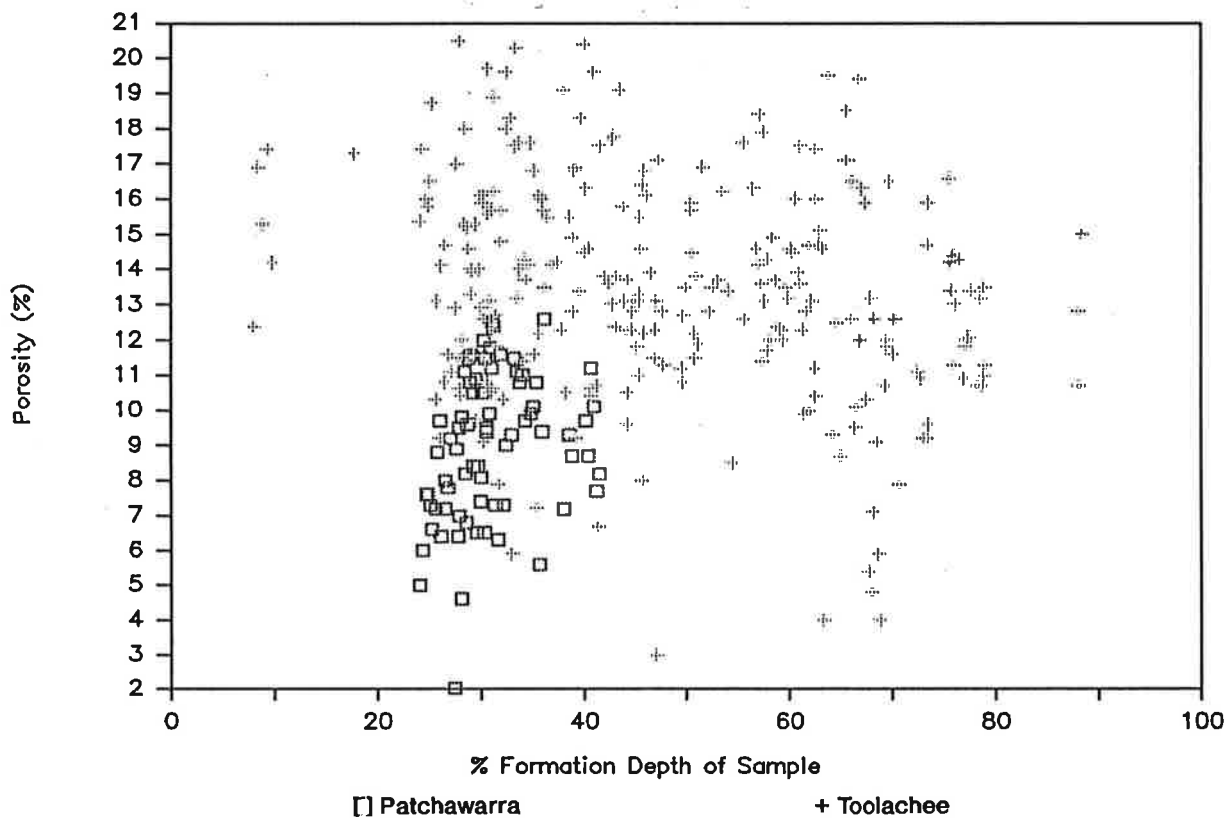


Figure 34: Plug porosity vs formation interval; 0% represents the top and 100% represents the bottom of the formation. Porosity similarly decreases towards the base of both the Patchawarra and Toolachee Formations.

Porosity vs basal Hutton Depth

Tool+Patch samples only

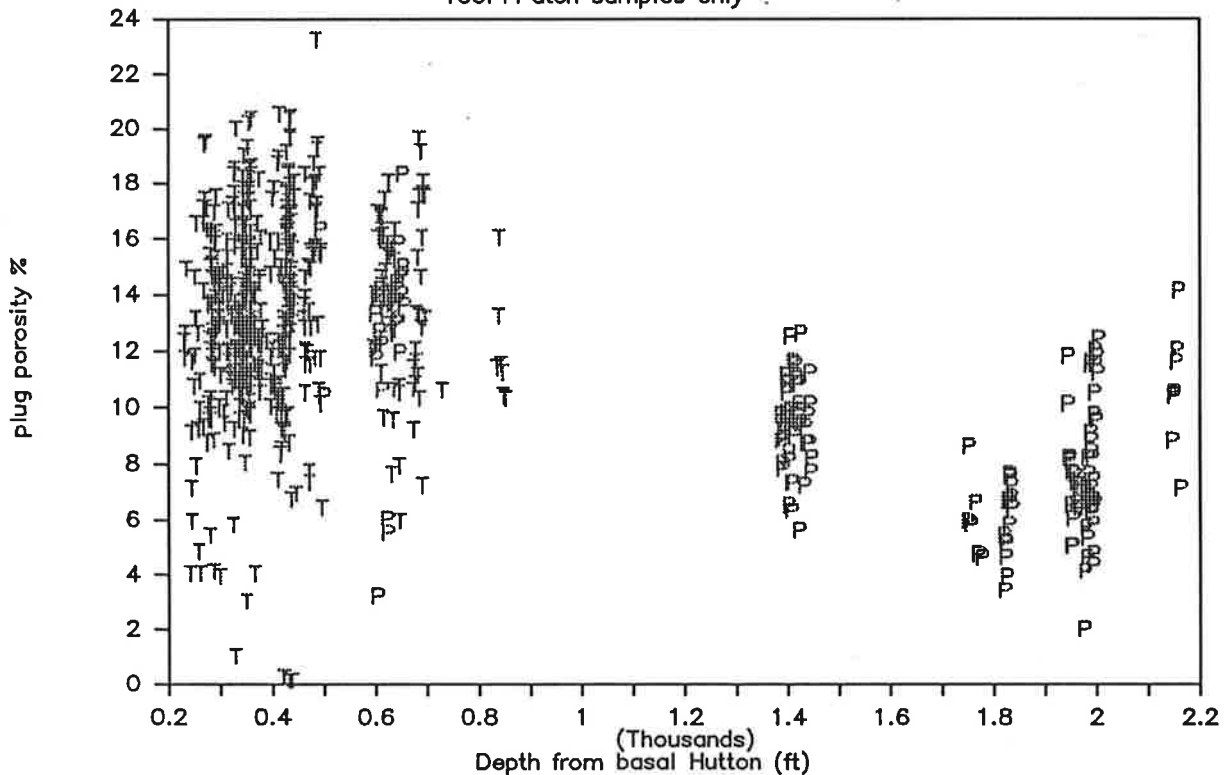


Figure 35: Porosity vs depth from Jurassic. Porosity generally decreases with depth and within 350 ft of the basal Hutton (Jurassic) unconformity. T=Toolachee Formation plug data, P=Patchawarra Formation plug data.

Porosity vs Depth

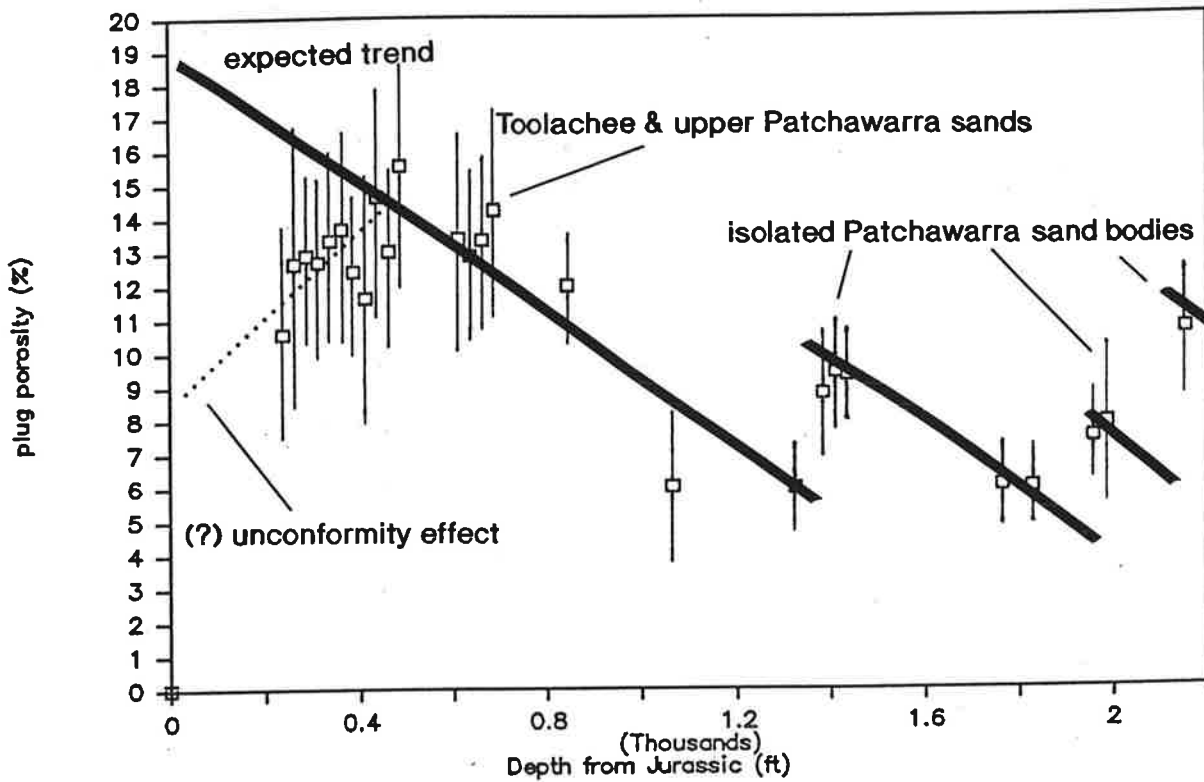


Figure 35(a): Porosity vs depth from Jurassic using the same data in Figure 35. Squares represent the average porosity over a 25 feet interval below the Jurassic, and bars represent one standard deviation of porosity on each side of the average porosity.

Plug Permeability vs Hutton Depth

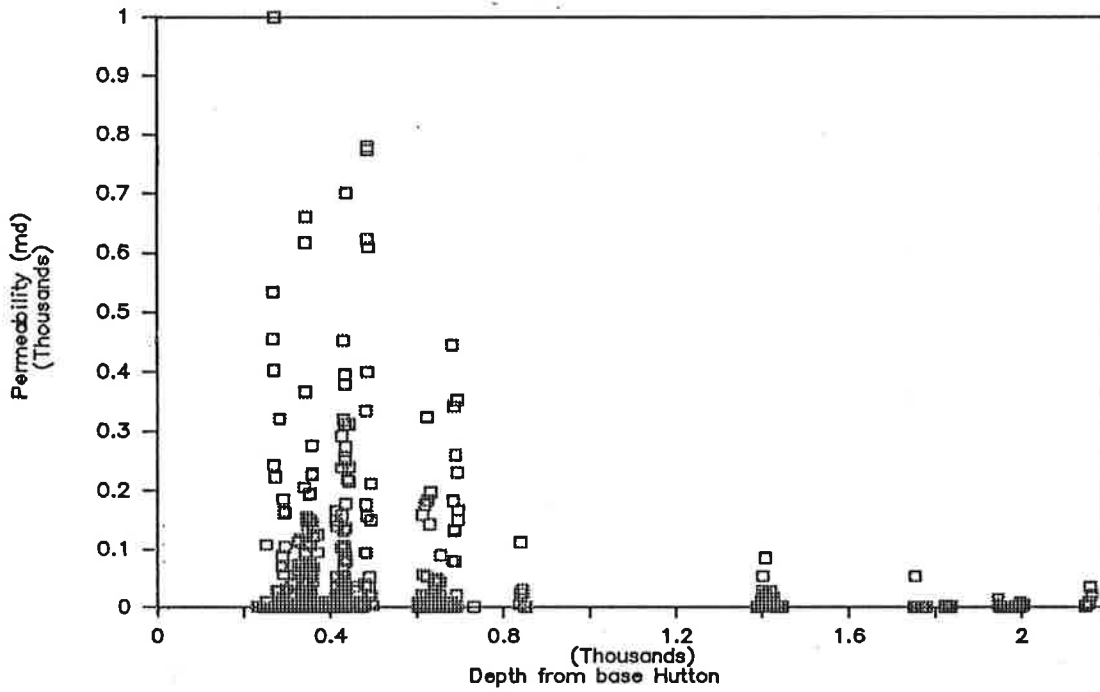


Figure 36: Plug permeability vs depth from Jurassic (basal Hutton Formation). Permeability decreases with depth and within 350 ft of the unconformity. See also Figure 34.

Plug Permeability vs Hutton Depth

673 samples

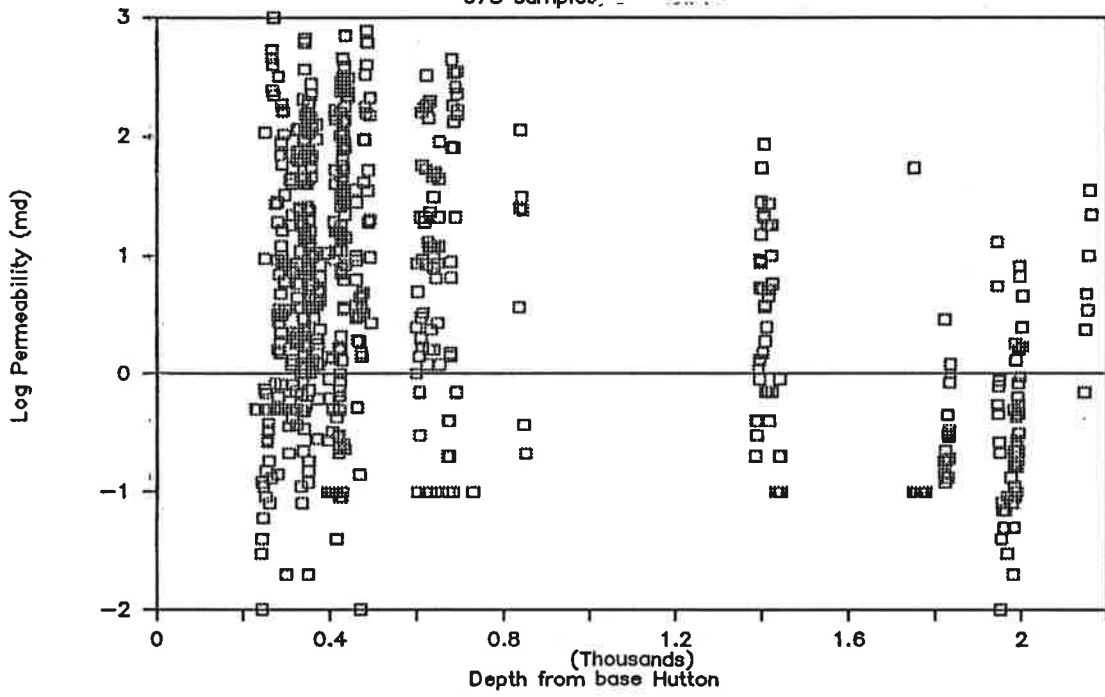


Figure 37: Log plug permeability vs depth from Jurassic.

Porosity vs Depth from Base Hutton

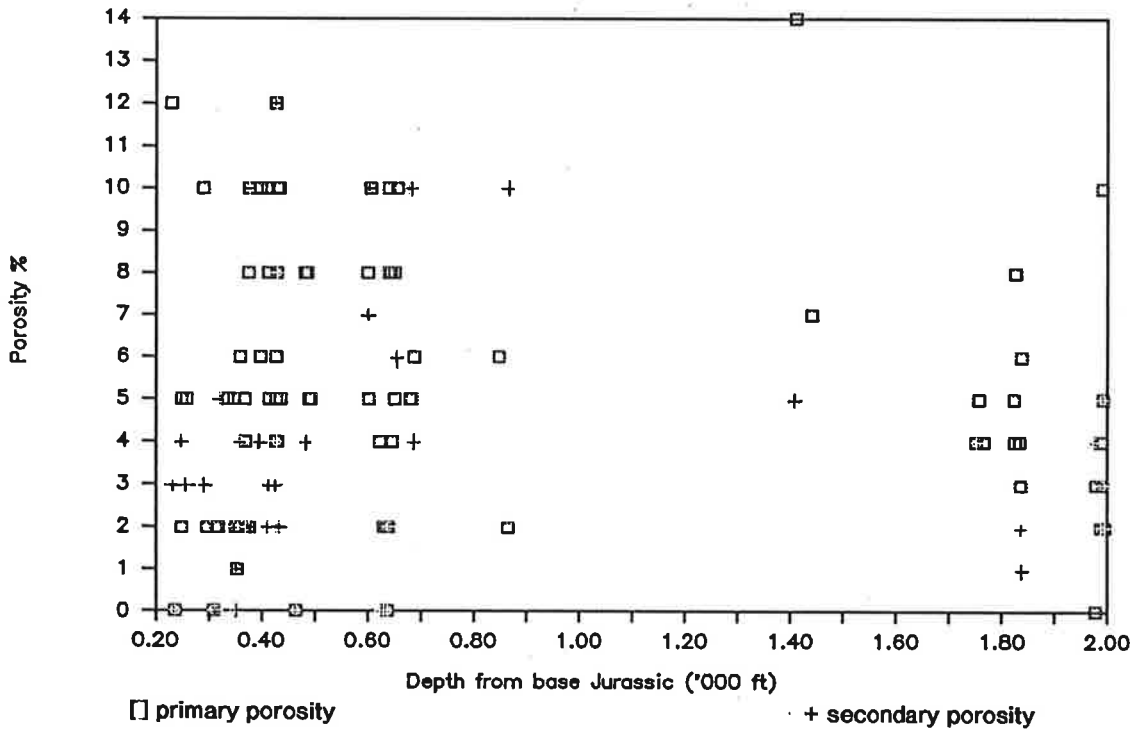


Figure 38: Primary and secondary porosity estimated by thin section vs depth from Jurassic. Similar to plug porosity vs depth in Figure 32.

Plug Residual Oil vs Hutton Depth

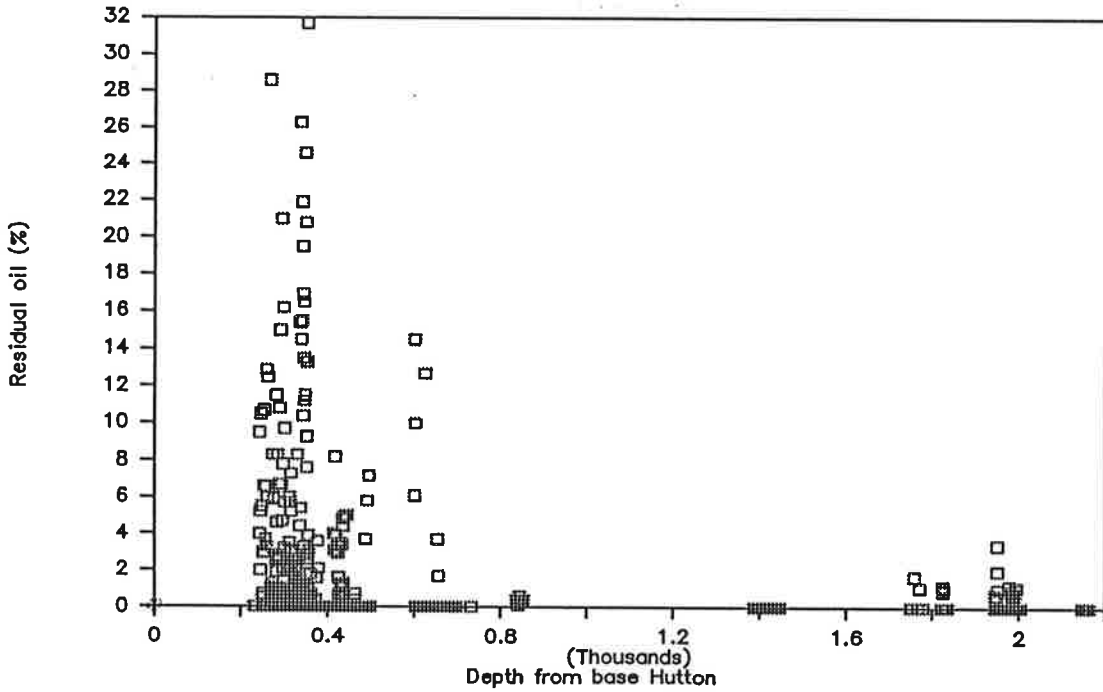


Figure 39: Plug residual oil vs depth from Jurassic. Most higher levels of residual oil are recorded from core plugs taken from 200 to 650 feet below the basal Jurassic unconformity.

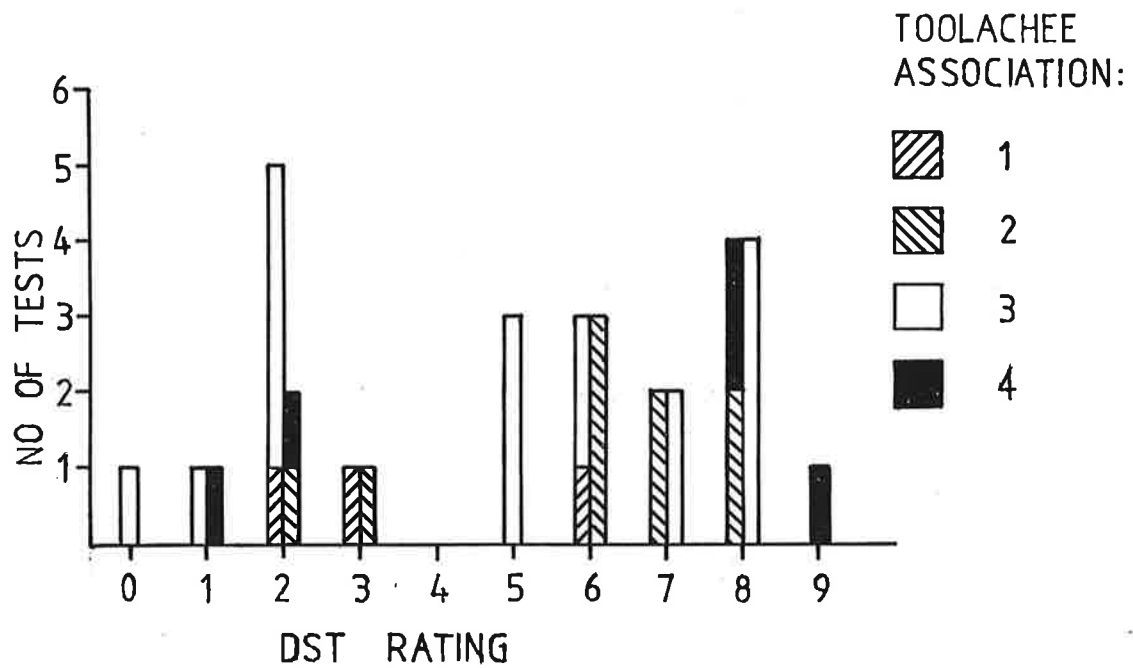


Fig. 40. 39 DST results from 4 Toolachee Formation facies associations.

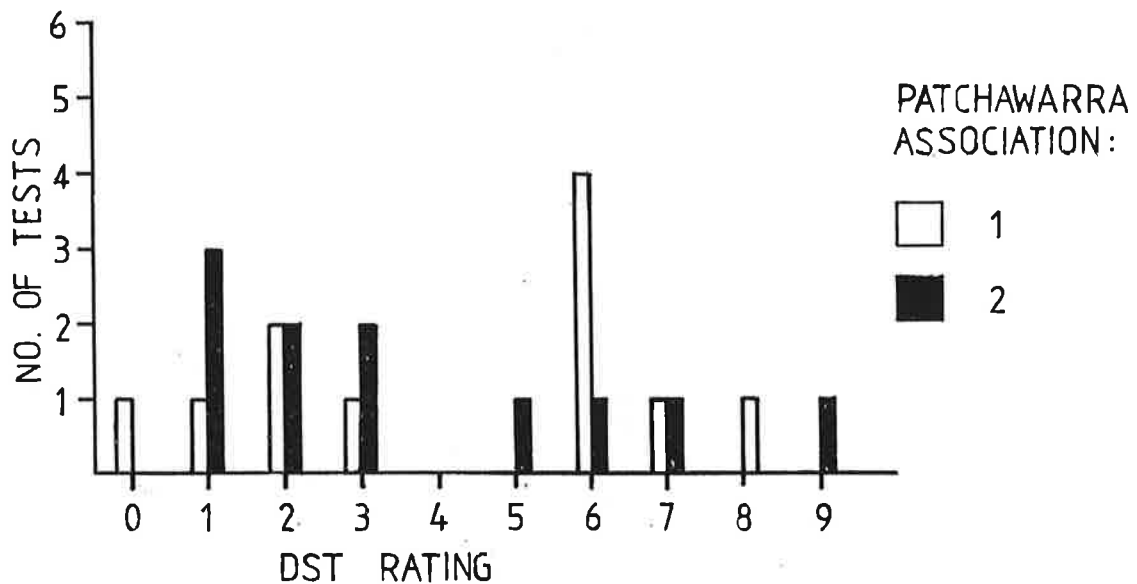


Fig. 41. 23 DST results from the upper two Patchawarra Formation facies associations.

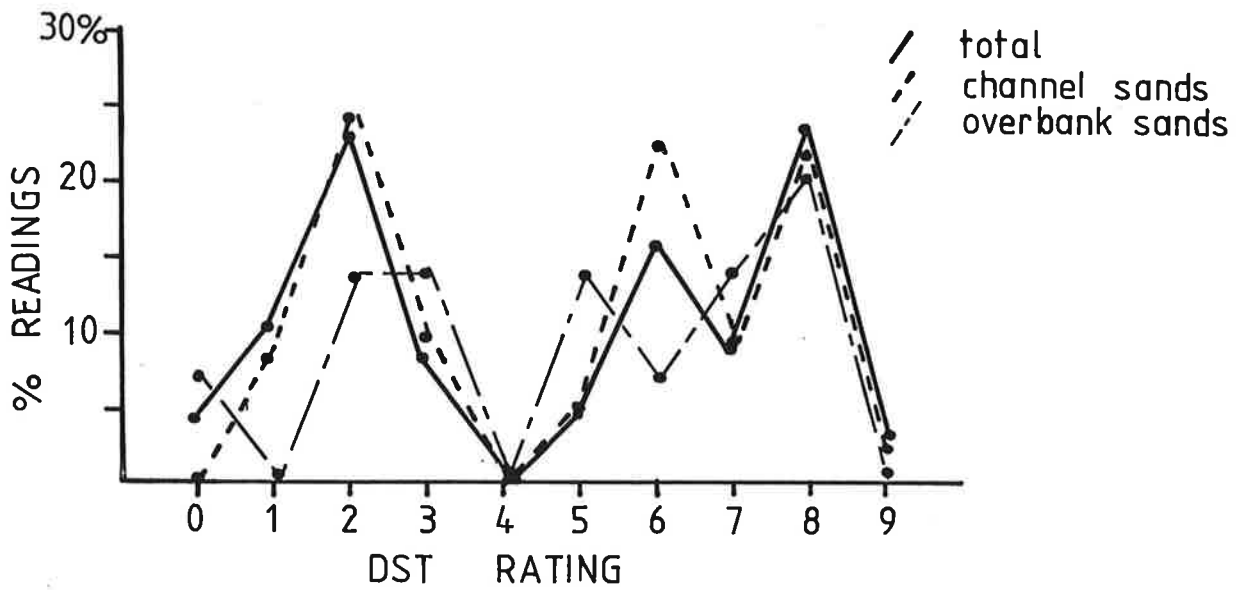


Fig. 42 DST results of testing 46 channel sands, 14 overbank sands and all sands (79 readings), Toolachee and Patchawarra Formations.

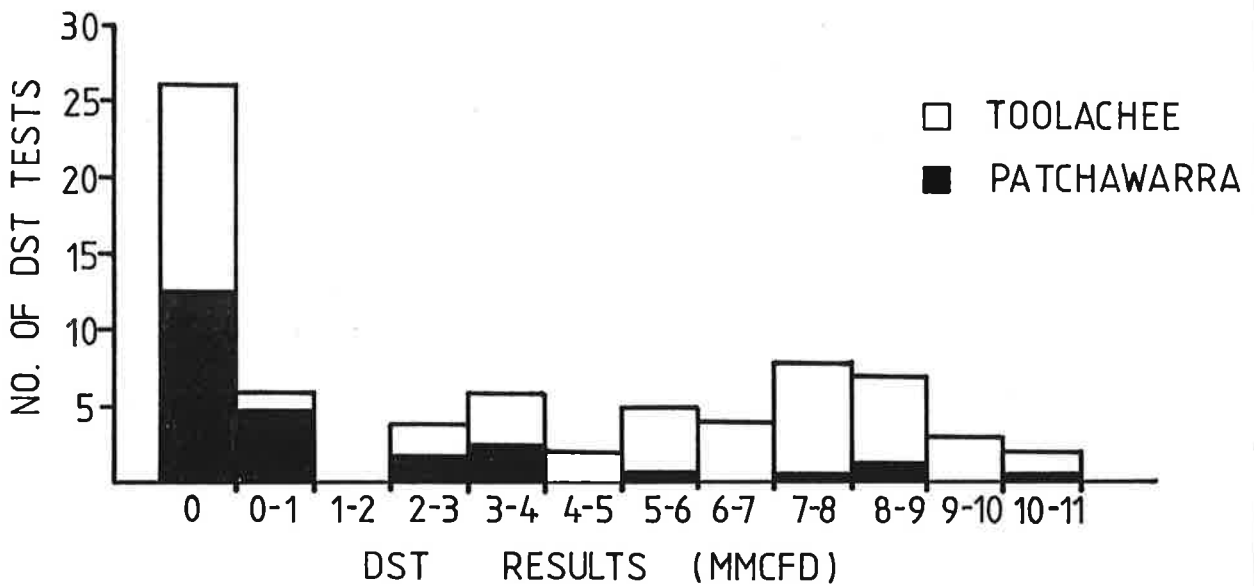


Fig. 43 Histogram of DST results, all sands.

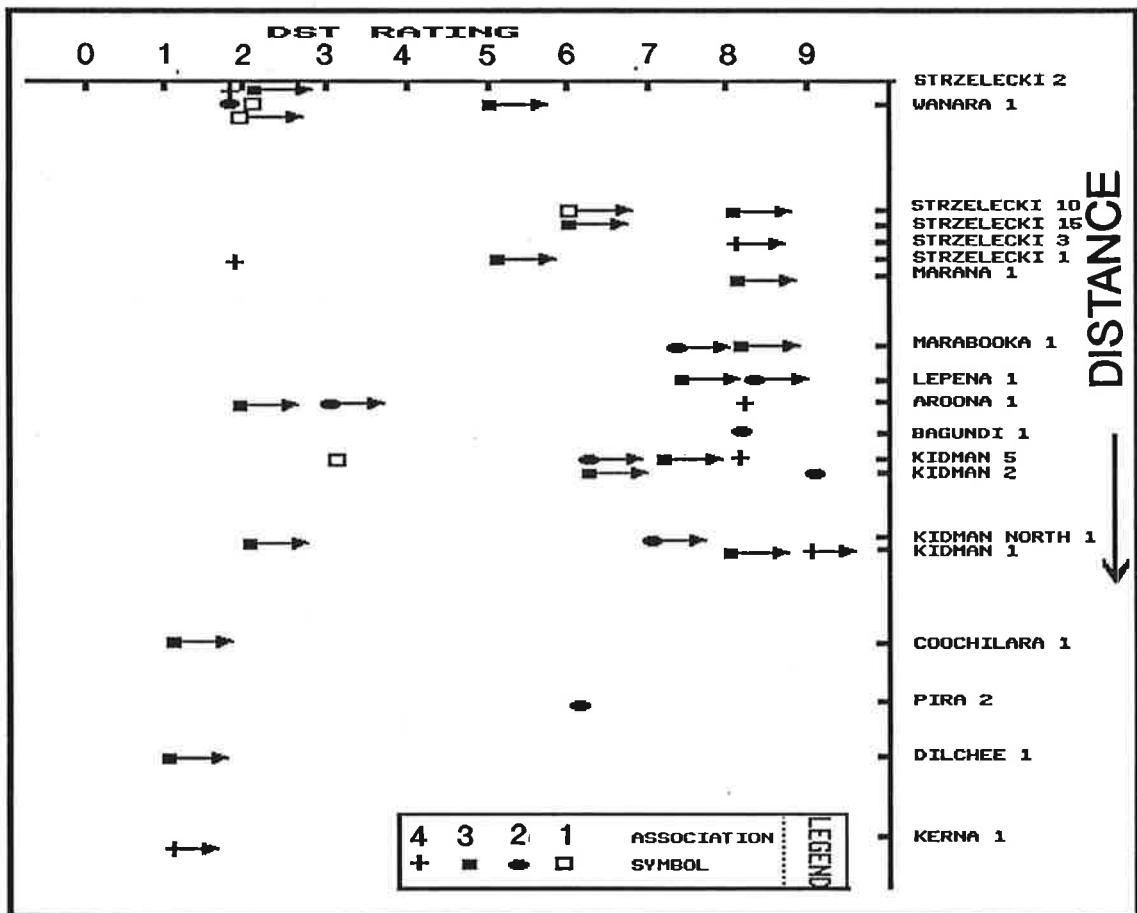


Fig. 44 Drill Stem Test ratings for Toolachee Formation facies associations, plotted as radial distance from Strzelecki 2 in the south-west of the study area. High DST ratings indicate good flow conditions. Arrows indicate a "greater than" DST rating. No pattern of DST results is apparent.

Depth from Jurassic vs TDS

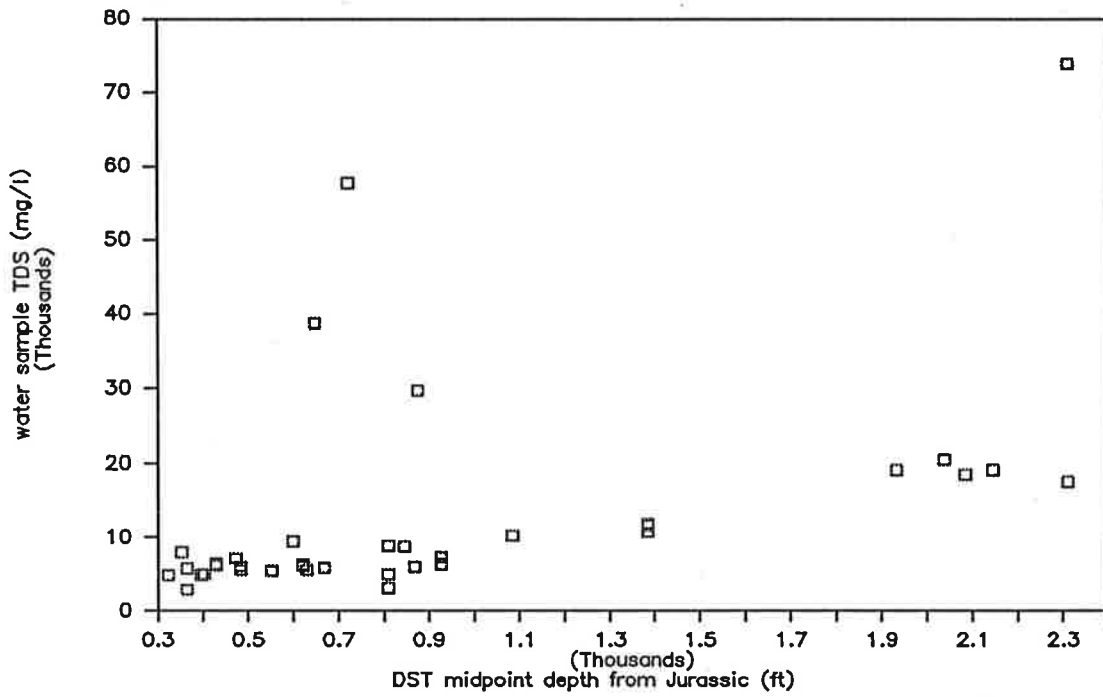


Figure 45: Groundwater TDS vs depth from Jurassic. TDS generally increases with depth. Peaks in salinity occur at 7000 feet and 2300 feet below the Jurassic and are possibly related to similar peaks in porosity, permeability and/or residual oil at 4000 and 2100 feet below the Jurassic, as evidenced in Figures 35, 36 and 39.

STRZELECKI 10

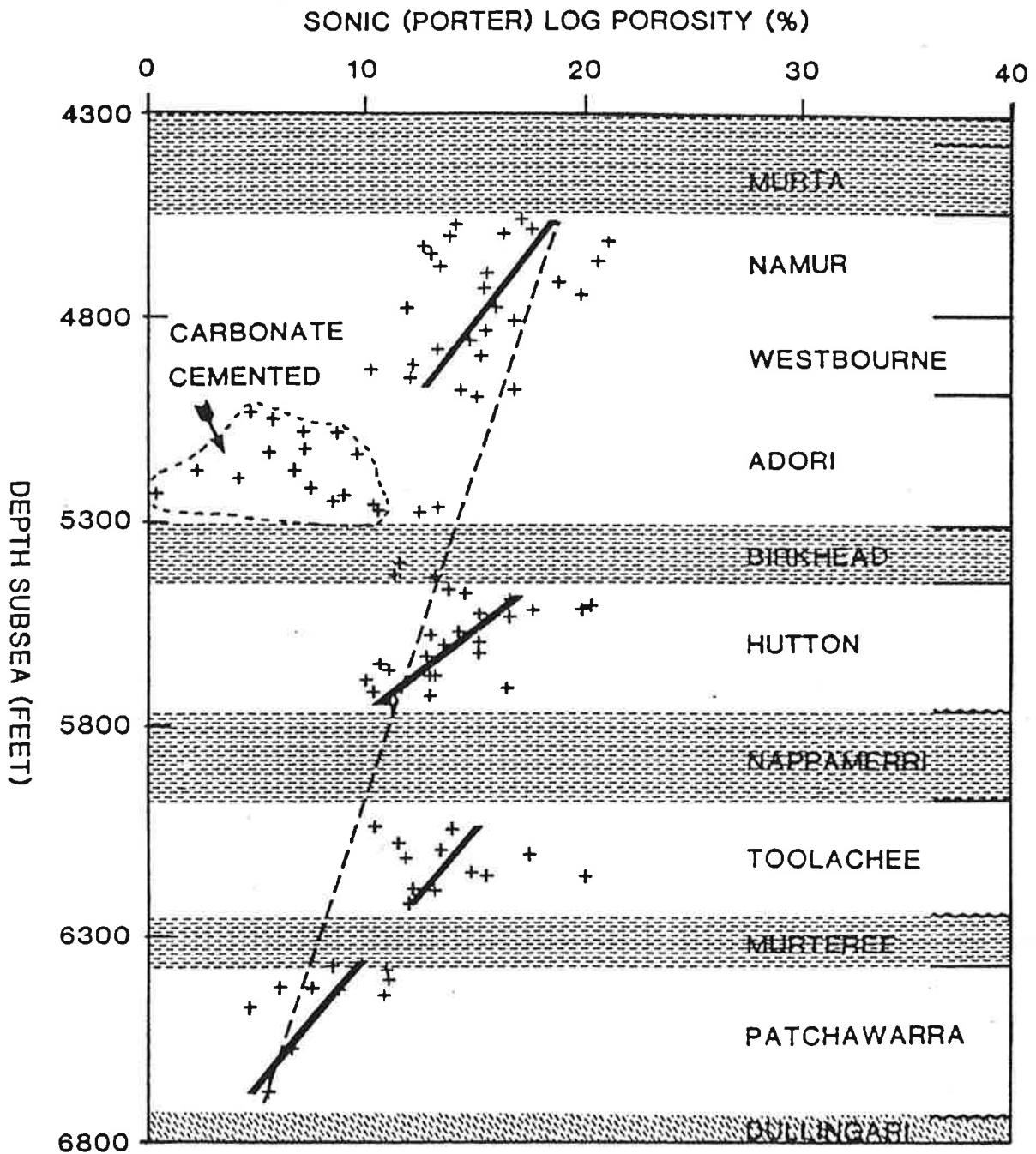


Figure 46 Strzelecki 10 porosity variation with depth, after Staughton (1985). Porosity is derived from sonic logs of arenites with less than 30% shale volume. Siltstone rich units are shaded. First order porosity variation is indicated by the dashed line and second order porosity variation is shown as thick lines within reservoir units.

Vr vs Depth

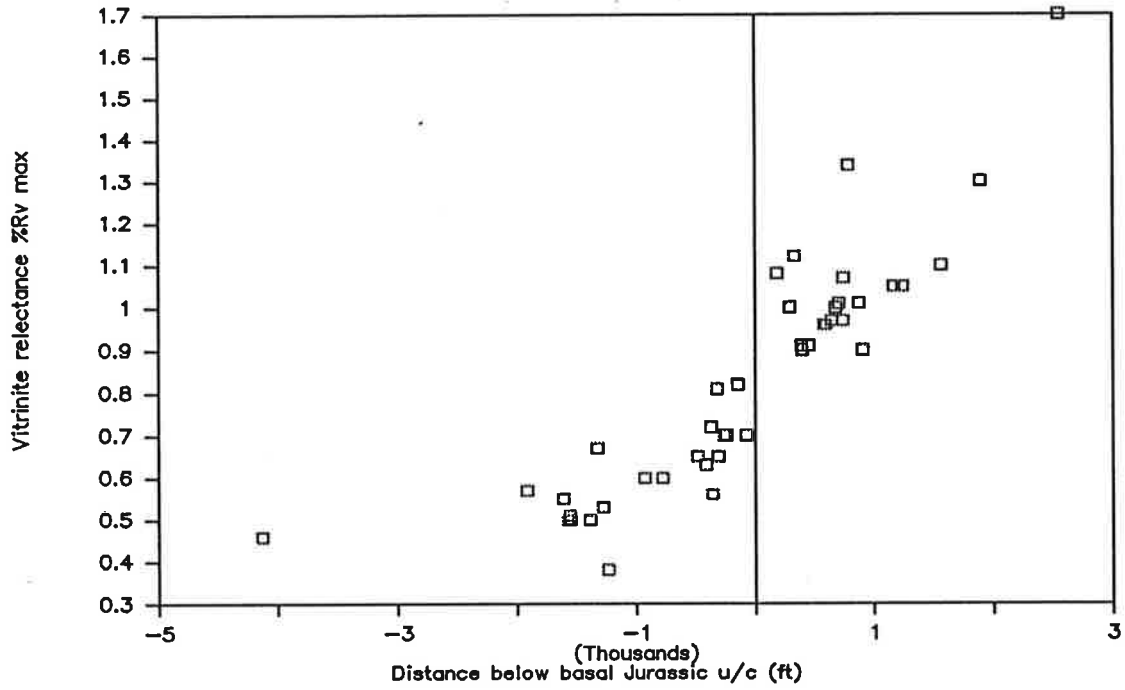


Figure 47: Vitrinite relectance vs depth from basal Jurassic. Gradient is steeper for the Cooper Basin. Data from Kantsler 1978, 1979(a),1979(b) and Keiraville Konsultants, 1984.

Porosity vs Depth

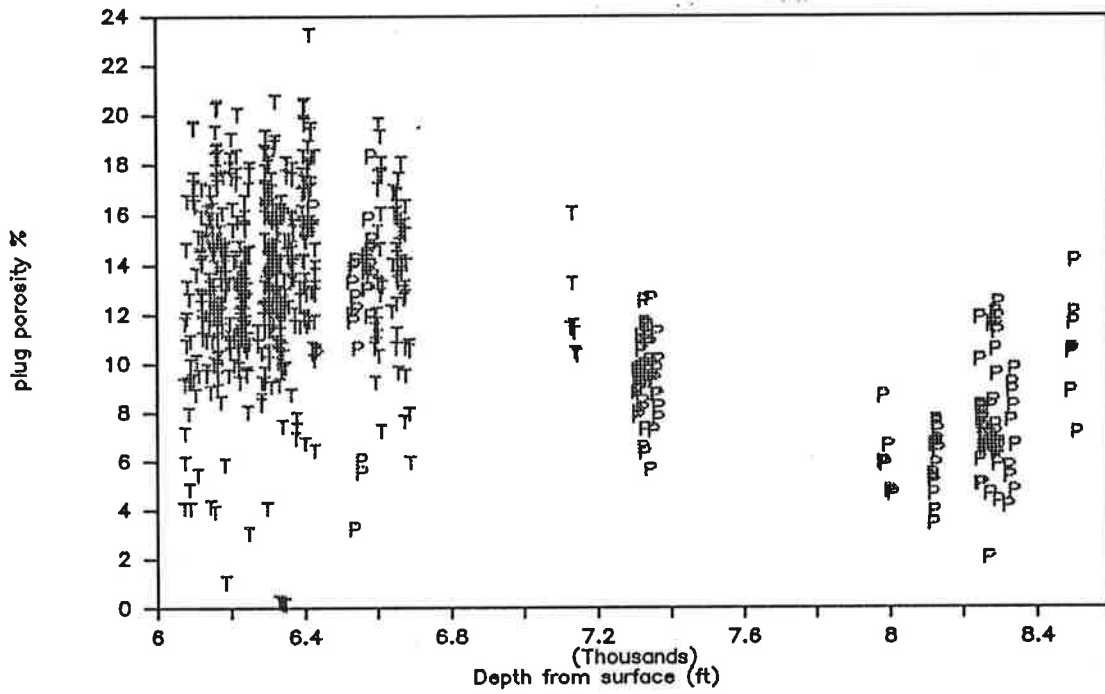


Figure 48: Plug porosity vs depth. Porosity generally decreases with depth. T=Toolachee, P=Patchawarra samples.

Dickite vs Plug Permeability

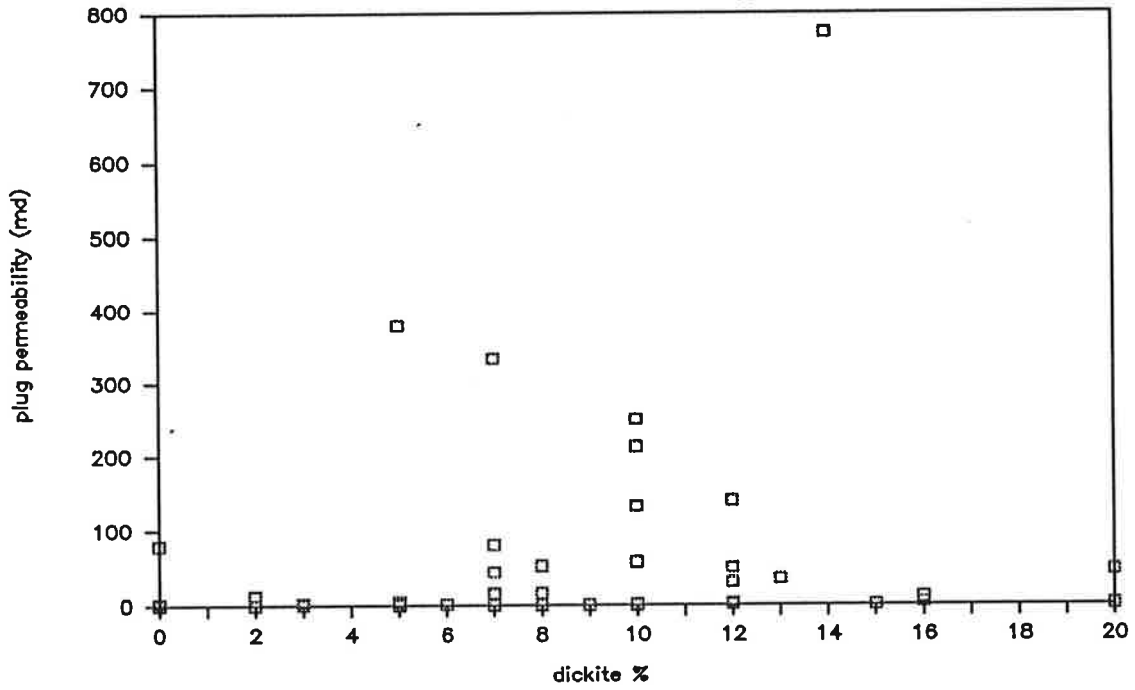


Figure 49

Dickite vs plug permeability. Permeability decreases with increasing dickite content. Microporosity associated with dickite does not appear to be a major factor in permeability.

Plug Permeability vs Grain Size

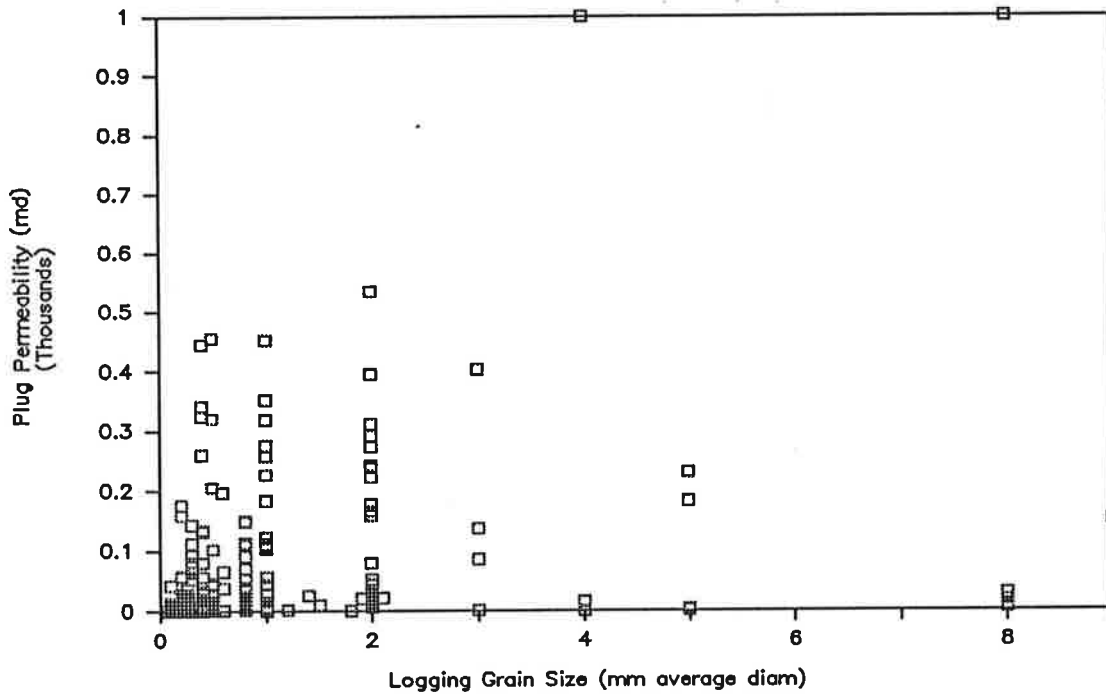


Figure 50: Plug permeability vs grain size. Permeability appears to be more variable in coarse grained sediments than fine grained sediments.

Log(permeability)/porosity vs Grain Size

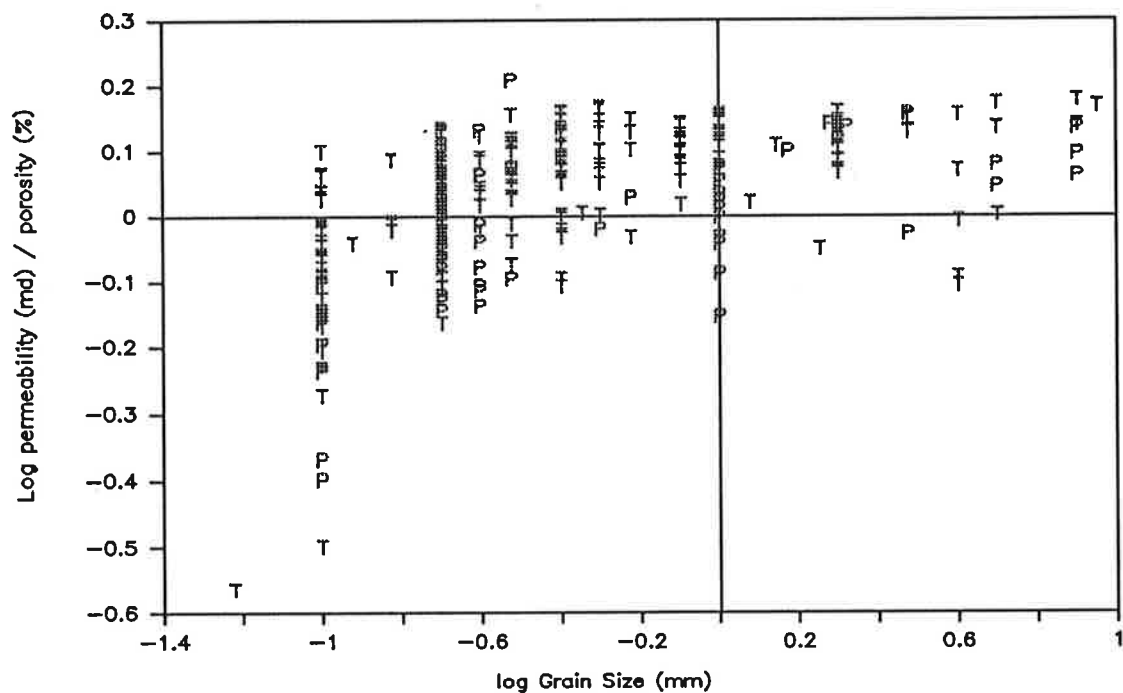


Figure 51: Log(permeability)/porosity vs grain size.

Log(permeability)/porosity vs Depth

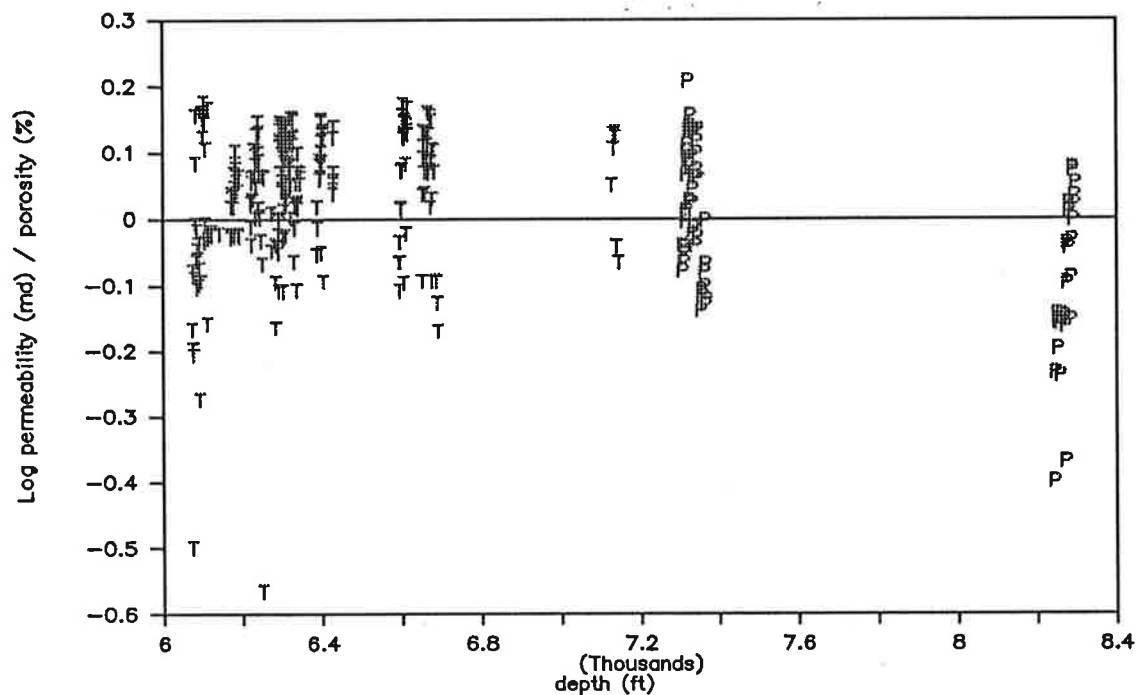


Figure 52: Log(permeability)/porosity vs depth.

Residual Oil vs Porosity

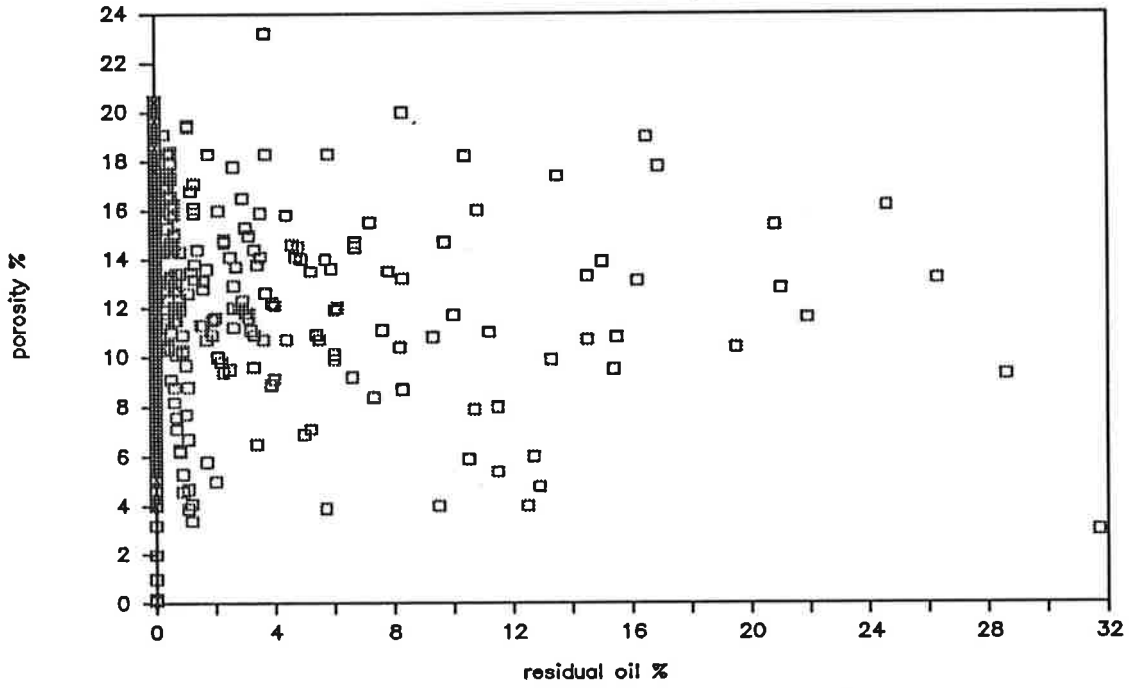


Figure 53: Porosity vs plug residual oil. Residual oil as recorded by core plug measurements is restricted to total core plug porosities of 3% to 21%.

Kaolin & Illite vs Depth from Jurassic

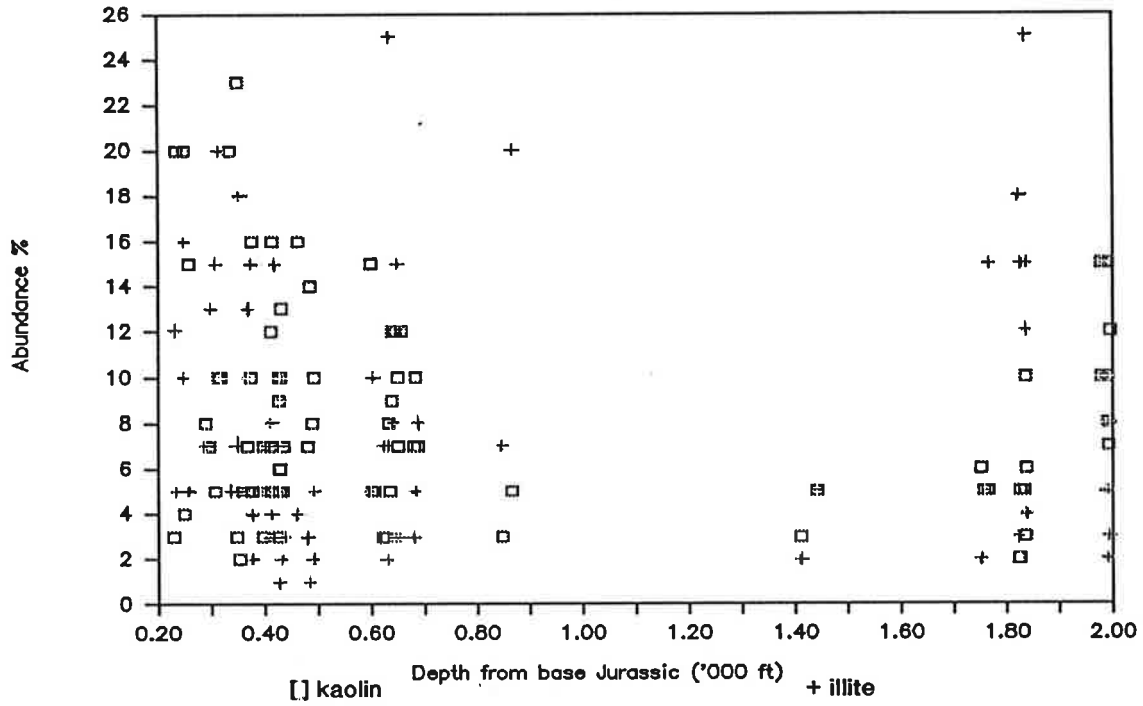


Figure 54: Kaolin & illite vs depth from Jurassic. These do not vary greatly with depth from Jurassic. See also Figures 55, 56 & 57.

Kaolin vs Depth from Jurassic

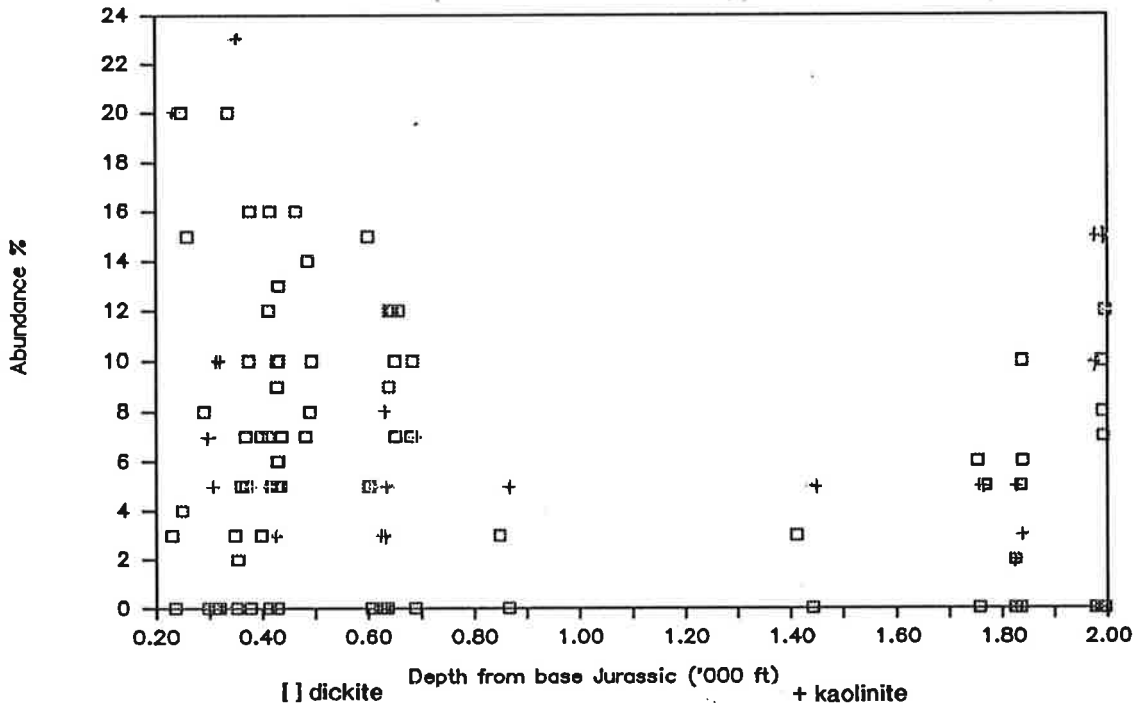


Figure 55: Kaolin vs depth from Jurassic.

Siderite vs Depth from Jurassic

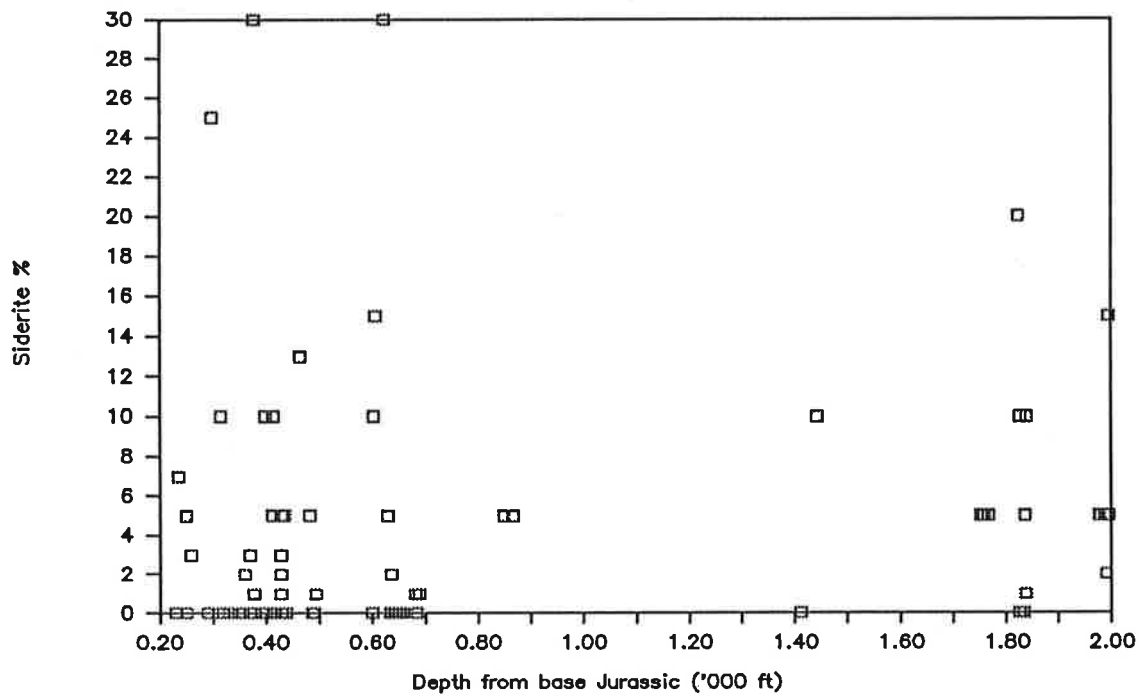


Figure 56: Siderite vs depth from Jurassic.

Illite / Kaolin vs Depth from Jurassic

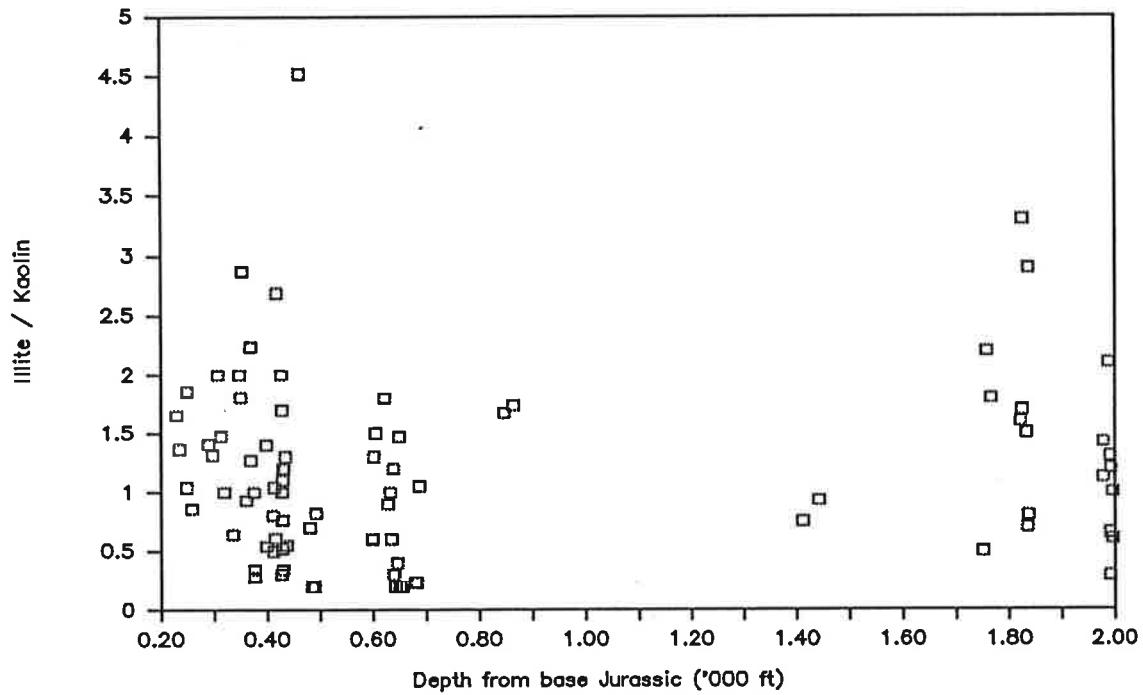


Figure 57: Illite/kaolin vs depth from Jurassic.

Porosity vs Position

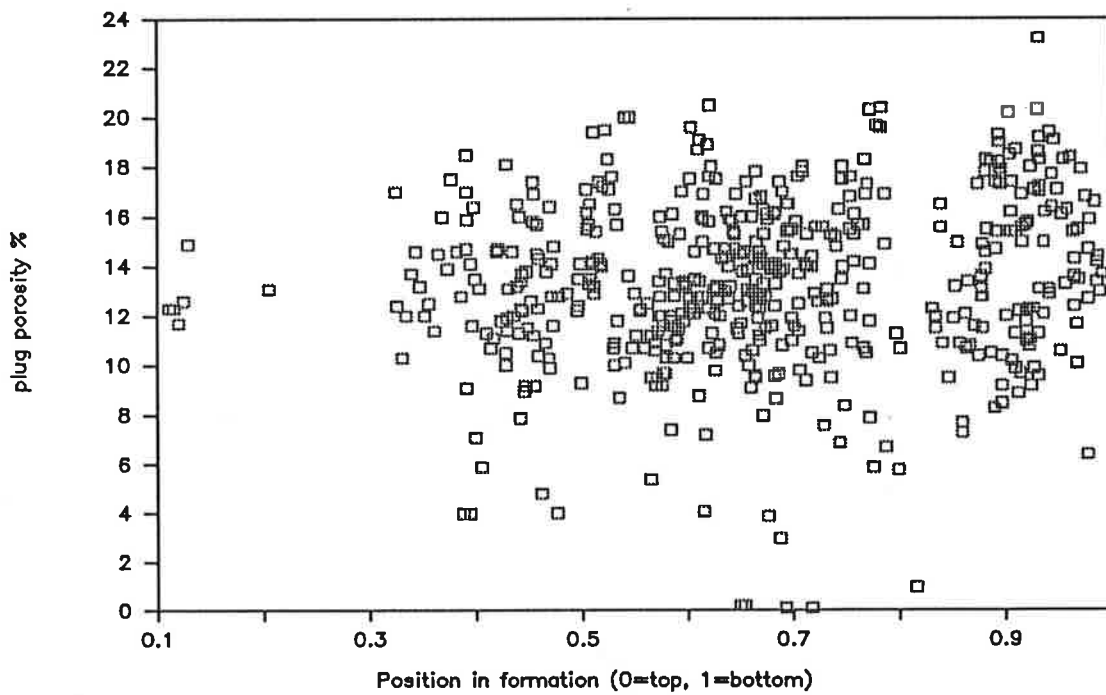


Figure 58: Plug porosity vs formation position.

Permeability vs Position

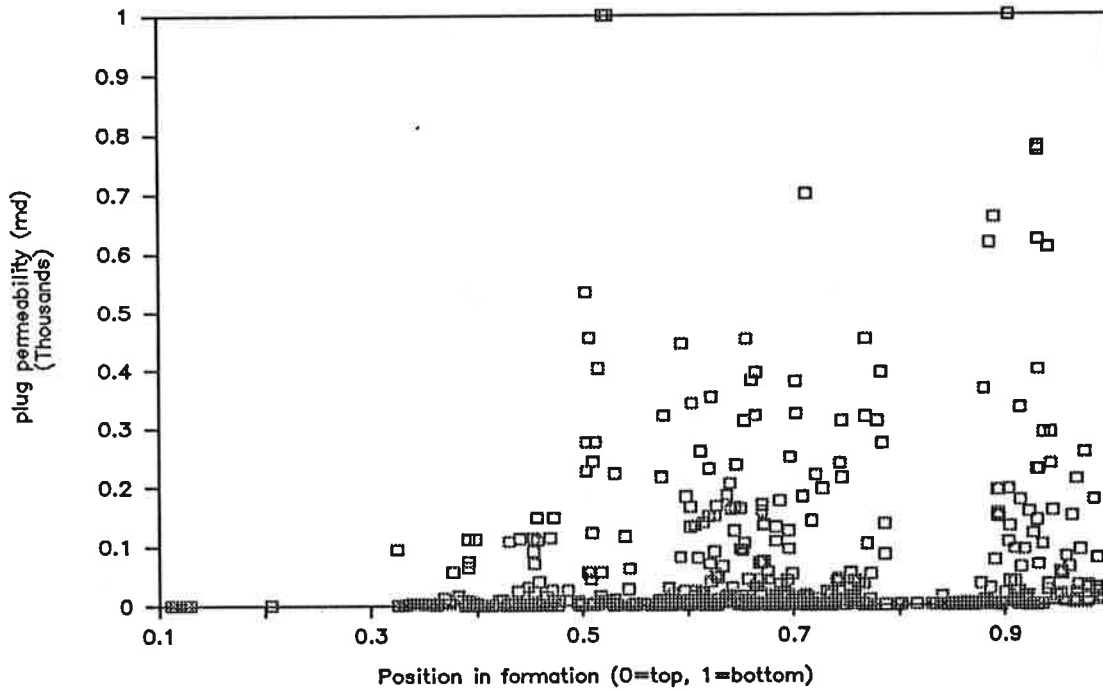


Figure 59: Plug permeability vs formation position. As with Figure 58, there appears to be no major variation in porosity and permeability across the Toolachee Formation. A similar pattern occurs for the Patchawarra Formation.

Log Permeability vs Porosity

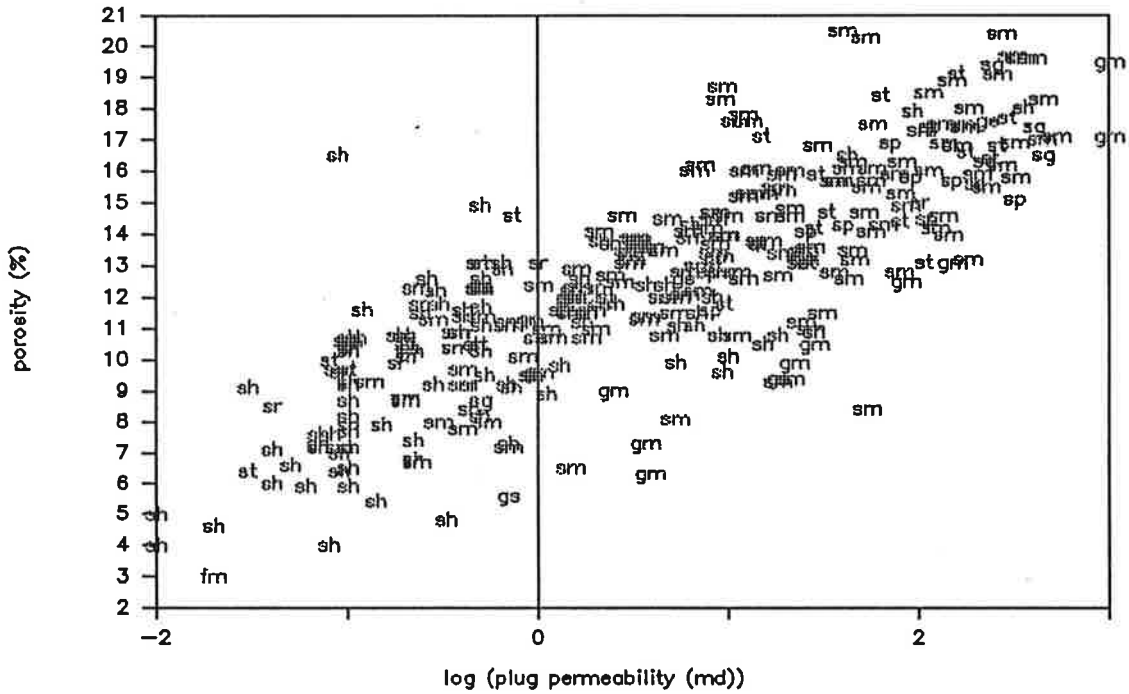


Figure 60(a) above and Fig 60(b) on the following page:

Log permeability vs porosity of 337 Toolachee and Patchawarra Formation lithofacies. fm = massive siltstone, gm = massive gravel, gs = stratified gravel, sg = sand with graded bedding, sh= sand with horizontal laminations, sm = massive sand, sp = planar cross bedded sand, st = trough crossbedded sand, sr = sand with ripple marks

Log Permeability vs Porosity

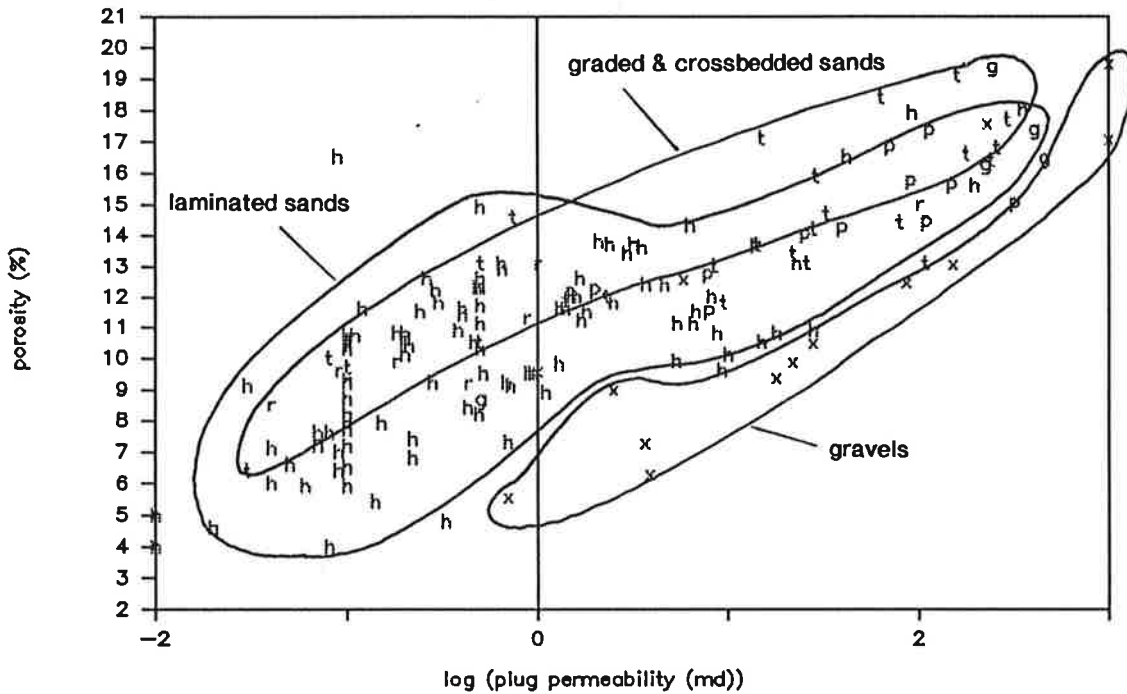


Figure 60(b) Log permeability vs porosity of 337 Toolachee and Patchawarra Formation lithofacies. The same data is plotted as Figure 60(a) except massive sands (sm). x = gravel, g = sand with graded bedding, h = sand with horizontal laminations, p = planar cross bedded sand, t = trough crossbedded sand, r = sand with ripple marks. Sands with graded bedding, planar and trough crossbeds are delineated and have higher porosities than horizontally laminated sands (delineated) and gravels (delineated) that commonly have clay matrix. Massive sands have variable porosity and permeability as seen in Figure 60(a).

Plug Permeability vs Porosity

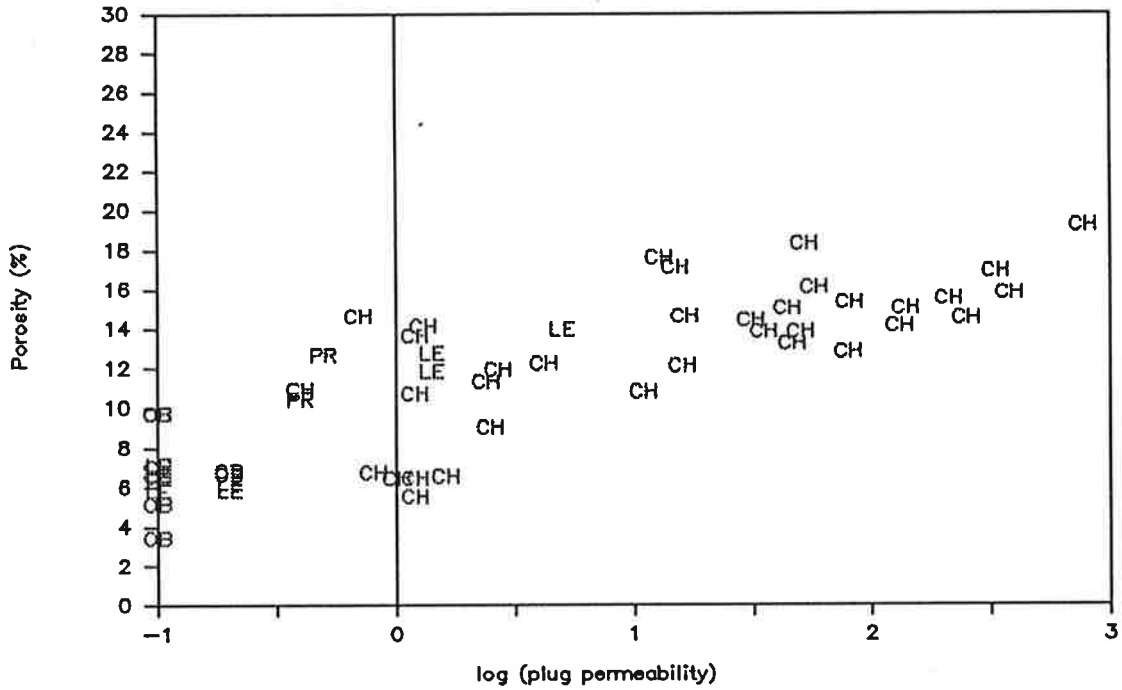


Figure 61

Log permeability vs porosity for various facies, 54 points. Channel deposits seem to have higher permeability and porosity values. CH = channel deposits, FP = floodplain deposits, LE = low energy channel deposits, OB = overbank deposits and PR = prograding deposits.

12 References

- AlDahan A.A. & Morad S. 1986. Mineralogy and chemistry of diagenetic clay minerals in Proterozoic sandstones from Sweden. *American Journal of Science* **286**, 29-80.
- Almon W.R. & Davies D.K. 1981. Fluid sensitivity analysis, Cooper Basin sandstones, Australia. Unpublished report from Davies, Almon & Associates to the South Australian Oil & Gas Corporation.
- Almon W.R., Fullerton L.B. & Davies D.K. 1976. Pore space reduction in Cretaceous sandstones through chemical precipitation of clay minerals. *Journal of Sedimentary Petrology* **46**, 89-96.
- AMDEL 1986. Determination of bulk and clay mineralogy of 47 plugs. Unpublished Report to the South Australian Department of Mines & Energy.
- Arndt L. 1986. Geophysical interpretation of the Kidman Area, Cooper Basin. Unpublished report to the South Australian Department of Mines & Energy.
- Barr T.M. & Youngs B.C. 1981. Cuttapiirrie 1; an oil discovery in the Early Jurassic of the Eromanga Basin. *Australian Petroleum Exploration Association Journal* **21**, 60-70.
- Battersby D.G. 1976. Cooper Basin gas & oil fields. In Leslie R.B., Evans H.J. & Knight C.L. eds. Economic geology of Australia and Papua New Guinea, 3. Petroleum. *Australasian Institute of Mining and Metallurgy Monograph* **7**, 321-368.
- Bayliss P. 1975. Nomenclature of the trioctahedral chlorites. *Canadian Mineralogist* **13**, 178-180.
- Berner R.A. 1981. A new geochemical classification of sedimentary environments. *Journal of Sedimentary Petrology* **51**, 359-365.
- Bjorlykke K. 1979. Cementation of sandstones. *Journal of Sedimentary Petrology* **49**, 1358-1359.
- Bjorlykke K. 1984. Formation of secondary porosity: How important is it?. In MacDonald D.A. & Surdam R.C. eds. Clastic diagenesis, *American Association of Petroleum Geologists Memoir* **37**, pp277-286.
- Bjorlykke K. 1988. Sandstone diagenesis in relation to preservation, destruction and creation of porosity. In Chilingarian G.V. & Wolf K.H. eds *Diagenesis 2, Developments in Sedimentology* **41**, pp555-588.
- Bjorlykke K. & Brendsdal A. 1986. Diagenesis of the Brent Sandstone in the Statfjord Field, North Sea. In Gautier D.L. ed. Roles of organic matter in sediment diagenesis. *Society of Economic Palaeontologists and Mineralogists, Special Publication* **30**, pp157-167
- Bjorkum P.A. & Gjelsvik N. 1988. An isochemical model for formation of authigenic kaolinite, K-feldspar and illite in sediments. *Journal of Sedimentary Petrology* **58**, 506-511.
- Blatt H. 1979. Diagenetic processes in sandstones. In Scholle P.A. & Schluger P.R. eds. Aspects of diagenesis, *Society of Economic Palaeontologists and Mineralogists, Special*

Paper 26, pp141-175.

Boles J.R. 1981. Clay diagenesis and effect on sandstone cementation In, Longstaffe L.J. (ed). Short course in clay and the resource geologist. *Mineralogical Association of Canada*, 148-168.

Boles J.R. & Franks S.G. 1979. Clay diagenesis in Wilcox sandstones of southwest Texas: implications of smectite diagenesis on sandstone cementation. *Journal of Sedimentary Petrology* **49**, 55-70.

Bone Y. 1988. Cooper/Eromanga Basin Palaeotemperatures: Implications of the correlation between fluid inclusion microthermometry and vitrinite reflectance. Adelaide University departmental research seminar, 16-3-88.

Bone Y. & Russell N.J. 1988. Geological note: correlation of vitrinite reflectivity with fluid inclusion microthermometry: Assessment of the technique in the Cooper/Eromanga Basins, South Australia. *Australian Journal of Earth Sciences* **35**, 567-570.

Bowering O.J.W. & Burnett P.J. 1980. Formation water salinities, Toolachee and Patchawarra-Tirrawarra Formations. Unpublished report to Delhi Petroleum Pty. Ltd.

Busch D.A. 1974. Stratigraphic traps in sandstone exploration. *American Association Petroleum Geologists Memoir* **21**.

Caruthers W. & Kharaka Y.K. 1978. Aliphatic anion acids in oil field waters - implications for the origin of natural gas. *American Association Petroleum Geologists Bulletin* **9**, 167-203.

Coles, Nikiforuk, Pennell 1987. Cooper Basin, Australia; Appraisal of reserves and deliverability. Report by C.N.P. Associates Ltd., Calgary, Canada to Santos Ltd.

Curtis C.D. 1978. Possible links between sandstone diagenesis and depth-related geochemical reactions occurring in enclosing mudstones. *Journal of the Geological Society of London* **135**, 107-117.

Curtis C.D. 1983. Geochemistry of porosity enhancement and reduction in clastic sediments. In Brooks J. *Petroleum geochemistry of NW Europe*, Geological Society of London Special Publication **12**, 113-126.

Curtis C.D., Hughes C.R., Whiteman J.A. & Wittle C.K. 1985. Compositional variation within some sedimentary chlorites and some comments on their origin. *Mineral Magazine* **49**, 375-387.

Dapples E.C. 1979. Silica as an agent in diagenesis. In Larsen G. & Chilingar G.V. eds. *Diagenesis in sediments and sedimentary rocks*, Developments in Sedimentology **25A**, pp99-141.

Davis S.W. 1964. Silica in streams and ground water. *American Journal of Science* **262**, 870-890.

Deer W.A., Howie R.A. & Zussman J. 1962. *Rock forming minerals 3, sheet silicates*. Longmans, London, 270p.

DeGolyer & MacNaughton 1986. Geological descriptions and maps of certain fields in

the Cooper and Eromanga Basins, Australia. Unpublished report to C.S.R. Petroleum Ltd.

Devine S.B. & Gatehouse C.G. 1977. Sandstone reservoir geometry of non-marine sediments in the Toolachee gas field. *Australian Petroleum Exploration Association Association Journal* 17, 50-57.

Dutton S.P. 1987. Diagenesis and burial history of the Lower Cretaceous Travis Peak Formation, East Texas. *Bureau of Economic Geology Report of Investigation* 164, 58p

Faridi H. & Hunt, J.W., 1987: Sedimentology, facies analysis and hydrocarbon prospectivity of the Patchawarra Formation in the Nappacoongee-Murteree and Toolachee Blocks. Regional studies team Delhi Petroleum. Unpublished Report to Delhi Petroleum Ltd.

Faehrmann A. 1986. "Permian" & "Jurassic" waters of the southern Cooper / Eromanga Basins - a discussion. Unpublished report to Santos Ltd.

Fairburn W.A. 1989. The geometry of Toolachee Unit 'C' fluvial sand trends, Moomba Field, Permian Cooper Basin, South Australia. In O'Neil B.J. ed. *The Cooper & Eromanga Basins, Australia*. Proceedings of Petroleum Exploration Society of Australia, Society of Petroleum Engineers, Australian Society of Exploration Geophysicists (SA Branches), Adelaide, 239-250.

Fuchtbauer H. 1967. Influence of different types of diagenesis on sandstone porosity. *7th. World Petroleum Congress* 2, 353-369.

Garrels R.M. & Howard P., 1959. Reactions of feldspar and mica with water at low temperatures and pressure. *Clays and Clay Minerals* 6, 58-88.

Gatehouse C.G. 1972. Formations of the Gidgealpa Group in the Cooper Basin. *Australasian Oil and Gas Review* 18, 10-15.

Gausden J. 1979. Northern Cooper Basin review, 1979. Unpublished report for Alliance Oil Development Australia N.L.

Gilby A.R. & Mortimore I.R. 1989. The prospects for Eromanga oil accumulations in the northern Cooper Basin region, Australia. In O'Neil B.J. ed. *The Cooper & Eromanga Basins, Australia*. Proceedings of Petroleum Exploration Society of Australia, Society of Petroleum Engineers, Australian Society of Exploration Geophysicists (SA Branches), Adelaide, 391-404.

Goodchild M.W. & Whitaker J.H.McD. 1986. A Petrographic study of the Rotliegendes Sandstone reservoir (Lower Permian) in the Rough Gas Field. *Clay Minerals* 21, 459-477.

Gordon H.M. 1978. Kidman Field reserves study. Unpublished Report to Delhi Corporation.

Grasso C.A. 1986. The palaeogeography of Permian sediments of the Munkarie and Brumby Gas Fields in the Southern Cooper Basin utilising Genetic Sequence of Strata. B.Sc. (Hons.) Thesis, University of Adelaide. (Unpubl.)

Gravestock D., Griffiths M. & Hill A. 1983. The Hutton Sandstone - Two separate reservoirs in the Eromanga Basin, South Australia. *Australian Petroleum Exploration*

Association Journal 23, 109-119.

Gravestock D.L. & Morton J.G.G. 1984. Geology of the Della Field, a perspective on the history of the Cooper Basin. *Australian Petroleum Exploration Association Journal* 24, 266-277.

Gretener P.E. 1978. *Pore pressure: Fundamentals, general ramifications and implications for structural geology*. American Association of Petroleum Geology, Continuing Education Course Note Series 4.

Hall P.L., Astill D.M. & McConnell J.D.C. 1986. Thermodynamic and structural aspects of the dehydration of smectites in sedimentary rocks. *Clay Minerals* 21, 633-648.

Hancock N.J. & Taylor A.M. 1978. Clay mineral genesis and oil migration in the Middle Jurassic Brent Formation. *Journal of the Geological Society of London* 135, 69-72.

Harder H. 1974. Illite mineral synthesis at surface temperature. *Chemical Geology* 14, 241-253.

Hawkins P.J. 1978. Relationship between diagenesis, porosity, reduction, and oil emplacement in late Carboniferous sandstone reservoirs, Bothamsall Oilfield, East Midlands. *Journal of the Geological Society of London* 135, 7-24.

Heald M.T. 1955. Stylolites in sandstones. *Journal of Geology* 63, 101-114.

Heath R.S., McIntyre S. & Gibbins N. 1989. A Permian origin for Jurassic reservoir oil in the Eromanga Basin. In O'Neil B.J. ed. *The Cooper & Eromanga Basins, Australia*. Proceedings of Petroleum Exploration Society of Australia, Society of Petroleum Engineers, Australian Society of Exploration Geophysicists (SA Branches), Adelaide, 405-416.

Hower J., Eslinger E.V., Hower M.E. & Perry E.A. 1976. Mechanism of burial metamorphism of argillaceous sediments: 1. Mineralogical and chemical evidence. *Bulletin of the Geological Society of America* 87, 725-737.

Huang W.L., Bishop A.M. & Brown R.W. 1986. The effect of fluid/rock ratio on feldspar dissolution and illite formation under reservoir conditions. *Clay Minerals* 21, 585-601.

Hunt J.M. 1979. *Petroleum geochemistry and geology*. W.H. Freeman & Co, San Francisco, 617p.

Hunt J.M. 1989. Generation and migration of petroleum from abnormally pressured fluid compartments. American Association of Petroleum Geologists 1989 annual convention, abstracts.

Hunt J.W. 1985. Porosity in the Cooper and Eromanga Basins. Unpublished report to Delhi Petroleum Pty. Ltd.

Hunt J.W. & Piper A.J. 1986. Interpretation of well results, progress report 2. Unpublished report to Santos Ltd.

Hunt J.W., Heath R.S. & McKenzie P. 1989. Thermal maturity & other geological controls on the distribution and composition of Cooper Basin hydrocarbons. In O'Neil B.J. ed. *The Cooper & Eromanga Basins, Australia*. Proceedings of Petroleum

Exploration Society of Australia, Society of Petroleum Engineers, Australian Society of Exploration Geophysicists (SA Branches), Adelaide, 509-524.

Hurst A.R. 1980. Occurrence of corroded authigenic kaolinite in a diagenetically modified sandstone. *Clays and Clay Minerals* 28, 393-396.

Hurst A. & Irwin H. 1982. Geological modelling of clay diagenesis in sandstones. *Clays and Clay Minerals* 17, 5-22.

Hurst V.J. & Kunkle A.C. 1985. Dehydroxylation, rehydroxylation, and stability of kaolinite. *Clays and Clay Minerals* 33, 1-14.

Imam M.B. & Shaw H.F. 1987 Diagenetic controls on the reservoir properties of gas bearing Neogene Surma Group sandstones in the Bengal Basin, Bangladesh. *Marine and Petroleum Geology* 4, 103-110.

James W.C. 1985. Early Diagenesis, Atherton Formation (Quaternary): A guide for understanding early cement distribution and grain modifications in nonmarine deposits. *Journal Sedimentary Petrology* 55, 135-146.

Jenkins C.C. 1989. Geochemical correlation of source rocks and crude oils from the Cooper and Eromanga Basins. In O'Neil B.J. ed. *The Cooper & Eromanga Basins, Australia*. Proceedings of Petroleum Exploration Society of Australia, Society of Petroleum Engineers, Australian Society of Exploration Geophysicists (SA Branches), Adelaide, 525-540.

Kantsler A.J. 1978. Coochillarra 1 vitrinite reflectance analysis. Unpublished report to Delhi Petroleum Pty. Ltd.

Kantsler A.J. 1979 (a). Strzelecki 3 petrographic descriptions of organic matter in sidewall cores. Unpublished report to Delhi Petroleum Pty. Ltd.

Kantsler A.J. 1979 (b). Kidman 3 Vr analyses and brief descriptions of coal cuttings and core. Unpublished report to Delhi Petroleum Pty. Ltd.

Kantsler A.J. & Cook A.C. 1979. Rank variation in the Cooper & Eromanga Basins central Australia. Unpublished report to Delhi Petroleum Pty. Ltd.

Kantsler A.J., Cook A.C. & Zwigulis M. 1986. Organic maturation in the Eromanga Basin. in Gravestock D.I., Moore P.S. & Pitt G.M. eds. *Contributions to the Geology and Hydrocarbon Potential of the Eromanga Basin*. Geological Society of Australia Special Publication 12, 305-322.

Kantsler A.J., Smith G.C. & Cook A.C. 1978. Lateral & vertical rank variation: Implications for hydrocarbon exploration. *Australian Petroleum Exploration Association Journal* 18, 143-156.

Kantsler A.J., Prudence T.J.C., Cook A.C. & Zwigulis M. 1983. Hydrocarbon habitat of the Cooper/Eromanga Basin, Australia. *Journal of the Australian Petroleum Exploration Association* 23, 75-92.

Kapel A.J. 1966. The Coopers Creek Basin. *Journal of the Australian Petroleum Exploration Association* 6, 71-75.

- Kapel A.J. 1972. The geology of the Patchawarra area, Cooper Basin. *Australian Petroleum Exploration Association Journal* **12**, 53-57.
- Keiraville Konsultants 1984. Organic Petrology of a suite of samples from Dilchee 1. Unpublished report to Delhi Petroleum Pty. Ltd.
- Kuang K.S. 1985. History and style of Cooper-Eromanga basin structures. *4th Australian Society of Exploration Geophysicists Conference*, Sydney. 245-248.
- Lonoy A., Akselsen J. & Ronning K. 1986. Diagenesis of a deeply buried sandstone reservoir: Hill Field, Northern North Sea. *Clay Minerals* **21**, 497-511.
- Loughnan P.F. & Roberts F.I. 1986. Dickite- and kaolinite-bearing sandstones and conglomerates in Illawarra Coal Measures of the Sydney Basin, New South Wales. *Australian Journal of Earth Science* **33**, 325-332.
- Manktelow N. 1979. Structure and tectonics of the Cooper Basin. Unpublished report to Delhi Petroleum Pty. Ltd.
- Martin K.R. 1980. A preliminary account of diagenesis and reservoir quality in the Toolachee Formation, Cooper Basin. Unpublished Report to Santos Ltd.
- Martin K.R. 1981. A comparison of the petrology of sandstone from the Daralingie Beds in Moomba 19 and 45 Wells, Cooper Basin. Unpublished Report to Santos Ltd.
- Martin K.R. 1982. A comparison of the reservoir quality of the Toolachee and Patchawarra Formations, Dullingari Field, Cooper Basin. Unpublished Report to Santos Ltd.
- Martin K.R. 1984. A petrological study of Patchawarra 76-1 Sand in Toolachee 14, Cooper Basin. Unpublished Report to Santos Ltd.
- Martin K.R. 1988. Petrology and reservoir quality of the Patchawarra Formation in Pira 2, Cooper-Eromanga Basin, South Australia. Unpublished Report to Santos Ltd.
- Martin K.R. & Hamilton N.J. 1981. Diagenesis and reservoir quality, Toolachee Formation, Cooper Basin. *Journal of the Australian Petroleum Exploration Association* **21**, 143-154.
- McBride E.F. 1989. Quartz cement in sandstones: a review. *Earth Science Reviews* **26**, 69-112.
- Molenaar N. 1986 The interrelation between clay infiltration, quartz cementation and compaction in Lower Givetian terrestrial sandstones, northern Ardennes, Belgium. *Journal of Sedimentary Petrology* **56**, 359-369.
- Moore P. 1985. Petroleum traps: their nature & origin. Unpublished report to Delhi Petroleum Pty. Ltd.
- Morad S. & AlDahan A.A. 1987. A SEM study of diagenetic kaolinisation and illitisation of detrital feldspars in sandstones. *Clay Minerals* **22**, 237-243.
- Muller G. 1967. Diagenesis in argillaceous sediments. In: G.Larsen and G.V. Chilingar (eds), *Diagenesis in sediments*, Developments in sedimentology 8. Elsevier, Amsterdam,

pp127-177.

O'Shea K.J. & Frapce S.K. 1988. Authigenic illite in the Lower Silurian Cataract Group Sandstones of Southern Ontario. *Bulletin of Canadian Petroleum Geology* **36**, 158-167.

Overton M. & Evanochko J. 1987. Petrophysical cut-offs review. Unpublished Report to Santos Ltd.

Overton M. & Hamilton N. 1986. A petrophysical review of unit fields, Cooper Basin, South Australia. Unpublished Report to Santos Ltd.

Padmasiri S. & Cook A.C. 1983. Organic petrology of suites of samples from Strzelecki 4 and 5 wells. Unpublished report to Delhi Petroleum Pty. Ltd. by Keiraville Konsultants.

Palanynk V.S. 1987. Strzelecki Field estimate of original oil in place. Unpublished Report to Delhi Petroleum Pty. Ltd.

Paul R. 1988. *Organic metamorphism and geothermal history*. Reidel, 273p

Perry E.A. & Hower J. 1970. Burial diagenesis in Gulf Coast pelitic sediments. *Clays and Clay Minerals* **18**, 165-177.

Petroleum Management Associates Pty. Ltd. 1986. A detailed analysis of the Cooper Eromanga Basins. Unpublished Report to Santos Ltd.

Pettijohn F.J., Potter P.E. & Siever R. 1987. *Sand and sandstone*. Springer - Verlag New York. 553p

Pitt G.M. 1986. Geothermal gradients, geothermal histories and the timing of thermal maturation of the Eromanga-Cooper Basins. in Gravestock D.I., Moore P.S. & Pitt G.M. eds. *Contributions to the Geology and Hydrocarbon Potential of the Eromanga Basin*. Geological Society of Australia Special Publication 12, 323-351.

Postma D. 1977. The occurrence and chemical composition of recent Fe-rich mixed carbonates in a river bog. *Journal of Sedimentary Petrology* **47**, 1089-1098.

Postma D. 1982. Pyrite and siderite formation in brackish and freshwater swamp sediments. *American Journal of Science* **282**, 1151-1183.

Powis G.D. 1989. Revision of Triassic stratigraphy at the Cooper Basin to Eromanga Basin transition. In O'Neil B.J. (ed), *The Cooper and Eromanga Basins, Australia*. Proceedings of Petroleum Society of Australia, Society of Petroleum Engineers, Australian Society of Exploration Geophysics (S.A. Branches), Adelaide, 265-277.

Price P.L., Fillatoff J., Williams A.J., Pickering S.A. & Woods G.R. 1985. Late Palaeozoic and Mesozoic palynostratigraphical units. Unpublished report to C.S.R. Oil and Gas Division.

Pyecroft M. 1973. The Della Field, Cooper Basin. *Australian Petroleum Exploration Association Journal* **13**, 58-67.

Raven M.D. & Milnes A.R. 1989. Mineralogical analysis of Cooper Basin drill core samples. CSIRO technical memorandum 18/1989, Unpublished Report to the National Centre of Petroleum Geology and Geophysics.

Reading H.G. ed., 1978. *Sedimentary environments and facies*. Blackwell, Oxford. 557p.

Reinson G.E. & Foscolos A.E. 1986. Trends in sandstone diagenesis with depth of burial, Viking Formation, Southern Alberta. *Bulletin of Canadian Petroleum Geology* **34**, 126-152.

Richards N.C. 1982. Kerna Field reserves report. Unpublished Report to Delhi Corporation.

Richards N.C. 1984. Strzelecki Field Study. Unpublished Report to Delhi Petroleum Pty. Ltd.

Rigby D. & Smith J.W. 1981. An isotopic study of gases and hydrocarbons in the Cooper Basin. *Australian Petroleum Exploration Association Journal* **21**, 222-229.

Russell N.J. & Bone Y. 1989. Palaeogeothermometry of the Cooper & Eromanga Basins, South Australia. In O'Neil B.J. ed. *The Cooper & Eromanga Basins, Australia*. Proceedings of Petroleum Exploration Society of Australia, Society of Petroleum Engineers, Australian Society of Exploration Geophysicists (SA Branches), Adelaide, 559-582.

Sarkisyan S.G. 1972. Origin of authigenic clay minerals and their significance in petroleum geology. *Sedimentary Geology* **7**, 1-22.

Schmidt V. & McDonald D.A. 1979. Secondary reservoir porosity in the course of sandstone diagenesis. *American Association of Petroleum Geology Education Course Note Series* **12**, p1-125.

Schultz-Rojahn J.P. & Phillips S.E. 1989. Diagenetic alteration of Permian reservoir sandstones in the Nappamerri Trough and adjacent area, southern Cooper Basin. In O'Neil B.J. ed. *The Cooper & Eromanga Basins, Australia*. Proceedings of Petroleum Exploration Society of Australia, Society of Petroleum Engineers, Australian Society of Exploration Geophysicists (SA Branches), Adelaide, 629-646.

Shanmugam G. 1989. Porosity prediction in sandstones using erosional unconformities. American Association of Petroleum Geologists 1989 annual convention, abstracts.

Shelton J.W. 1964. Authigenic kaolinite in sandstone, *Journal of Sedimentary Petrology* **34** pp.102-111

Smith M.J. 1987. Facies interpretation and genetic unit mapping of the Epsilon Formation in the Toolachee Field area, Southern Cooper Basin, South Australia. Unpublished honours thesis, Adelaide University.

Smosna R. 1988. Low temperature, low pressure diagenesis of Cretaceous sandstones, Alaskan North Slope. *Journal of Sedimentary Petrology* **58** 644-655.

Smyth M. 1983 Nature of source material for hydrocarbons in the Cooper Basin, Australia. *American Association of Petroleum Geologists Bulletin* **67**, 1422-1428.

Stanley D.J. & Halliday G. 1984. Massive hydraulic fracture stimulation of the early Permian gas reservoirs, Big Lake Field, Cooper Basin. *Journal of the Australian Petroleum Exploration Association* **24**, 170-179.

Stanton R.L. 1972. *Ore Petrology*. McGraw Hill, Sydney. 713p.

Staughton D.B. 1985. The diagenetic history and reservoir quality evaluation of the Strzelecki hydrocarbon field, Cooper/Eromanga Basins, South Australia. Unpublished Bachelor of Science Honours thesis, Department of Earth Sciences, Monash University.

Stewart D.J. 1986. Diagenesis of the shallow marine Fulmar Formation in the central North Sea. *Clay Minerals* **21**, 537-564.

Stevenson B.G. 1985. Petrography and petrophysical analysis of Tirrawarra 46. Amdel Report F6190/85.

Stuart W.J. 1976. The genesis of Permian and Lower Triassic reservoir sandstones during phases of southern Cooper Basin development. *Australian Petroleum Exploration Association Journal* **16**, 41-48.

Stuart W.J., Kennedy S. & Thomas A.D. 1988. The influence of structural growth and other factors on the configuration of fluviatile sandstones, Permian Cooper Basin. *Australian Petroleum Exploration Association Journal* **28**, 255-266.

Surdam R.C., Boesse S.W. & Crossley L.J. 1984. The chemistry of secondary porosity. In McDonald D.A. & Surdam R.C. (eds), *Clastic diagenesis*. *American Association of Petroleum Geologists Memoir* **37**, 127-150.

Taylor G.H., Liu S.Y. & Smyth M. 1988. New light on the origin of Cooper Basin oil. *Australian Petroleum Exploration Association Journal* **28**, 303-309.

Taylor R.J. & Thomas A.D. 1989. Seismic character of fluvial sandbody geometry, upper Toolachee Formation, central Patchawarra Trough, Cooper Basin, South Australia. In O'Neil B.J. ed. *The Cooper & Eromanga Basins, Australia*. Proceedings of Petroleum Exploration Society of Australia, Society of Petroleum Engineers, Australian Society of Exploration Geophysicists (SA Branches), Adelaide, 215-225.

Thornton R.C.N. 1973. Lithofacies study on the Toolachee Formation, Gidgealpa - Moomba - Big Lake area, Cooper Basin, South Australia. *Australian Petroleum Exploration Association Journal* **13**, 41-48.

Thornton R.C.N. 1978. Regional lithofacies and palaeogeography of the Gidgealpa Group. *Australian Petroleum Exploration Association Journal* **17**, 52-63

Thornton R.C.N. 1979. Regional stratigraphic analysis of the Gidgealpa Group, southern Cooper Basin, Australia. *Bulletin of the Geological Survey of South Australia* **49**.

Tybor P. 1986. Crude oil - parent source rock correlation study, Strzelecki Field South Australia. Unpublished report from Analabs to Delhi Petroleum Pty. Ltd.

Wall V.J. 1987. Hydrocarbon reservoir quality in the Cooper/Eromanga Basins. Department of Earth Sciences, Monash University, NERDDP Project No.808 (ref.84/4067) (unpublished).

Weaver C.E. & Beck K.C. 1971. Clay water diagenesis during burial: How mud becomes gneiss. *Geological Society of America Special Paper* **134**, 96p.

Wehl P.K. 1959. Pressure solution and the force of crystallisation, a phenomenological theory. *Journal of Geophysical Research* **64**, 2001-2025.

Weaver C.E. & Pollard L.D. 1973. *The chemistry of clay minerals* Elsevier, Developments in Sedimentology 15, 213p.

Williams B.P.J. 1982. Facies analysis of Gigealpa Group reservoir rocks, southern Cooper Basin, South Australia. Unpublished report for the South Australian Oil and Gas Corporation Pty. Ltd.

Williams B.P.J. & Wild E.K. 1984. The Tirrawarra sandstone and Merrimelia Formation of the southern Cooper Basin, South Australia- The sedimentation and evolution of a glaciofluvial system. *Australian Petroleum Exploration Association Journal* **24**, 377-392.

Wilson M.D. & Pitman E.D. 1977. Authigenic clays in sandstones: Recognition and influence on reservoir properties and palaeoenvironmental analysis. *Journal of Sedimentary Petrology* **27**, 3-31.

Windsor C.N. 1983. Structural geology and genesis within the Nappacoongee- Murteree Block of the Cooper Basin, South Australia - evidence of hydrocarbon potential. Delhi Petroleum Report.

Wolf K.H. & Chilingarian G.V. 1976. Diagenesis of sandstones and compaction. In Wolf K.H. & Chilingarian (Eds), *Compaction of coarse grained sediments 2 (Developments in sedimentology 18B)*. Elsevier, Amsterdam, pp69-444.

Wopfner H. 1972. Climate & deposition in Permian and Early Triassic in South Australia. Abstracts 44th ANZAAS Congress, Sydney, 95-96.

Yew C.C. & Mills A.A. 1989. The occurrence and search for Permian oil in the Cooper Basin, Australia. In O'Neil B.J. ed. *The Cooper & Eromanga Basins, Australia*. Proceedings of Petroleum Exploration Society of Australia, Society of Petroleum Engineers, Australian Society of Exploration Geophysicists (SA Branches), Adelaide, 339-360.

Zhou S. 1989. Subsidence history of the Eromanga Basin, Australia. In O'Neil B.J. ed. *The Cooper & Eromanga Basins, Australia*. Proceedings of Petroleum Exploration Society of Australia, Society of Petroleum Engineers, Australian Society of Exploration Geophysicists (SA Branches), Adelaide, 329-336.

APPENDIX 1

Core logging methods and results.

APPENDIX 1: Core logging description

Section:	Contents:
1	Introduction
2	Physical measurements
3	Sedimentary facies determination
4	Reference sheet
5	Logging forms
6	References

1 Introduction

This appendix contains the details of the logging of 1040 feet of core in 14 drill holes within the study area, as listed in Table 1.

<u>WELL</u>	<u>INTERVAL</u>	<u>FT</u>	<u>FMN</u>
Kidman 1	6592'-6621'6"	29'5"	Toolachee
Kidman 2	6651'-6691'	40'	"
Marabooka 1	6402'7"-6491'	87'5"	"
Marana 1	6319'-6348'5"	29'5"	"
Pira 2	7128'-7781'2"	53'	"
Strzelecki 1	6287'-6378'	91'	"
Strzelecki 1	6400'-6445'	45'	"
Strzelecki 2	6120'-6192'	72'	"
Strzelecki 5	6057'-6114'6"	57'6"	"
Strzelecki 10	6294'-6349'7"	55'7"	"
Strzelecki 10	6376'-6435'	59'	"
Strzelecki 15	6274'-6306'6"	32'6"	"
Strzelecki 16	6220'-6279'6"	59'6"	"
	<u>Subtotal:</u>	<u>711'4"</u>	
Strzelecki 15	6306'6"-6335'	23'6"	Murteree
Coochilara 1	7977'-8016'6"	39'6"	Patchawarra
Dilchee 1	8256'-8301'	45'	"
Kerna 1	8090'6"-8136'	45'6"	"
Kidman 1	7307'-7367'	60'	"
Pira 2	8240'-8296'8"	56'8"	"
Strzelecki 1	6531'-6589'	58'	"
	<u>Subtotal:</u>	<u>304'8"</u>	
Total		1039'6"	

Table 1. Study area drillhole core logged and presented in this Appendix.

(2)

Generally the condition of the core is sound. All core is cut longitudinally into two pieces with the exception of core from Marana 1 which is still whole. No signs of rock substance slaking was observed. Minor thin brown clay coating of the outside of all core is commonly dessicated and presumably originates from drilling operations. Core recovery is quite good.

Minor localised core diameter increases are observed of up to 5mm, typically in carbonaceous shales, and core diameter decreases of up to 10mm typically in coals. This indicates that swelling of either organic matter or clays, dewatering, depressurisation or stress relief has occurred after drilling of the core. Caliper tool traces recorded on the well logs of the drill holes indicates similar physical effects of the rock mass immediately surrounding the drillhole opening. This indicates that this type of swelling and shrinkage of the rock mass occurs immediately after drilling and not as a response to exposure to air.

All core has been stored for several years within wooden core boxes at room temperature with little or no exposure to extremes of temperature or humidity. The age of core is indicated in Table 2 below.

	<u>WELL</u>	<u>DATE DRILLED</u>
1	Coochilara 1	April 1978
2	Dilchee 1	Oct 1981
3	Kerna 1	May 1981
4	Kidman 1	Sept 1977
5	Kidman 2	May 1979
6	Marabooka 1	Dec 1980
7	Marana 1	Oct 1982
8	Pira 2	April 1986
9	Strzelecki 1	Dec 1970
10	Strzelecki 2	Nov 1971
11	Strzelecki 5	Oct 1981
12	Strzelecki 10	June 1982
13	Strzelecki 15	April 1983
14	Strzelecki 16	July 1983

Table 2 Drilling dates of study area drill holes that were logged.

2 Physical measurements

Characterisation of the core follows the format of Swanson 1981 (commonly referred to as the Shell sample examination manual).

2.1 Depth

All core logging is recorded relative to driller's depth marks included with the core, at a scale of 1cm representing 1 foot of core. The driller's depth to logger's depth conversion (obtained from well completion cards) and the logger's conversion of driller's depth to the top of the core interval (obtained from the composite well logs) are listed in Table 3 below. By comparing geophysical well logging traces (gamma, sonic) with core logging results another driller's depth to core depth conversion was often indicated. Well log to core log comparisons are presented in Appendix 6 and conversions to obtain core depth from driller's depths of each examined well are included in Table 3.

Well	Core		A	B	C
Kidman 1	1	Toolachee	+12	+18	+18
Kidman 2	1	"	-3	-2	-2
Marabooka1	3,4	"	+8	+7	+15
Marana 1	1	"	+1	+1	+1
Pira 2	1	"	+10	+8	+8
Strz 1	1	"	-2	+1	+1
Strz 1	2	"	-2	+6	+8
Strz 1	3	"	-2	+6	+6
Strz 2	1,2	"	+4	+4	+2
Strz 5	5	"	0	+9	+12
Strz 10	1	"	+7	+9	+9
Strz 10	2	"	+7	+12	+11
Strz 15	1,2	"	+2	0	0
Strz 16	1,2	"	+7	+6	+5
Coochilara 1	2	Patchawarra	+9	-1	-1
Dilchee 1	1	"	+3	+3	+13
Kerna 1	2	"	+13	+19	+19
Kidman 1	2	"	+12	+9	+9
Pira 2	2	"	+10	+10	+14
Strz 1	4	"	-2	+5	+5

Table 3. Driller's depth to logger's depth conversion. All depths are in feet. A = logger's conversion for non core interval, B = logger's conversion for core interval, C = conversion for core interval estimated in this report.

2.2 Others

Grain size was defined using the Wentworth scale distribution of average grain diameter and was obtained by comparison with a visual estimation chart.

Rock type identification uses the classification by Folk (1974). Most sands are sublithic quartz arenites (slqa) and lithic arenites (lqa) because of their high quartz content, variable rock fragment content and low feldspar content.

Sorting as defined by Folk (1974) decreases from well sorted material with S.D.= 0.2 at the left of the sorting column to poorly sorted material with S.D.=1.2 at the right of the sorting column.

Roundness as defined by Swanson (1981) varies from angular (0.1) to well rounded (0.9) from left to right of the roundness column.

Sphericity as defined by Swanson (1981) varies from low (0.3) to high (0.9) from left to right of the sphericity column.

Visible porosity is recorded as trace = -, 1 = poor, 2 = fair, good = 3 and excellent = 4.

Sorting, roundness, sphericity and porosity are all visually estimated.

Sedimentary structures are recorded to the right of the mud column as shown on the reference sheet.

3 Sedimentary facies determination.

Sedimentary rock type descriptions uses lithofacies codes as outlined by Miall (1978). Their definition and inferred environment of deposition are listed below. It is important to note that more than one sedimentary environment can form deposits with similar combinations of lithic types, sedimentary structures, thicknesses and adjacent related lithic assemblages.

3.1 Gravels

Gravel facies comprise intraformational or channel lag deposits formed by traction load in upper flow regimes. Facies **Gms (matrix supported gravel)** and **Gm (massive or crudely bedded gravel)** are patchy and generally less than 10 cm wide. Some imbrication of the gravel size particles is observed in Gm type gravels indicating crude bedding whereas Gms gravel deposits sometimes have intraformational, framework size clasts of silt typical of bank collapse material that indicates lateral and basal stream reworking.

Some gravel deposits are associated with an erosional scour (e.g. the basal Toolachee unconformity in Strzelecki 15 at 6306 feet) and are termed Facies **Ge (scour structure with gravel base)** deposit.

Most gravel intervals that were logged are Gms.

3.2 Sandstones

The most common sand lithofacies are **Sm (massive sandstone)** and **Sh (horizontally laminated)** and are commonly identified together. Sm type sands often have patchy mostly sub-horizontal laminations as found with Sh type sands indicating reworking or fluid escape (see also Williams 1982) which has destratified its internal structure. The horizontal bedding of Sh type sands is a product of deposition in laminar flow in either lower or upper flow regimes.

Sr (ripple cross laminated sandstone), St (trough cross bedded sandstone), Sp (planar cross bedded sandstone) and Sg (sandstone with graded bedding) all indicate depositional facies that produce sands identified with each sedimentary structure.

Sr (ripple cross laminated sandstone) sands occur in a lower energy regime in the upper portions of a point bar or a crevasse splay deposit. The sands are generally very fine to fine grained, sorting is generally moderate to good and the ripple cross lamination structures are sometimes disrupted due to burrowing organisms.

Sp (planar cross bedded sandstones) sands are fine to coarse grained and indicate fluvial channel deposition in laterally migrating linguoid bars, transverse bars and sand waves of the lower flow regime (Williams 1982). Pebbles are occasionally found, sorting ranges from poor to moderate and the planar crossbeds are low angle.

(6)

St (trough cross bedded sandstone) sands are fine to coarse grained sediments deposited in laterally migrating fluvial channels. The trough crossbeds are the result of migrating dunes under lower flow regime conditions (Williams 1982).

Sx (crossbedded [type unknown] sandstone) lithofacies code is attributed to core where a distinction cannot always be made between the planar and trough types of crossbeds of Sp and St lithofacies described above.

Sb (bioturbated sandstone) type sands are common, generally fine grained and have disrupted or chaotic laminae caused by burrowing organisms and plant roots. This facies occurs in crevasse splay deposits and proximal overbank deposits where burrowing organisms can rework the sands during periods of non deposition.

Sd (soft sediment deformed sandstone) sands are fine to very fine grained, well sorted sediments that display chaotic bedding and microfaulting caused by slumping, subsidence, compaction and fluid escape from the sediment. This deformation mostly occurs with compactional subsidence of flood basin to lacustrine deposits and prodelta muds.

Sg (sandstones with graded bedding) sands are well sorted fine to coarse grained sediments that are generally horizontally laminated indicating deposition in lower flow regimes possibly associated with pulses of sedimentation such as proximal overbank deposits.

Sw/Fw (interlaminated sandstone and mudstone) very fine grain sediments form by the interbedding of wave rippled sands and silts with flaser bedding common in mixed lithology laminae. This facies originates in overbank marshes or lakes where the fine to very fine sands and muds are deposited and wind driven waves create ripple patterns in the bottom sediments on the leeward side of the prevalent wind direction.

3.3 Mudstones

Fl (Planar, finely laminated mudstone) silts and clays are common and consist of finely laminated sands, silts and muds deposited as overbank deposits during the waning stages of floods. They often contains very small ripples and may be bioturbated.

(7)

Fm (laminated to massive mudstone) represent laminated to massive silts and clays deposited on flood plains during the waning stages of floods and can be thick. They generally overly F1 sediment types and may be overlain by coals.

Fb (bioturbated mudstone) and **Fd (soft sediment deformed mudstone)** are the fine grained lithofacies equivalents of Sb and Sd.

C (Coal) represent coal rich sediments and coals. All coals were assigned one code. Coals consists of plant remains and carbonaceous shales which have undergone coalification processes and are the result of deposition in quiet water flood basin swamps and oxbow lakes where the anoxic waters preserve the organic matter. The coals are mostly inertinite rich with varying amounts of liptinites.

4 Reference sheet (see over)

5 Logging forms (see over)

6 References

Miall A.D. 1978. Lithofacies types and vertical profile models in braided river deposits: a summary. In Miall A.D. (Ed.) *Fluvial Sedimentology*, Canadian Society of Petroleum Geology, Memoir 5, 597-604

Miall A.D. 1988. Reservoir heterogeneities in fluvial sandstones: lessons from outcrop studies. *American Association of Petroleum Geologists Bulletin* 72, 682-697.

Swanson R.G. 1981. Sample examination manual. *American Association of Petroleum Geologists*, Tulsa.

Williams B.P.J. 1982. Facies analysis of Gidgealpa Group reservoir rocks, southern Cooper Basin, South Australia. A preliminary report. Unpublished Report to South Australian Oil & Gas Pty. Ltd.

Reference Sheet for logging forms

AM-DEL		DEPTH	LITHO LOGY:	SEDIM. STRUCT	LITHOFACIES	NOTES	ROCK TYPE	COLOR	SORT	ROUND	SPHER	EST. ϕ
ϕ	k		MUD	SAND	GRAVEL							

LITHOFACIES

Gms	massive
Gm	horizontal bedding
Ge	scour, gravel base
Sm	massive sand
St	trough crossbed
Sp	planar crossbed
Sr	ripple mark
Sh	horizontal laminae
Se	erosional scour
Sd	soft sed deformed
Sg	graded bedding
Sb	bioturbated
Sw/Fb	wave rippled, interlaminated
Sx	crossbedded
Sl	low angle crossbed
F1	fine laminated
Fm	fine massive
Fb	bioturbated
Fr	ripple mark
Fw	starved ripples
Fg	graded bedding
Fd	deformed laminae

FILL PATTERNS

	sandstone
	siltstone
	shale
	silty sand
	carb shale
	gravel
	coal
	scour base

ABBREVI'S

s	sub
l	lithic
q	quartz
a	arenite
carb	carbonaceous
c	coal
stne	stone
shle	shale
l	light
dk	dark
brn	brown
blck	black

POROSITY

-	trace
1	poor (1-5%)
2	fair (5-10%)
3	good (10-15%)
4	excellent (>15%)

MISCELLANEOUS

SORTING varies from $\sigma = 0.2$ (left) to $\sigma = 1.2$ (right)

ROUNDNESS varies from 0.1 (angular, left) to 0.9 (well rounded, right)

SPHERICITY varies from low 0.3 (left) to high 0.9 (right)

POROSITY ϕ in %

PERMEABILITY k in millidarcies

DEPTH from drill core markers

SEDIMENTARY STRUCTURES

	ripple crosslamination
	climbing ripples
	ripple marks
	planar crossbeds
	trough crossbeds
	organic stringers
	intraclasts
	low angle crossbedding
	load casts
	sediment deformation
	microfaulting
	roots, bioturbation
	stylolites

AM-DEL	DEPTH	LITHO LOGY:	SEDIM. STRUCT	LITHOFACIES		NOTES	ROCK TYPE	COLOR	SORT	ROUND	SPHER	EST. #
				MUD	SAND							
	7977					START CORE 2						
	78											
	79											
	7980											
	81					SAMPLE 488 * Well indurated quartz	slqabuff					1
	82											
	83					F1						-
	84											
	85					Sn	slqabuff					1
	86					F1						
	87					Sn	slqabuff					1
	88											
	89											
	7990					Sw/Fb	slqabuff					1
	91					minor siderite	to grey					
	92											
	93											
	94											
	95											
	96					Sn	" "					1
	97											
	98					Sw/Fb	" "					1
	99					F1	carb. shale black					
	8000											
	01					Sn, (Sb)						1
	8002					F1	slqabuff					

AM-DEL	DEPTH	LITHO LOGY:	SEDIM. STRUCT	LITHOFACIES	NOTES	ROCK TYPE	COLOR	SORT	ROUND	SPHER	EST. Ø
		MUD	SAND	GRAVEL							
	8002			F1, Sn		slq	buff				1
	03			F1, Sn							
	04										
	05			F1, (Fb)							
	06			C		coa	black				
	07										
	08										
	09										
	8010			F1, (Fb)							
	11										
	12					silt-					
	13					stone					
	14					black					
	15				← angular dropstones to 11mm & disrupted bedding underneath	to					
	16					grey					
				END CORE 2							

AM-DEL		DEPTH	LITHO LOGY:	SEDIM. STRUCT.	LITHOFACIES	NOTES	ROCK TYPE	COLOR	SORT	ROUND	SPHER	EST. Ø
Ø	k											
		8281	-----		F1	carb. shale	black					
		82				increasing silt content ↑						
		83										
		84										1
		85					slqabuff					
		86			Sh							
		87				uniform, minor grey thin silt bands						
		88										1
		89				SAMPLE 483 *						
		8290										
		91										
		92				SAMPLE 484 *						
		93			Sn, (Sh):	grain size variation between both. Occasional patchy siderite sometimes associated with carbonaceous material.	"	"				2
		94			F1	SAMPLE 485						
		95			Sn							
		96			Sp		"	"				2
		97			Sn	SAMPLE 486 * SAMPLE 487 *						
		98			F1, (Fb)							-
		99										
		8300				Carbonaceous shale						-
		8301				END CORE 1						






AM-DEL	DEPTH	LITHO LOGY:	SEDIM. STRUCT	LITHOFACIES	NOTES	ROCK TYPE	COLOR	SORT	ROUND	SPHER	EST. Ø
		MUD	SAND	GRAVEL							
	8115			Sw, Fb		see pg. 1					
	16										
	17				minor bands of brown siderite associated with dark silt bands.						
	18										
	19				SAMPLE 476 *						
	20				SAMPLE 477 *						
	8120				(- drop stone 40mm x 15mm						
	21										
	22				SAMPLE 478 *						
	23			Sh			slqabuff				
	24						grey				1
	25										
	26										
	27										
	28			Sh							
	29			Sd	Large slump(?) structure 70 mm thick.	SAMPLE 479 *					
	30			Sh							
	8130										
	31			Sm	minor patchy brown siderite blebs.	SAMPLE 480 *	slq	dk. grey			
	32					SAMPLE 481 *					
	33			F1, (Fb)	minor brown laminated siderite.	SAMPLE 482 *	shale	black			
	34										
	35			C			coal	black			
	8136				END CORE 2						

AM-DEL	DEPTH	LITHO LOGY:	SEDIM. STRUCT	LITHOFACIES	NOTES	ROCK TYPE	COLOR	SORT	ROUND	SPHER	EST. #
	7307				START CORE 2	slqabuff					3
	08			Sn							
	09			Sh, fine banding		slqagrey					
	7310										
	11			Sn, (Sh)		slqabuff					3
	12										
	13										
	14										
	15					slqabuff					3
	16										
	17			Sh, 5mm regular banding							
	18										
	19										
	7320										
	21										
	22										
	23			Sn		slqabuff					3
	24										
	25										
	26										
	27										
	28			Gn		slqabuff					4
	29										
	7330					slqagrey					2
	31			Sn		lqagrey brn					3
	7332			Gns, Sh							

AM-DEL	DEPTH	LITHO LOGY:	SEDIM. STRUCT	LITHOFACIES	NOTES	ROCK TYPE	COLOR	SORT	ROUND	SPHER	EST. Ø
	7332			Sn		slqa	buff				3
	33			Sn							
	34										
	35										
	36										
	37										
	38			Sn, (Sh)							
	39					slqa	buff				3
	7340										
	41										
	42					lqa	grey to buff				3
	43			Sh							
	44										3
	45			Gns		lqa	"				4
	46										2
	47			Sn							4
				C		coal	black				-
	48										
	49			F1			dk grey				1
	7350										
	51										
	52			Sh		slqa	buff				3
	53			F1		"	grey buff				1
	54			Sh		"	grey				1
	55			F1							
	55			Sh, (Sn)							
	56					"	buff				3
	7357			St							

AM-DEL	DEPTH	LITHO LOGY:	SEDIM. STRUCT.	LITHOFACIES		NOTES	ROCK TYPE	COLOR	SORT	ROUND	SPHER	EST. Ø		
				MUD	SAND								GRAVEL	
	7357													
	58													
	59						St, patchy disseminated brown siderite.	slqabuff				■	■	3
	7360													
	61						SAMPLE 330 *							
	62													
	63						Sn	slqabuff						3
	64													
	65													
	66				Sh	slqabuff					■	■	3	
	7367				END CORE 2									

AM-DEL	DEPTH	LITHOLOGY:	SEDIM. STRUCT	LITHOFACIES	NOTES	ROCK TYPE	COLOR	SORT	ROUND	SPHER	EST. Ø
		MUD	SAND	GRAVEL							
2-D 0-016	6592				START CORE 1						
	93										
	94										
	95				Sh		slqabuff				3
	96										
	97										
	98										3
	99										
	6600			~	Sm						3
	01				Sh	CORE PLUG 306 * SAMPLE 307 *					4
	02			^							
	03			~	Sm	SAMPLE 308 *	slqabuff				4
	04				Sm Sh						
	05										
	06						" "				3
	07										
	08			~	Sm	SAMPLE 309 *					
09											
6610											
11											
12				Ge						3	
13				Sh		slqabuff				3	
14				Gm							
15				Sm						3	
16											
6117				F1						-	

AM-DEL		DEPTH	LITHO LOGY:	SEDIM. STRUCT	LITHOFACIES	NOTES	ROCK TYPE	COLOR	SORT	ROUND	SPHER	EST. Ø
Ø	k		MUD	SAND	GRAVEL							
		6617			F1							
		18			C		C	black				
		19										
		6620				F1, (Fb) Minor layered fine brown siderite.	siltbrn/stnegrey					-
		6621			Fm							
					END CORE 1							

KIDMAN 2 / TOOLACHEE / CORE 1 / 6651'- 6691' / PAGE 1 OF 2

AM-DEL	DEPTH	LITHO LOGY:		LITHOFACIES	NOTES	ROCK TYPE	COLOR	SORT	ROUND	SPHER	EST. #
		MUD	SAND								
	6651				START CORE 1						
	52				Sn, (Sh)						
	53										
	54					slqabuff					3
	55										
	56				Sh, siderite Sn						
	57				Sh, common patchy siderite						
	58										
	59				Sn						3
	60										
	61				Sh						
	62										
	63										
	64				Sn						
	65										
	66										
	67					slqabuff					4 3 4
	68										3
	69				Sh						3
	70				Sn						3
	71				Sn						
	72				F1						2
	73					slqabuff					
	74				Sh						3
	75										
	6676				Sh						




AM- DEL	DEPTH	LITHO LOGY:	SEDIM. STRUCT	LITHOFACIES	NOTES	ROCK TYPE	COLOR	SORT	ROUND	SPHER	EST. Ø
		MUD	SAND	GRAVEL							
	6676			Sh							3
	77										
	78					slqabuff					2
	79			Sm							
	6680										3
	81										
	82										
	83					carbblack shale					-
	84			F1,Fn							
	85										
	86										
	87										2
	88					slqgrey brn					
	89			Sh, (Sb)							
	90										2
	6691				END CORE 1						

AM-DEL	DEPTH	LITHOLOGY:		LITHOFACIES	NOTES	ROCK TYPE	COLOR	SORT	ROUND	SPHER	EST. #
		MUD	SAND								
	6319				START CORE 1						
	20				Sn	slqabuff					2
	21										
	22										
	23				Sn becomes grey with more lithic component	grey					
	24				C	coalblack					
	25										
	26				Fm	carbgrey shale					-
	27										
	28				SAMPLE 303 * CORE PLUG 304 *						
	29					slqabuff					2
	6330										
	31				Sh						2
	32										
	33					slqabuff					2
	34										
	35				Sn						
	36										
	37				SAMPLE 305 *						2
	38										
	39				Sh, (Sb)	" "					3
	6340										
	41					siltgrey					-
	42				F1	-stne					
	43				F1 continues to end of Core 1 i.e. to 6348'5"						
	6344										

13.0

13.5

AM-DEL	DEPTH	LITHO LOGY:	SEDIM. STRUCT	LITHOFACIES	NOTES	ROCK TYPE	COLOR	SORT	ROUND	SPHER	EST. Ø
		MUD	SAND	GRAVEL							
	6477										
	78						slqabuff				
	79					<- hydrocarbons present SAMPLE 336 x					
	6480										3
	81					several dark grey dissolution seams up to 20mm long.					
	82										
	83			nn							
	84			nn	Sn						3
	85										
	86										
	87			g							
	88			Sn						3	
	89										
	90			Sn						3	
	6491				END CORE 3						

AM-DEL		DEPTH	LITHO LOGY:	SEDIM. STRUCT	LITHOFACIES	NOTES	ROCK TYPE	COLOR	SORT	ROUND	SPHER	EST. Ø
Ø	k		MUD	SAND	GRAVEL							
		7178			C			black				
		79			Sh, (Sb) patchy brown siderite near top.		slqa	buff				
		80										
		7181			END CORE 1							



AM-DEL	DEPTH	LITHO LOGY:	SEDIM. STRUCT.	LITHOFACIES	NOTES	ROCK TYPE	COLOR	SORT	ROUND	SPHER	EST. Ø
		MUD	SAND	GRAVEL							
	8290	[Patterned]						[Dotted]			
	91										
	92										
	93				Sh, Sp						3
	94								[Solid]		
	95										
	96										
	8297				END CORE 2						

AM-DEL		DEPTH	LITHO LOGY:	SEDIM. STRUCT	LITHOFACIES	NOTES	ROCK TYPE	COLOR	SORT	ROUND	SPHER	EST. Ø
Ø	k		MUD	SAND	GRAVEL							
		6287				START CORE 1						
		88										
		89				F1, (Sb)						1
		6290										
		91										
		92										
		93										
		94										
		95										
		96										
		97										
		98				Sp, (Fb)						1
		99										1
		6300										
		01										
		02										
		03										
		04				Sw/Fb						1
		05										
		06										1
		07										
		08				Sg common dark brown weathered clay.	slqa					1
		09] hydrocarbon beading	SAMPLE 458 * SAMPLE 459 *		buff brown				2
		6310				F1						
		11				C brown siderite bands near top.	coal					-
		6312				Fb						







AM-DEL	DEPTH	LITHO LOGY:	SEDIM. STRUCT	LITHOFACIES	NOTES	ROCK TYPE	COLOR	SORT	ROUND	SPHER	EST. #
	6312										
	13			Fb							
	14										
	15										
	16										
	6317				END CORE 1						
	18										
	6319				START CORE 2						
	20										
	21										
	22			C		coal					
	23						black				
	24										
	25										-
	26										
	27										
	28										
	29					slqa					
	6330			Sm, (Sh) common white stockwork clay, common patchy blebs of brown siderite to 1mm. SAMPLE 460 *		buff					3
	31										
	32										
	33										
	34			Sp	common patchy siderite blebs to 1mm diameter.						1
	35										
	36										-
	6337			F1							

AM-DEL	DEPTH	LITHO LOGY:		LITHOFACIES	NOTES	ROCK TYPE	COLOR	SORT	ROUND	SPHER	EST. Ø
		MUD	SAND								
	6337			F1							
	38			C							
	39			Sh, (Sb) common dispersed siderite & carbonaceous stringers.		slqa	mauve grey				2
	6340										
	41			Fb		slqa					1
	42										
	43			Sg	SAMPLE 461 *	slqa	buff				
	44				SAMPLE 462 *		grey				4
	45										
	46			C							
	47			Fm	carb shale		black				-
	48			C							
	49			Fm							-
	6350										
	51										
	52										
	53			F1, (Fn)							-
	54										
	55			Sw/Fb		slqa					1
	56						buff				
	57										
	58			S1, (Sn) common carb. stringers common white clay minor brown siderite.		slqa					2
	59						buff				3
	6360										2
	61] hydrocarbon beading	SAMPLES 463						3
	6362			S1, (Sn)	464 *						2
					465 *						
					466 *						
					467 *						

AM-DEL	DEPTH	LITHO LOGY:	SEDIM. STRUCT	LITHOFACIES	NOTES	ROCK TYPE	COLOR	SORT	ROUND	SPHER	EST. Ø
	6362		~	Sm		slqa	buff	/	■	■	1
	63				SAMPLE 469 *	slqa	grey	/			4
	64				SAMPLE 470 *			/			
	65							/			4
	66] hydrocarbon beading SAMPLE 471 *			/	■	■	
	67			Sm, (St.)				/			4
	68							/			
	69			Gm C				/			2
	6370			F1		carb silt	dk. grey				-
	71							/			
	72							/			
	73			Sw/Fb				/	■	■	1
	74							/			
	75							/			
	76				minor patchy blebs of			/			
	77				siderite			/			
	6378				END CORE 2						
					START CORE 3						
	6400				minor light brown blebs of siderite to 1mm diameter.	slqa	lt.	/			2
	01							/			
	02						buff	/	■	■	
	03			Sm			to brn	/			
	04							/			
	05							/			2
	06							/			
	6307							/			

AM- DEL	DEPTH	LITHO LOGY:	SEDIM. STRUCT	LITHOFACIES	NOTES	ROCK TYPE	COLOR	SORT	ROUND	SPHER	EST. Ø	
		MUD	SAND	GRAVEL								
	6432											
	33											
	34				F1		siltgrey					
	35						stone					1
	36											
	37											
	38											
	39											
	6440											
	41											
	42											
	43											
	44											
	6445				END CORE 3							

AM-DEL	DEPTH	LITHO LOGY:	SEDIM. STRUCT.	LITHOFACIES	NOTES	ROCK TYPE	COLOR	SORT	ROUND	SPHER	EST. Ø
	6556			Sh, S(b)	SAMPLE 494 *	slqa					1
	57										
	58										
	59			F1							-
	6560										
	61										
	62				SAMPLE 495						
	63				30mm brown sideritic band *						
	64					shale/ slqa					
	65				SAMPLE 496 *		grey buff				
	66			Sw/Fb							
	67				Minor scour & fill. Few congl. & coarse s/s bands with clay matrix.						
	68				SAMPLE 497 *						
	69										
	6570										
	71				SAMPLE 498 H/C beading strong. Some H/C restricted to coarser bands. *						1
	72				SAMPLE 499 SAMPLE 500 *	slqa	buff				
	73				SAMPLE 501 *						1
	74			H/C beading common.							
	75				SAMPLE 502 *						
	76										2
	77			Sh, laminations to 1mm thick.							
	78			F1							-
	79			Sh							
	80				SAMPLE 503 *	slqa	buff grey				3
	6581			Sm, Sh							

AM-DEL	DEPTH	LITHOLOGY:		LITHOFACIES	NOTES	ROCK TYPE	COLOR	SORT	ROUND	SPHER	EST. %
		MUD	SAND								
	6581				Sn, (Sh)	slqa	buff	///			3
	82				Laminations 10mm of grey silt.						
	83					SAMPLE 504 x					
	84										
	85										
	86				Sn, (Sh)	slqa	buff	///			3
	87				SAMPLE 505 x						
	88										
	6589				END CORE 4						

AM-DEL	DEPTH	LITHO LOGY:	SEDIM. STRUCT.	LITHOFACIES	NOTES	ROCK TYPE	COLOR	SORT	ROUND	SPHER	EST. #
	6120				START CORE 2	slqabuff					3
	21			Sh, St							
	22										
	23			Sh, St	SAMPLE 294 *	slqabuff					3
	24										
	25			Sh, common siderite along fine bands							2
	26										
	27										
	28					cartblack					
	29			F1		shale					
	6130										
	31			Sd, minor siderite along fine layers		slqagrey					3
	32		d			buff					
	33		d								
	34			Fm							
	35		z								
	36			Sh		slqa					
	37										
	38			St, Sh							2
	39			as for 6141'							
	6140			St	SAMPLE 295						
	41			F1, common patchy elongate siderite to 5mm long	*						
	42			St, brn siderite along fine bands							
	43			Sn		slqabuff					3
	44										
	6145			Fh							

AM-DEL	DEPTH	LITHO LOGY:	SEDIM. STRUCT	LITHOFACIES	NOTES	ROCK TYPE	COLOR	SORT	ROUND	SPHER	EST. Ø
	6170										
	71			Interlayered Sn (coarser) and Sh (finer)		slqa buff					2
	72										
	73										
	74										
	75					slqabuff					3
	76					to					
	77					lt.					
	78					brown					
	79			Sn, common intraclasts							3
	6180										
	81										
	82										
	83										
	84										
	85										3
	86										
	87										
	88										
	89			Sh, patchy siderite along fine laminations							3
	6190										
	91										
	6192			Sn							
				END CORE 2							

← H/C present — strong beading & smell

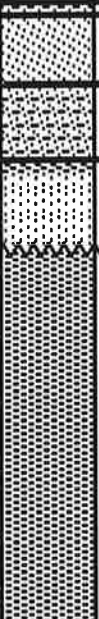
AM-DEL	DEPTH	LITHO LOGY:	SEDIM. STRUCT	LITHOFACIES	NOTES	ROCK TYPE	COLOR	SORT	ROUND	SPHER	EST. Ø
	6082			St							1
	83			C		coalblk					
	84					slqabuff					1
	85										
	86			Sh, minor Sb							2
	87										
	88										2
	89										
	6090				SAMPLE 293 *						2
	91			Sr							2
	92			Sh, minor Sb							1
	93										-
	94			F1		carbblk silt					-
	95										
	96			C F1		coalblk					-
	97			Sn		slqabuff					1
	98										4
	99										4
	6100			Sg							4
	01										4
	02			Gm							4
	03			Sh Gms							4
	04			Sg							4
	05			Sg							3
	06			Sg, no apparent grading Sn							3
	6107			C		coalblk					-

AM-DEL	DEPTH	LITHO LOGY:	SEDIM. STRUCT	LITHOFACIES	NOTES	ROCK TYPE	COLOR	SORT	ROUND	SPHER	EST. #
		MUD	SAND	GRAVEL							
	6107				C						3
	08				Sm common patchy siderite						3
	09				Fm	slqabuff					1
	6110				Sh, (Sb)						1
	11										
	12										1
	13				Sp						3
	6114				Sp						3
				END CORE 1							

AM-DEL	DEPTH	LITHOLOGY:	SEDIM. STRUCT	LITHOFACIES	NOTES	ROCK TYPE	COLOR	SORT	ROUND	SPHER	EST. Ø
		MUD	SAND	GRAVEL							
	6410				C						
	11				F1 common patchy siderite above 6411'						1
	12										
	13					slqagrey					
	14										1
	15										
	16										
	17										
	18										
	19										
	6420										
	21				Sh, Sr						1
	22										
	23										1
	24										
	25										
	26										
	27				Sh patchy siderite common on fine laminations						
	28				St, Sh						
	29				Sn, reverse graded bedding	slqa lt.					
	30				Sh	brn					
	31				Sn						2
	6430				Sr						
	32				Gm						3
	33				Sw, Fw minor siderite in bands to 12mm						1
	34										
	6435				Sb, Sh						1

AM-DEL	DEPTH	LITHO LOGY:	SEDIM. STRUCT	LITHOFACIES	NOTES	ROCK TYPE	COLOR	SORT	ROUND	SPHER	EST. Ø
	6274			C			blk				-
	75										
	76			C							
	77			rootlets		slq	brn				-
	78			Fm/Sn			to				
	79						grey				
	6280			F1/Sh							-
	81			Sh/F1	SAMPLE 274						
	82			Sr patchy siderite - 1mm diam *		slq	off				1
	83			Sr			white				1
	84			Sh			to				2
	85			Sr			pale				-
	86			Sr			brn/				-
	87			Sh			grey				2
	88			Sr							-
	89			Sp							1
	6290			Sr							2
	91			Sn							2
	92			Sr							3
	93			Sp							3
	94			St							3
	95										3
	96				SAMPLE 270 * SAMPLE 271 *						3
	97			Sn							3
	98			St							3
	6299			Sh							

AM-DEL		DEPTH	LITHO LOGY:	SEDIM. STRUCT	LITHOFACIES	NOTES	ROCK TYPE	COLOR	SORT	ROUND	SPHER	EST. #
Ø	k											
		6245			Sm							
		46					carb	blk				
		47			Fm		silt					
		48										
		49										
		6250			Sh, Sb	END CORE 1 SAMPLE 288 * START CORE 2	slq	buff	/			2
		51				SAMPLE 289 *			/			
		52			Sm				/			3
		53							/			
		54							/			
		55			C		coal	blk				
		56										
		57										
		58										
		59			Fm							
		6260			Sb	minor intact laminae	slq	dk	/			1
		61							/			
		62			Sh			grey	/			
		63						to	/			
		64						lite	/			
		65						grey	/			1
		66			Sr	planar crossbeds well preserved			/			
		67							/			
		68							/			1
		69							/			
		6270							/			

AM- DEL	DEPTH	LITHO LOGY:	SEDIM. STRUCT	LITHOFACIES	NOTES	ROCK TYPE	COLOR	SORT	ROUND	SPHER	EST. Ø	
		MUD	SAND	GRAVEL								
	6270			Sr		slq	dark grey to lite grey				1	
	71			Sh								
	72											
	73				Sm	SAMPLE 290 x					3	
	74											
	75					F1 minor patchy siderite in bands to 12 mm wide.						-
	76											
	77											
	78											
	6279				END CORE 2							

APPENDIX 2
Petrological descriptions.

Appendix 2: Petrological details

Section:	Contents:
1	Abbreviations used
2	Thin section details
3	Thin section sedimentary estimates
4	Modal estimates
5	Porosity details

1 Abbreviations

Ave	Average grain size (mm)
C.M.	Carbonaceous material (%)
Frac	Fracture porosity (%)
Ill	Illite (%)
Kao	Kaolin (%)
Max	Maximum grain size (mm)
Mic	Micritic siderite (%)
Min	Minimum grain size (mm)
Murt	Murteree
Oil stain	Oil staining (1=absent, 2=rare, 3=common)
Other	Other rock constituents (%)
Patc	Patchawarra
Plug perm	Core plug permeability (md)
Plug por	Core plug porosity (%)
Prim	Primary porosity
Qtz	Quartz (%)
RF	Rock fragments (%)
Roundness	Roundness, 0.1=angular, 0.9=well rounded
Sec	Secondary porosity
Spar	Sparry siderite (%)
Sphericity	Sphericity, 0.3=low, 0.9=high
Tool	Toolachee
Type	Type of other rock constituent

(2)
Appendix 2, Section 1 Thin section details

Sample No.	Well Name	Well No.	Depth	Formation
0270	STRZELECKI	15	6278.5	TOOL
0271	STRZELECKI	15	6298.9	TOOL
0272	STRZELECKI	15	6306.3	TOOL
0273	STRZELECKI	15	6334.9	MURT
0274	STRZELECKI	15	6283.5	TOOL
0287	STRZELECKI	16	6242.2	TOOL
0288	STRZELECKI	16	6256.8	TOOL
0289	STRZELECKI	16	6259.5	TOOL
0290	STRZELECKI	16	6280.8	TOOL
0291	STRZELECKI	05	6066	TOOL
0292	STRZELECKI	05	6080	TOOL
0293	STRZELECKI	05	6090	TOOL
0294	STRZELECKI	02	6126.7	TOOL
0295	STRZELECKI	02	6145.8	TOOL
0296	STRZELECKI	02	6186.7	TOOL
0297	STRZELECKI	10	6334	TOOL
0298	STRZELECKI	10	6343.8	TOOL
0302	MARANA	01	6325	TOOL
0303	MARANA	01	6328.8	TOOL
0305	MARANA	01	6338	TOOL
0307	KIDMAN	01	6613.5	TOOL
0308	KIDMAN	01	6615	TOOL
0309	KIDMAN	01	6620.5	TOOL
0310	KIDMAN	02	6689.5	TOOL
0311	PIRA	02	7150.4	TOOL
0312	PIRA	02	7168.8	TOOL
0329	KIDMAN	01	7343.8	PATC
0330	KIDMAN	01	7373	PATC
0331	MARABOOKA	01	6415	TOOL
0332	MARABOOKA	01	6426.7	TOOL
0333	MARABOOKA	01	6432.2	TOOL
0334	MARABOOKA	01	6437.8	TOOL
0335	MARABOOKA	01	6466.8	TOOL
0336	MARABOOKA	01	6487.3	TOOL
0337	PIRA	02	8279	PATC
0338	PIRA	02	8280.2	PATC
0339	PIRA	02	8293.8	PATC
0340	PIRA	02	8293.9	PATC
0458	STRZELECKI	01	6307.3	TOOL
0459	STRZELECKI	01	6307.8	TOOL
0460	STRZELECKI	01	6328.5	TOOL
0461	STRZELECKI	01	6341.5	TOOL
0462	STRZELECKI	01	6342	TOOL
0463	STRZELECKI	01	6358.4	TOOL
0464	STRZELECKI	01	6358.7	TOOL
0465	STRZELECKI	01	6358.9	TOOL
0466	STRZELECKI	01	6359.3	TOOL

(3)

Appendix 2, Section 1 Thin section details (continued)

Sample No.	Well Name	Well No.	Depth	Formation
0467	STRZELECKI	01	6360	TOOL
0468	STRZELECKI	01	6360.5	TOOL
0469	STRZELECKI	01	6361.5	TOOL
0470	STRZELECKI	01	6362.3	TOOL
0471	STRZELECKI	01	6364.2	TOOL
0472	STRZELECKI	01	6412.5	TOOL
0473	STRZELECKI	01	6415.1	TOOL
0474	STRZELECKI	01	6420.7	TOOL
0475	STRZELECKI	01	6423	TOOL
0476	KERNA	01	8131.5	PATC
0477	KERNA	01	8132.8	PATC
0478	KERNA	01	8134.8	PATC
0479	KERNA	01	8142	PATC
0480	KERNA	01	8144.3	PATC
0481	KERNA	01	8144.8	PATC
0482	KERNA	01	8145.1	PATC
0483	DILCHEE	01	8292.2	PATC
0484	DILCHEE	01	8295	PATC
0485	DILCHEE	01	8296.5	PATC
0486	DILCHEE	01	8299	PATC
0487	DILCHEE	01	8299.6	PATC
0488	COOCHILARA	01	7990	PATC
0489	COOCHILARA	01	7995.3	PATC
0490	COOCHILARA	01	8004.4	PATC
0491	STRZELECKI	01	6530.5	PATC
0492	STRZELECKI	01	6533	PATC
0493	STRZELECKI	01	6536.8	PATC
0494	STRZELECKI	01	6554.4	PATC
0495	STRZELECKI	01	6560.9	PATC
0496	STRZELECKI	01	6563	PATC
0497	STRZELECKI	01	6566	PATC
0498	STRZELECKI	01	6569.3	PATC
0499	STRZELECKI	01	6569.5	PATC
0500	STRZELECKI	01	6570.6	PATC
0501	STRZELECKI	01	6571.3	PATC
0502	STRZELECKI	01	6573.3	PATC
0503	STRZELECKI	01	6577.8	PATC
0504	STRZELECKI	01	6582.1	PATC
0505	STRZELECKI	01	6586	PATC
0611	STRZELECKI	10	6277	TOOL
0612	STRZELECKI	10	6257	TOOL
0613	STRZELECKI	10	6187	DARA
0614	STRZELECKI	10	6377	TOOL
0615	STRZELECKI	10	6607	PATC
0616	STRZELECKI	10	6677	PATC
0617	STRZELECKI	10	6727	TIRR

(4)

Appendix 2, Section 1 Thin section details (continued)

Sample No.	Well Name	Well No.	Depth	Formation
0618	STRZELECKI	10	6787	TIRR
0619	STRZELECKI	10	6827	TIRR
0620	STRZELECKI	10	6907	MERR
0621	KIDMAN	01	6372	DARA
0622	KIDMAN	01	6422	TOOL
0623	KIDMAN	01	6502	TOOL
0624	KIDMAN	01	6572	TOOL
0625	KIDMAN	01	6722	TOOL
0626	KIDMAN	01	6762	TOOL
0627	KIDMAN	01	6902	EPSI
0628	KIDMAN	01	7037	EPSI
0629	KIDMAN	01	7062	EPSI
0630	KIDMAN	01	7232	PATC
0631	KIDMAN	01	7412	PATC
0632	KIDMAN	01	7472	PATC
0633	KIDMAN	01	7562	PATC

Appendix 2, Section 2 Thin section sedimentary details

No.	Grain size (mm)			Roundness	Sphericity	Sorting
	Min	Ave	Max			
270	0.1	0.25	0.5	0.7	0.7	moderate
271	0.1	0.5	1.2	0.7	0.5	fair-poor
272	0.1	0.3	0.5	0.7	0.5	fair-good
273	0.01	0.05	2	0.3	0.3	poor
274	0.05	0.1	0.2	0.5	0.3	good
287	0.1	0.2	2	0.7	0.5	poor
288	0.01	0.01	0.02	0.7	0.7	good
289	0.2	0.1	0.5	0.7	0.5	fair
290	0.05	0.15	0.5	0.7	0	moderate
291	0.01	0.2	0.05	0.5	0.3	poor
292	0.1	0.2	0.4	0.3	0.5	good
293	0.1	0.2	0.5	0.5	0.7	poor
294	0.05	0.15	0.3	0.3	0.5	fair-poor
295	0.01	0.05	0.3	0.3	0.5	poor
296	0.05	0.3	1	0.7	0.5	poor
297	0.01	0.4	1	0.7	0.7	fair
298	0.05	0.1	0.9	0.5	0.7	poor
302	0.1	0.3	2.5	0.7	0.5	very poor
303	0.01	0.1	0.2	0.5	0.9	fair
305	0.1	1.5	12	0.3	0.5	very poor
307	0.1	0.4	1	0.5	0.5	poor
308	0.2	0.4	1.5	0.3	0.5	very poor
309	0.1	0.3	0.5	0.5	0.5	fair

(5)

Appendix 2, Section 2: Thin section sedimentary details (contd)

No.	Grain size (mm)			Round ness	Spher- icity	Sorting
	Min	Ave	Max			
310	0.05	0.2	0.4	0.5	0.7	moderate
311	0.05	0.25	0.4	0.5	0.5	fair-good
312	0.03	0.05	0.2	0.7	0.9	good
329	0.1	2	12	0.7	0.3	very poor
330	0.02	0.06	0.25	0.7	0.7	good
331	0.01	0.08	0.2	0.5	0.7	poor
332	0.01	0.1	0.3	0.7	0.7	good
333	0.01	0.05	0.5	0.5	0.5	medium
334	0.03	0.15	0.4	0.3	0.5	good
335	0.02	0.15	2	0.5	0.7	good
336	0.05	0.1	0.5	0.5	0.7	fair
337	0.05	0.2	0.5	0.3	0.5	fair
338	0.05	0.2	0.6	0.3	0.5	fair
339	0.02	0.2	0.5	0.3	0.3	poor
340	0.1	0.4	1	0.3	0.5	poor
458	0.01	0.3	0.8	0.3	0.5	poor
459	0.1	0.4	1.2	0.5	0.5	very poor
460	0.01	0.1	0.2	0.3	0.5	poor
461	0.01	0.3	4	0.5	0.5	very poor
462	0.05	0.2	1.5	0.5	0.5	poor
463	0.05	0.2	1.5	0.3	0.5	very poor
464	0.01	0.2	2	0.3	0.5	very poor
465	0.05	0.3	0.6	0.7	0.7	fair
466	0.05	0.3	1.2	0.5	0.5	poor
467	0.05	0.3	3	0.3	0.5	very poor
468	0.1	0.15	0.4	0.5	0.7	fair
469	0.1	0.4	0.8	0.7	0.7	fair
470	0.05	0.6	1.2	0.7	0.5	very poor
471	0.1	0.3	0.8	0.5	0.7	poor
472	0.1	0.3	1	0.5	0.7	poor
473	0.1	0.7	2	0.5	0.7	poor
474	0.05	0.05	8	0.3	0.5	very poor
475	0.1	0.3	3.5	0.5	0.7	very poor
476	0.1	0.25	1.4	0.5	0.5	poor
477	0.1	0.3	0.6	0.7	0.7	good
478	0.1	0.2	0.5	0.5	0.7	good
479	0.05	0.2	0.3	0.7	0.7	good
480	0.1	0.3	10	0.5	0.7	poor
481	0.1	0.5	15	0.3	0.5	very poor
482	0.05	0.4	2	0.3	0.7	poor
483	0.1	0.2	1.5	0.7	0.5	good
484	0.1	0.25	0.5	0.7	0.7	fair-good
485	0.05	0.4	0.8	0.3	0.5	poor
486	0.05	0.35	0.5	0.5	0.5	good
487	0.05	0.8	2.5	0.1	0.5	very poor
488	0.01	1.5	0.04	0.3	0.5	very poor

(6)

Appendix 2, Section 2: Thin section sedimentary details (cont'd)

No.	Grain size (mm)			Round ness	Spher- icity	Sorting
	Min	Ave	Max			
489	0.01	0.04	0.03	0.5	0.7	good
490	0.05	0.3	0.4	0.3	0.5	good
491	0.05	0.3	1.5	0.7	0.7	poor
492	0.1	0.3	0.4	0.5	0.7	good
493	0.05	0.2	0.4	0.7	0.7	good
494	0.1	0.25	0.4	0.7	0.7	fair-good
495	0.1	0.25	0.4	0.9	0.7	very good
496	0.05	0.2	15	0.5	0.7	very poor
497	0.05	0.2	1	0.7	0.7	good
498	0.05	0.25	0.5	0.5	0.7	fair-good
499	0.1	0.25	0.5	0.7	0.3	fair
500	0.05	0.4	1.1	0.3	0.5	poor
501	0.1	0.4	0.8	0.5	0.7	poor-fair
502	0.1	0.3	0.5	0.5	0.7	fair
503	0.05	0.2	0.5	0.7	0.5	fair
504	0.1	0.4	0.7	0.7	0.7	fair
505	0.1	0.3	0.9	0.3	0.5	fair
611		0.15	0.4			
612		0.15	0.3			
613		0.15	0.25			
614		0.1	0.2			
615		0.25	0.15			
616		0.3	0.1			
617		0.25	1			
618		0.3	1			
619		0.2	0.8			
620		0.2	0.8			
621		0.1	0.2			
622		0.1	0.2			
623		0.1	0.2			
624		0.25	0.5			
625		0.2	1.1			
626		0.25	0.8			
627		0.25	0.8			
628		0.2	0.3			
629		0.06	0.1			
630		0.2	0.3			
631		0.3	1.2			
632		0.2	0.4			
633		0.25	0.7			

(7)

Appendix 2 Section 3 Petrological modal estimates

Sample No.	Rock constituents (%)								Oil stain	
	Qtz	Kao	Ill	RF	Spar	Mic	CM	Other		
0270	70	7	5	15	0	0	3	1	musc	2
0271	65	10	5	15	0	0	5	1	musc	2
0272	65	7	3	20	0	0		1	musc	3
0273	55	16	4	5	0	13	7			1
0274	60	5	5	5	10	0	5			1
0287	50	20	5	20	0	0	3	1	musc	3
0288	50	23	7	5	0	0	15	4	musc	2
0289	60	2	18	2	2	0	5	2	musc	1
0290	55	10	15	10	0	0	3	2	musc,tourm	1
0291	50	20	5	5	7	0	7	5	musc	1
0292	50	20	10	10	0	0	3	2	musc,tourm	2
0293	65	15	5	7	1	0	3	2	musc,tourm	2
0294	65	3	12	5	5	0	10	2	musc	2
0295	55	4	16	10	5	0	15	2	musc,tourm	2
0296	40	8	7	30	0	0		2	musc,tourm	2
0297	60	5	5	25	2	0	3	1	musc,tourm	2
0298	60	7	13	2	0	0	10	4	musc	2
0302	70	16	4	15	0	0	3	2	musc	3
0303	50	5	15	10	0	0	15	2	musc,tourm	1
0305	35	9	1	45	0	0	3	2	musc	1
0307	65	7	3	10	1	0	3	2	musc	2
0308	50	10	5	25	0	0	3	2	musc	3
0309	50	7	8	25	1	0	3	2	musc	2
0310	50	10	15	15	0	0	3	2	musc,tourm	2
0311	70	3	7	10	5	0	3	2	musc,tourm	1
0312	50	5	20	2	5	0	5	10	musc,tourm	1
0329	50	3	2	30	0	0			biotite	1
0330	40	5	5	30	0	10	5	5	musc	3
0331	40	7	13	10	0	25	10			2
0332	50	5	15	30	0	30	10			2
0333	50	10	20	5	0	10	7	1	musc	1
0334	65	10	10	5	0	0		2	musc,tourm	3
0335	75	3	7	5	0	0	10	5	musc	1
0336	60	5	10	5	0	1	3	2	musc	2
0337	50	15	10	15	0	5	3	5	musc	3
0338	50	10	15	15	0	5	3	5	musc	3
0339	60	15	5	10	0	5	3	3	musc,tourm	3
0340	55	8	2	25	1	0	1	1	musc	2
0458	50	5	2	13	30	0	1	1	musc,tourm	1
0459	60	16	4	10	0	0	10	1	musc	3
0460	75	3	7	5	0	10	3	1	musc	2
0461	60	7	3	10	0	0	10	3	musc	2
0462	60	12	8	15	0	0	1	1	musc,tourm	3
0463	65	5	5	10	4	1	10	1	musc,tourm	2
0464	65	5	10	5	3	0	3	2	musc	2

Appendix 2 Section 3 Petrological modal estimates (continued)

Sample No.	Rock constituents (%)								Oil stain	
	Qtz	Kao	Ill	RF	Spar	Mic	CM	Other		
0465	65	3	7	15	1	0	1			2
0466	60	6	7	5	5	0	10	5	musc,tourm	3
0467	60	10	5	5	5	0	3	5	musc,tourm	2
0468	60	6	9	5	5	0	3	5	musc,tourm	2
0469	65	13	2	10	5	0	1	1	musc,tourm	2
0470	60	10	5	10	5	0	1	1	musc,tourm	2
0471	65	5	10	10	5	0	1	1	musc,tourm	2
0472	70	7	3	10	5	0	1	1	musc,tourm	2
0473	70	14	1	15	0	0	1	1	musc	2
0474	45	8	2	40	0	0	1	1	musc,tourm	2
0475	65	10	5	10	0	1	10	1	musc	2
0476	60	2	3	10	18	2	7	1	musc,tourm	3
0477	65	2	18	5	2	10	1	1	musc,tourm	2
0478	75	5	15	1	0	1	1	1	tourm	2
0479	60	5	25	1	1	0				2
0480	65	3	12	10	0	1	1	1	musc,tourm	2
0481	65	10	15	10	0	5	3	1	musc,tourm	3
0482	65	6	4	10	0	10	1	1	musc,tourm	3
0483	50	15	5	10	5	0	1	1	musc	3
0484	75	10	10	0	5	0	1	1	tourm	3
0485	70	7	8	10	0	5	1	1	musc,tourm	3
0486	60	12	8	2	15	0	1	1	musc	3
0487	35	12	3	40	4	1	1	1	musc	3
0488	65	6	2	15	5	0	1	1	musc,tourm	1
0489	65	5	5	5	5	0	1	1	musc,tourm	3
0490	65	5	15	10	5	0	1	1	musc,tourm	1
0491	50	15	5	30	0	0	1			3
0492	65	5	10	10	1	0	1	1	musc,tourm	2
0493	65	5	10	5	10	0	1	1	musc,tourm	3
0494	60	3	7	10	15	0	10	1	tourm	3
0495	55	3	2	5	15	0	1	1	musc,tourm	1
0496	65	8	7	10	5	0	10	1	musc,tour	1
0497	50	5	25	5	15	0	1	1	tourm	3
0498	70	9	8	10	0	0	1	1	tourm	3
0499	65	12	3	10	0	0	1	1	tourm	2
0500	65	12	3	10	0	0	1	1	tourm	2
0501	65	12	3	10	0	0	1	1	tourm	2
0502	65	12	3	10	0	0	1	1	tourm	1
0503	65	12	3	10	0	0	1	1	tourm	2
0504	70	7	3	10	0	0	1	1	tourm	1
0505	60	12	3	15	0	0	10	1	musc	3
0611	65	7	13	5	0	2	10	0		A
0612	55	10	10	2	4	1	15	1	tourm	R
0613	55	5	15	2	4	1	15	1	tourm	R

(9)

Appendix 2 Section 3 Petrological modal estimates (continued)

Sample No.	Rock constituents (%)								Oil stain	
	Qtz	Kao	Ill	RF	Spar	Mic	CM	Other		
0614	65	10	5	10	5	0	2	1	tourm	C
0615	70	5	15	2	7	0	0	1	tourm	R
0616	65	3	12	0	15	0	2	1	tourm	A
0617	65	5	10	10	5	0	2	0		A
0618	65	7	8	10	0	0	2	0		A
0619	65	5	10	15	0	0	2	0		A
0620	70	5	10	5	5	0	2	0		R
0621	55	3	17	2	2	3	15	1	tourm	A
0622	65	5	10	10	10	0	2	1	tourm	C
0623	55	10	10	2	4	1	15	1	tourm	R
0624	65	5	10	10	5	0	2	1	tourm	C
0625	65	7	8	10	5	0	2	1	tourm	C
0626	65	5	10	10	0	0	2	0		C
0627	55	5	15	2	2	3	15	1	tourm	R
0628	65	5	10	10	1	0	2	0		C
0629	65	3	17	0	0	15	10	0		A
0630	65	3	7	5	18	2	10	1	tourm	C
0631	65	5	10	20	0	0	2	0		C
0632	65	5	10	10	0	0	2	0		R
0633	65	7	3	10	0	0	2	0		R

Section 3 Porosity details

Sample No.	Section porosity:			Plug por	Plug perm
	Prim	Sec	Frac		
0270	10	0	0	17.1	15
0271	12	3	0	16.1	57
0272	5	2	0		
0273	0	0	1		
0274	8	2	0		
0287	5	0	0	13.2	46
0288	2	0	0		
0289	1	1	0	17.6	12.8
0290	8	2	0	10.7	1.2
0291	0	0	1		
0292	2	4	0	14.6	0.7
0293	5	3	0	10.9	0.4
0294	12	3	0	12.6	0.5
0295	5	0	0		
0296	10	3	0	14.6	16.4
0297	6	4	0		
0298	5	0	0		

Appendix 2 Section 3 Porosity details (continued)

Sample No.	Section porosity:			Plug por	Plug perm
	Prim	Sec	Frac		
0302	5	3	0	10.8	11
0303					
0305	5	12	0	9.7	0.1
0307	5	10	0	15.3	81
0308	5	10	0		
0309	6	4	0	12.8	80
0310	8	0	0		
0311	6	0	0	10.4	0.4
0312	2	10	0		
0329	14	5	0	9.0	2.5
0330	7	0	0	9.7	0.1
0331	2	0	0		
0332					
0333	2	0	1		
0334	2	5	0		
0335	5	2	0		
0336	4	2	0		
0337	0	4	2	2.0	0.1
0338	3	0	0	7.0	0.1
0339	3	0	0		
0340	10	5	0	6.5	0.1
0458	2	10	0	11.3	2.4
0459	10	2	0	12.2	4.2
0460	6	4	0	11.8	1.4
0461	8	2	0	12.1	16
0462	10	0	0	15	140
0463	4	0	0		
0464	6	8	0	14.1	1.3
0465	8	4	0		
0466	4	2	0		
0467	4	2	0	14.1	132
0468	4	2	0		
0469	10	2	0	13.8	35
0470	10	2	0	14.5	250
0471	10	2	0	15.8	380
0472	8	0	0	16.9	334
0473	8	4	0	19.2	773
0474	5	0	0	18.3	52
0475	5	0	0	15.5	212
0476	5	0	0	3.4	0.1
0477	4	0	0	5.1	0.1
0478	8	0	0	6.6	0.2
0479	4	2	0	6.8	0.2
0480	3	0	0	6.4	1.0
0481	3	1	0		
0482	6	1	0	6.4	1.2

Appendix 2 Section 3 Porosity details (continued)

Sample No.	Section porosity:			Plug por	Plug perm
	Prim	Sec	Frac		
0483	2	2	0	7.1	0.1
0484	4	3	0	6.2	0.2
0485	5	0	0	5.8	0.2
0486	2	2	1	6.7	0.8
0487	2	2	4	6.5	1.6
0488	4	4	0		
0489	5	0	0	5.8	0.1
0490	4	0	0	6.6	0.1
0491	8	7	1		
0492	5	10	0	13.9	5.0
0493	10	0	0	12.7	1.4
0494	4	0	1	5.5	1.2
0495	2	0	2		
0496	2	0	2		
0497	0	0	9		
0498	2	0	0		
0499	8	2	1		
0500	10	2	1	14.4	31
0501	10	0	0		
0502	8	0	0	13.8	50
0503	4	0	0	11.9	2.7
0504	5	0	1	15	44
0505	10	6	0	13.6	1.2
0611	2	0	1		
0612	2	0	0		
0613	2	0	0		
0614	2	0	0		
0615	2	0	0		
0616	2	0	0		
0617	2	0	0		
0618	2	0	0		
0619	2	0	0		
0620	1	0	1		
0621	3	0	0		
0622	5	0	0		
0623	2	0	0		
0624	1	5	1		
0625	4	0	1		
0626	1	5	0		
0627	2	0	0		
0628	0	3	0		
0629	2	0	0		
0630	2	0	0		
0631	4	0	0		
0632	6	2	0		
0633	5	0	0		

APPENDIX 3
XRD results and analysis.

Appendix 3: XRD data.

Section	Contents
1	Methods
2	Results
3	References

1 Methods

Bulk mineral identification of all samples was carried out by X-Ray Diffraction (XRD) analysis. Samples of total rock were wet ground for 30 seconds using ethanol in a tungsten-carbide mill, then oven dried at temperatures less than 100^o C. Samples were run as front mounted powder pressings from 3 to 75^o 2 θ at 4^o per minute in a "Siemens" X-Ray diffractometer at 50kV and 35mA using Co K α radiation.

These procedures follow guidelines for sample handling outlined by Phillips (1989). Interpretation of results used data captured from the diffractometer and analysed using the program XPLOT (Raven & Self 1988). Broad estimates of mineral abundance are made by comparing the relative peak count sizes of the scan angles for each mineral present.

Dickite was recognised from the presence of a peak with a 'd' spacing of 3.79 A^o, which differentiates it from kaolinite which has a nearby peak at 3.74 A^o.

The ratio of illite to kaolin was calculated by measuring the height of the illite/muscovite peak at approximately 10 A^o and the height of the kaolin peak at 7 A^o, then dividing twice the illite peak height with the kaolin peak height.

Typical XRD traces of samples 270 and 273 are shown as Figure 1 and 2.

2 Results

The results of the analysis of XRD traces are tabulated in Table 1 overleaf. Abbreviations used are:

D=dominant	i/k=illite to kaolin ratio
C=codominant	Qtz=quartz
M=minor	Kaol=kaolinite
T=trace	Dick=dickite
A=absent	Sid=siderite

3 References

Phillips S.P. 1988. Sample preparation procedures for X-Ray diffraction. Unpublished memo to the National Centre for Petroleum Geology and Geophysics, Adelaide.

Raven M. & Self P.G. 1988. XPLOTT-user manual, manipulation of powder X-Ray diffraction data. *CSIRO Technical Memorandum 30/1988*, 29p.

Table 1: XRD details.

Well Name	No.	Sample	Qtz.	Kaol	Dick	ill.	Sid	i/k
STRZELECKI	15	0270	D		M	T		0.54
STRZELECKI	15	0271	D		T	T		0.52
STRZELECKI	15	0272	D		M	T		0.55
STRZELECKI	15	0273	C		T	M	C	4.52
STRZELECKI	15	0274	D	S		S	T	1.04
STRZELECKI	16	0287	S		M	M		0.64
STRZELECKI	16	0288	D	M		M		1.81
STRZELECKI	16	0289	D		M	M		2.87
STRZELECKI	16	0290	D		M	M		1
STRZELECKI	05	0291	S	M		M	M	1.36
STRZELECKI	05	0292	D		M	M		1.04
STRZELECKI	05	0293	S		M	T		0.86
STRZELECKI	02	0294	D		M	M	M	1.65
STRZELECKI	02	0295	D		M	M		1.85
STRZELECKI	02	0296	D		M	T		1.4
STRZELECKI	10	0297	D		T	T		0.93
STRZELECKI	10	0298	D		M	M	M	1.27
MARANA	01	0302	D		M	M		0.61
MARANA	01	0303	D		M	M		2.69
MARANA	01	0305	D		M	T		0.3
KIDMAN	01	0307	D		M	T		0.23
KIDMAN	01	0308	D		T	T		0.23
KIDMAN	01	0309	D	T		T		1.05
KIDMAN	02	0310	D		M	M		1.47
PIRA	02	0311	D		T	T		1.67
PIRA	02	0312	D	M		M		1.74
KIDMAN	01	0329	D		T	T		0.75
KIDMAN	01	0330	D	M		M		0.93
MARABOOKA	01	0331	D	M		M	T	1.31
MARABOOKA	01	0332	D	T		M	S	2
MARABOOKA	01	0333	D	M		M	T	1.47
MARABOOKA	01	0334	D	T		T		1

(3)

Appendix 3, Table 1: XRD details (continued).

Well Name	No.	Sample	Qtz	Kaol	Dick	ill	Sid	i/k
MARABOOKA	01	0335	D		T	T		2
MARABOOKA	01	0336	D		T	M		2.24
PIRA	02	0337	D	M		M	T	1.12
PIRA	02	0338	D	M		M	T	1.42
PIRA	02	0339	D	M		M	T	0.65
PIRA	02	0340	D		M	T		0.29
STRZELECKI	01	0458	D	M		T	M	0.34
STRZELECKI	01	0459	D		M	T		0.28
STRZELECKI	01	0460	D		M	M	T	1.4
STRZELECKI	01	0461	D		M	T		0.5
STRZELECKI	01	0462	D		T	T		0.8
STRZELECKI	01	0463	D		T	T		1
STRZELECKI	01	0464	D		T	T		2
STRZELECKI	01	0465	D	T		T		1.7
STRZELECKI	01	0466	D		M	M		1.1
STRZELECKI	01	0467	D		T	T		0.76
STRZELECKI	01	0468	D		M	M	M	1.2
STRZELECKI	01	0469	D		T	T		0.34
STRZELECKI	01	0470	D		M	M	S	1.2
STRZELECKI	01	0471	D		T	T	T	1.3
STRZELECKI	01	0472	D		M	T		0.7
STRZELECKI	01	0473	D		M	T		0.2
STRZELECKI	01	0474	D		M	T		0.2
STRZELECKI	01	0475	D		M	M		0.82
KERNA	01	0476	D		M	M	M	1.6
KERNA	01	0477	D	M		M	M	3.3
KERNA	01	0478	D	M		M		1.7
KERNA	01	0479	D		M	M	T	1.5
KERNA	01	0480	D	M		S	M	2.9
KERNA	01	0481	D		M	M		0.7
KERNA	01	0482	D		M	M	T	0.8
DILCHEE	01	0483	D	M		M	T	2.1
DILCHEE	01	0484	D		M	M		1.3
DILCHEE	01	0485	D		M	M	M	1.2
DILCHEE	01	0486	D	M		M	T	1
KERNA	01	0487	D		M	M	T	0.6
COOCHILARA	01	0488	D		M	M	T	0.5
COOCHILARA	01	0489	D	M		M	M	2.2
COOCHILARA	01	0490	D		M	M	M	1.8
STRZELECKI	01	0491	D		M	T	T	0.6
STRZELECKI	01	0492	D		T	T	T	1.3
STRZELECKI	01	0493	D	M		M	M	1.5
STRZELECKI	01	0494	D	M		M	M	1.8
STRZELECKI	01	0495	D	M		M	M	0.9
STRZELECKI	01	0496	D	M		M	T	1
STRZELECKI	01	0497	D	M		T	M	0.6

(4)

Appendix 3, Table 1: XRD details (continued).

Well Name	No.	Sample	Qtz	Kaol	Dick	ill	Sid	i/k
STRZELECKI	01	0498	D		M	M		1.2
STRZELECKI	01	0499	D		S	T		0.3
STRZELECKI	01	0500	D		M	T		0.3
STRZELECKI	01	0501	D		T	T		0.3
STRZELECKI	01	0502	D		M	T		0.2
STRZELECKI	01	0503	D		M	T		0.4
STRZELECKI	01	0504	D		M	T		0.2
STRZELECKI	01	0505	D		T	T		0.2
STRZELECKI	10	0611	D	A	M	M	T	0.84
STRZELECKI	10	0612	D	A	M	M	M	1.16
STRZELECKI	10	0613	D	A	M	M	M	2
STRZELECKI	10	0614	D	A	M	M	A	0.67
STRZELECKI	10	0615	D	M	A	M	M	1.38
STRZELECKI	10	0616	D	T	T	T	T	1.6
STRZELECKI	10	0617	D	A	T	T	A	1.71
STRZELECKI	10	0618	D	T	T	T	T	1
STRZELECKI	10	0619	D	T	A	T	T	2
STRZELECKI	10	0620	D	T	T	T	T	3.6
KIDMAN	01	0621	D	M	M	M	M	3.7
KIDMAN	01	0622	D	T	A	T	T	2.44
KIDMAN	01	0623	D	M	A	M	T	0.58
KIDMAN	01	0624	D	T	A	T	T	2.4
KIDMAN	01	0625	C	T	A	T	C	1.41
KIDMAN	01	0626	D	T	A	T	M	2
KIDMAN	01	0627	D	M	A	M	T	3.09
KIDMAN	01	0628	D	T	T	T	T	2
KIDMAN	01	0629	D	A	M	M	T	2.9
KIDMAN	01	0630	D	A	M	M	M	3.2
KIDMAN	01	0631	D	A	T	T	T	1
KIDMAN	01	0632	D	A	T	T	T	1.11
KIDMAN	01	0633	D	A	T	T	A	0.5

Table 1 XRD determination of bulk mineralogy.

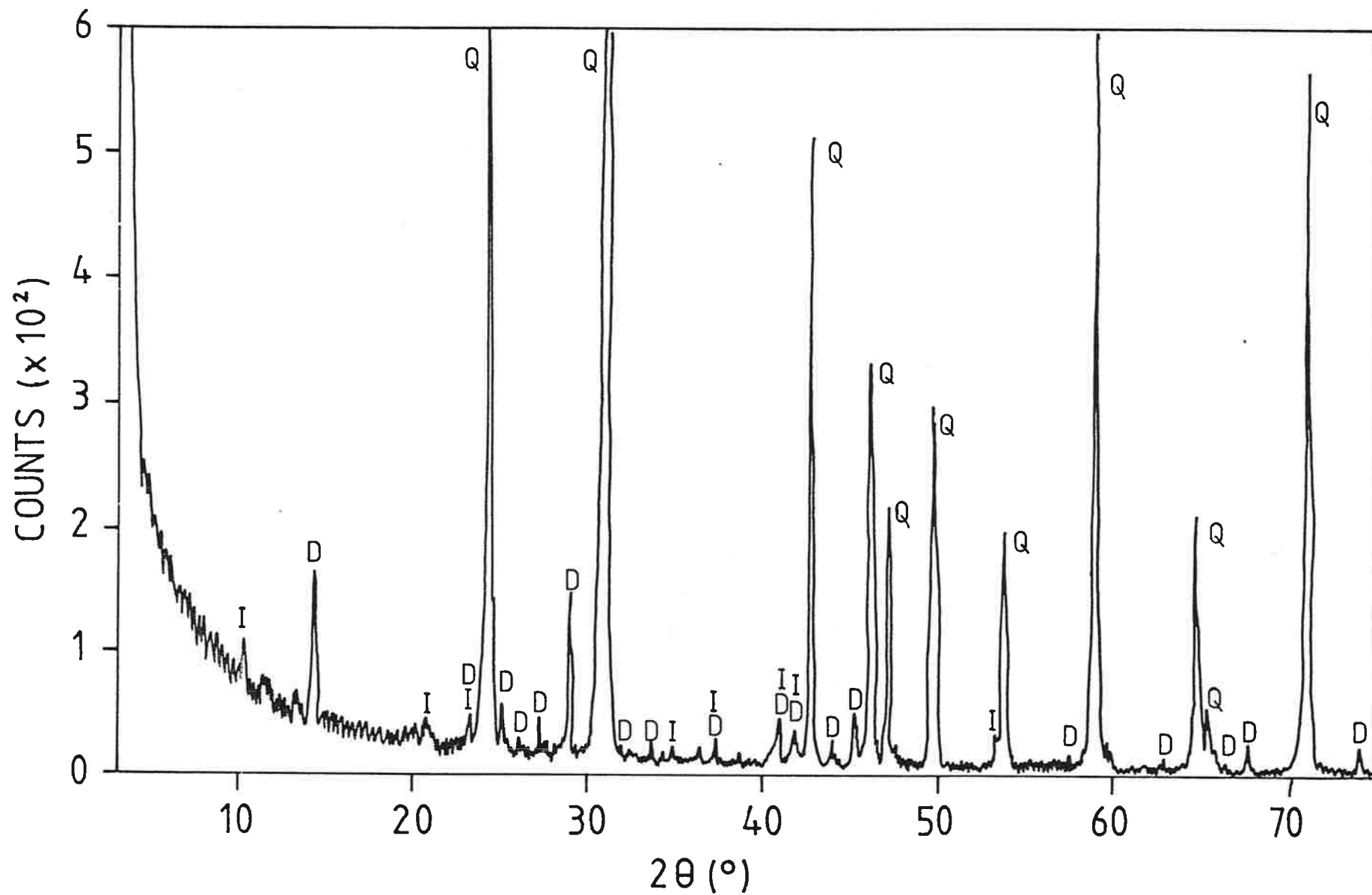


Fig. 1 Typical XRD trace of sample 270 with peaks marked.

Q = quartz, D = dickite, I = illite.

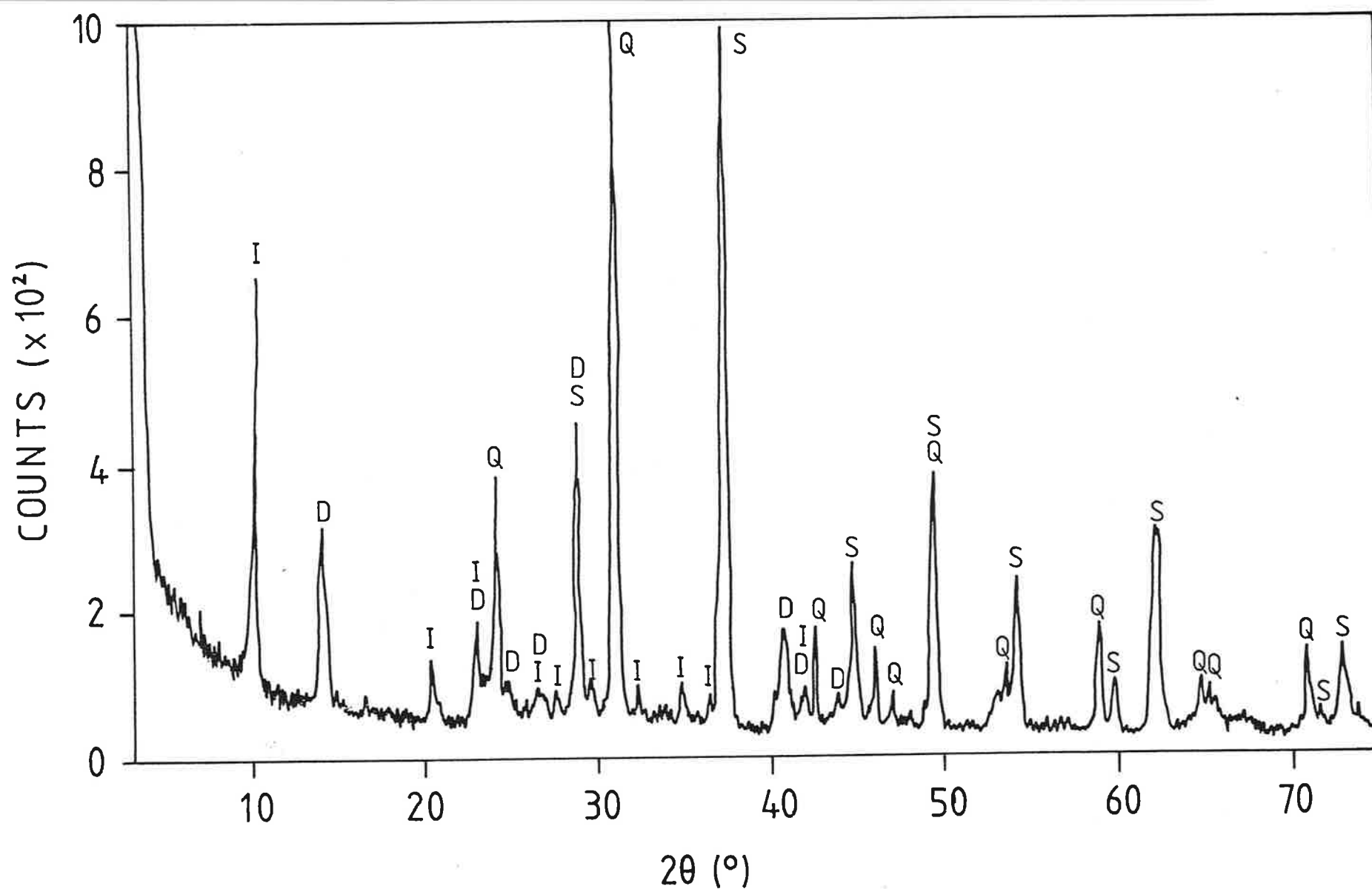


Fig. 2 Typical XRD trace of sample 273 with peaks marked.

Q = quartz, D = dickite, I = illite, S = siderite.

APPENDIX 4
Miscellaneous data.

Appendix 4: Miscellaneous data.

Section	Contents
1	Well details
2	Formation tops
3	Summary of CSIRO (1989) memo

Section 1: Well details

Wellname	Easting (m)	Northing (m)	K.B. (ft)	T.D. (ft)
Aroona 1	371262	1501898	213	7250
Bagundi 1	373564	1501423	213	7310
Bagundi 2	372177	1501875	224	7385
Baratta 1	366228	1491965	190	7573
Coochilara 1	385997	1500864	260	9001
Coochilara 2	383297	1499481	256	8966
Dieri 1	375017	1494816	212	7894
Dilchee 1	391827	1501943	265	9153
Kerna 1	397170	1499132	285	8531
Kerna 2	398685	1499159	287	8914
Kerna 3	397567	1498359	291	8428
Kerna 4	398012	1496193	276	8643
Kidman 1	381148	1498383	241	7732
Kidman 2	377094	1498404	255	7523
Kidman 3	379344	1496400	252	7635
Kidman 4	380910	1497107	241	7968
Kidman 5	376074	1499548	232	7438
Kidman Nth 1	379604	1502214	256	7599
Kidman Nth 2	379174	1503278	259	7611
Marabooka 1			181	7164
Marabooka 2			200	7285
Marabooka 3			194	7176
Marabooka 4				
Lepena 1	368613	1503457	233	7467
Marana 1	365935	1497570	216	6874
Nanima 1	359660	1493905	182	7018
Pira 1	388745	1502756	275	9057
Pira 2	387544	1502930	273	9296
Strzelecki 1	361236	1500756	201	6813
Strzelecki 2	357182	1492059	187	7054
Strzelecki 3	363034	1498543	196	6368
Strzelecki 4	361555	1499099	232	5865
Strzelecki 5	361990	1498216	208	6294
Strzelecki 6	362462	1498744	212	5690
Strzelecki 7	361055	1499167	209	5686
Strzelecki 8	362072	1498555	209	5691
Strzelecki 9	362677	1498335	208	5679
Strzelecki 10	363250	1495638	217	7010
Strzelecki 11	362057	1499179	198	5693
Strzelecki 12	361655	1499541	220	5715

(2)

Appendix 4, Section 1: Well details (continued)

Wellname	Easting (m)	Northing (m)	K.B. (ft)	T.D. (ft)
Strzelecki 13	362599	1499194	202	5687
Strzelecki 14	362159	1499586	214	5691
Strzelecki 15	363501	1496997	200	6535
Strzelecki 16	360924	1498181	221	6447
Strzelecki 17	361160	1499605	212	6254
Strzelecki 18	361508	1498647	215	5924
Strzelecki 19	362928	1498184	199	5911
Strzelecki 20	362890	1498668	210	5718
Strzelecki 21	362380	1498227	198	5702
Strzelecki 22	362089	1499020	204	5703
Strzelecki 23	362445	1498665	210	5715
Strzelecki 24	360171	1499429	218	6817
Strzelecki 25	362034	1496616	187	6730
Wanara 1	356730	1493691	216	6868

Table 2: Formation depths

Well	Depth to formations (ft)									
	Nap	Too	Dar	Ros	Eps	Mur	Pat	Mer	Tir	PrePm
Aroona 1	6029	6469	0	0	0	6756	6885	7076	0	7124
Bagundi 1	6087	6423	0	0	6714	6772	6906	0	0	7012
Bagundi 2	6108	6518	0	0	6795	6840	6976	0	0	7258
Baratta 1	6130	6489	0	6814	6860	7013	7168	7454	0	7508
Cooch 1	6238	6868	7298	7316	7539	7714	7896	0	0	8921
Cooch 2	6250	6805	0	7206	7354	7550	7740	0	0	8818
Dieri 1	6101	6570	6889	6949	7045	7233	7400	0	0	7789
Dilchee 1	6304	7006	7428	7526	7774	7974	8170	0	0	9052
Kerna 1	6308	6839	7374	7426	7675	7856	8049	0	0	8413
Kerna 2	6346	6999	7462	7548	7818	8004	8206	0	0	8814
Kerna 3	6341	6789	7312	7358	7607	7777	7962	0	0	8289
Kerna 4	6315	6820	7372	7459	7724	7884	8076	0	0	8516
Kidman 1	5932	6367	0	6763	6879	7048	7210	0	0	7583
Kidman 2	6039	6422	6768	6788	6876	6944	7135	7336	0	7393
Kidman 3	5977	6374	6773	6785	6890	7065	7229	7462	0	7477
Kidman 4	6364	6438	0	6850	7004	7186	7366	0	0	7874
Kidman 5	6082	6378	0	6758	6768	6890	7028	7212	0	7318
Kid Nth 1	6074	6484	0	6816	6863	6986	7127	0	0	7475
Kid Nth 2	6082	6526	0	6852	6886	6998	7134	0	0	7487
Mrbka 1	6117	6326	0	0	0	0	6526	0	0	7061
Mrbka 2	6143	6350	0	0	0	6551	6592	0	0	7183
Mrbka 3	6130	6319	0	0	0	0	6526	0	0	7078
Mrbka 4	0	6367	0	0	0	0	6645	0	0	0
Lepena 1	6096	6510	0	0	0	6705	6772	0	0	7367
Marana 1	5910	6170	0	0	0	6414	6492	6714	0	6738
Nanima 1	6009	6175	0	0	0	6410	6530	0	0	6837
Pira 1	6270	6957	7364	7446	7691	7873	8069	0	0	0
Pira 2	6302	6944	7372	7452	7695	7876	8073	0	0	9196
Strz 1	5930	6212	0	0	0	6433	6495	0	0	6729

(3)

Appendix 4, Section 2: Formation depths (continued)

Well	Depth to formations (ft)									
	Nap	Too	Dar	Ros	Eps	Mur	Pat	Mer	Tir	PrePm
Strz 2	5895	6094	0	0	0	6327	6405	0	0	6959
Strz 3	5816	5994	0	0	0	0	0	0	0	6180
Strz 4	5812	0	0	0	0	0	0	0	0	0
Strz 5	5831	5990	0	0	0	0	0	0	0	6205
Strz 6	0	0	0	0	0	0	0	0	0	0
Strz 7	0	0	0	0	0	0	0	0	0	0
Strz 8	0	0	0	0	0	0	0	0	0	0
Strz 9	0	0	0	0	0	0	0	0	0	0
Strz 10	5974	6186	0	0	0	6462	6588	6840	6683	0
Strz 11	0	0	0	0	0	0	0	0	0	0
Strz 12	0	0	0	0	0	0	0	0	0	0
Strz 13	0	0	0	0	0	0	0	0	0	0
Strz 14	0	0	0	0	0	0	0	0	0	0
Strz 15	5870	6078	0	0	0	6308	6368	0	0	6404
Strz 16	5905	6096	0	0	0	0	6318	0	0	6368
Strz 17	5798	5956	0	0	0	0	0	0	0	6095
Strz 18	5846	0	0	0	0	0	0	0	0	0
Strz 19	5812	0	0	0	0	0	0	0	0	0
Strz 20	0	0	0	0	0	0	0	0	0	0
Strz 21	0	0	0	0	0	0	0	0	0	0
Strz 22	0	0	0	0	0	0	0	0	0	0
Strz 23	0	0	0	0	0	0	0	0	0	0
Strz 23	5936	6234	0	0	0	6454	6565	0	0	6728
Strz 25	5900	6128	0	0	0	6365	6440	0	0	6601
Wanara 1	5876	6018	0	0	0	6225	6264	0	0	6726

The following results are tabulated from Raven M.D. & Milnes A.R. 1989 Mineralogical analysis of Cooper Basin drill core samples, C.S.I.R.O. Technical Memorandum 18/1989.

Table 1:

No.	FeOx	MnOx	TiO2	CaO	K2O	P2O5	SiO2	Al2O3	MgO	CEC	Total
298	1.08	0.03	0.96	0.03	3.08	0.24	47.6	32.3	0.55	4	85.9
302	1.09	0.03	2.32	0.06	3.59	0.80	46.0	27.9	0.83	4	82.5
309	1.03	0.04	0.98	0.05	3.33	0.24	49.3	27.7	0.75	11	83.7

Table 2:

No.	Qtz	Siderite	Illite	Kaolin	Chlorite	Total
298	10	2	30	53	0	96
302	12	2	36	37	0	84
309	15	2	33	38	4	88

All data comes from the testing of <10um size fraction of samples 298, 302 and 309. Both kaolinite and dickite clays were found in sample 298 while dickite was found as the only kaolin clay type in samples 302 and 309.

The first table tabulates CEC in milli-equivalents per 100g of sample, and XRF conducted on oven dried samples and expressed in element oxide %. Presumably there is substantial interstitial water in the clays. The second table lists estimates of mineral abundance from XRD analysis.

No smectite was found. The sharp XRD peak for mica suggests mica (detrital illite) rather than illite or interstratified or mixed clays. Sample 309 had anomalous CEC vs K2O indicating CEC value is not substantially accounted for by mica or illite present in the sample.

APPENDIX 5

Facies associations limits for wells.

Appendix 5 Facies associations limits for wells

Abbreviations:

Assn No	association number
DST	drill stem test
H ₂ O	mostly water recovered
MMCFD	Million cubic feet of gas per day
NGTS	no gas to surface
RTSM	rate too small to measure
Thick	facies association thickness in feet
T1..T4:	Toolachee Formation facies association 1 to 4
P1..P3:	Patchawarra Formation facies association 1 to 3

Assn No.	Top (ft)	Thick (ft)	Depositional Association	DST result (MMCFD)
Bagundi 1				
T1	6423	63	prograde	?
T2	6486	68	prograde	7.6
T3	6554	100	channels	?
T4	6654	64	channels	?
P1	6907	68	prograde	8.4
P3	6975	37	flood plain	?
Bagundi 2				
T1	6518	66	prograde	?
T2	6584	62	prograde, lacustrine	?
T3	6644	92	channels	?
T4	6736	60	channels	4.5
P1	6977	71	channel overlain by prograde	9.8
P2	7048	131	stacked channels	0.2
P3	7189	71	channel over flood plain	H ₂ O
Baratta 1				
T1	6489	80	flood plain	?
T2	6569	26	thin channels	?
T3	6595	175	stacked channels	?
T4	6770	42	stacked thick channel	?
Cochilara 1				
T1	6867	172	channel over progrades	?
T2	7039	36	channel	?
T3	7075	178	stacked channels	NGTS
T4	7253	46	channel	?
P1	7895	124	prograde + 1 channel	?
P2	8013	715	stacked thick channels	?
P3	8728	200	flood plain, 1 channel	?

Appendix 5, Page 2

Assoc Top No.	Thick (ft)	Depositional Association	DST result (MMCFD)
Dieri 1			
T1	6570	88 progrades	?
T2	6658	36 thin channels	?
T3	6694	87 stacked channels	?
T4	6821	67 stacked channels	?
P1	7400	172 prograde over floodplain	1.0
P2	7572	97 thick stacked channels	?
P3	7665	123 overbank	?
Dilchee 1			
T1	7008	160 prograde	?
T2	7168	22 overbank/lacustrine	?
T3	7190	146 stacked thin channels	RTSM
T4	7336	94 overbank over channel	?
P1	8170	109 prograde, 1 channel	3.6
P2	8279	531 stacked thick channels	?
P3	8810	200 crevasse splay, channels, coal	?
Kerna 1			
T1	6837	197 overbank	?
T2	7034	30 overbank	?
T3	7064	195 thin stacked channels	?
T4	7259	118 stacked thick channels	?
P1	8049	103 prograde over thin channels	3.0
P2	8152	269 stacked channels	7.0
Kerna 2A			
P1	8215	111 3 stacked channels	3.2
P2	8316	413 thick stacked channels	RTSM
P3	8730	84 overbank	?
Kerna 3			
P1	7961	100 prograde + thin channels	?
P2	8061	227 stacked channels	?
Kerna 4			
P1	8067	102 prograde + thin channels	H ₂ O
P2	8169	343 stacked thick channels	H ₂ O
Kidman 1			
T1	6369	31 prograde	?
T2	6500	100 stacked thick channels	?
T3	6600	108 stacked thick channels	9.5
T4	6708	32 thick channel	10.9
P1	7210	90 floodplain	RTSM
P2	7300	283 stacked thick channels	RTSM
Kidman 2			
T1	6422	72 prograde/lacustrine	?
T2	6494	59 thick stacked channel	7.7
T3	6553	185 stacked channels	3.6
T4	6538	30 channel	?
P1	7136	77 prograde, thin channel	?
P2	7214	108 stacked channels	?
P3	7322	84 flood plain	?

Appendix 5, Page 3

Assoc No.	Top (ft)	Thick (ft)	Depositional Association	DST result (MMCFD)
Kidman 3				
T1	6371	101	prograde/lacustrine	?
T2	6472	101	stacked thick channel	8.6
T3	6520	183	multiple channels	10.4
T4	6703	70	thick stacked channel	10.4
P1	7218	94	prograde over thin channels	RTSM
P2	7312	116	stacked channels	2.2
P3	7428	50	stacked channels	H ₂ O
Kidman 5				
T1	6378	74	prograde	0.8
T2	6454	61	stacked channels	4.5
T3	6515	165	stacked channels	5.4
T4	6680	79	stacked channels	8.3
P1	7030	80	2 stacked channels	3.7
P2	7110	162	stacked channels over overbank	H ₂ O
P3	7272	88	overbank	?
Lepena 1				
T1	6511	61	progrades	?
T2	6573	33	thin channels	?
T3	6606	54	thin channels	5.2
T4	6660	49	thin channels	?
P1	6766	75	thin channels	5.3
P2	6831	384	thick stacked channels	?
P3	7215	155	stacked crevasse splay sands	?
Marabooka 1				
T1	6326	37	prograde	?
T2	6363	49	thick channel	6.9
T3	6412	57	stacked thin channels	8.4
T4	6469	58	thick channel	?
P1	6526	68	thin progrades	RTSM
P2	6594	394	stacked channels	RTSM
P3	6968	92	stacked channels	?
Marana 1				
T1	6169	60	lacustrine	?
T2	6229	25	prograde channel	?
T3	6244	107	stacked channels	8.4
T4	6361	53	stacked thick channel	H ₂ O
P1	6591	225	major prograding lacustrine	?
Pira 2				
T1	6995	116	prograde	?
T2	7111	41	thick channel	RTSM
T3	7152	141	prograde over stacked channels	RTSM
T4	7393	80	overbank over channel	?
P1	8073	117	channel over prograde	RTSM
P2	8190	870	stacked channels	0.6
P3	8980	156	? prograde	?

Appendix 5, Page 4

Assoc Top No.	(ft)	Thick (ft)	Depositional Association	DST result (MMCfD)
Strzelecki 1				
T1	6229	56	prograde	5.0
T2	6285	35	thin channels	5.0
T3	6320	70	stacked channels	5.0
T4	6390	105	stacked channel	RTSM
P1	6495	196	thick stacked channels	RTSM
P2	6691	39	thick channel	?
Strzelecki 2				
T1	6103	68	prograde	RTSM
T2	6171	31	channel	RTSM
T3	6202	71	stacked channel	H ₂ O
T4	6290	38	channel	H ₂ O
P1	8401	40	prograde	H ₂ O
P2	6441	524	stacked thick channels	H ₂ O
Strzelecki 3				
T1	5993	55	prograde/lacustrine	?
T2	6048	18	thin channel	8.0
T3	6066	78	stacked channels	8.0
T4	6144	37	stacked channel	7.3
Strzelecki 10				
T1	6186	84	prograde over channel	4.2
T2	6270	35	thin channels	?
T3	6305	113	multiple stacked channels	7.1,oil
T4	6418	42	thin channel	?
P1	6583	99	prograde over 1 channel	?
P2	6682	161	stacked thick channels	?
Strzelecki 15				
T1	6078	62	prograde over minor channel	?
T2	6140	28	thin channel over overbank	?
T3	6168	104	multiple channels	9.2
T4	6272	34	stacked channels	9.2
Strzelecki 17				
T1	5954	46	prograde	?
T2	6000	31	thin channels	?
T3	6031	55	stacked channels	?
T4	6086	10	thin channel	?

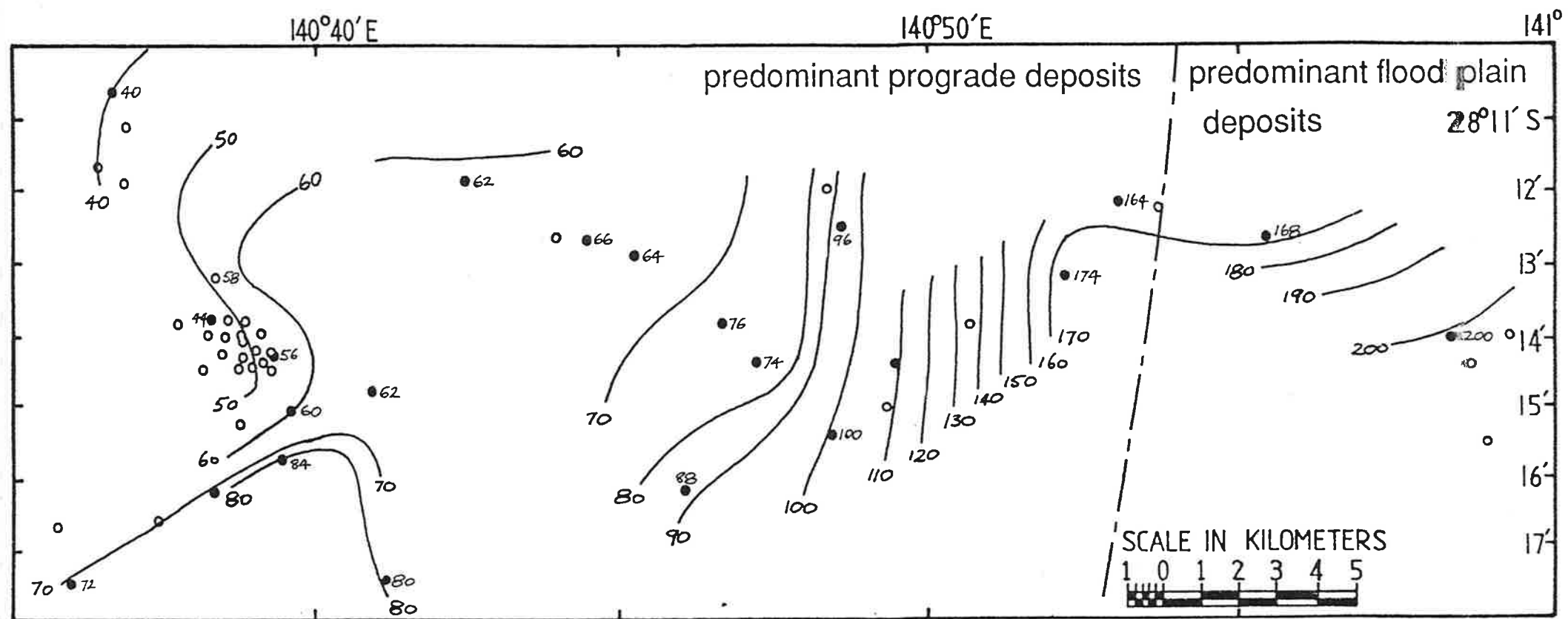


Fig. 1 Toolachee Fm. Association 1 isopach map. Isopachs in feet.

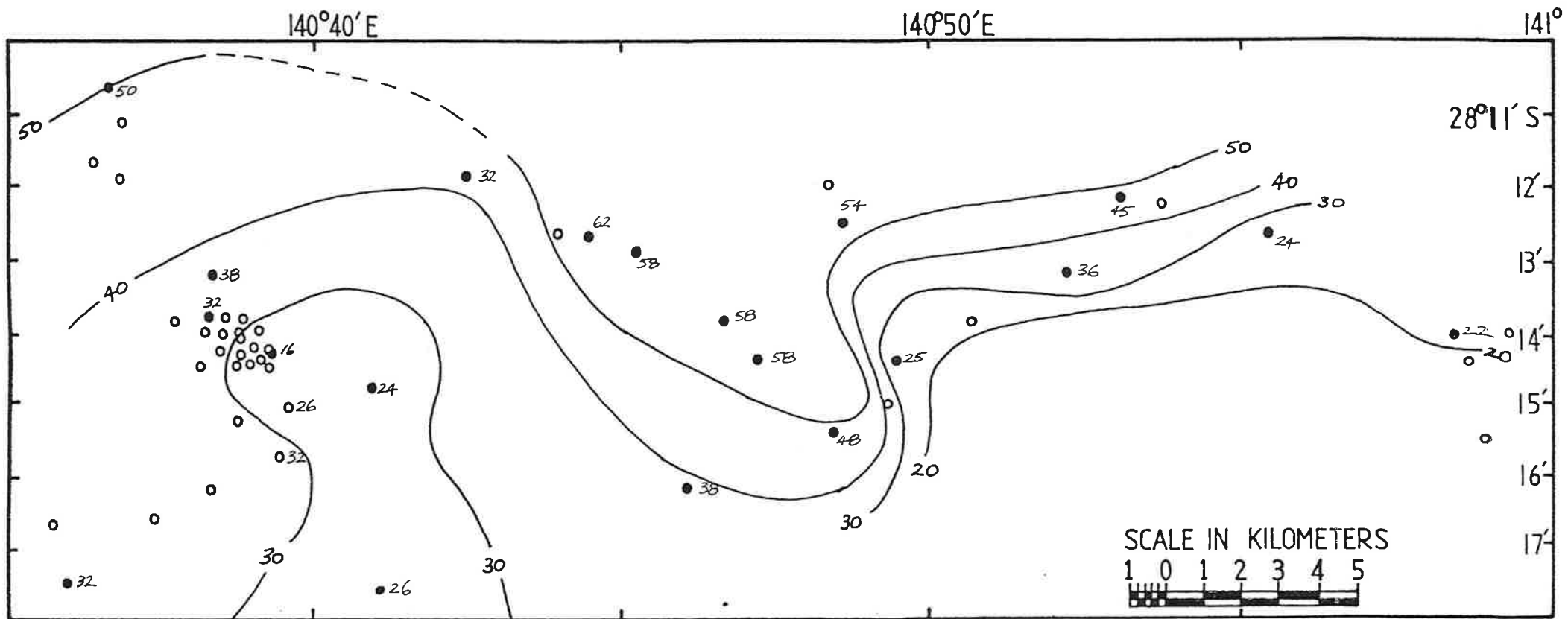


Fig. 2 Toolachee Fm. Association 2 isopach map. Isopachs in feet.

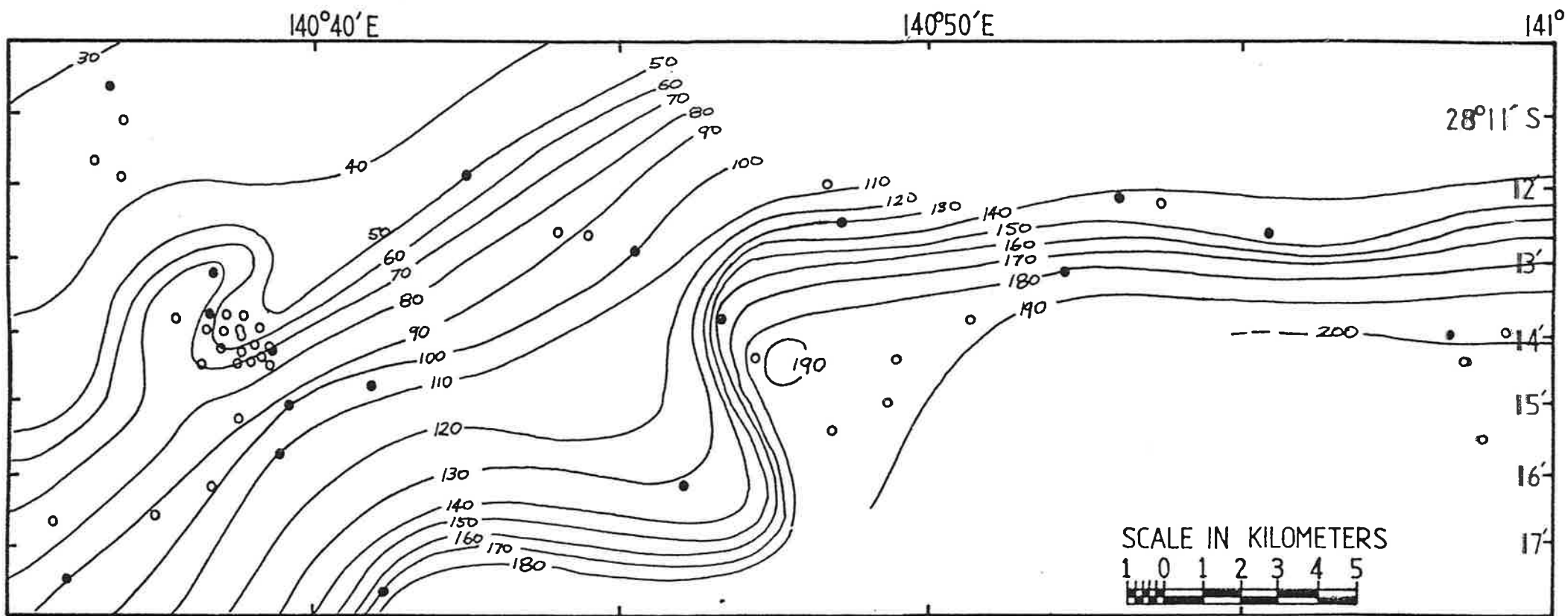


Fig. 3 Toolachee Fm. Association 3 isopach map. Isopachs in feet.

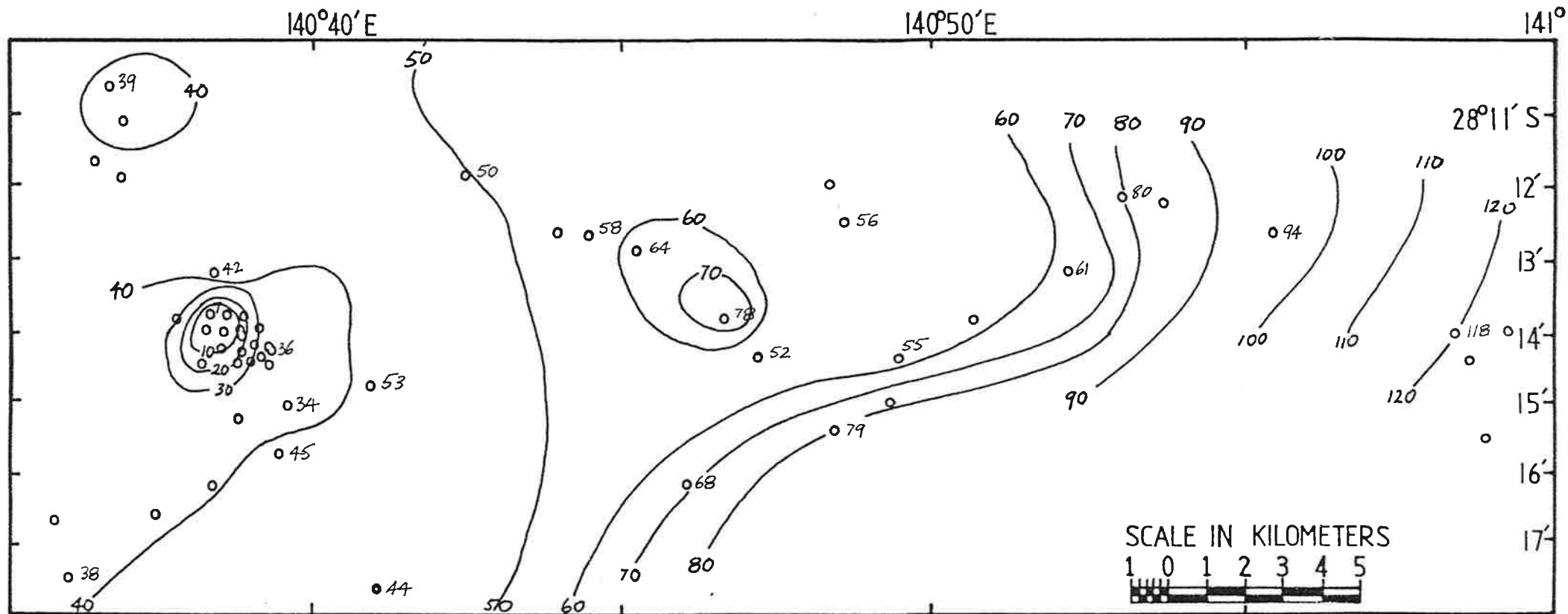


Fig. 4 Toolachee Fm. Association 4 isopach map. Isopachs in feet.

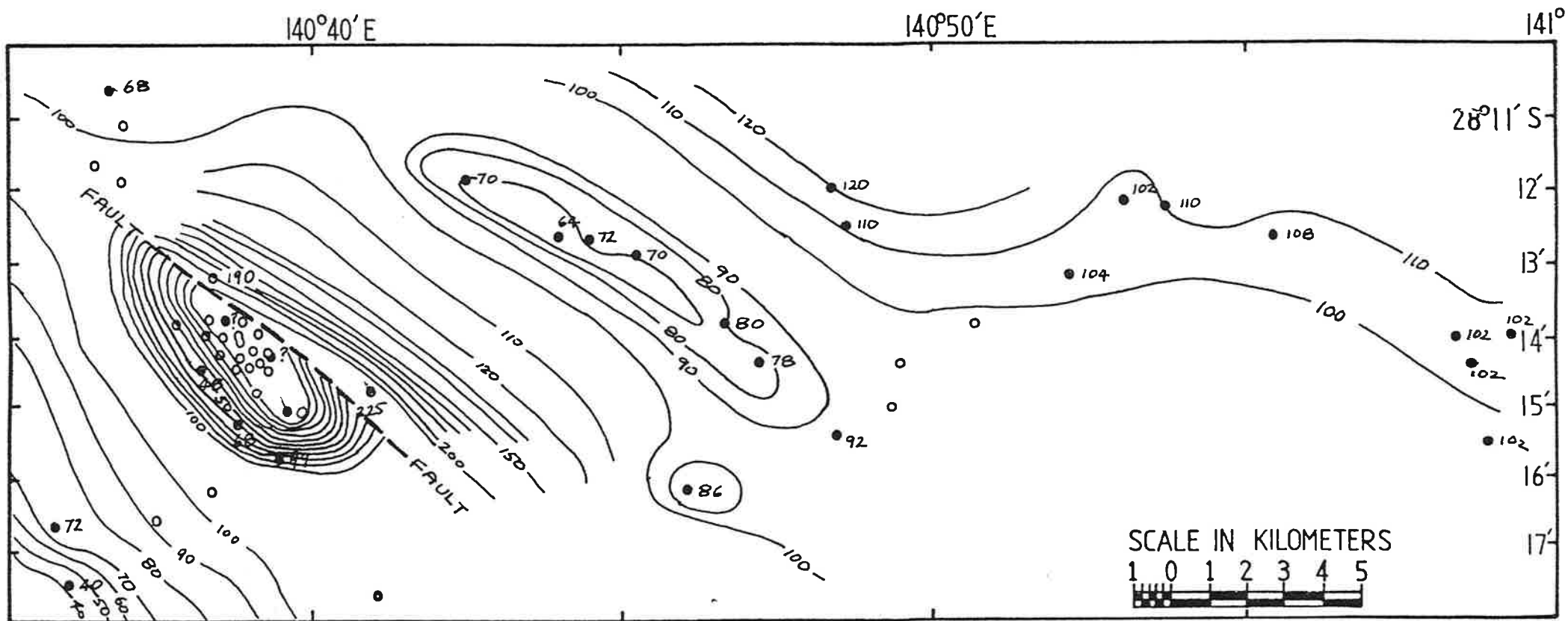


Fig. 5 Patchawarra Fm. Association 1 isopach map. Isopachs in feet.

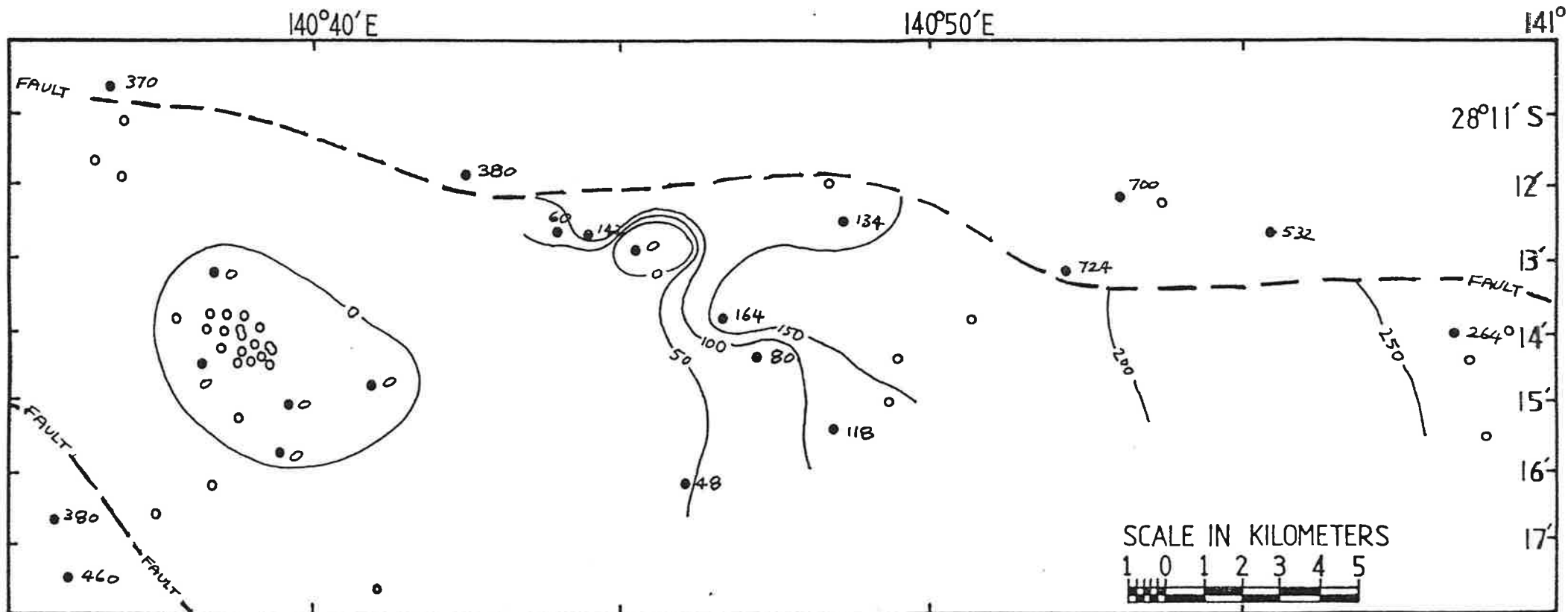


Fig. 6 Patchawarra Fm. Association 2 isopach map. Isopachs in feet.

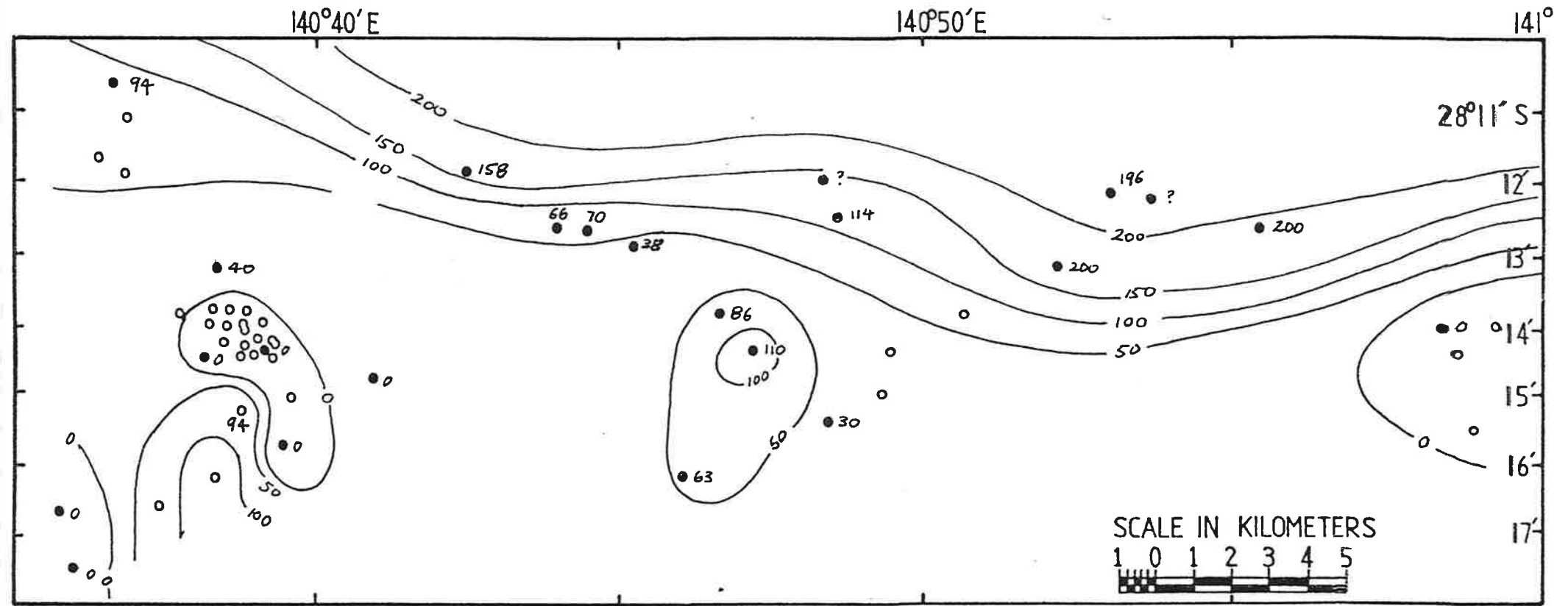


Fig. 7 Patchawarra Fm. Association 3 isopach map. Isopachs in feet.

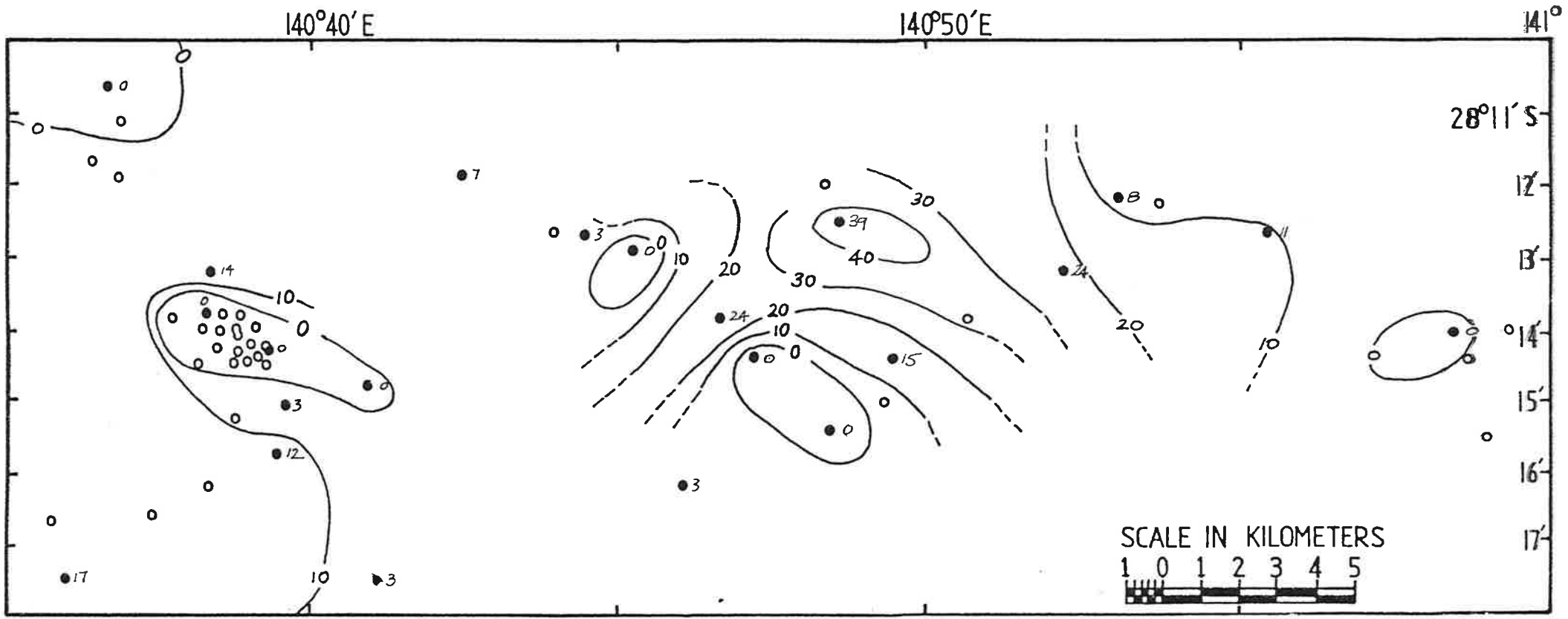


Fig. 8 Toolachee Fm. Association 1 sandstone % map.

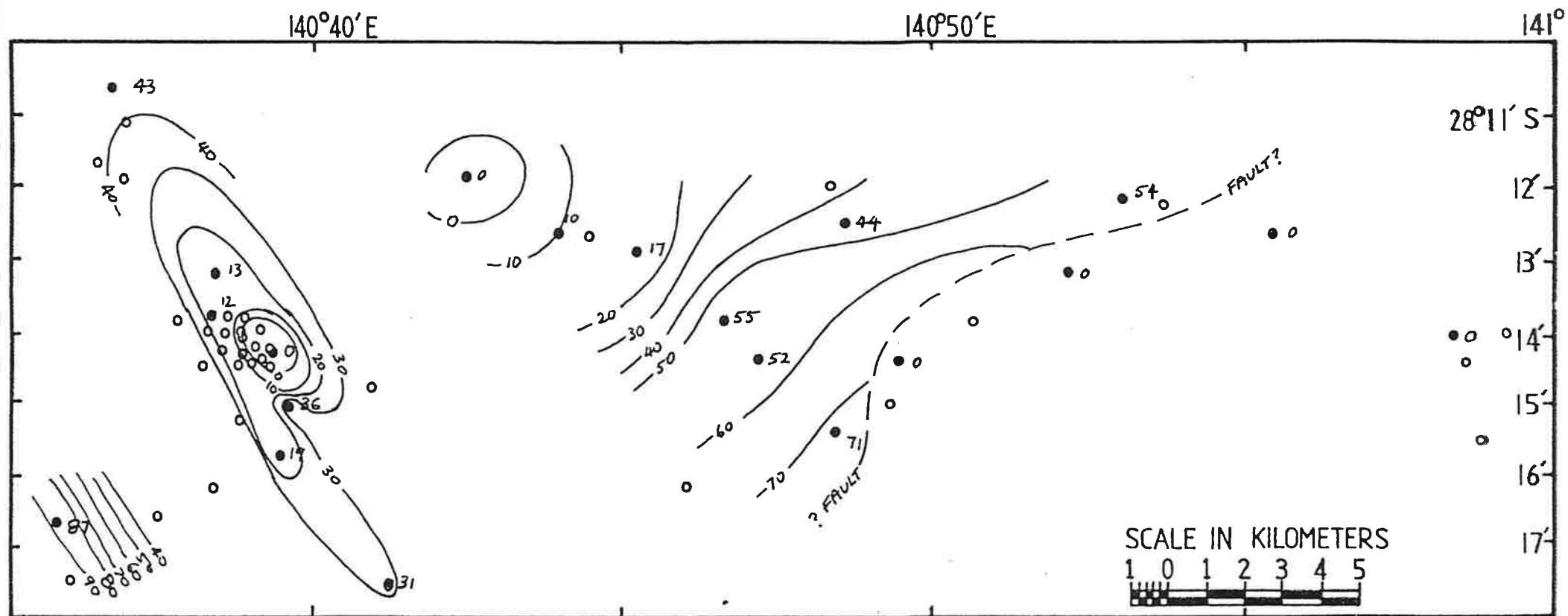


Fig. 9 Toolachee Fm. Association 2 sandstone % map.

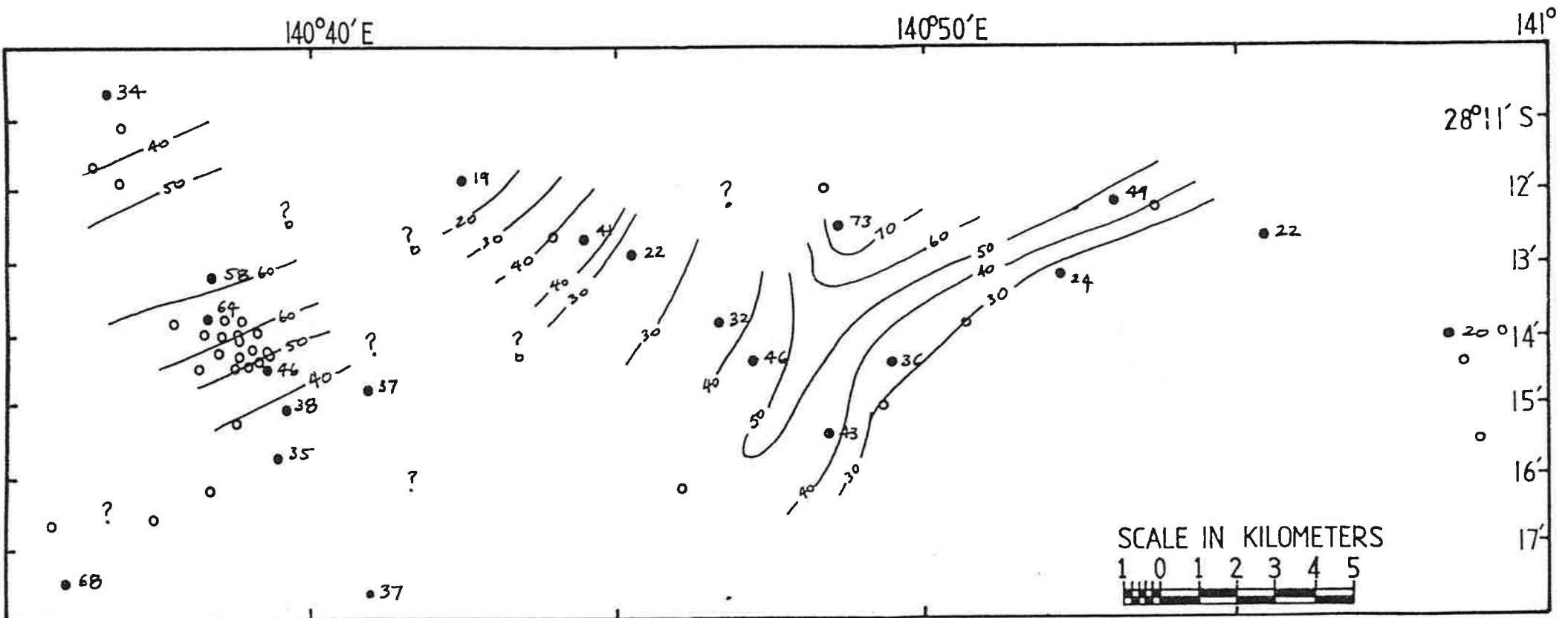


Fig. 10 Toolachee Fm. Association 3 sandstone % map.

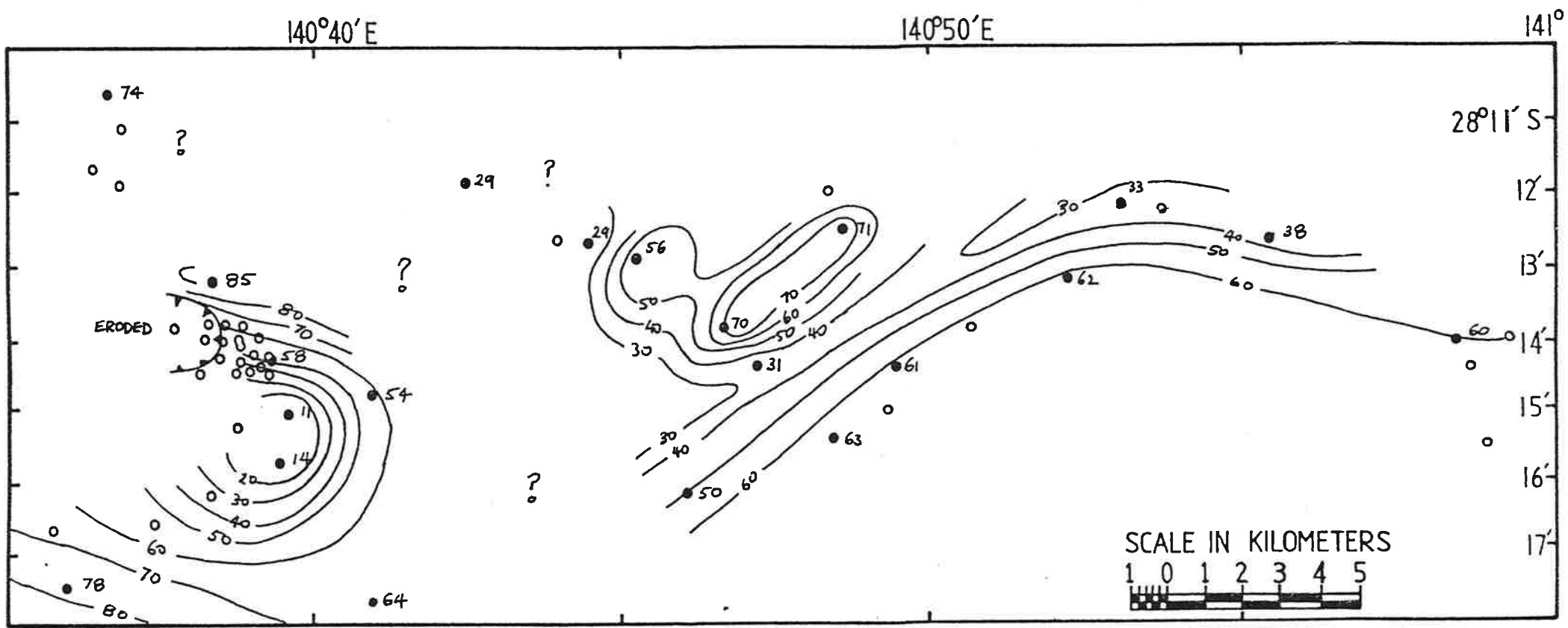


Fig. 11 Toolachee Fm. Association 4 sandstone % map.

APPENDIX 6

Electrical log to core logging correlations.

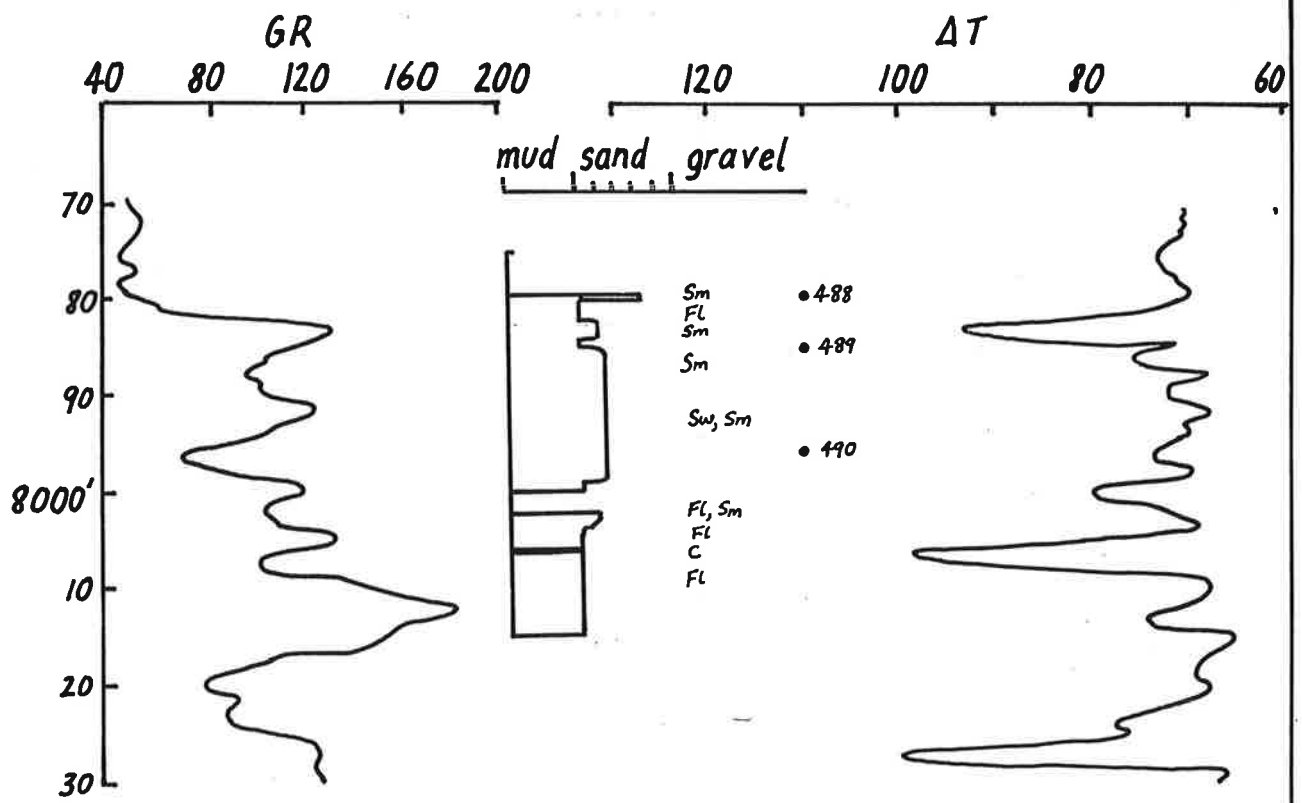


Fig. 1. Coochilara 1, core 2, Patchawarra Fmn.
Overbank, low energy channel deposits.

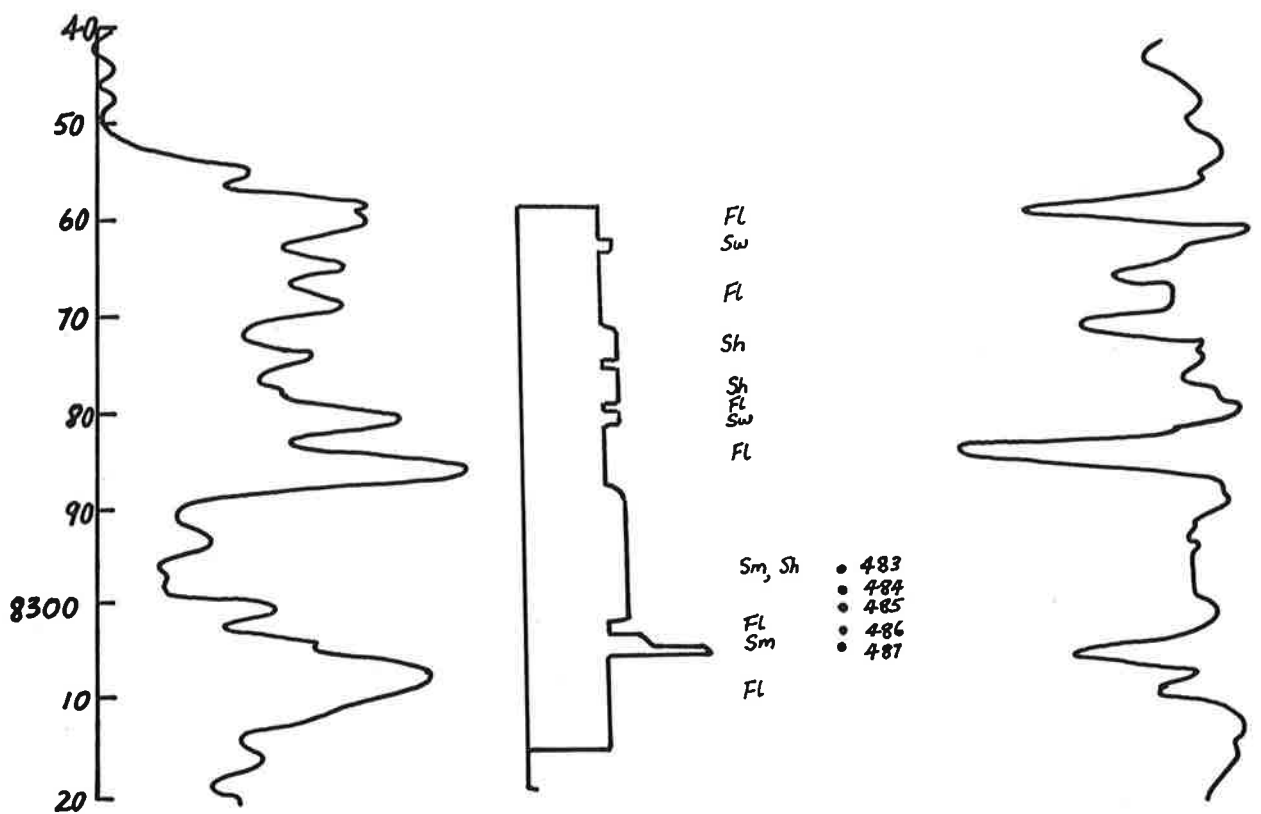


Fig. 2. Dilchee 1, core 1, Patchawarra Fmn.
Low energy fluvial to flood plain deposits

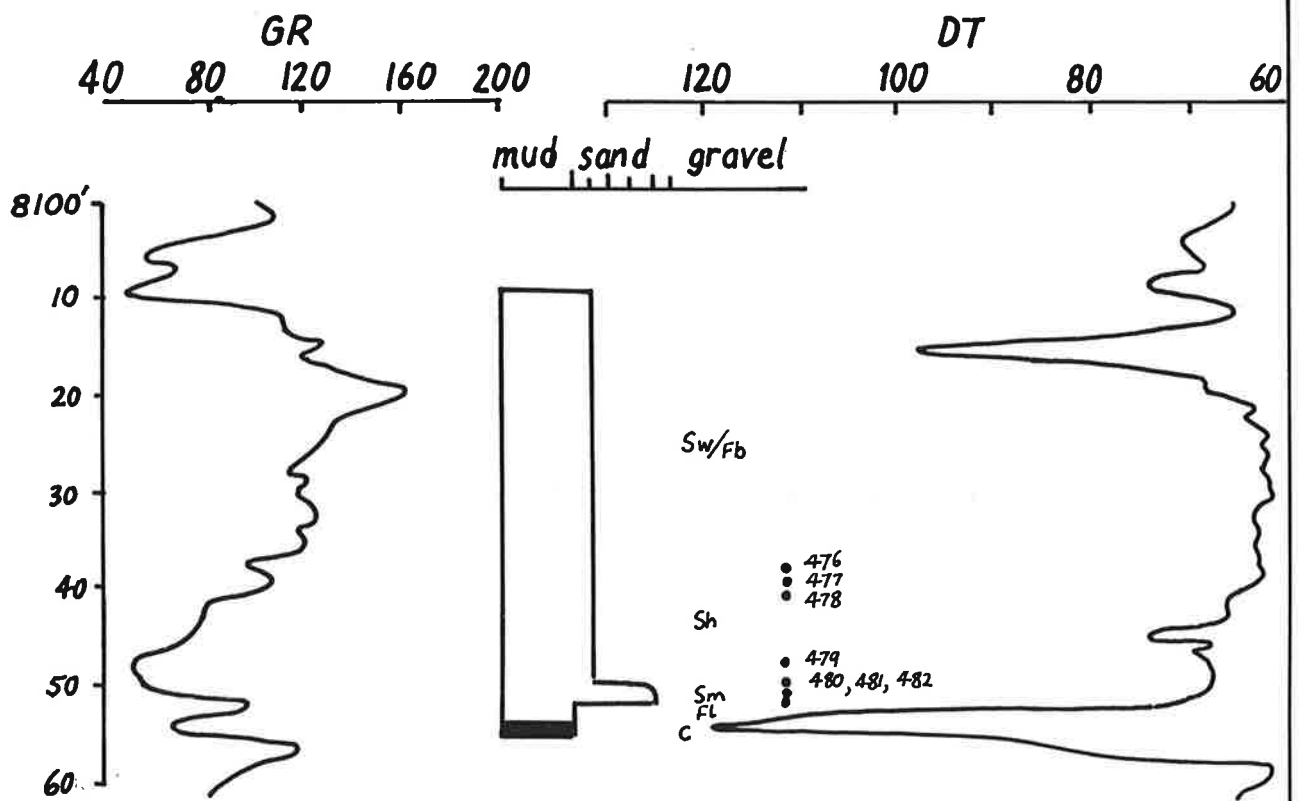


Fig. 3. Kerna 1, core 2, Patchawarra Fmn.
Floodplain and minor channel deposits.

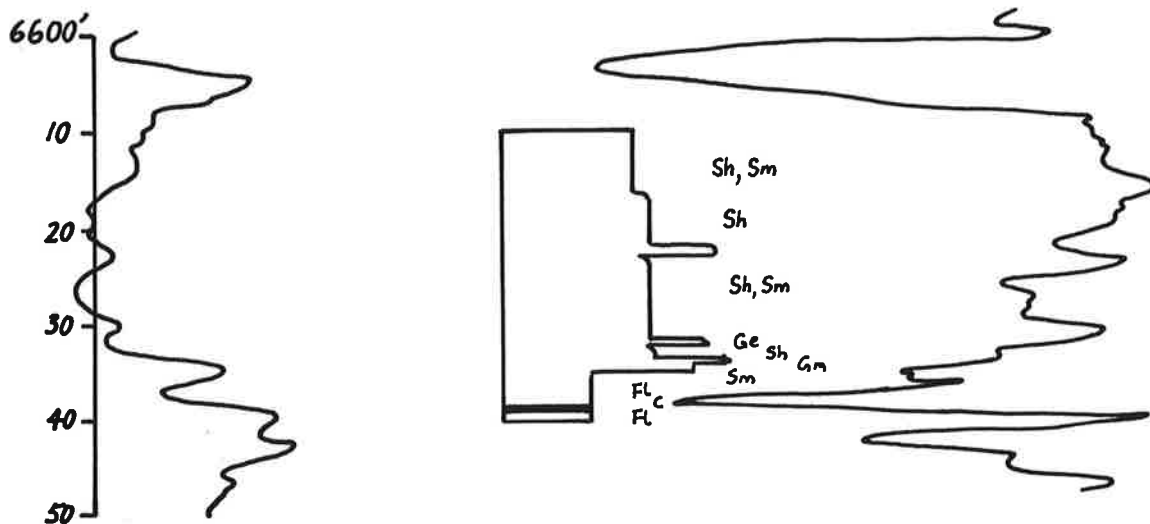


Fig. 4. Kidman 1, core 1, Toolachee Fmn.
Stacked channel deposits.

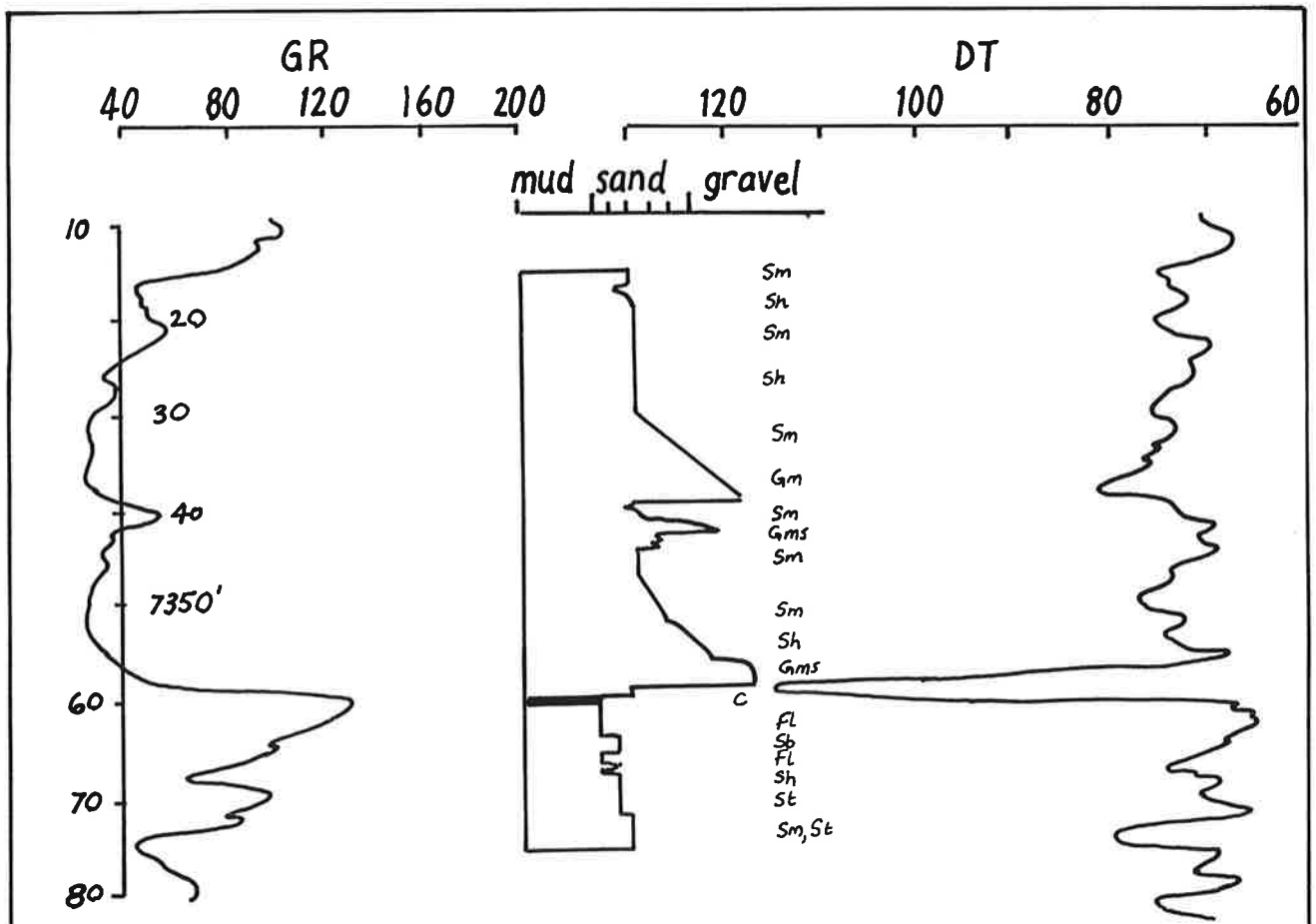


Fig. 5. Kidman 1, core 2, Patchawarra Fmn.
Bed load channel deposits.

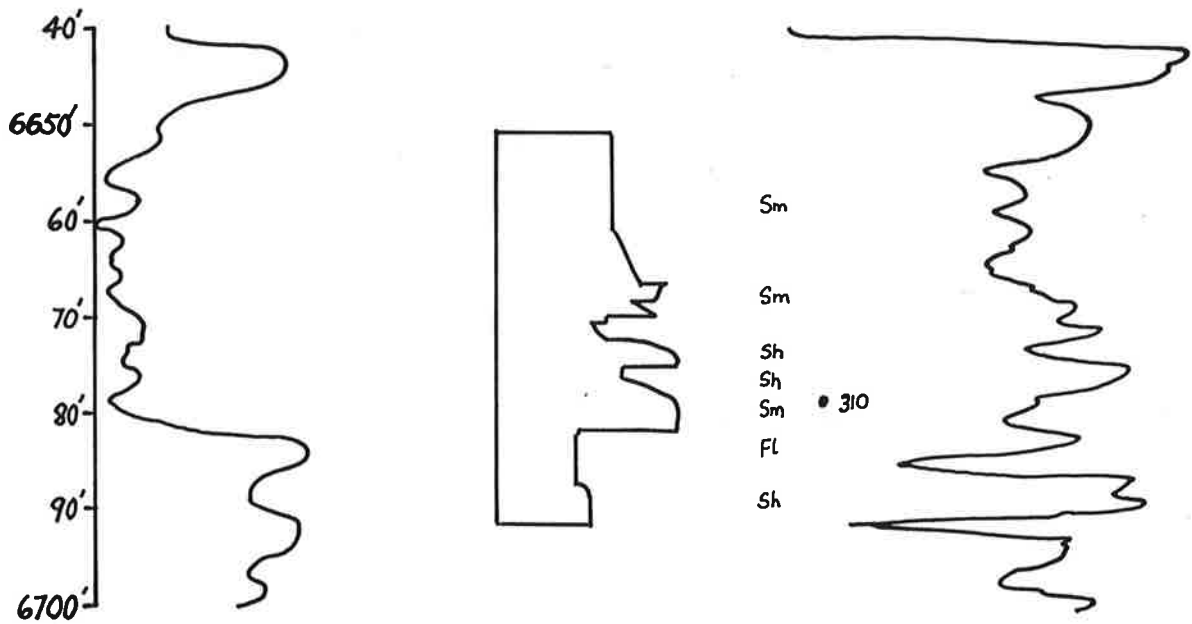
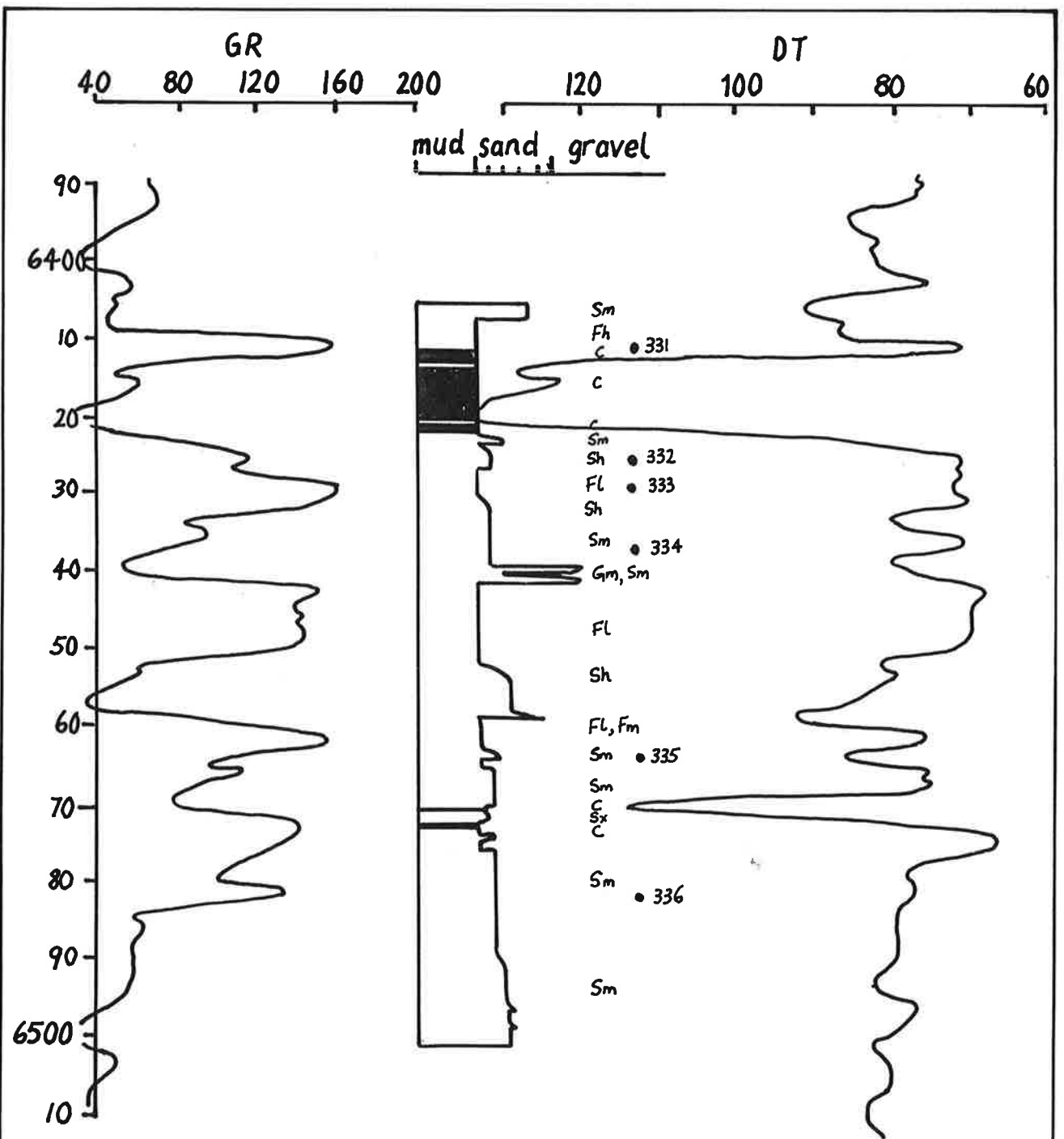
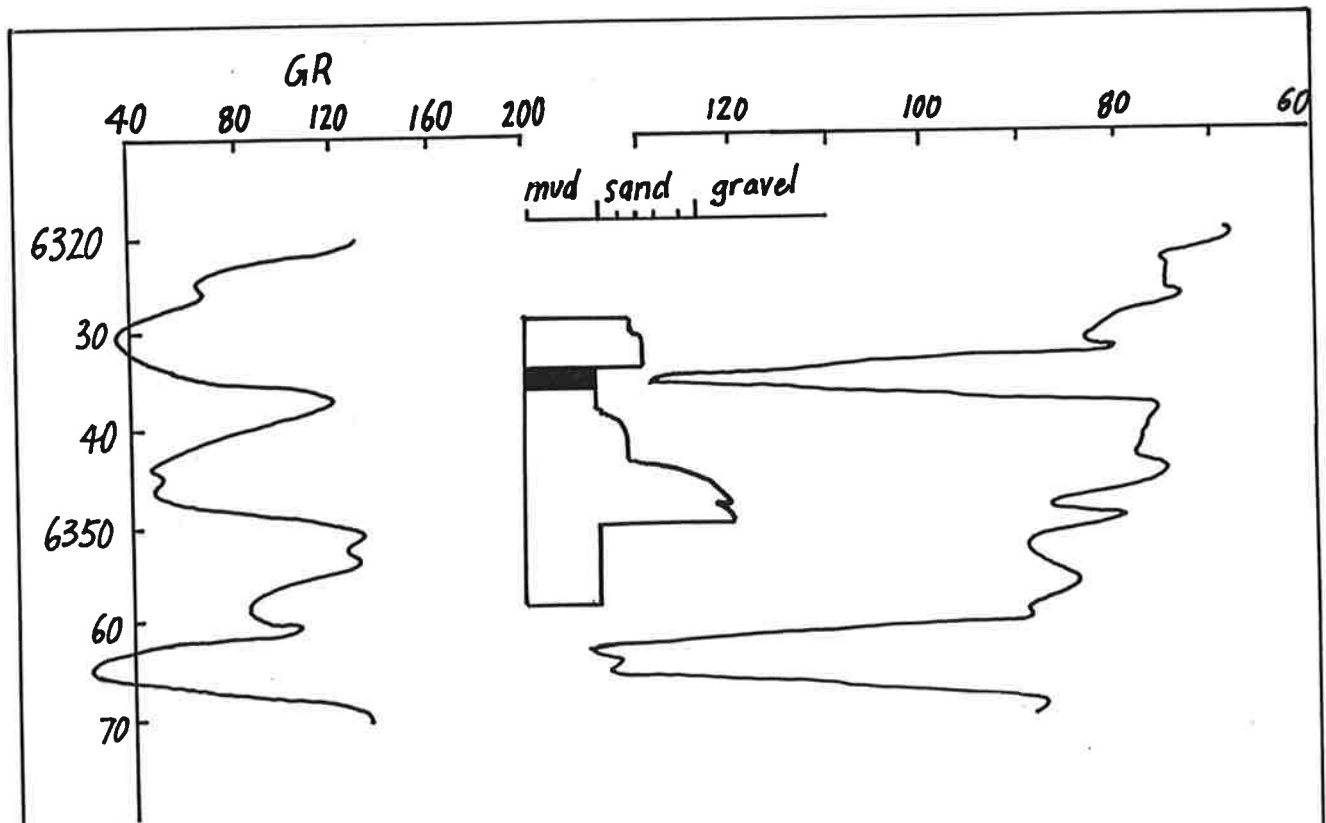


Fig. 6. Kidman 2, core 1, Toolachee Fmn.
Channel deposits, minor prograde



**Fig. 7. Marabooka 1, core 3, Toolachee Fmn.
Stacked channel & minor overbank deposits**



**Fig. 8 Marana 1, core 1, Toolachee Formation.
Channel deposits.**

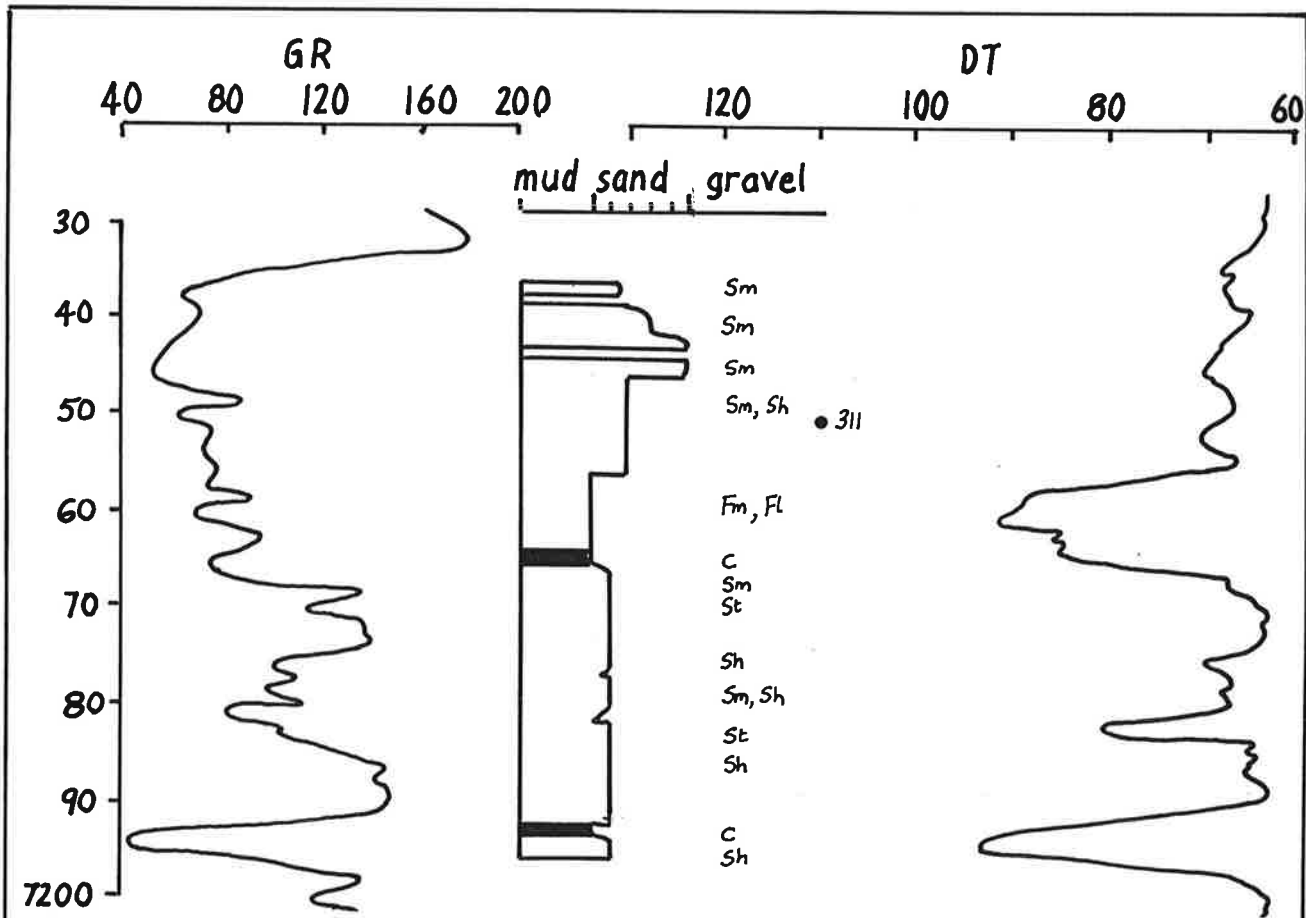


Fig. 9. Pira 2, core 1, Toolachee Fmn.

Mostly prograding deposits.

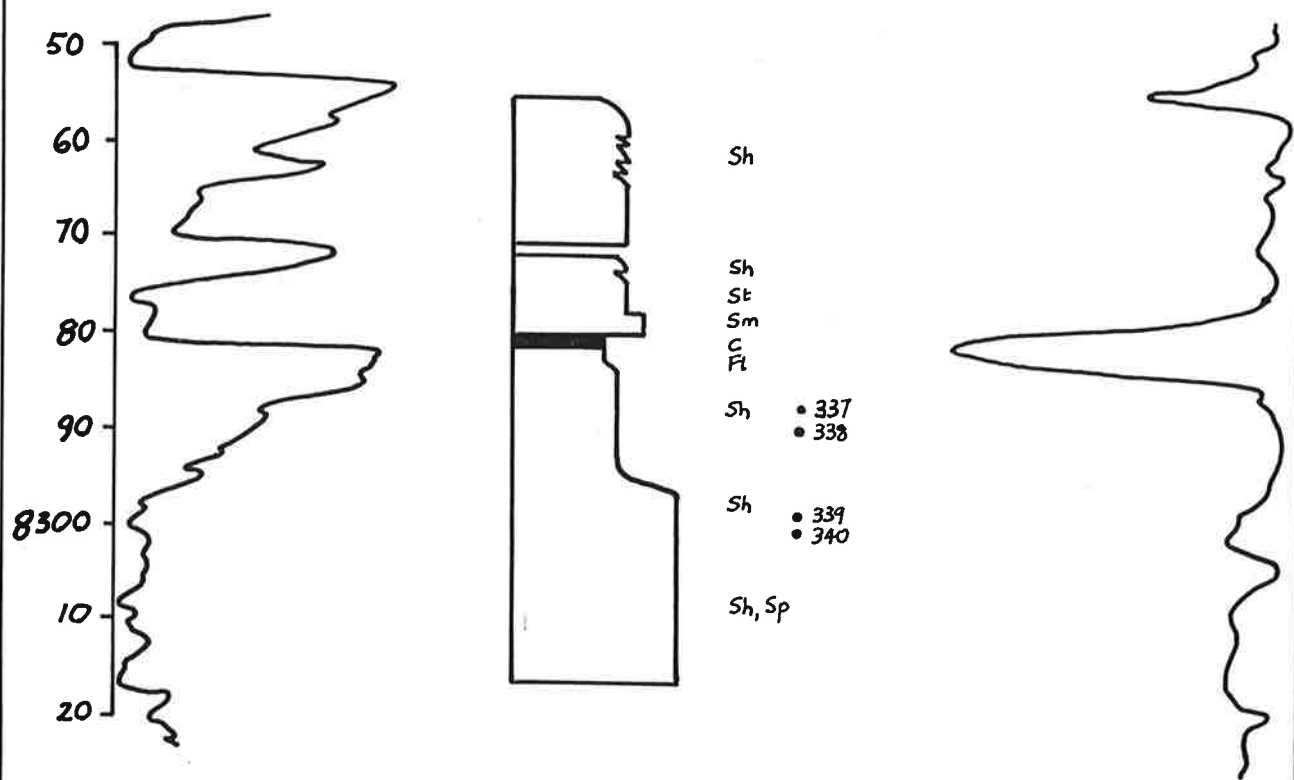


Fig. 10. Pira 2, core 2, Patchawarra Fmn.

Stacked channel deposits.

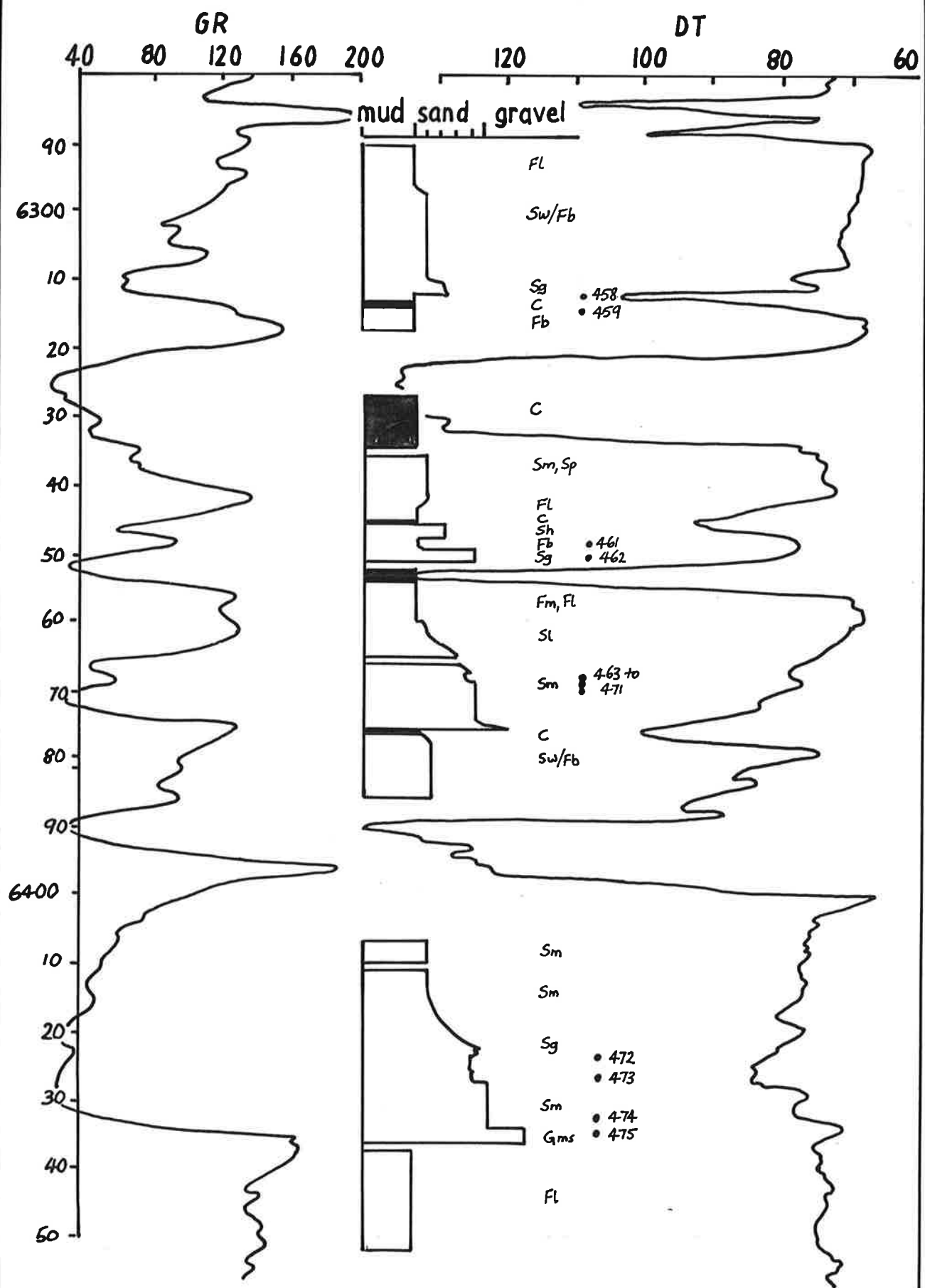
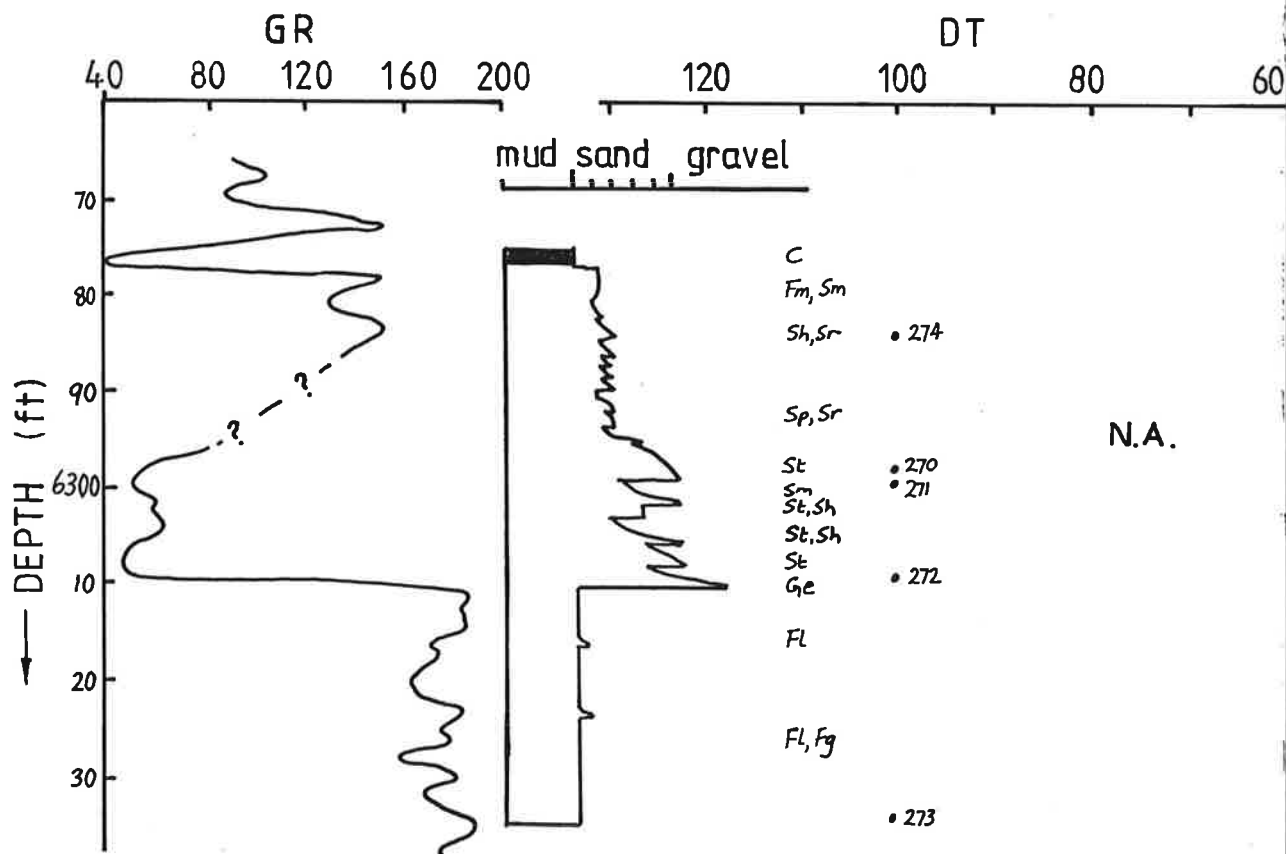
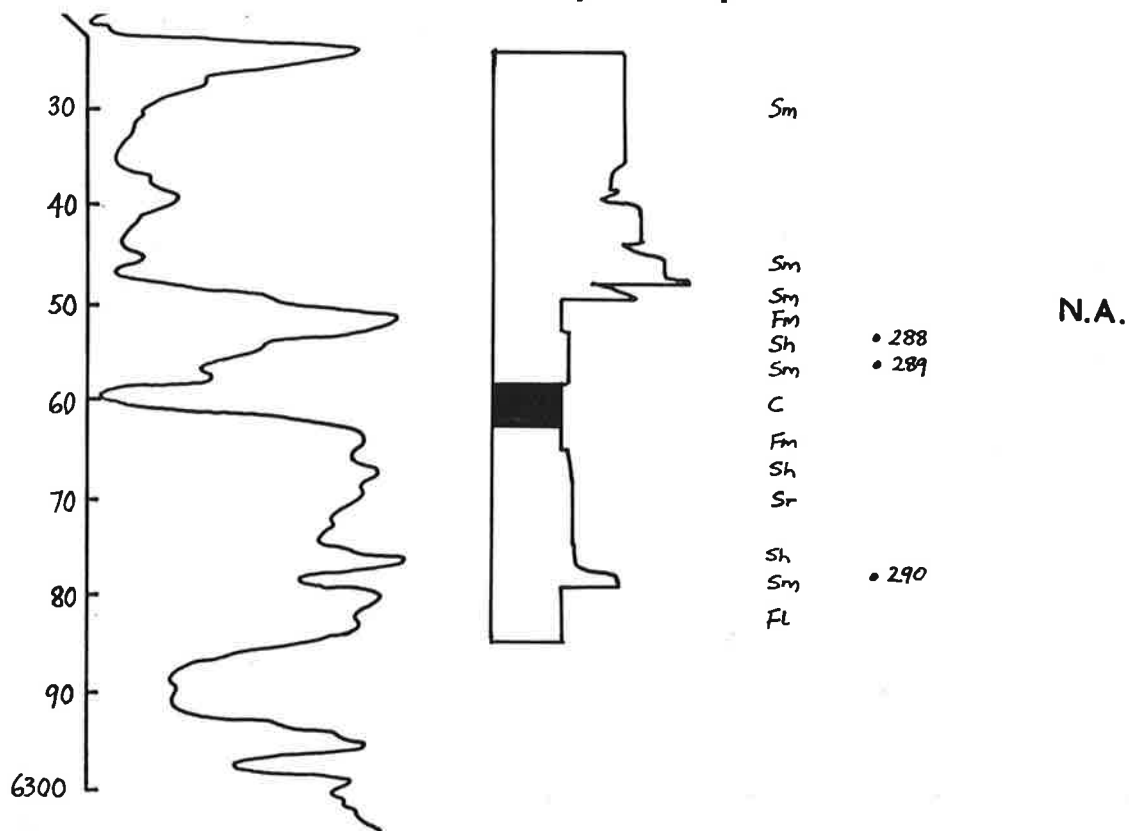


Fig. 11. Strzelecki 1, cores 1,2,3, Toolachee Fmn.
Stacked channel deposits.



**Fig. 16. Strzelecki 15, cores 1,2, Toolachee, Murteree Fmns.
Lacustrine, channel, floodplain deposits**



**Fig. 17. Strzelecki 16, cores 1,2, Toolachee Fmn.
Floodplain & channel deposits.**

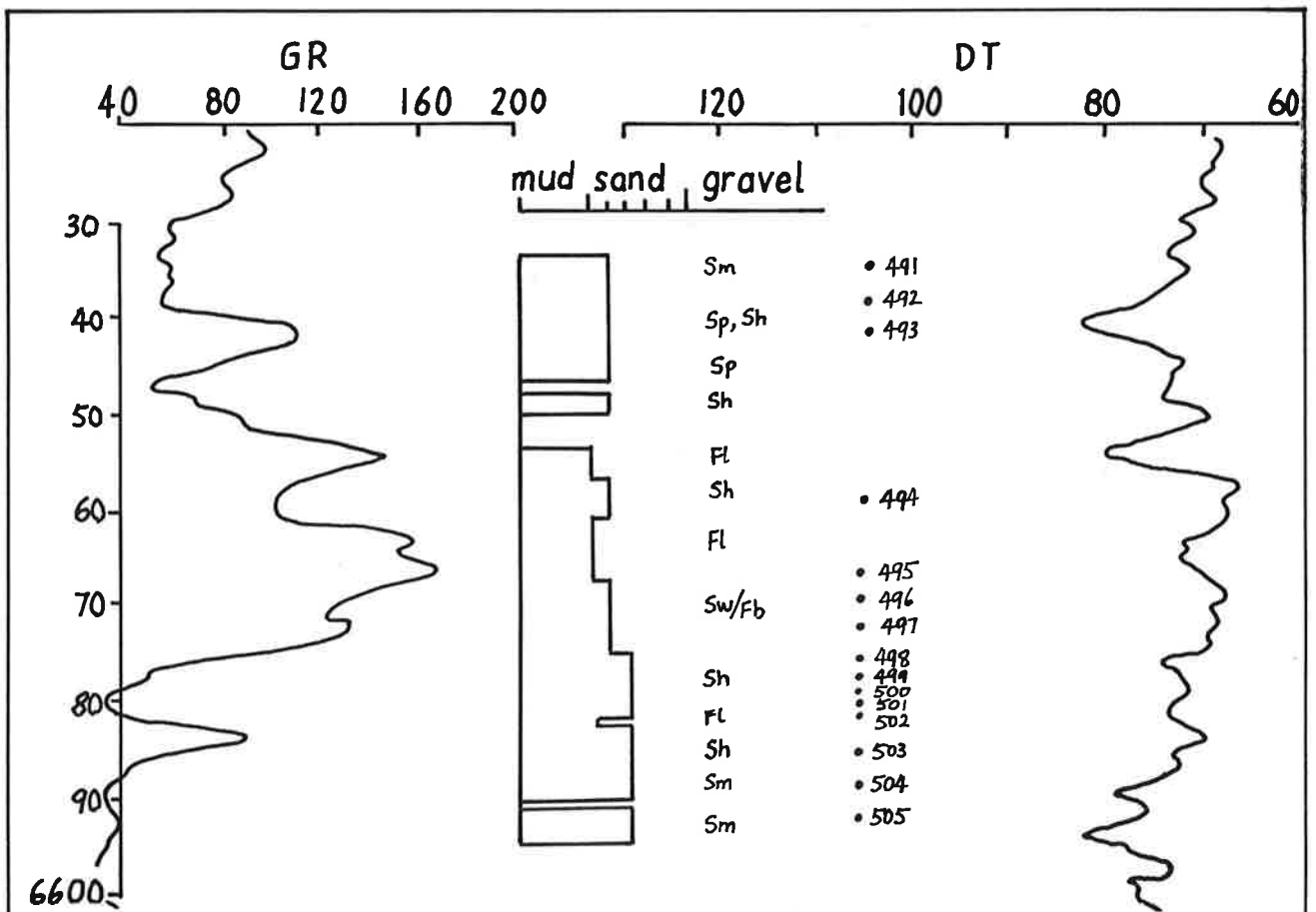


Fig. 12. Strzelecki 1, core 4, Patchawarra Fmn.

Floodplain deposits.

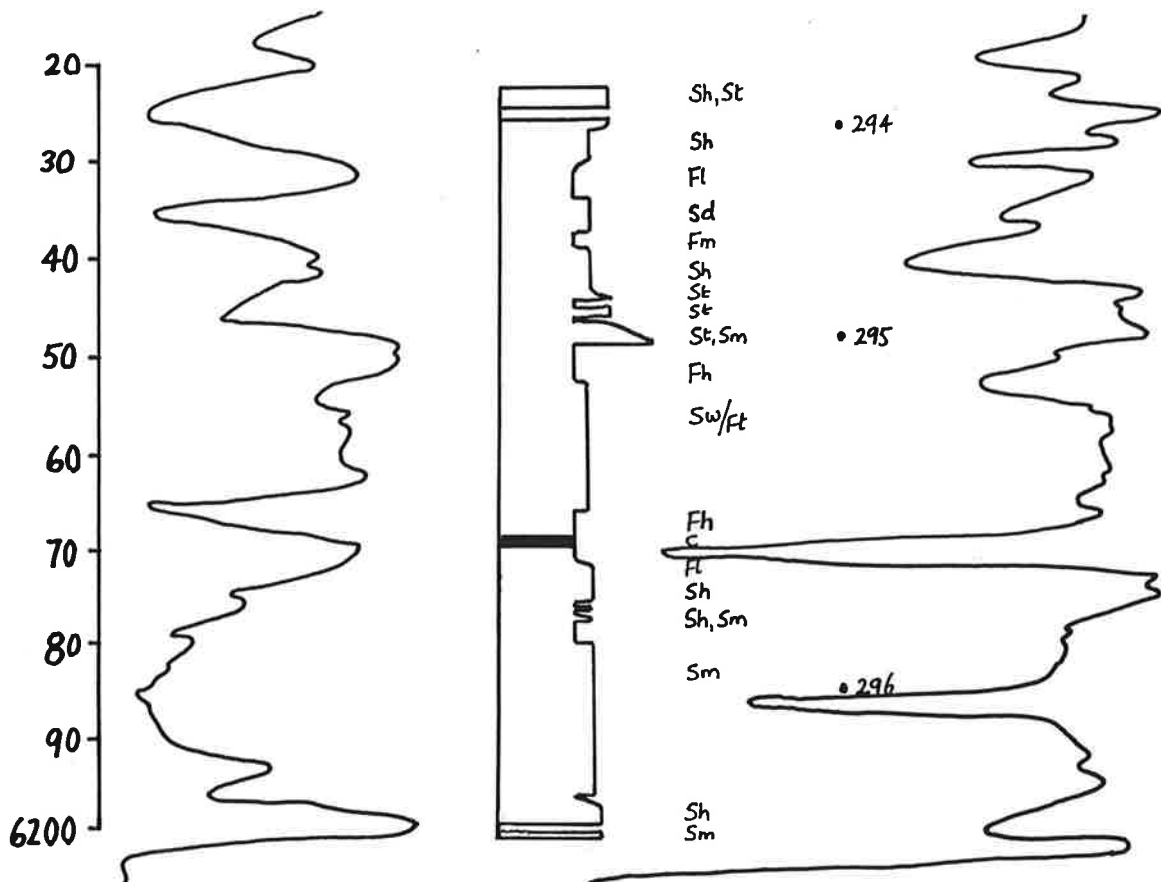
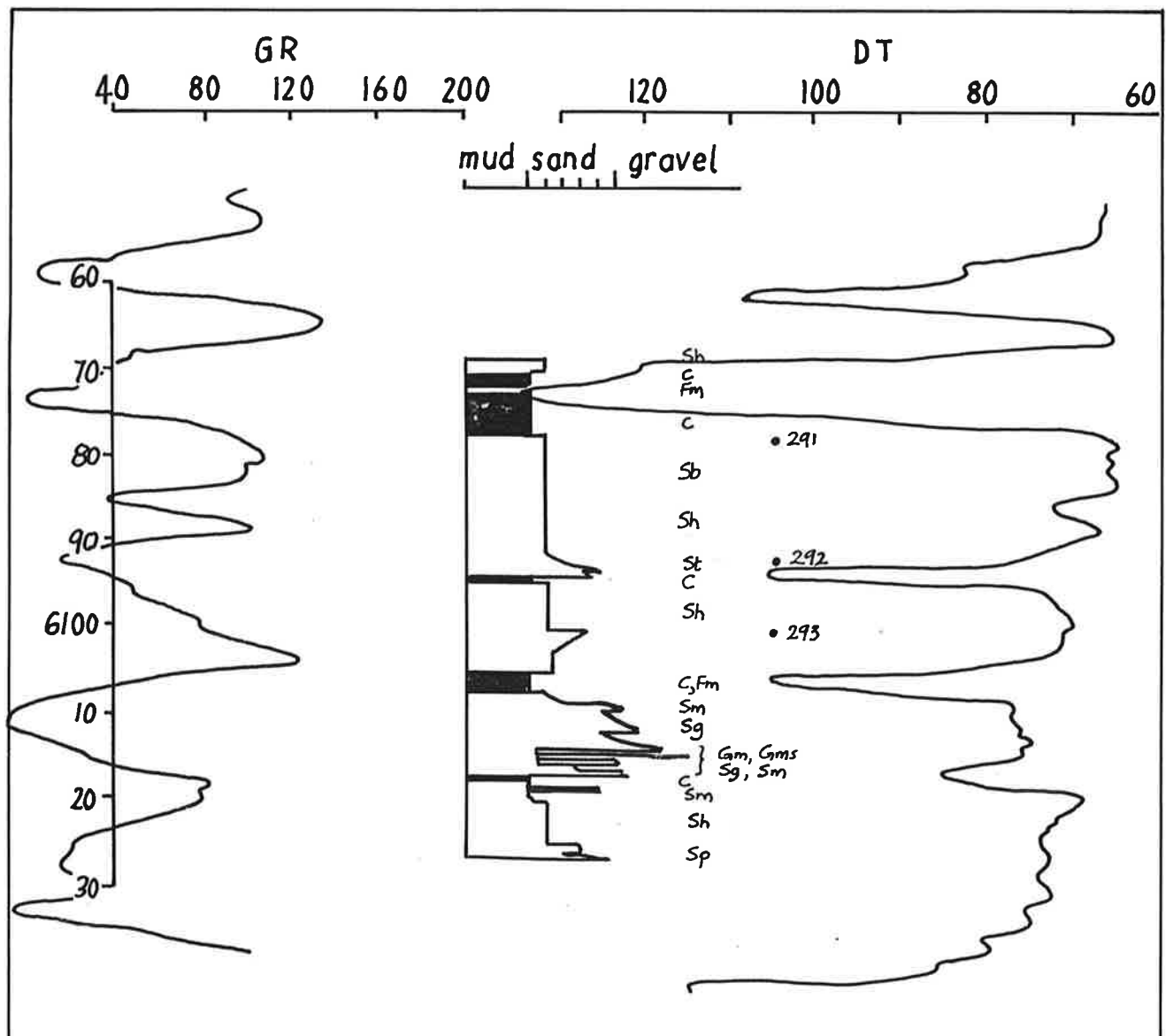


Fig. 13. Strzelecki 2, core 1, Toolachee Fmn.

Channel & overbank deposits.



**Fig. 14. Strzelecki 5, core 5, Toolachee Fmn.
Floodplain deposits.**

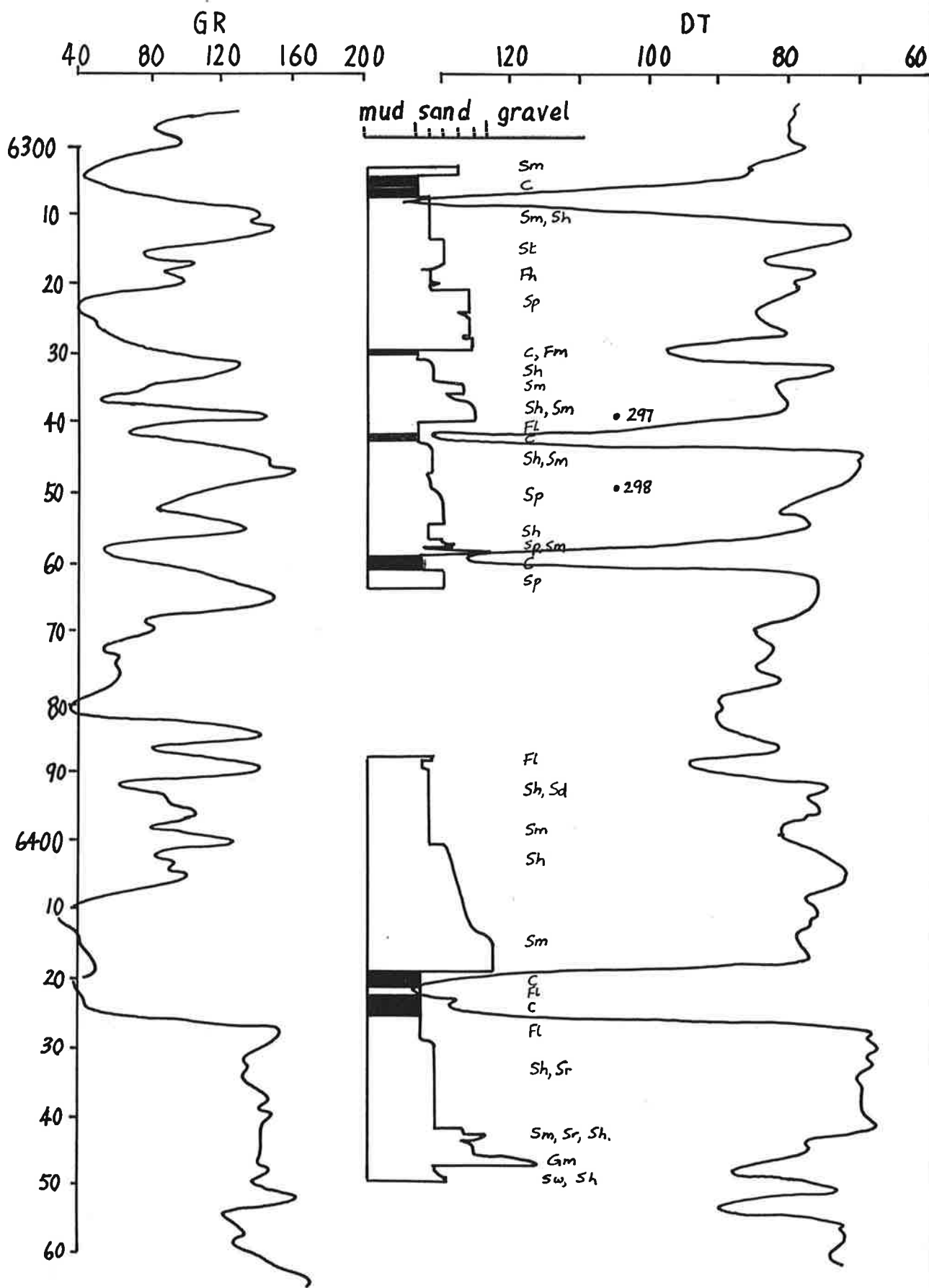


Fig. 15. Strzelecki 10, cores 1,2, Toolachee Fmn.
Stacked channel deposits.

APPENDIX 7

Drill Stem Test results and analysis.

Appendix 7: Drill Stem Test results.

Section	Contents
1	Introduction
2	Results
3	Analysis
4	Discussion

1 Introduction

This appendix presents the data and results of the pressure testing, or Drill Stem Tests (DST's) of intervals of drillholes within the study area. All DST's were performed over intervals of Patchawarra and Toolachee Formations sands, with few other formations tested.

2 Data

Data in Table 2 and Table 3 contains all 79 DST results for drillholes within the study area intersecting the sands of the Toolachee and Patchawarra Formations respectively. Genetic strata associations (as defined in Appendix 5, this report) and the number and inferred origin of sand units within these associations that were tested by DST's are also listed.

Data are wholly derived from the composite logs of all wells in the study area with most, if not all, DST's performed during or immediately after drilling. Depositional facies of tested sands are inferred from their gamma ray and sonic well logging trace.

Associations that were partly tested are enclosed in brackets.

Terminology used in the listing of the DST results in Tables 2 and 3 are shown in Table 1 below.

(Appendix 7, Page 2)

DST rating: DST results:

- 0.....water
- 1.....tight, no gas to surface (NGTS)
- 2.....trace gas, rate too small to measure (RTSM)
- 3.....0.1 to 1 million cubic feet per day (MMCFD)
- 4.....1 to 2 MMCFD
- 5.....2 to 3 "
- 6.....3 to 5 "
- 7.....5 to 7 "
- 8.....7 to 10 "
- 9.....> 10 "

Inferred depositional facies of sands:

- CH.....channel deposit
- FP.....flood plain
- LE.....low energy fluvial deposit
- OV.....overbank deposit
- PR.....prograding deposit
- XX.....mixed origin or unclear facies interpretation

Table 1. Terminology used in the listing of DST results in Tables 2 and 3, this Appendix. Numbers in front of the facies notation of sands refer to the number of genetic increments of strata intersected by the DST.

Well Name	DST no.	Association no.	Facies	Rating	DST (MMCFD)
Aroona 01	1	(2)	1OB	3	0
Aroona 01	2	(3)	1OB	2	0
Aroona 01	3	4	3OB	8	8.2
Bagundi 01	3	2	1CH	8	7.6
Cochilara 01	1	(3)	1CH	1	0
Dilchee 01	2	(3)	1CH	2	0
Kerna 01	1	(4)	2CH	2	0
Kidman 01	1	(3)	1OB	8	9.55
Kidman 01	2	(4)	1CH	9	10.8
Kidman 02	1	2	1CH	8	7.7
Kidman 02	2	(3)	2CH	6	3.3
Kidman 02	3	(3)	1CH	5	2.7
Kidman 05	1	1	1OB	3	0.78
Kidman 05	2	(2)	1CH	6	4.5

(continued next page...)

(Appendix 7, Page 3)

(...continued from previous page)

Well Name	DST no.	Association no.	Facies	Rating	DST (MMCFD)
Kidman 05	6	(3)	1CH	7	5.4
Kidman 05	3	4	1CH	8	8.3
Kidman 05	7	(4)	1CH	1	0
Kidman North 1	1	(2)	1OB	7	6.5
Kidman North 1	2	(3)	1CH	2	0
Marabooka 01	5	(2)	1CH	7	6.9
Marabooka 01	6	(3)	2CH	8	8.4
Marana 01	3	(3)	2CH	8	8.35
Marana 01	4	(3)	2CH	2	0
Lepena 01	1	(3)	1OB	7	5.3
Lepena 01	2	(4)	1CH	8	8.4
Pira 01	1	2	1CH	6	4.8
Pira 02	1	2,(3)	XX	2	0
Strzelecki 01	1	1,2,(3)	XX	8	5.2
Strzelecki 01	2	4	1CH	2	0
Strzelecki 01	9	1,2	4OB	0	0
Strzelecki 01	8	(3)	XX	0	0
Strzelecki 01	7	(3)	1OB	5	
Strzelecki 02	3	1,2	XX	2	0
Strzelecki 02	7	2	1CH	2	0
Strzelecki 02	4	(3)	1CH	2	0
Strzelecki 02	5	4,(3)	XX	2	0
Strzelecki 03	4	(1),2,(3)	XX	8	8.0
Strzelecki 03	5	(4)	1CH	8	7.3
Strzelecki 05	4	(1),2,(3)	XX	8	9.2
Strzelecki 10	1	(1)	XX	6	4.24
Strzelecki 10	2	(3)	XX	8	7.06
Strzelecki 10	3	(3)	1CH	6	6.84
Strzelecki 15	1	(3)	1CH	6	3.92
Strzelecki 15	2	(3),(4)	1CH	8	9.16
Strzelecki 16	1	(3),(4)	2CH	8	8.1
Strzelecki 24	1	(2),(3)	1CH	6	3.82
Strzelecki 25	2	(2),(3)	XX	8	7.56
Strzelecki 25	1	(2)	1CH	6	7.56
Wanara 01	3	(1)	XX	2	0
Wanara 01	4	(1),2,(3)	1CH	7	5.3
Wanara 01	5	(3)	1OB	5	2.2

Table 2. Drill Stem Test (DST) results of the Toolachee Formation sands intersected by the study area wells. Refer to Table 1 for terminology; for example, Wanara 1 DST number 5 tested one overbank sand unit that forms part of the Toolachee Formation facies association 3 and resulted in a gas flow of 2.2 MMCFD that is given a rating of 5. Facies associations with partly tested intervals are denoted by brackets.

(Appendix 7, Page 4)

Well Name	DST no.	Association no.	Facies	Rating	DST (MMCFD)
Aroona 01	4	(1),(2)	1CH	8	8.5
Bagundi 01	4	(1)	1OB	8	8.4
Coochilara 01	4	(2)	3CH	6	0.35
Coochilara 01	3	(1)	XX	1	0
Dilchee 01	4	(1)	1CH	6	3.65
Dilchee 01	5	(1),(2)	XX	1	0
Dilchee 01	6	(2)	XX	1	0
Kerna 01	7	(2)	4CH	7	7.0
Kerna 01	5	(2)	1CH	5	3.0
Kerna 01	4	(1)	XX	6	3.0
Kerna 02	4	(1)	3CH	6	3.25
Kerna 02	5	(2)	1CH	1	0
Kerna 02	7	(2)	1CH	2	0
Kerna 02	8	(2)	2CH	2	0
Kidman 01	4	(1),(2)	XX	2	0
Kidman 05	4	(1)	1OB	6	3.7
Kidman 05	5	(2)	1CH	1	0
Kidman North 1	4	(1)	1OB	9	10.3
Lepena 01	3	(1)	XX	7	5.3
Marabooka 01	7	(1),(2)	1CH	2	0
Pira 01	3	(1)	1CH	3	0.7
Pira 01	4	(2)	1CH	3	0.24
Pira 02	5	(2)	1CH	3	0.64
Pira 02	4	(2)	1CH	3	0.62
Pira 02	2	(1)	XX	0	0
Pira 02	3	(1)	1OB	2	0
Strzelecki 01	3	(1),(2)	XX	1	0
Strzelecki 15	3	(1)	1CH	2	0

Table 3 Drill Stem Test (DST) results of Patchawarra Formation sands intersected by the study area wells.

3 Analysis

DST results are plotted in Figures 40,41,42,43 and 44 of the report. DST results are compared with depositional facies associations and inferred depositional facies in Figures 41 and 42. DST results are plotted for the four Toolachee Formation depositional facies associations defined in Appendix 5 of this report in Figure 40 and similarly DST results are plotted for the two upper most Patchawarra Formation depositional facies associations in Figure 41. No DST spanning more than one of each association sand body is plotted. Frequency histograms are also plotted for all DST results as DST ratings in Figure 42 and as absolute flow rates in Figure 43.

DST results for the four Toolachee Formation facies associations are plotted against radial distance from Strzelecki 2, located in the south west corner of the study area, in Figure 44. Again, only single association test results are used and where only part of a single association was tested, DST results are reported as being greater than the highest DST result for that association.

Interpretation of data presented in these graphs is presented in Section 8.2 of the report.

4 Discussion

Rigorous analysis of DST flowrate data is not possible in any situation where gas flow comes from a less than ideal gas reservoir.

Systematic errors arise from the undefined nature of the geological rock mass being tested at depth. The only direct indication of these rock mass properties are the suite of geophysical logs that are run across the tested intervals. Problems of using these logs are the poor resolution of thin high flow rate intervals, no confirmation of lateral continuity of geological substances and the mostly empirical field wide determination of sand rock types that are considered permeable.

Another systematic error occurs in applying attributes of perfect porous media flow to geological materials that are not perfect hydraulic media.

(Appendix 7, Page 6)

Specific errors in DST flowrate analysis may come about from formation damage caused by mud filtrate invasion or the blockage of pore throats by interstitial clay particles, water reactive minerals, the short length of time during DST testing and fracturing of the test interval.

However, the lack of reactive clays, the relatively strong nature of the Cooper Basin rock substances and the lack of past history of well drilling problems in the Cooper Basin preclude permanent formation damage.

APPENDIX 8

Water sample chemistry data.

Appendix 8. Water sample chemistry data.

Test	Wellname	No.	Fmn	DST	pH	Na	K
1	Bagundi	1	Patc	4	6.9	2300	12100
2	Cooch	1	Tool	1	7.9	1958	23
3	Cooch	1	Tool	1	7.3	2476	36
4	Cooch	1	Tool	1	7.5	2417	34
5	Cooch	1	Tool	1	7.9	1958	23
6	Kerna	1	Tool	1	6.9	2000	23
7	Kerna	2	Patc	7	6.9	6300	150
8	Kerna	2	Patc	8	6.8	6670	153
9	Kidman	1	Tool	1	7.2	1865	24
10	Kidman	1	Tool	2	7.2	775	21
11	Kidman	1	Tool	2	6.5	1440	22
12	Kidman	1	Tool	2	6.7	2900	43
13	Kidman	1	Patc	4	6.8	4112	65
14	Kidman	1	Patc	4	6.5	4188	81
15	Kidman	1	Patc	4	6.5	3688	81
16	Kidman	2	Tool	1	7.4	2500	75
17	Kidman	2	Tool	2	7.4	1750	27
18	Kidman	2	Tool	2	7.2	1745	27
19	Kidman	2	Tool	3	7.1	2105	26
20	Kidman	2	Tool	3	7	1990	25
21	Kidman	5	Tool	6	7.9	2100	1600
22	Kidman	5	Tool	3	7.4	4000	13000
23	Kidman	5	Patc	5	7.5	3100	385
24	Lepena	5	Patc	3	8.3	2170	27000
25	Marana	1	Tool	4	6.7	2200	23
26	Marana	1	Tool	4	7.8	1800	25
27	Pira	2	Patc	5	7.5	3020	3960
28	Pira	2	Tool	1	8	2200	1080
29	Pira	2	Patc	2	7.4	2750	5350
30	Pira	2	Patc	4	7.2	5550	2350
31	Pira	2	Patc	5	6.9	7180	28000
32	Strz	1	Tool	2	7	2022	16
33	Strz	1	Tool	2	6.9	1897	14
34	Strz	1	Patc	3	7	1826	18
35	Strz	2	Tool	4	6.8	1591	21
36	Strz	2	Tool	5	6.9	1600	18
37	Strz	3	Tool	4	6.7	1640	15
38	Strz	3	Tool	5	6.6	1000	11
39	Strz	3	Tool	5	6.8	1950	20
40	Strz	10	Tool	2	6.9	2750	20

(Appendix 8, page 2)

No.	Ca	Mg	Cl	HCO ₃	SO ₄	NO ₃	DST top	DST base
1	25	3.3	13400	1140	790	4	6947	6977
2	218	126	3419	501	79	1	7110	7220
3	54	12	2936	1741	43	1	7110	7220
4	43	11	2923	1571	252	1	7110	7220
5	218	126	3419	501	79	1	7110	7220
6	2	7.5	2340	1556	21	4	7142	7210
7	370	105	9285	2174	137	4	8400	8462
8	150	90	10870	1170	40	4	8465	8518
9	46	15	1434	2033	406	5	6578	6622
10	508	12	1452	201	142	5	6709	6774
11	365	12	2314	402	363	5	6709	6774
12	328	12	3899	916	741	5	6709	6774
13	98	30	4925	1845	536	2	7266	7367
14	129	39	5463	1531	443	2	7266	7367
15	128	36	5335	1374	60	2	7266	7367
16	41	5	2718	829	990	2	6478	6545
17	42	8	1868	1693	100	2	6564	6620
18	36	5	1871	1659	89	2	6564	6620
19	30	5	2204	1803	89	2	6630	6691
20	25	5	2197	1734	95	2	6630	6691
21	40	5	3600	1800	270	4	6660	6700
22	300	88	15200	3700	2390	4	6700	6761
23	235	14	4570	1860	100	4	7154	7178
24	76	62	24700	2320	1400	4	6794	6842
25	58	8.4	2520	1561	45	4	6318	6359
26	265	115	2823	134	900	20	6318	6359
27	400	90	8210	312	1580	4	8589	8639
28	45	7.9	3350	1960	100	4	7098	7196
29	250	92	8920	446	1350	4	8194	8277
30	290	75	11400	692	190	4	8314	8365
31	680	150	31200	2600	4000	4	8589	8639
32	18	6	2090	1840	40		6384	6445
33	8	2	2045	1555	20		6384	6445
34	17	3	1766	1910	35		6529	6591
35	24	6	1660	1515	10		6196	6240
36	32	5	1630	1565	25		6239	6344
37	2	10	1304	955	960	5	6196	6240
38	22	2	1008	183	609	5	6146	6215
39	40	6	1880	755	1103	5	6146	6215
40	42	6.9	3054	1222	900	4	6300	6354

(Appendix 8, page 3)

<u>No.</u>	<u>Anions</u>	<u>Cations</u>	<u>TDS</u>
1	14428.3	15334	29762.3
2	2325	4000	6325
3	2578	4721	7299
4	2505	4747	7252
5	2325	4000	6325
6	2051.5	3921	5972.5
7	6925	11600	18525
8	7063	12084	19147
9	1950	3878	5828
10	1316	1800	3116
11	1839	3084	4923
12	3283	5561	8844
13	4305	7308	11613
14	4437	7439	11876
15	3933	6771	10704
16	2621	4539	7160
17	1827	3663	5490
18	1813	3621	5434
19	2166	4098	6264
20	2045	4028	6073
21	3745	5674	9419
22	17388	21294	38682
23	3734	6534	10268
24	29308	28424	57732
25	2289.4	4130	6419.4
26	2205	3877	6082
27	7470	10106	17576
28	3332.9	5414	8746.9
29	8442	10720	19162
30	8265	12286	20551
31	36010	37804	73814
32	2062	3970	6032
33	1921	3620	5541
34	1864	3711	5575
35	1642	3185	4827
36	1655	3220	4875
37	1737	3224	4961
38	1035	1805	2840
39	2016	3743	5759
40	2818.9	5180	7998.9